



**THE ROLE OF DIHYDROCERAMIDE
DESATURASE AND SPHINGOSINE KINASES IN
CELL SURVIVAL/APOPTOSIS AND
INFLAMMATION PATHWAYS**

By

Mariam B Alsanafi

A thesis submitted in the fulfillment of the requirements for the degree of
Doctor of Philosophy

January 2020

Strathclyde Institute of Pharmacy and Biomedical Sciences (SIPBS)
Glasgow, UK

DECLARATION

This thesis is the result of the author's original research. It has been composed by the author and has not been previously submitted for examination which has led to the award of a degree.

The copyright of this thesis belongs to the author under the terms of the United Kingdom Copyright Acts as qualified by University of Strathclyde Regulation 3.50. Due acknowledgement must always be made of the use of any material contained in, or derived from, this thesis.

Signed:

Date:

ACKNOWLEDGEMENTS

In the name of Allah (God), the most gracious, the most merciful, I would like to thank several people for the contributions they made while I was developing and writing my PhD dissertation.

First, I would like to thank my supervisors, Prof. Nigel Pyne and Prof. Susan Pyne, for their amazing help, inspiration, recommendations, and encouragement throughout this project. I will never forget the experience and would highly recommend such a great experience to everyone. I also would like to thank all the members of the Pyne research group, including Salha Tawati, Ashref Elburi, Mohammed Alrofai, Abir Mohammed, Ryan Brown, Melissa McNaughton, and Ahmed Alfaqih, who helped me through hard times and laughed with me during more enjoyable times.

Many thanks also go to Dr. Rothwelle Tate, Margaret MacDonald, and Graeme Mackenzie for their continued laboratory help and support. In addition, I would like to thank members of my previous cardiovascular lab, including Zuhair Alsulti, Abdulhadi Buruzangi, Molly Huq, and Abdulwahab Alamri, who provided continued support and friendship. Furthermore, I am grateful to the office members, including Samiyah Alenezi, Samiyah Alshehri, Hanin Alyamani, Nouf Abutheraa, Aliyah Alhuwaiti, Najla Altuwaijery, Lina Akil, Bayan Ainousah, and Kanidta Niwasabutra—all of whom were always extremely supportive while making the office fun.

My gratitude goes to the Kuwait government for offering me a scholarship to pursue my PhD degree at the University of Strathclyde.

My infinite appreciation and thanks go to my parents, Bader and Awatif, as well as my sisters, Haya and Fatma, and brothers, Nasser and Mohammad, for their never-ending support, prayers, motivation, love, caring, and for giving me the courage to make it.

My greatest thanks go to my children. To my beloved twin boys, Abdullah and Abdulrahman, thank you for not only sharing this journey with me, but also embracing the Scottish accent—aye ;) You are a precious gift. I am so grateful to have you in my life, and I regret not being able to give you more time throughout my PhD journey. To my little baby girl, Athari, who arrived while I was writing this dissertation, I'm really sorry for producing so many stress hormones during my pregnancy, but I am truly thankful that you were with me while writing up my work.

I will miss Scotland, my second home, and will never forget the wonderful memories, stressful moments, daily lab work, and relaxing time on weekends and during Christmas holidays. I will miss the great few sunny days and even the mostly rainy weather, for which I always forget my umbrella and get wet. This has been a fascinating period in my life. Although it was at times stressful and I cried a lot, now that the journey is drawing to an end, I wish I could continue it. Now I have to go back to my home, Kuwait, but I will take with me all these lovely memories and friendships, keeping them with me forever. I cannot wait to return to Glasgow to visit during the holidays as I really love this country.

It is my sincere hope that this effort, which took years of my life, will be beneficial to future researchers seeking to discover new pharmacological targets to treat various diseases, including cancer. “Allah makes the way to Heaven easy for him who treads the path in search of knowledge.” ~Prophet Mohammad (PBUH)

DEDICATION

This thesis is dedicated in loving memory of my grandmother, Amina, my grandfather, Hasan, and my best friend in high school, Anwar, who passed away during my PhD journey. I'm so sorry that I did not have the chance to attend your funerals. I know that you would love seeing me get my PhD degree. Words cannot heal the pain of losing you. How I miss you!

TABLE OF CONTENTS

DECLARATION.....	II
ACKNOWLEDGEMENTS.....	III
DEDICATION	V
TABLE OF CONTENTS	VI
LIST OF FIGURES	IX
LIST OF TABLES.....	XII
ABBREVIATIONS	XIII
PUBLICATIONS AND POSTER PRESENTATIONS	XVI
ABSTRACT	XVII
CHAPTER1: GENERAL INRODUCTION	2
1.1 SPHINGOLIPIDS SYNTHESIS AND METABOLISM	2
1.2 SPHINGOLIPID RHEOSTAT.....	7
1.3 SPHINGOLIPID METABOLITES	10
1.3.1 <i>Sphingomyelin (SM) and dihydrosphingomyelin (dhSM)</i>	10
1.3.2 <i>Sphingosine (Sph)</i>	11
1.3.3 <i>Ceramide (Cer) and dihydroceramide (dhCer)</i>	14
1.3.4 <i>Sphingosine-1-phosphate (S1P)</i>	19
1.4 SPHINGOLIPID METABOLISING ENZYMES.....	27
1.4.1 <i>Dihydroceramide desaturase 1 (Degs1)</i>	27
1.4.2 <i>Sphingosine kinases (SKs)</i>	30
1.5 SPHINGOSINE KINASE INHIBITORS.....	35
1.5.1 <i>Non-selective SK inhibitor [SKI-II inhibitor (SKi)]</i>	37
1.5.2 <i>Selective SK1 inhibitors</i>	39
1.5.2.1 PF-543	39
1.5.2.2 FTY720	40
1.5.3 <i>Selective SK2 inhibitors</i>	41
1.5.3.1 ABC294640	41
1.5.3.2 ROME [(R)-FTY720-OMe].....	43
1.5.3.3 K145.....	44
1.6 POST-TRANSLATIONAL MODIFICATION AND UBIQUITINATION OF PROTEINS	45
1.7 ENDOPLASMIC RETICULUM (ER) STRESS PATHWAY.....	49
1.7.1 <i>ER stress sensors</i>	52
1.7.2 <i>Pharmaceutical ER stress inducers</i>	55
1.8 TUMOUR SUPPRESSOR PROTEIN (P53)	56
1.8.1 <i>p53</i>	56
1.8.1.1 Mdm2 and p53	57
1.8.2 <i>p63, p73, and p90</i>	59
1.9 NUCLEAR FACTOR KAPPA B (NF-KB).....	62
1.9.1 <i>The NF-κB family</i>	63
1.9.2 <i>Inhibitory kappa B (IκB)</i>	64
1.9.3 <i>The Inhibitory kappa B kinases (IKKs)</i>	64
1.9.4 <i>Three distinctive pathways of NF-κB activation</i>	66
1.9.4.1 Classical (canonical) pathway.....	67
1.9.4.2 Alternative (non-canonical) pathway.....	68
1.9.4.3 Atypical pathway.....	68
1.10 ACTIVATOR PROTEIN-1 (AP-1).....	69

1.11	PROJECT AIMS	72
CHAPTER2: MATERIALS AND METHODS		74
2.1	MATERIALS	74
2.1.1	General reagents.....	74
2.1.2	Cell culture.....	75
2.1.3	Antibodies.....	75
2.1.4	Agonists and inhibitors.....	77
2.1.5	Molecular biology.....	78
2.1.6	Radioisotopes.....	79
2.2	METHODS	80
2.2.1	Cell culture.....	80
2.2.2	Treatment protocol.....	81
2.2.3	Plasmid DNA transformation and purification.....	82
2.2.4	Cell transfections	83
2.2.4.1	siRNA transfections	83
2.2.4.2	Transient plasmid transfection	83
2.2.5	Immunoprecipitation.....	84
2.2.6	Preparation of the pellet and supernatant fractions:.....	85
2.2.7	Preparation of cell lysates for western blotting analysis of protein expression.....	85
2.2.8	SDS-PAGE and western blotting	86
2.2.8.1	Preparation of polyacrylamide gels.....	86
2.2.8.2	Polyacrylamide gel electrophoresis (SDS-PAGE)	86
2.2.8.3	Transfer to nitrocellulose membranes.....	87
2.2.8.4	Western blotting.....	88
2.2.8.5	Stripping and re-probing nitrocellulose membranes.....	89
2.2.8.6	Quantification and statistical analysis of western blots	89
2.2.9	[³ H]-Thymidine incorporation assay.....	90
2.2.10	Luciferase reporter assay.....	90
2.2.11	Immunofluorescence microscopy.....	92
2.2.12	Lipidomics (Cell pellet preparation for mass spectrometry for sphingolipid analysis).....	93
2.2.13	Statistical analysis.....	94
CHAPTER 3: THE ROLE OF DIHYDROCERAMIDE DESATURASE IN REGULATING THE SURVIVAL OF HUMAN EMBRYONIC KIDNEY CELLS		96
3.1	INTRODUCTION.....	96
3.2	RESULTS.....	101
3.2.1	Effect on <i>Degs1</i> expression in HEK293T and parental HEK293 cells.....	101
3.2.2	Effect of SKi and ABC294640 on <i>Degs1</i> expression in HEK293T cells.....	101
3.2.3	Effect of proteasome inhibitors on the polyubiquitination of <i>Degs1</i> in HEK293T cells.....	108
3.2.4	Effect of SKi, ABC294640, and MG132 on <i>Degs1</i> expression in parental HEK293 cells.....	113
3.2.5	Effect of NAC on <i>Degs1</i> expression in HEK293T cells	115
3.2.6	Assessment of the role of SK1 and SK2 in regulating <i>Degs1</i> ladder formation in HEK293T cells.....	118
3.2.7	Effect of SKi and ABC294640 on apoptosis and DNA synthesis in HEK293T cells.....	126
3.2.8	Effect of SKi and ABC294640 on p38 MAPK and JNK activation in HEK293T cells.....	139
3.2.9	Effect of SKi, ABC294640, and tunicamycin on PERK and XBP-1s levels in HEK293T cells.....	153
3.2.10	Effect of SKi and ABC294640 on sphingolipid levels in HEK293T cells.....	162

3.3 DISCUSSION.....	164
CHAPTER 4: THE ROLE OF SPHINGOSINE KINASES 1 AND 2 IN REGULATING P53, P38 MAPK, JNK AND XBP-1S SIGNALLING IN HUMAN EMBRYONIC KIDNEY CELLS	175
4.1 INTRODUCTION.....	175
4.2 RESULTS.....	179
4.2.1 <i>Effect of SKi and ABC294640 on post-translational modification of p53 in HEK293T and parental HEK293 cells</i>	179
4.2.2 <i>Effect of NAC on SKi-induced p63/p90 formation in HEK293T cells</i>	192
4.2.3 <i>Effect of SKi on p38 MAPK and JNK activation in HEK293T cells</i>	194
4.2.4 <i>Role of p53 and apoptosis in HEK293T cells</i>	198
4.2.5 <i>Role of p53 in regulating XBP-1s levels in HEK293T cells</i>	201
4.2.6 <i>Effect of SKi on sphingolipid levels in HEK293T cells</i>	209
4.2.7 <i>Effect of SKi, ABC294640, and MG132 on p53 with immunofluorescence microscopy in HEK293T cells</i>	210
4.3 DISCUSSION.....	213
CHAPTER 5: SPHINGOSINE KINASES LINK WITH NUCLEAR FACTOR KAPPA B- AND ACTIVATOR PROTEIN-1-MEDIATED SIGNALLING IN KERATINOCYTES	225
5.1 INTRODUCTION.....	225
5.2 RESULTS.....	231
5.2.1 <i>Effect of SK inhibitors on NF-κB signalling and transcriptional activity in NCTC-NF-κB reporter keratinocytes</i>	231
5.2.2 <i>Effect of SK inhibitors on JNK/ERK-1/2 signalling and AP-1 transcriptional activity in NCTC-AP1 reporter keratinocytes</i>	244
5.3 DISCUSSION.....	257
CHAPTER 6: GENERAL DISCUSSION AND FUTURE DIRECTIONS	264
6.1 GENERAL DISCUSSION	264
6.2 CONCLUSION AND FUTURE DIRECTIONS.....	270
CHAPTER 7: REFERENCES	272
APPENDIX: SUPPLEMENTARY DATA	317

LIST OF FIGURES

CHAPTER 1

Figure 1.1 <i>Sphingolipid metabolism</i>	6
Figure 1.2 <i>The sphingolipid rheostat</i>	8
Figure 1.3 <i>Sphingodynamics</i>	9
Figure 1.4 <i>S1P receptors, G-protein-coupling and signalling pathways</i>	23
Figure 1.5 <i>Intracellular and extracellular actions of S1P</i>	26
Figure 1.6 <i>The ubiquitin proteasome system</i>	46
Figure 1.7 <i>Ubiquitin modifications and related diverse cellular functions</i>	47
Figure 1.8 <i>Types of ubiquitination</i>	48
Figure 1.9 <i>ER stress and UPR</i>	51
Figure 1.10 <i>p53-Mdm2 auto-regulatory loop</i>	59
Figure 1.11 <i>Modular structure of the p53 family members</i>	62
Figure 1.12 <i>The three distinctive NF-κB pathways</i>	66

CHAPTER 2

Figure 2.1 <i>Cells' morphology</i>	81
Figure 2.2 <i>Luciferase reaction</i>	91

CHAPTER 3

Figure 3.1 <i>Effect of SKi and ABC294640 on Dags1 protein expression in HEK293T cells</i>	104
Figure 3.2 <i>Confirmation of SKi-induced Dags1 ladder identity using siRNA in HEK293T cells</i>	105
Figure 3.3 <i>Dags1 location change according to cell harvesting method in HEK293T cells</i>	106
Figure 3.4 <i>Dags1 immunoprecipitation in HEK293T cells</i>	107
Figure 3.5 <i>Effect of MG132 on Dags1 protein expression in HEK293T cells</i>	110
Figure 3.6 <i>Confirmation of MG132 and MG132/SKi-induced Dags1 ladder identity using siRNA</i>	111
Figure 3.7 <i>Effect of Bortezomib on Dags1 protein expression in HEK293T cells</i>	112
Figure 3.8 <i>SKi and MG132 induce post-translational modification of Dags1 in parental HEK293 cells</i>	114
Figure 3.9 <i>Effect of NAC on the SKi-induced formation of the Dags1 ladder in HEK293T cells</i>	116
Figure 3.10 <i>The effect of NAC on Fenretenide- and MG132-induced formation of the Dags1 ladder in HEK293T cells</i>	117
Figure 3.11 <i>Effect of SKi or ABC294640 on SK1 protein expression in HEK293T cells and role of oxidative stress</i>	120
Figure 3.12 <i>siRNA knockdown of SK1 expression in HEK293T cells</i>	121
Figure 3.13 <i>Effect of SK1 siRNA on the Dags1 ladder in HEK293T cells</i>	122
Figure 3.14 <i>Effect of PF-543 on formation of Dags1 ladder in HEK293T cells</i>	123
Figure 3.15 <i>RT-qPCR analysis of mRNA transcript levels of SK2 in HEK293T cells</i>	124
Figure 3.16 <i>Effect of SK2 siRNA on the Dags1 ladder in HEK293T cells</i>	125
Figure 3.17 <i>Effect of SKi or ABC294640 on PARP cleavage in HEK293T cells</i>	127
Figure 3.18 <i>Effect of SKi, ABC294640, or MG132 on CHOP expression in HEK293T cells</i>	128
Figure 3.19 <i>Effect of SKi or ABC294640 on DNA synthesis in HEK293T cells</i>	129
Figure 3.20 <i>Effect of Dags1 siRNA on ABC294640-induced PARP cleavage in HEK293T cells</i>	131
Figure 3.21 <i>Effect of Dags1 siRNA on DNA synthesis in HEK293T cells</i>	132
Figure 3.22 <i>Effect of SK1 siRNA on ABC294640-induced PARP cleavage in HEK293T cells</i>	133
Figure 3.23 <i>Effect of SK1 siRNA on DNA synthesis in HEK293T cells</i>	134
Figure 3.24 <i>Effect of SK2 siRNA on ABC294640-induced PARP cleavage in HEK293T cells</i>	135

Figure 3.25 Effect of SKi and ABC294640 on P-Akt expression in HEK293T cells.....	137
Figure 3.26 Effect of SKi and ABC294640 on LC3B expression in HEK293T cells.....	138
Figure 3.27 Effect of SKi on levels of phosphorylated p38 and JNK protein expressions in HEK293T cells.....	141
Figure 3.28 Effect of ABC294640 on levels of phosphorylated p38 and JNK protein expression in HEK293T cells.....	143
Figure 3.29 Effect of JNK inhibitor (SP600125) and the p38 MAPK inhibitor (SB203580) on PPAR cleavage in HEK293T cells.....	145
Figure 3.30 Effect of the p38 MAPK inhibitor (SB203580) pre-treatment to SKi on DNA synthesis in HEK293T cells.....	146
Figure 3.31 Effect of Degr1 siRNA on SKi-induced p38 MAPK and JNK pathways in HEK293T cells.....	149
Figure 3.32 Effect of SK1 siRNA on p38 MAPK and JNK pathways in HEK293T cells.....	150
Figure 3.33 Effect of SK2 siRNA p38 MAPK and JNK pathways in HEK293T cells.....	151
Figure 3.34 Effect of p38 MAPK inhibitor (SB203580) on the polyubiquitination of Degr1 in response to SKi in HEK293T cells.....	152
Figure 3.35 Effect of SKi, ABC294640, or Tunicamycin on PERK mobility shift in HEK293T cells.....	155
Figure 3.36 Lack of effect of Degr1 siRNA on PERK mobility shift in HEK293T cells.....	156
Figure 3.37 Lack of effect of SK1 siRNA on PERK mobility shift in HEK293T cells.....	157
Figure 3.38 Lack of effect of SK2 siRNA on PERK mobility shift in HEK293T cells.....	158
Figure 3.39 Effect of SKi or ABC294640 in combination with MG132 to XBP-1s levels in HEK293T cells.....	160
Figure 3.40 Effect of Degr1 siRNA on XBP-1s levels in HEK293T cells.....	161
Figure 3.41 Different roles of native and polyubiquitinated Degr1 forms.....	166

CHAPTER 4

Figure 4.1 Effect of SKi and ABC294640 on p53 in HEK293T and parental HEK293 cells ...	181
Figure 4.2 Confirmation of p53, p63 and p90 identities using siRNA in HEK293T cells.....	182
Figure 4.3 p53 and location change according to cell harvesting method in HEK293T cells.....	183
Figure 4.4 p53 immunoprecipitation in HEK293T cells.....	184
Figure 4.5 Effect of HA-tagged ubiquitin plasmid transfection on SKi-induced post-translationally modified forms of p53 in HEK293T cells.....	187
Figure 4.6 Effect of MG132 on p53 post-translationally modified forms in HEK293T cells.....	188
Figure 4.7 Effect of SK1 siRNA on p53 post-translationally modified forms in HEK293T cells.....	189
Figure 4.8 Effect of SK2 siRNA on p53 post-translationally modified forms in HEK293T cells.....	190
Figure 4.9 Effect of Degr1 siRNA on p53 post-translationally modified forms in HEK293T cells.....	191
Figure 4.10 The effect of NAC on post-translational modification of p53 in HEK293T cells.....	193
Figure 4.11 Effect of SK1 siRNA on SKi-induced p38 MAPK and JNK pathways in HEK293T cells.....	195
Figure 4.12 Effect of SK2 siRNA on SKi-induced p38 MAPK and JNK pathways in HEK293T cells.....	196
Figure 4.13 Effect of p53 siRNA on SKi-induced p38 MAPK and JNK pathways in HEK293T cells.....	197
Figure 4.14 Effect of p53 siRNA on ABC294640-induced PARP cleavage in HEK293T cells.....	199
Figure 4.15 Effect of p53 siRNA on DNA synthesis in HEK293T cells.....	200
Figure 4.16 Effect of SK1 siRNA on XBP-1s levels in HEK293T cells.....	203
Figure 4.17 Effect of SK2 siRNA on XBP-1s levels in HEK293T cells.....	204
Figure 4.18 Effect of p53 siRNA on XBP-1s levels in HEK293T cells.....	205
Figure 4.19 Effect of SK1 siRNA on PARP cleavage in HEK293T cells.....	206
Figure 4.20 Effect of SK2 siRNA on PARP cleavage in HEK293T cells.....	207

Figure 4.21 Effect of p53 siRNA on PARP cleavage in HEK293T cells.....	208
Figure 4.22 Immunofluorescence microscopy images showing the effect of SKi, ABC294640, and MG132 on p53 in HEK293T cells.....	212

CHAPTER 5

Figure 5.1 Effect of SK inhibitors on SK1 protein expression in NCTC-NF- κ B reporter keratinocytes	232
Figure 5.2 Effect of TNF α on I κ B degradation in NCTC-NF- κ B reporter keratinocytes.....	235
Figure 5.3 Effect of SK inhibitors on I κ B degradation in NCTC-NF- κ B reporter keratinocytes... ..	238
Figure 5.4 Effect of SK inhibitors on NF- κ B-mediated signalling in NCTC-NF- κ B reporter keratinocytes	243
Figure 5.5 Effect of SK inhibitors on SK1 protein expression in NCTC-AP1 reporter keratinocytes	245
Figure 5.6 Effect of PMA on JNK phosphorylation and ERK-1/2 activation in NCTC-AP1 reporter keratinocytes	248
Figure 5.7 Effect of SK inhibitors on PMA-activated JNK and ERK1/2 in NCTC-AP1 reporter keratinocytes	251
Figure 5.8 Effect of SK inhibitors on AP1-mediated signalling in NCTC-AP1 reporter keratinocytes	256

APPENDIX

Figure S1 MS analysis of dihydroceramide levels in HEK293T cells treated with SKi or ABC294640	317
Figure S2 MS analysis of sphingoid bases levels in HEK293T cells treated with SKi or ABC294640	318
Figure S3 MS analysis of ceramide levels in HEK293T cells treated with SKi or ABC294640.....	319
Figure S4 MS analysis of sphingomyelin levels in HEK293T cells treated with SKi or ABC294640	320
Figure S5 MS analysis of dihydrosphingomyelin levels in HEK293T cells treated with SKi or ABC294640	321
Figure S6 MS analysis of sphingolipid levels in HEK293T cells treated with SK1 siRNA and SKi.....	322
Figure S7 MS analysis of sphingolipid levels in HEK293T cells treated with SK2 siRNA and SKi.....	323

LIST OF TABLES

CHAPTER 1

Table 1.1 <i>Structures and potencies of SK inhibitors</i>	36
--	----

CHAPTER 2

Table 2.1 <i>Pre-stained molecular weight marker standards</i>	87
--	----

ABBREVIATIONS

3-KSR, 3-keto-sphinganine reductase; 3KdhSph, 3-keto-dihydrosphingosine; ABC, ATP binding cassette; ABC294640, 3-(4-chlorophenyl)-adamantane-1-carboxylic acid (pyridin-4-ylmethyl)amide; AC, adenylyl cyclase; AKAPs, A-kinase anchoring proteins; AML, acute myeloid leukemia; ANP32A, acidic leucine-rich nuclear phosphoprotein-32A; AP-1, activator protein-1; APS, ammonium persulfate; ASK-1, apoptosis signal regulating kinase 1; ATF4, activating transcription factor 4; ATF6, activating transcription factor 6; Atg5, autophagy related 5; BAFF, B-cell-activating factor of the TNF family; BCL-3, B-cell lymphoma 3; BiP, binding Ig protein; BMS345541, N¹-(1,8-dimethylimidazo[1,2-a]quinoxalin-4-yl)-1,2-ethanediamine; BSA, bovine serum albumin; bZIP, basic leucine-zipper; C/EBP, CCAAT-enhancer-binding protein; C16 dhCer, N-hexadecanoyldihydrosphingosine; C1P, ceramide-1-phosphate; Ca²⁺, calcium; CD11b⁺, cluster of differentiation 11b; CD3⁺, cluster of differentiation 3; CDase, ceramidase; Cer, ceramide; CERK, ceramide kinase; CerS, ceramide synthase; CERT, ceramide transfer protein; CHK1, cell cycle kinase; CHOP, C/EBP homologous protein; cIAP2, cellular inhibitor of apoptosis protein 2; CK2, casein kinase II; CKII, casein kinase II; COPD, chronic obstructive pulmonary disease; COX-2, cyclooxygenase-2; CPTP, C1P-specific transfer protein; CXCL1, C-X-C motif chemokine ligand 1; CXCL2, C-X-C motif chemokine ligand 2; D-MAPP, dimethylallyl diphosphate; DBD, DNA-binding domain; Degs1, dihydroceramide desaturase; dh-GluCer, dihydroglucosylceramide; dhCer, dihydroceramide; dhCerS, dihydroceramide synthase; dhS1P, dihydrosphingosine-1-phosphate; dhSM, dihydrosphingomyelin; dhSph, dihydrosphingosine; DTT, dithiothreitol; DUB, Deubiquitination; E1, ubiquitin-activating enzyme; E2, ubiquitin-conjugating enzyme; E3, ubiquitin ligase; EAE, experimental autoimmune encephalomyelitis; EBV, Epstein-Barr virus; ECL, enhanced chemiluminescence; EDEM, ER degradation-enhancing α -mannosidase-like protein; EGF, epidermal growth factor; ER, endoplasmic reticulum; ERAD, ER-associated degradation; ERK1/2, extracellular signal-regulated kinases 1 and 2; ERSE, ER stress response element; ER α , estrogen receptor α ; FAPP2, four-phosphate adaptor protein 2; FB1, Fumonisin B1; FTY720, 2-amino-2-[2-(4-octylphenyl)ethyl]propane-1,3-diol; GCase, glycosidase; GluCer, glucosylceramide; GPCRs, G-protein coupled

receptors; GPT, glutamate pyruvate transaminases; GSL, glycosphingolipids; GTPase, guanosine triphosphatase; GWAS, genome-wide association studies; HCC, hepatocellular carcinoma; HDAC1/2, histone deacetylases 1 and 2; HDAC3, histone deacetylase 3; HLH, helix-loop-helix; HRP, horseradish peroxidase; IBD, inflammatory bowel disease; IFN- γ , interferon gamma; IKK, I κ B kinase; IL-1, Interleukin-1; IL-12, Interleukin-12; IP3R, inositol 1,4,5-trisphosphate receptor; IRE1, inositol requiring 1; IRF1, interferon-regulatory factor 1; I κ B, Inhibitor of NF- κ B; JNK, c-JUN N-terminal kinase; K145, 3-(2-amino-ethyl)-5-[3-(4-butoxyphenyl)-propylidene]-thiazolidine-2,4-dione; K_i, competitive inhibition constant; K_{iu}, uncompetitive inhibition constant; LMP, latent membrane protein; LPA, lysophosphatidic acid; LPP, lipid phosphate phosphatase; LPS, lipopolysaccharide; Lyso-PI, lysophosphatidylinositol; Lyso-SM, lysosphingomyelin; LZ, leucine-zipper; MAPK, mitogen activated protein kinase; MAPKK, MAPK kinase; MAPKKK, MAPK kinase kinase; MFsd2b, major facilitator superfamily domain containing 2B; MG132, carbobenzoxy-Leu-Leu-leucinal; MHP, (S)-methyl 2-(hexanamide)-3-(4-hydroxyphenyl) propanoate; MS, multiple sclerosis; NAC, N-acetyl-L-cysteine; NF- κ B, nuclear factor kappa B; NIK, NF- κ B-inducing kinase; NLS, nuclear localisation sequence; ODN, oligodeoxynucleotide; ORMDL, orosomucoid-like; p53BS, p53 binding site; PARP, poly (ADP-ribose) polymerase; PBS, phosphate-buffered saline; PDGF, platelet-derived growth factor; PDI, protein disulfide isomerase; PDPK1, 3-phosphoinositide-dependent protein kinase 1; PERK, protein kinase r-like endoplasmic reticulum kinase; PHA, phytohemagglutinin; PHB2, prohibitin 2; PI3K, phosphatidylinositol 3-kinase; PKB, protein kinase B; PKC, protein kinase C; PLA, phospholipase A; PLC, phospholipase C; PMA, Phorbol 12-Myristate 13-Acetate; PTMs, post-translational modifications; RA, rheumatoid arthritis; RANTES, regulated on activation normal T cell expressed and secreted; REs, response elements; RHD, Rel homology domain; RIP, ring-finger interacting protein; RIP1, Receptor interacting protein 1; RNAi, ribonucleic acid interference; ROCK, rho-associated kinase; ROME, (R)-FTY720-methyl ether; ROS, reactive oxygen species; RSK2, ribosomal S6 kinase 2; S1P, sphingosine 1-phosphate; S1P₁₋₅, sphingosine 1-phosphate receptors 1 to 5 receptors; S1PP, S1P phosphatase; SAPKs, stress-activated protein kinases; SB203580, 4-(4-Fluorophenyl)-2-(4-

methylsulfanylphenyl)-5-(4-pyridyl)1H-imidazole; SDK1, sphingosine-dependent protein kinase; SEM, standard error margin; SK1, sphingosine kinase 1; SK2, sphingosine kinase 2; SKi, 2-(p-hydroxyanilino)-4-(p-chlorophenyl) thiazole; SM, sphingomyelin; SMase, sphingomyelinases; SMS, sphingomyelin synthase; SOCS3, suppressor of cytokine signalling; SP600125, Anthra(1,9-cd)pyrazol-6(2H)-one, 1,9-Pyrazoloanthrone; Sph, sphingosine; SPL, S1P lyase; SPNS2, spinster homologue protein 2; SPT, serine palmitoyl transferase; TA, transactivation; TAD, transactivation domain; TCA, trichloroacetic acid; TEMED, tetramethylethylenediamine; TGFb, transforming growth factor b; Th1 cells, T helper cell type 2; TLRs, toll-like receptors; TNBC, triple-negative breast cancer; TNF- α , tumour necrosis factor alpha; TPA, tumour-promoting agent; TRADD, TNF receptor-associated death domain; TRAF-2, TNF receptor-associated factor 2; TRE, TPA-response element; TRITC, tetramethyl rhodamine isothiocyanate; Ub, ubiquitin; UBP, ubiquitin-binding protein; UC, ulcerative colitis; ULK1, Unc-51-like autophagy-activating kinase 1; UPR, unfolded protein response; UPRE, UPR element; UPS, ubiquitin-proteasome system; UV, ultraviolet; VEGF, vascular endothelial growth factor; WT, wild type; XBP-1s, X-box DNA-binding protein-1s.

PUBLICATIONS AND POSTER PRESENTATIONS

PUBLICATIONS

Alsanafi, M., Kelly, S. L., Jubair, K., McNaughton, M., Tate, R. J., Merrill, A. H., & Pyne, N. J. (2018). Native and polyubiquitinated forms of dihydroceramide desaturase are differentially linked to human embryonic kidney cell survival. *Molecular and Cellular Biology*, 38(23), e00222-18.

Alsanafi, M., Kelly, S. L., McNaughton, M., Merrill Jr, A. H., Pyne, N. J., & Pyne, S. (2020). The regulation of p53, p38 MAPK, JNK and XBP-1s by sphingosine kinases in human embryonic kidney cells. *Biochimica et Biophysica Acta (BBA)-Molecular and Cell Biology of Lipids*, 158631.

POSTER PRESENTATIONS IN CONFERENCES

Alsanafi, M., Pyne, N.J., and Pyne, S. The role of sphingosine-1-phosphate (S1P) in pancreatic β -cells survival and insulin secretion (2016). SIPBS Annual Research Symposium, University of Strathclyde, Glasgow, UK.

Alsanafi, M., Pyne, N.J., and Pyne, S. Sphingosine kinase inhibitors SKi and ABC294640 induce endoplasmic reticulum stress and promote post-translational modification of p53 in human embryonic kidney 293T cells (2017). XII Sphingolipid club meeting, Trabia, Italy.

ABSTRACT

The literature details significant controversy regarding the role of dihydroceramide desaturase (Degs1) in regulating cell survival/apoptosis and therefore this study primarily examined the molecular basis of the reported opposing roles of Degs1. The sphingosine kinase inhibitor SKi [2-(*p*-hydroxyanilino)-4-(*p*-chlorophenyl)thiazole] or the Degs1 inhibitor fenretinide promoted the polyubiquitination of Degs1 (Mr = 40-140 kDa) through a mechanism involving p38 mitogen-activated protein kinase (MAPK), oxidative stress, and Mdm2 (E3 ligase) in HEK293T cells. The polyubiquitinated forms of Degs1 acquire a “gain of function” and activate pro-survival pathways, p38 MAPK/c-Jun N-terminal kinase (JNK), and X-box protein 1s (XBP-1s) in HEK293T cells. In contrast, the sphingosine kinase inhibitor, ABC294640 [3-(4-chlorophenyl)-adamantane-1-carboxylic acid (pyridin-4-ylmethyl)amide] (25 to 50 μ M), did not promote formation of polyubiquitinated Degs1 forms and induced apoptosis of HEK293T cells via a mechanism involving native Degs1. Native Degs1 appears to function in this context via substrate induction to increase *de novo* synthesis of apoptotic ceramides. These results were achieved using siRNA transfections, western protein analysis of protein expression, immunoprecipitation, [³H]-Thymidine incorporation assay, and mass spectrometry. These novel findings are the first to reveal that the polyubiquitinated forms of Degs1 exhibit opposing function compared with the native form, which could explain the controversy concerning the role of this enzyme in apoptosis *versus* cell survival described within literature.

The study next investigated the role of sphingosine kinases (SK1, SK2) in regulating p53, stress activated protein kinases, and XBP-1s in HEK293T cells since SK inhibitors are known to promote p53-dependent cell death. SKi stimulated polyubiquitination of p53 to form two higher molecular mass proteins (63 and 90 kDa), which might represent inactive forms of p53. The formation of p63/p90 in response to SKi was enhanced by completely eliminating SK1 from HEK293T cells using a combination of SK1 siRNA and SKi. In addition, sphingolipid measurements showed a decrease in the levels of S1P and increase in the levels of

sphingosine under these conditions. However, SK2 or Degs1 had no role in regulating the formation of p63/p90. In addition, the complete elimination of SK1 enhanced the activation of p38 MAPK/JNK pro-survival pathways in response to SKi. Taken together with the effect on p53, these findings suggest that SK1 opposes pro-survival signalling pathways in HEK293T cells. The proteasome inhibitor, MG132 also induced expression of the pro-survival protein XBP-1s and this was enhanced when HEK293T cells were treated with SKi. SK2 siRNA reduced XBP-1s levels in response to MG132/SKi while p53 siRNA promoted this effect. These findings were achieved using siRNA and transient plasmid transfections, western protein analysis of protein expression, immunoprecipitation, [³H]-Thymidine incorporation assay, mass spectrometry, and immunofluorescence microscopy which suggest that SK2 opposes the death promoting function of p53.

Lastly, the role of SK1 and SK2 in regulating inflammation-based transcriptional factors in keratinocytes was investigated using western protein analysis of protein expression and luciferase reporter assays. SK2 inhibitors, such as ABC294640 or SKi or K145 or (R)-methylether FTY720 (ROME) were shown to reverse the degradation of inhibitor kappa B (IκB) and transcriptional regulation of nuclear factor kappa B (NF-κB) in response to TNFα. In contrast, the potent SK1 inhibitor, PF-543 did not reverse IκB degradation and only weakly inhibited transcriptional regulation of NF-κB at a concentration that is 50-fold higher than the K_i for inhibition of SK1 activity. Thus SK2 and not SK1 is proposed to regulate NF-κB signalling and transcription. The effect of the sphingosine kinases on transcriptional regulation of Activator Protein-1 (AP-1) was also investigated. SK2 inhibitors, ABC294640 or K145 reduced phorbol myristate acetate (PMA) stimulated phosphorylation of JNK and ERK-1/2 and transcriptional activity of AP-1. In contrast, other SK inhibitors including PF-543, SKi and ROME did not inhibit JNK and ERK-1/2 signalling and only produced a minimal reduction in AP-1 transcriptional activity, thereby suggesting that the effects of SK2 inhibitors on JNK/ERK signalling and AP-1 transcriptional activity are likely to be ‘off-target’.

These novel significant findings provide improved understanding of the role of Degr1, SK1 and SK2 in regulating cell survival and inflammation and this might ultimately aid in the identification of novel signalling networks and therapeutic targets for treatment of various diseases, including cancer.

CHAPTER 1:
GENERAL INRODUCTION

CHAPTER1: GENERAL INRODUCTION

1.1 Sphingolipids synthesis and metabolism

Sphingolipids comprise a class of lipids commonly found in cell membranes characterised by sphingoid backbones of 18-carbon amino-alcohol that are synthesised from non-sphingolipid precursors in the endoplasmic reticulum (ER) (Gault *et al.*, 2010). Changes of this basic structure give rise to the sphingolipids family, including sphingomyelin (SM), dihydrosphingomyelin (dhSM), lysosphingomyelin (Lyso-SM), ceramide (Cer), dihydroceramide (dhCer), sphingosine (Sph), sphingosine-1-phosphate (S1P), and ceramide-1-phosphate (C1P). Sphingolipids are an essential component of eukaryotes' cellular membranes and several of them function as regulatory signalling molecules involved in cell growth, proliferation, migration, inflammation, angiogenesis, adhesion, differentiation, intracellular trafficking, survival, and cell death in health and disease (Hannun and Obeid, 2008).

Sphingolipid metabolism involves a complex interconnected network of reversible reactions catalysed through different enzymes, and there is often more than one route to the generation and breakdown of each molecule (Gault *et al.*, 2010). Despite this, sphingolipids have a sole metabolic entry point (serine palmitoyl transferase; SPT) that forms the first sphingolipid in the *de novo* pathway, and they meet on a sole exit point (S1P lyase (SPL), that breaks S1P down into non-lipid precursors) (Gault *et al.*, 2010; Hannun and Obeid, 2008). The main sphingolipid, sphingomyelin (SM), is formed by transfer of the phosphocholine headgroup from phosphatidylcholine to Cer, catalysed by the enzyme sphingomyelin synthase (SMS). SM is hydrolysed by a

family of sphingomyelinases (SMase) into Cer due to many stresses (i.e., cytotoxic agents, UV irradiation, and pathogens) or the stimulation of particular receptors (e.g., interferon gamma [IFN- γ], tumour necrosis factor alpha [TNF α], and interleukin-1 [IL-1]) (Pyne and Pyne, 2011). In this complex network, Cer (and, to a lesser degree, dihydroceramide) is considered the main centre of sphingolipid biosynthesis and metabolism (Hannun and Obeid, 2008).

Cer can be synthesised through two different metabolic pathways: the *de novo* and salvage pathways. The *de novo* pathway occurs on the cytoplasmic surface of the endoplasmic reticulum (ER) and starts with the condensation of serine and palmitoyl CoA catalysed through the enzyme serine palmitoyltransferase (SPT), the rate-limiting step, to form 3-keto-dihydrosphingosine (3KdhSph), known as 3-keto-sphinganine (Merrill, 2002). SPT is a heterotrimeric complex negatively regulated by orosomucoid-like (ORMDL) proteins (Breslow *et al.*, 2010). Interestingly, a genetic variant that raises ORMDL3 expression has been related through genome-wide association studies (GWAS) with increasing susceptibility to the development of childhood asthma (Han *et al.*, 2009). Next, two rapid enzymatic reactions occur: first, 3KdhSph is reduced into dihydrosphingosine (dhSph), also called sphinganine, catalysed by the enzyme 3-keto-sphinganine reductase (3-KSR) in a NADH-dependent reaction; and second, dhSph is converted into dhCer through N-acylation by the enzyme dihydroceramide synthase. This enzyme uses different chain lengths of fatty acyl CoAs to produce multiple dihydroceramide species (and subsequently Cers with different chain lengths depending on the acyl CoA used). Finally, dhCer is converted to Cer catalysed by the enzyme dihydroceramide desaturase (Degs1)

(thereby producing a *trans* 4,5-double bond). Cer and dhCer are transported from the ER to the Golgi apparatus through either vesicular trafficking or a non-vesicular transport through Cer transfer protein (CERT) (a cytoplasmic protein that contains a phosphatidylinositol-4-phosphate-binding domain and a putative catalytic lipid transfer domain) (Hanada *et al.*, 2003). Once Cer and dhCer are in the Golgi apparatus, they are used to form SM and dhSM respectively, through the action of the enzyme sphingomyelin synthase (SMS) on the luminal side of the Golgi. Alternatively, glucosylceramide (GluCer) and dihydroglucosylceramide (dh-GluCer) are formed through the action of the enzyme glucosylceramide synthase (GCerS) on the cytosolic surface of the Golgi apparatus (Van Meer and Holthuis, 2000). After the translocation of GluCers into the Golgi lumen through four-phosphate adaptor protein 2 (FAPP2), they are further converted into lactosylceramides and other more complex glycosphingolipids (GSL), essential components of eukaryotic cell membranes involved in the regulation of cell differentiation, growth and neoplastic transformation (Spiegel and Milstien, 2003).

Cer can also be formed through the salvage pathway, a less energy-consuming route than the *de novo* pathway of Cer synthesis. In the salvage pathway, Cer is synthesised by re-acylation of Sph that has been formed by sphingomyelin hydrolysis to Cer, catalysed by the enzyme sphingomyelinase (SMase), and Cer deacylation. Cer can also be phosphorylated by ceramide kinase (CERK) to produce ceramide 1-phosphate (C1P). Finally, SM and GSLs are transported to the plasma membrane by vesicular transport and C1P by a C1P-specific transfer protein (CPTP) (Kolesnick and Hemer, 1990).

The sphingoid base Sph is not synthesised *de novo*; the only pathway known to generate Sph is through the deacylation of Cer catalysed by ceramidase (CDase) (Hannun and Obeid, 2008). This can be from the degradation of plasma membrane SM and glycosphingolipids (via Cer) in the endocytic recycling pathway, which is called the salvage pathway. At the ER, Sph and dhSph can be phosphorylated by sphingosine kinase 1, SK1, to form S1P and dihydro-S1P, respectively (Hait *et al.*, 2006; Pitson, 2011b; Pyne and Pyne, 2011). Subsequently, dephosphorylation of S1P to Sph is catalysed by either S1P phosphatases (S1PP) or lipid phosphate phosphatases (LPP); alternatively, S1P can be irreversibly converted to hexadecenal and phosphoethanolamine by S1P lyase (SPL) (Pyne and Pyne, 2011; Fyrst and Saba, 2010). Additionally, a second isoform of sphingosine kinase, SK2, shuttles between the cytoplasm and the nucleus (Wattenberg, 2010). S1P produced in the nucleus by SK2 inhibits histone deacetylases (HDAC) signalling and thereby exerts epigenetic regulation (Hait *et al.*, 2009). Membrane sphingolipids are internalised through the endocytic pathway and degraded in the lysosome via acidic forms of SMase, glycosidase (GCase) and CDase (Maceyka and Spiegel, 2014). The sphingolipids' biosynthesis and metabolism is illustrated in Figure 1.1.

1.2 Sphingolipid rheostat

The 'sphingolipid rheostat' was first proposed in 1996 to connect several findings that demonstrate the ability of Cer and S1P to regulate cell survival and growth by modulating opposing signalling pathways (Cuvillier *et al.*, 1996; Pyne *et al.*, 1996). This concept was established according to the findings that higher levels of Cer induce apoptosis and cell growth arrest (Obeid *et al.*, 1993) whereas S1P production promotes proliferation in response to growth factors (Olivera and Spiegel, 1993) while also suppressing Cer-mediated apoptosis (Cuvillier *et al.*, 1996). Moreover, these sphingolipids were shown to have differential effects upon protein kinase cascades that regulate cell fate, such as ERK-1/2 and JNK (Pyne *et al.*, 1996). Although many enzymes are involved in the regulation of the sphingolipid rheostat, SKs are proposed to play a critical role in reducing the intracellular levels of pro-apoptotic Cer/Sph while concurrently increasing pro-survival S1P levels (Spiegel and Milstien, 2003). Indeed, many studies have provided evidence that SK1 is a major regulator of cell fate that correlates inversely with intracellular Cer amounts in various cellular systems (Olivera *et al.*, 1999; French *et al.*, 2003; Maceyka *et al.*, 2005; Nava *et al.*, 2002; Taha *et al.*, 2006b; Gault and Obeid, 2011). S1P, Cer, and Sph play roles in the aetiologies of several human diseases, including cancer, by affecting biological programmes and cellular responses (Newton *et al.*, 2015). Many studies have aimed to clarify the signalling pathways and molecular mechanisms by which these sphingolipids exert their effects as well as how the balance of S1P/Cer is controlled in order to direct cells to specific pathways. This may provide new strategies to produce therapeutics for specific diseases, such as cancers and cardiovascular and metabolic disorders.

Therefore, the sphingolipid rheostat is considered to be a sensing mechanism to coordinately regulate cellular fate by the inter-conversion of S1P, Sph, and Cer (Newton *et al.*, 2015). Changes in the regulation of the S1P-to-Cer ratio could result in an imbalance of the sphingolipid rheostat as shown in Figure 1.2 (Fyrst and Saba, 2010). However, the sphingolipid rheostat is only one of many factors that contribute to cellular fate.

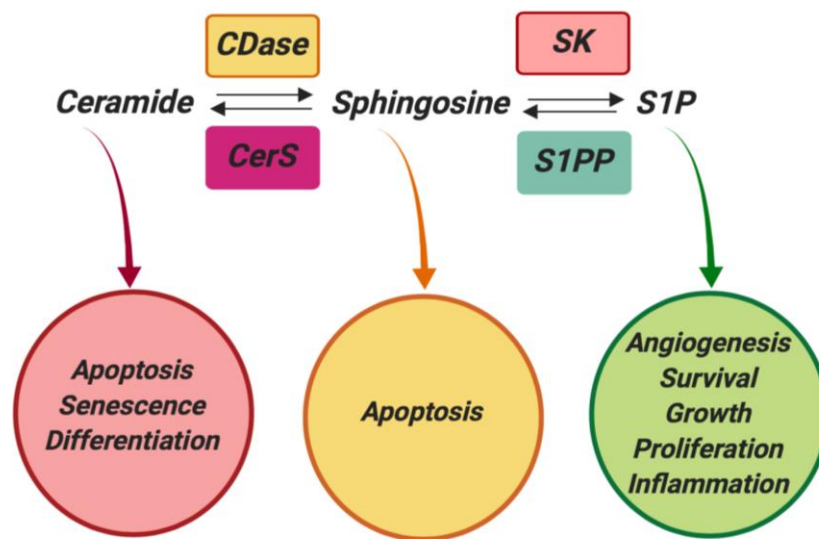


Figure 1.2 The sphingolipid rheostat. Cer has been linked with apoptosis, senescence, or differentiation. Sph also exhibits pro-apoptotic properties whereas S1P promotes cellular growth, survival, and proliferation. The sphingolipid rheostat functions to regulate the levels of sphingolipid metabolites through interconversion of the pro-apoptotic sphingolipids Cer and Sph and the proliferative sphingosine-1-phosphate (S1P) in order to control cell fate [Adapted from (Gault and Obeid, 2011)]. CDase, ceramidase; CerS, ceramide synthase; S1P, sphingosine 1-phosphate; S1PP, S1P phosphatases; SK, sphingosine kinase.

Importantly, the effects of sphingolipids on cellular fate are modulated by their cellular import/export, subcellular localisation, receptor or other protein target expression, and protein carrier binding. Indeed, in certain cases, it is difficult to determine how sphingolipids will affect cell behaviour. For example, opposing

signals derived from different pathways may be stimulated by different S1P receptor subtypes. Additionally, tissue gradients of S1P can be produced by the opposite actions of SK and SPL. Moreover, as an extension of the rheostat concept, it has also been suggested that ceramide kinase (CERK) plays a critical role in regulating the balance between Cer and C1P (Fyrst and Saba, 2010; Chalfant and Spiegel, 2005). Therefore, the multidimensional “sphingodynamics” model has been utilised to represent the intricacy of sphingolipid-mediated biology, as shown in Figure 1.3 (Fyrst and Saba, 2010).

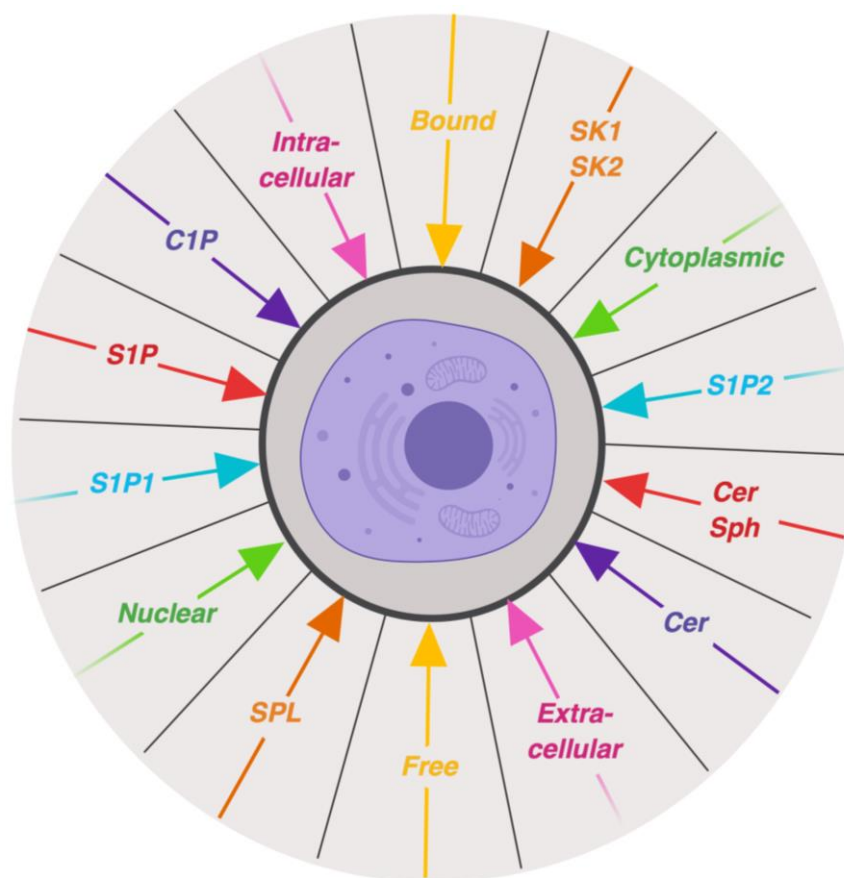


Figure 1.3 Sphingodynamics. A sphingodynamics model illustrates the complexity of factors affecting cellular outcomes mediated by bioactive sphingolipids [Adapted from (Fyrst and Saba, 2010)]. C1P, ceramide-1-phosphate; Cer, ceramide; S1P, sphingosine 1-phosphate; S1P1, sphingosine 1-phosphate receptor 1; S1P2, sphingosine 1-phosphate receptor 2; SK1, sphingosine kinase 1; SK2, sphingosine kinase 2; Sph, sphingosine; SPL, S1P lyase.

1.3 Sphingolipid metabolites

1.3.1 Sphingomyelin (SM) and dihydrosphingomyelin (dhSM)

SM is a lipid discovered and named by Johann L.W. Thudicum in the 1880s when he first isolated it from brain tissue (Thudicum, 1884). Pick and Bielschowsky determined the structure of SM to be N-acyl-sphingosine-1-phosphorylcholine (Pick and Bielschowsky, 1927). SM is produced by the SM synthase (SMS) enzymes that convert Cer and phosphatidylcholine into SM and diacylglycerol. SMS1 is mainly found in the trans-Golgi membranes whereas SMS2 is localised in the plasma membrane and concentrated structures in the Golgi complex (Huitema *et al.*, 2004; Hayashi *et al.*, 2014). Moreover, a SMS-related protein localised in ER has been recognised to affect SM homeostasis at the Golgi complex (Vacaru *et al.*, 2009). SMS1 is considered the main producer of bulk cellular SM because SMS1 in the Golgi is proximal to the movement of newly synthesised Cers from the ER (Huitema *et al.*, 2004). SM is an essential class of phospholipids in eukaryotic plasma membranes and key components of sphingolipid domains (Abe and Kobayashi, 2014; Frisz *et al.*, 2013; Kishimoto *et al.*, 2016) and cholesterol-dependent raft domains (Sezgin *et al.*, 2012; Lin and London, 2015; Lingwood and Simons, 2010). For example, SM is essential in the formation of raft-based FAS-associated signalling clusters that lead to cell apoptosis (Miyaji *et al.*, 2005). The rafts are considered critical in lipid and protein transport and sorting as well as in numerous signalling networks (Simons and Ikonen, 1997). In most mammalian tissues, SM content ranges from 2% to 15% of total organ phospholipids, although even greater levels are found in the brain, peripheral nerve tissue, ocular lenses, and erythrocytes

(Koval and Pagano, 1991; Talbott *et al.*, 2000). Meanwhile, dhSM accounts for almost 50% of all phospholipids in human ocular lens membranes (Byrdwell and Borchman, 1997). In addition to its structural role in membranes, SM and its metabolites contribute to cell signalling cascades related to cell cycle arrest, apoptosis, cell senescence, T-cell receptor signalling, differentiation, lipid transport and many more (Merrill, 2008; Huwiler *et al.*, 2000; Hannun *et al.*, 2001).

1.3.2 Sphingosine (Sph)

Sph is the simplest sphingolipid and is generated by deacylation of Cer, catalysed by a family of ceramidases localised in plasma membrane, lysosomes, mitochondria, and Golgi (Mao and Obeid, 2008; Tani *et al.*, 2007). A family of five ceramidases exists, encoded by five different genes and which have their highest activities in acidic, neutral, and alkaline environments; thus acid ceramidase, neutral ceramidase, and alkaline ceramidases 1–3, respectively (Mao and Obeid, 2008). Several studies have reported that high cellular Sph levels are associated with apoptosis (Cuvillier, 2002). For example, Sweeney *et al.* showed that Sph induced apoptosis of HL-60 cells through the stimulation of caspase (Sweeney *et al.*, 1998). Moreover, the treatment of breast cancer MCF-7 cells with doxorubicin stimulated Sph accumulation along with the production of Cer that led to a release of cytochrome c and the activation of caspase-7 (Cuvillier *et al.*, 2001). In certain cell lines, the induction of cell death by exogenous Sph was inhibited by the alkaline ceramidase inhibitor, dimethylallyl diphosphate (D-MAPP), and by the ceramide synthase inhibitor, fumonisin B1 (FB1). Therefore, it was proposed that exogenous Sph could

first be acetylated to Cer and then deacetylated to Sph to promote apoptosis (Cuvillier *et al.*, 2001).

Sph has been shown to inhibit the activity of the mitogen activated protein kinases (MAPKs), ERK-1/2 and concurrently stimulate stress-activated protein kinases (SAPKs) including JNK and p38 in various cell types (Ruvolo, 2003; Cuvillier, 2002). The imbalance of MAPKs and SAPKs has also been shown to induce cell apoptosis as a result of growth factor withdrawal (Xia *et al.*, 1995). The time course of MAPK inhibition and SAPK activation induced by Sph is consistent with the time course of Sph accumulation, however, the effect of Sph on MAPK activation has been demonstrated in *in vitro* studies to be in-direct effect (Sakakura *et al.*, 1997) suggesting that Sph acts upstream of ERKs in de-activating the MAPK pathway. Sph-induced apoptosis has been shown to be through the mitochondrial pathway. For example, cells treated with Sph have been associated with down-regulation of the PI3K-Akt pathway, resulting in de-phosphorylation of Bad and stimulation of mitochondrial apoptotic pathways (Siskind, 2005). Over-expression of active-Akt has been shown to partially counteract Sph apoptotic activity (Cuvillier, 2002). Whereas, over-expression of Bcl-2 has a protective effect against Sph-apoptosis through opposing permeabilisation of Sph on mitochondrial outer membrane, an essential step in the induction of apoptosis (Patwardhan *et al.*, 2016). In contrast, Sph has direct effects on signalling kinases such as inhibiting protein kinase C (PKC) (Smith *et al.*, 2000) and calmodulin-dependent kinases (Cuvillier, 2002), whereas stimulating signalling of the epidermal growth factor receptor (EGFR) (Davis *et al.*, 1988), casein kinase II (CKII) (McDonald *et al.*, 1991), p21-activated kinase 1

(Bokoch *et al.*, 1998), and 3-phosphoinositide-dependent protein kinase 1 (PDPK1) (King *et al.*, 2000). Thus Sph can positively and negatively affect kinase activities without being restricted to membrane fractions, making it an ideal second messenger. Due to the complexity of Sph signalling, investigators have taken more universal approaches to distinguish effectors involved. Two different research groups characterised kinase activities which are directly activated by Sph in Jurkat (MYu *et al.*, 1992) and Balb/3T3 cell extracts (Megidish *et al.*, 1998). Megidish *et al.* isolated a kinase activity that specifically phosphorylated members of the 14-3-3 protein family in response to Sph and this was described as a Sph-dependent kinase 1 (SDK1) (Megidish *et al.*, 1998). The 14-3-3 proteins are a family of ubiquitously expressed dimeric phosphoserine binding proteins which regulate functions of vital cellular proteins associated in signalling (Bridges and Moorhead, 2005). The dimeric 14-3-3 molecule is phosphorylated at a site at the interface through SDK1 resulting in disruption of the protein dimeric structure (Woodcock *et al.*, 2003). This finding is important since the dimeric 14-3-3 was shown to protect cells from apoptosis through affecting pro-apoptotic mediators such as Bad, and the SAPK-activating kinase apoptosis signal regulating kinase (ASK-1), while promoting cell survival and proliferation such as enabling the efficient activation of Raf-1 (Xing *et al.*, 2000; Bridges and Moorhead, 2005). Therefore, Sph-induced monomerisation of 14-3-3 protein could promote cell apoptosis via disruption of the anti-apoptotic function of 14-3-3 protein. Thus there is a potential for targeting 14-3-3 protein dimerisation for therapeutic applications through destabilisation of the dimeric 14-3-3 proteins as Woodcock *et al.* provided novel approach to anti-cancer therapeutics (Woodcock *et al.*, 2015). SDK1 has been subsequently identified as the caspase-

cleaved fragment of PKC δ (Hamaguchi *et al.*, 2003), which further emphasised the potential role of this pathway in Sph-induced apoptosis. PKC δ is well-known in promoting apoptosis induced via various DNA damaging agents such as UV radiation and chemotherapeutic agents (Brodie and Blumberg, 2003). Sph has also been shown to activate protein kinase A (PKA), a cAMP-dependent kinase (Ma *et al.*, 2005) and the localisation of PKA to the plasma membrane through A-kinase anchoring proteins (AKAPs) places it in a suitable position to be a front-line effector of Sph signalling (Manni *et al.*, 2008). Moreover, Sph has been shown to interact with acidic leucine-rich nuclear phosphoprotein-32A (ANP32A), which activates PP2A phosphatase resulting in increasing the expression of p38 stress-activated protein kinase (SAPK) and cyclooxygenase (COX)-2 in human endothelial cells (Habrukowich *et al.*, 2010). Recently, Sph has been shown to interact with flotillin proteins which increase recruitment of Sph to cell membranes thereby maintaining cellular S1P levels (Riento *et al.*, 2018).

1.3.3 Ceramide (Cer) and dihydroceramide (dhCer)

Cer is a significant signalling molecule as well as a central metabolic and structural precursor for several other sphingolipids. Cer is involved in cell responses, such as apoptosis, senescence, and cell cycle arrest. Various extracellular agents and stress stimuli, such as environmental stresses, cytokines, TNF α , chemotherapeutic agents, and irradiation, cause Cer accumulation (Hannun and Luberto, 2000). Roles for Cers produced from either *de novo* synthesis and/or the activation of sphingomyelinase in cytochrome c release from mitochondria or the stimulation of apoptosis are firmly established. Roles include effects on members of the Bcl-2 family that regulate

apoptosis (Ruvolo *et al.*, 1999; Lee *et al.*, 2011), the formation of large stable channels in mitochondrial outer membranes (thereby increasing small proteins' permeability) (Siskind and Colombini, 2000; Colombini, 2013), the inhibition of the pro-survival Akt/PKB kinase (Zhou *et al.*, 1998), and the clustering of death receptors within the plasma membrane (Grassmé *et al.*, 2002; Grassmé *et al.*, 2001; Colombini, 2010). In addition, certain functions of Cer are specific to different ceramide chain lengths due to multiple intracellular pools of Cer which can differentially affect cellular fate (Grösch *et al.*, 2012).

In contrast to Cers, dhCers were first considered only as intermediates in Cer biosynthesis, and the conversion of dhCer to Cer was assumed to be a fundamental step for obtaining any biological response. Indeed, many studies stated that the addition of exogenous dhCers did not promote cellular growth arrest or apoptosis (Bielawska *et al.*, 1993; Sugiki *et al.*, 2000). Contrastingly, the concept of dhCer being biologically inactive was opposed when Rodriguez-Cuenca *et al.* proposed that dhCer-mediated effects did not correlate with the functions of Cer (Rodriguez-Cuenca *et al.*, 2015). For example, the specific Dega1 inhibitor XM462 promoted accumulation of dhCer in HCG27 gastric carcinoma cells that resulted in delayed cell cycle G1/S transition, ER stress and autophagy. These effects were recapitulated by addition of short chain dhCers (Gagliostro *et al.*, 2012). The role of dhCer in apoptosis remains controversial. Some studies have linked dhCers to the induction of apoptosis. Thus, inhibitors of dihydroceramide desaturase (Dega1), such as fenretenide and resveratrol, promote apoptosis in transformed cell lines (Signorelli *et al.*, 2009; Erdreich-Epstein *et al.*, 2002; Hail *et al.*, 2006; Delmas *et al.*, 2011). In

contrast, others suggest that dhCers could oppose Cer-induced cell death e.g., Degr1 knockdown in human head and neck squamous carcinoma cells reduced photodynamic therapy-induced apoptosis (Breen *et al.*, 2013). This was accompanied by attenuated mitochondrial depolarization, reduced cell death and late apoptosis together with an increase in the levels of dhCers without affecting the levels of Cers. DhCers disrupt the formation of Cer channels in mitochondria (Stiban *et al.*, 2006), even when dhCer was only 10% of Cer. Thus it was proposed that the proportions of Cers and dhCers could be an important factor in the induction of apoptosis by Cer.

Cer mediates apoptosis through intrinsic (mitochondrial) and extrinsic (receptor-mediated) signalling pathways (Morad and Cabot, 2013). In the intrinsic pathway, chronic stress up-regulates *de novo* Cer synthesis while acute stress produces Cer with a faster route through SM hydrolysis, which then acts on intracellular target proteins to induce apoptosis (Oskouian and Saba, 2010). Cer activates signalling of the tumour suppressor serine/threonine protein phosphatases 2A (PP2A), which either activates pro-apoptotic Bax (Bidère *et al.*, 2003) or in-activates anti-apoptotic Bcl-2 (Xin and Deng, 2006) (members of the Bcl-2 protein family). Thus, these Bcl-2 family proteins, which govern the permeabilisation of the mitochondria outer membrane, are essential downstream mediators of Cer action (von Haefen *et al.*, 2002; Lee *et al.*, 2011). Moreover, Cer activates the protease cathepsin D, which cleaves BID, a member of the Bcl-2 family, resulting in its activation and translocation to the outer mitochondrial membrane, where it can induce apoptosis (Heinrich *et al.*, 2004). In contrast, the extrinsic apoptotic pathway is initiated

through activation of FAS death receptors at the cell surface and through the up-regulation of FAS receptor clusters to enhance FAS ligand binding (Park *et al.*, 2008). Interestingly, cancer cells down-regulate FAS receptor expression as a means of cancer progression and increase resistance to apoptosis (Paschall *et al.*, 2015).

Cer can also induce cell senescence. Venable *et al.* reported that exogenous Cer led to the induction of a senescent phenotype (inhibition of DNA synthesis and mitogenesis) in young WI-38 fibroblasts as well as a 4-fold increase in levels of endogenous Cer in these fibroblasts as they aged (reached replicative senescence) (Venable *et al.*, 1995). Similarly, Venable and Yin reported that Cer could induce senescence in endothelial cells (Venable and Yin, 2009). Cer is also linked to the senescent mediator p53; Dbaibo *et al.* reported that the accumulation of Cer in response to cell stress was dependent on accumulation of p53 (Dbaibo *et al.*, 1998). This was a result of up-regulation of CerS5 involving p53 and consequent C16 Cer accumulation. Various other studies have also reported Cer as an essential downstream mediator of the p53 response (Kim *et al.*, 2002; El-assaad *et al.*, 2003; Villani *et al.*, 2006). In contrast, others report Cer and p53 to be activated concomitantly in response to cellular stress or that cellular accumulation of ceramide occurs irrespective of p53 status (Villani *et al.*, 2006; Deng *et al.*, 2009; Nasr *et al.*, 2005).

Cer can also trigger autophagy by interfering with the activation of Akt/PKB upstream of the mTOR-signalling pathway (Scarlati *et al.*, 2004) and phosphorylation of Bcl-2 when it first dissociates from the Beclin 1:Bcl-2 complex

involving c-Jun N-terminal kinase 1 (JNK1)-mediated signalling (Wei *et al.*, 2008). Autophagy requires the conversion of short-chain Cers (C2-Cer and C6-Cer) into long-chain Cers facilitated by the enzyme ceramide synthase; this was observed when treating cells with tamoxifen or PDMP (an inhibitor of glucosylceramide synthase that converts Cer to glucosylceramide), resulting in higher intracellular levels of long-chain Cers (Pattingre *et al.*, 2009). Interestingly, Cer has previously been shown to interfere with the transport of amino acids at the plasma membrane (Hyde *et al.*, 2005). Following this observation, Guenther *et al.* showed that Cer starve cells by blocking amino acids entry, thereby stimulating autophagy through the down-regulation of nutrient transporters (Guenther *et al.*, 2008). Cers have a higher affinity for the mature autophagosomal protein LC3-II (which is a phosphatidylethanolamine-bound form) rather than LC3-I (which is cytosolic and uncleaved). Cer binding to LC3 involves a central hydrophobic domain that is similar to the CERT structure (Hernández-Corbacho *et al.*, 2017), where Ile35 and Phe52 are required (Sentelle *et al.*, 2012; Jiang and Ogretmen, 2013). Cer may work as a ‘receptor’ to target LC3-II-containing autophagosomes to the mitochondrial membrane. In contrast, the exact mechanism that links dhCer to autophagy is still unclear. However, Siddique *et al.* (2013) showed that knocking down Ddgs1 reduced ATP synthesis in embryonic fibroblasts. This resulted from the diminished activity of the electron transport chain, affecting the ability of one or more dihydrosphingolipids to interrupt the activity of electron transport chain components (Siddique *et al.*, 2013).

Like Cers, there are various molecular species of dhCers with different chain lengths. A full analysis of their specific properties that has yet to be made. Moreover, the specific intracellular targets of dhCer as well as the precise regulation affecting Cer and dhCer balances have yet to be fully defined. The overall abundance of dhCer to Cer would be integrated with the Cer to S1P ratio in two rheostat models (with S1P/Cer regulating the survival/apoptosis axis and dhCer/Cer directing the adaptation/apoptosis axis).

1.3.4 Sphingosine-1-phosphate (S1P)

S1P is a bioactive lipid mediator formed by Sph phosphorylation, catalysed by either SK1 or SK2. S1P has different concentrations depending on compartment, low in intracellular or interstitial fluids, whereas enriched in, lymph and blood creating a steep S1P gradient in the sub-micromolar range (Hla *et al.*, 2008). S1P is maintained at very low nano molar concentrations under normal basal conditions. However, upon receptor stimulation, the concentration of intracellular S1P can rapidly increase due to either high rates of formation by activation of SK or a lower rate of breakdown by S1PPs and SPL (Spiegel and Milstien, 2003). S1P is subject to tight regulation, but dysregulated S1P production can contribute to the pathogenesis of cancers, inflammatory and other diseases (Pyne and Pyne, 2010). S1P has well-established roles in both normal physiology and in pathophysiology. Examples of the effects of S1P at a cellular level are on the promotion of cell proliferation (Zhang *et al.*, 1991), the suppression of apoptosis (Goetzl *et al.*, 1999), the modulation of tumour invasiveness and cell motility (Sadahira *et al.*, 1992), and platelet activation

(Yatomi *et al.*, 1997). At an organismal level, S1P is established as a major regulator of cardiovascular, immune and nervous system functions (Blaho and Hla, 2014).

S1P mediates its effect through both intracellular target proteins and by S1P-specific G protein-coupled receptors (GPCR) activation at the plasma membrane, as shown in Figure 1.5. To date, most reported S1P effects are receptor-mediated (Strub *et al.*, 2010). Receptor-mediated S1P signalling occurs by binding to one of five mammalian S1P-specific G-protein coupled receptors (GPCRs), termed S1P₁–S1P₅ (Chun *et al.*, 2010). Interestingly, S1P receptors are closely related to lysophosphatidic acid and cannabinoid receptors. S1P exhibits low nanomolar affinity and all S1P receptors bind S1P with high affinity to stimulate cellular responses through defined G protein-coupling mechanisms (see Figure 1.4) (Chun *et al.*, 2002). The biological functions of each receptor subtype were identified with the use of receptor-selective antagonists, agonists and murine receptor knockout models, combined with the characterisation of particular receptor expression patterns (Choi *et al.*, 2008; Skoura and Hla, 2009a). S1P can bind to S1PRs in both a paracrine and autocrine manner in a process termed ‘inside-out signalling’ which involves the S1P release from cells to bind and activate S1P receptors (i.e., S1P released into the extracellular milieu) (Takabe *et al.*, 2008). Several transporters of S1P have been discovered, including ATP binding cassette (ABC) transporters ABCC1, ABCA1, and ABCG2 (Nishi *et al.*, 2014), spinster homologue protein 2 (SPNS2) (Kawahara *et al.*, 2009), and major facilitator superfamily transporter 2b (Mfsd2b) (Vu *et al.*, 2017). Alternatively, S1P can be partitioned into a lipid microenvironments that has privileged access to S1P receptors (Takabe *et al.*, 2008). S1P is concentrated in

plasma ($\sim 1 \mu\text{M}$) and mainly carried via the the apolipoprotein ApoM⁺ subfraction of high density lipoproteins HDL ($\sim 65\%$; ApoM⁺HDL) (Christoffersen *et al.*, 2011), with the remainder bound to plasma albumin ($\sim 35\%$) (Hla *et al.*, 2008). These carriers act as biased agonists that control the signalling and levels of S1P in blood (Galvani *et al.*, 2015). Additionally, S1P may move between two transmembrane helices of S1P₁ to access the binding pocket, as suggested by Hanson *et al.* (Hanson *et al.*, 2012b) who crystallised S1P₁, in complex with an antagonist. Recently, S1PRs has been shown to laterally diffuse through the cell membrane in endosomes which can also contain S1P. Then, this S1P is able to mediate ‘intracrine signalling’ to induce intracellular responses (Adada *et al.*, 2015). S1P receptor signalling leads to many physiological functions, including vascular system maturation, modulation of the permeability of blood vessels and pathological angiogenesis (S1P_{1,2}), the regulation of blood pressure, the clearance of histamine, and recovery from anaphylaxis (S1P₂), immune cell egress from tissue compartments (S1P_{1,5}), development of inner ear (S1P₂), pulmonary epithelial integrity (S1P₃), perinatal survival (S1P_{2,3}), hematopoietic, stem cell, and vascular survival as well as cytokine production (S1P_{1,4}) and neuronal functions such as oligodendrocyte survival and axon guidance (S1P₅) (Skoura and Hla, 2009b; Strohlic *et al.*, 2008; Miron *et al.*, 2010; Olivera *et al.*, 2010; Pébay *et al.*, 2005).

The activation of S1P receptors results in their differential coupling to heterotrimeric G-proteins (G_i, G_q, and G_{12/13}) to activate downstream effector enzymes (e.g., small guanosine triphosphatase proteins (GTPase), Ras, Rac, and Rho, extracellular signal-regulated kinase (ERK-1/2), phosphatidylinositol 3-kinase (PI3K), protein kinase B

(PKB/Akt), protein kinase C (PKC), phospholipase C (PLC), adenylyl cyclase (AC)), thereby stimulating cellular responses, including survival, proliferation, migration, and gene expression, as shown in Figure 1.4 (Pyne and Pyne, 2000; Spiegel and Milstien, 2003; Strub *et al.*, 2010). In addition to S1P receptors signalling on their own, they can functionally interact ‘cross-talk’ with growth factors, including the platelet-derived growth factor (PDGF), epidermal growth factor (EGF), transforming growth factor β (TGF β), and vascular endothelial growth factor (VEGF) (Lebman and Spiegel, 2008). For example, a functional PDGF β receptor–S1P₁ receptor signalling complex has been reported in Long *et al.* to enhance PDGF-stimulated migration of mouse embryonic fibroblasts (MEF) (Long *et al.*, 2006). The S1P/S1P₁ axis is necessary for cell migration toward PDGF, as Hobson *et al.* demonstrated that ablating SK1 or S1P₁ blocks PDGF-induced cell motility as it blocks the cross-talk between PDGF and S1P signalling pathways (Hobson *et al.*, 2001). In contrast with S1P₁, S1P₂ inhibits PDGF-induced cell migration (Goparaju *et al.*, 2005). These opposing effects of the two receptor subtypes results in regulation of cell motility.

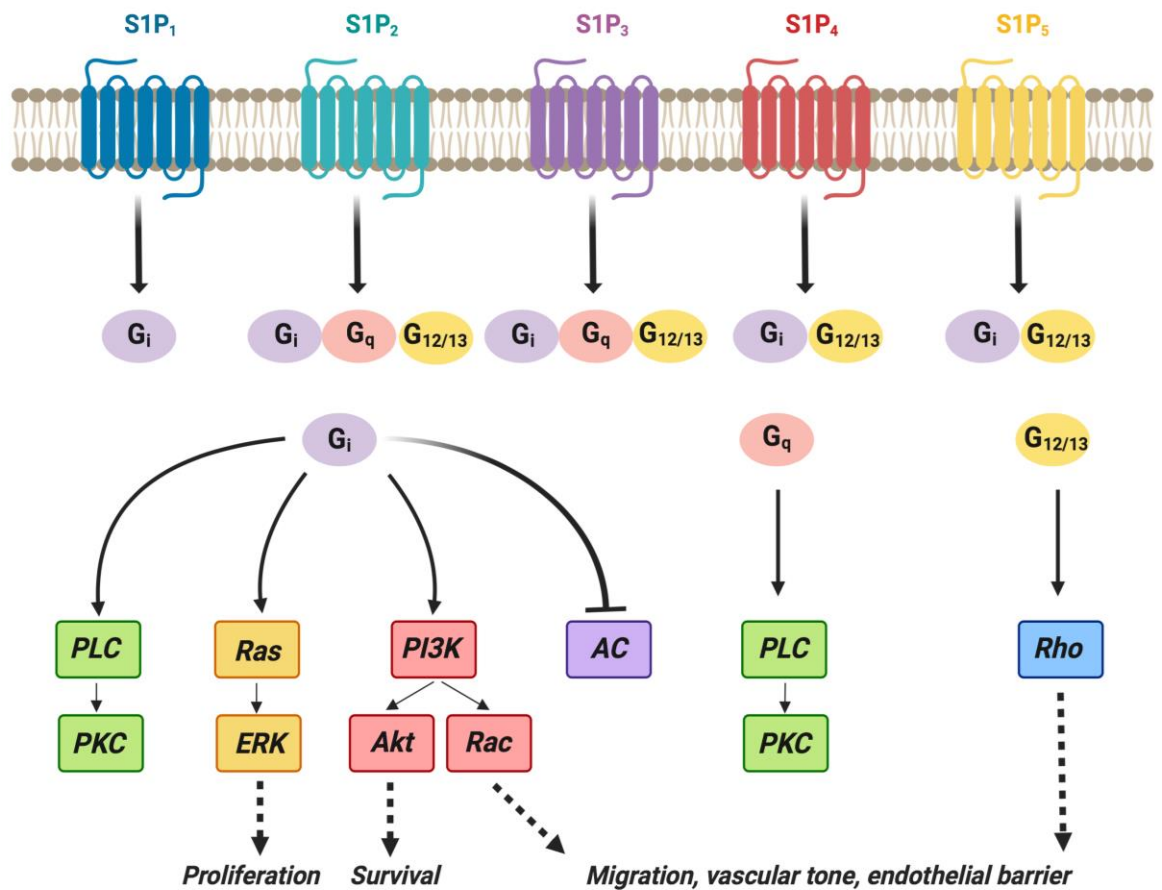


Figure 1.4 S1P receptors, G-protein-coupling and signalling pathways. The differential coupling of S1P receptors to G_i, G_q, and G_{12/13} proteins and their major signalling downstream effectors. Signalling via G_i protein can stimulate 1) activation of Ras and ERK-1/2 to stimulate proliferation; 2) activation of PI3K and PKB/Akt to promote survival and prevent apoptosis; 3) induction of PI3K and Rac to promote migration, induce vasodilation, and enhance endothelial barrier function; and 4) activation of PLC to increase intracellular free calcium [Ca²⁺] and activate PKC that is required for many cellular responses. Moreover, signalling through G_i can inhibit AC thereby preventing cAMP synthesis. Signalling through G_q primarily activates PLC pathways, and signalling through G_{12/13} can promote activation of the small GTPase Rho and the Rho-associated kinase (ROCK) to inhibit migration, reduce function of endothelial barrier and promote vasoconstriction [Adapted from (Brinkmann, 2007)]. AC, adenylyl cyclase; ERK, extracellular signal-regulated kinases; G, G protein; PI3K, phosphatidylinositol 3-kinase; PKC, protein kinase C; PLC, phospholipase C; S1P₁₋₅, sphingosine-1-phosphate receptors 1-5.

Direct intracellular molecular S1P targets have only been recently characterised despite the available evidence of receptor-independent actions and intracellular signalling by S1P (Maceyka *et al.*, 2012). There are various intracellular target proteins of S1P that are differentially regulated by SK1 and SK2, according to SK differential subcellular localisation. For example, intracellular cytoplasmic S1P, derived from SK1, has been shown to be essential for the activity of TNF receptor-associated factor 2 (TRAF2) E3 ubiquitin ligase, which catalyses the Lys63-polyubiquitination of the protein kinase RIP1 (Xia *et al.*, 2002; Alvarez *et al.*, 2010). RIP1 is crucial for the activation of the important pro-inflammatory transcription factor NF- κ B in response to TNF α that regulates cell survival, inflammatory and immune responses (Alvarez *et al.*, 2010). In addition, the interaction of TRAF2 with TRAF-interacting protein (TRIP), which attenuates the activity of TRAF2 E3 ligase and reduces production of pro-inflammatory cytokines, decreases S1P binding to the TRAF2 RING domain (Park *et al.*, 2015). In contrast, others have reported that TRAF2 regulates signalling of TNF and NF- κ B independently of SK1 to suppress apoptosis and skin inflammation in *Sk1*^{-/-} cells (Etemadi *et al.*, 2015). Moreover, nuclear S1P, produced from SK2, has been shown to control epigenetic-mediated gene expression through the inhibition of histone deacetylases 1 and 2 (HDAC1/2), which in turn enhances the transcription of senescence marker p21 and the transcription factor c-FOS (Hait *et al.*, 2009). Nuclear SK2-phosphorylated FTY720 has been shown to similarly inhibit HDAC resulting in suppression of breast cancer development, restoration of oestrogen receptor alpha (ER α) expression, and promotion of therapeutic sensitivity to tamoxifen in mouse models of breast cancer acting independently of S1P receptors (Hait *et al.*, 2015). S1P also interacts with

prohibitin 2 (PHB2), a protein that regulates the assembly and the function of mitochondria. Mitochondrial S1P is mainly derived from SK2 that localises to the inner membrane of mitochondria (Strub *et al.*, 2011). SK2 knockdown has been shown to impair mitochondrial respiration due to defective assembly of the respiratory chain complex (Strub *et al.*, 2011). Moreover, *Sk2*^{-/-} mice are not protected from ischaemic heart injury by preconditioning, comparing to the WT mice, and knockdown of SK2 or PHB2 or cytochrome c oxidase in cardiomyocytes has been shown to similarly abolish cytoprotection (Gomez *et al.*, 2011). These reports suggest that interaction of mitochondrial S1P with PHB2 is essential for regulation of mitochondrial function including assembly of cytochrome-c oxidase, mitochondrial respiration, and cytoprotection. However, others reported that SK2-derived S1P inhibits the translocation of the mitochondrial protein, BAK, which affect mitochondrial outer membrane potential and inhibits cytochrome c release leading to apoptosis (Chipuk *et al.*, 2012). Therefore, the role of mitochondrial S1P could be cell context dependent. Moreover, S1P has been shown to stimulate phospholipase D (PLD) through activation of protein kinase C delta (PKC δ) in human lung adenocarcinoma cells (Meacci *et al.*, 2003). Main intracellular actions of S1P are shown in figure 1.5.

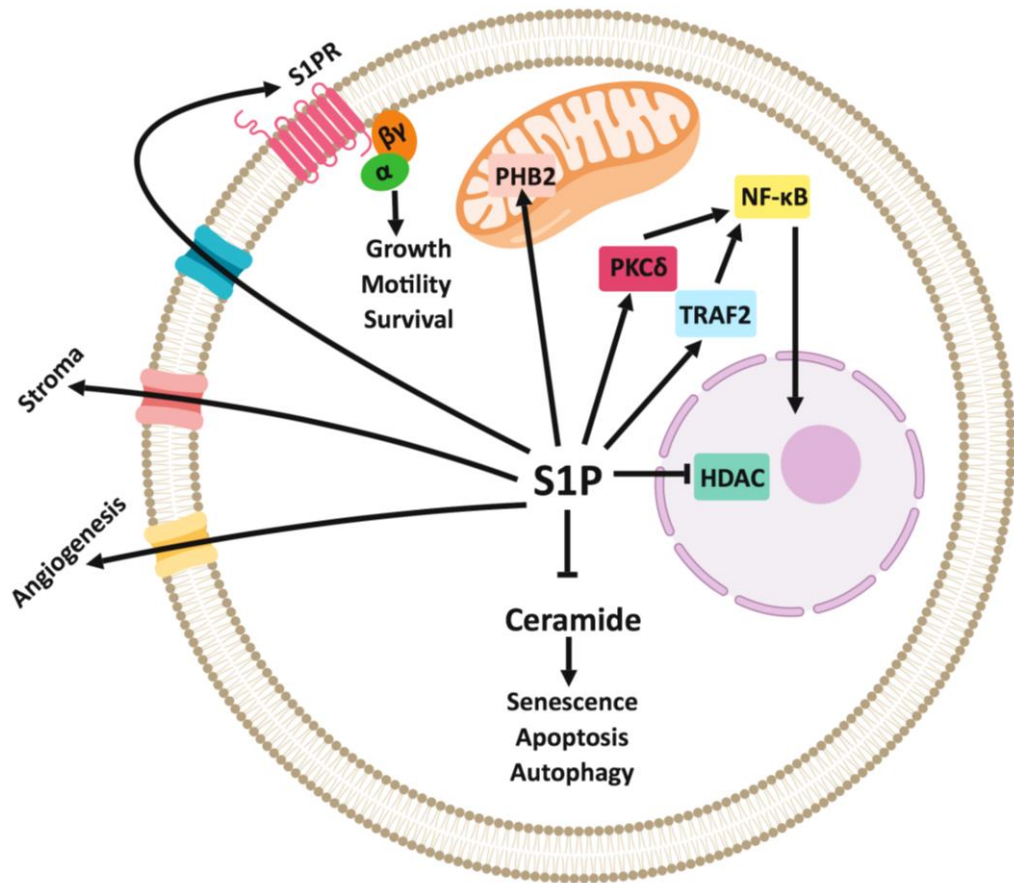


Figure 1.5 Intracellular and extracellular actions of S1P. Intracellular S1P can oppose pro-apoptotic Cer, which is associated with apoptosis, senescence, and autophagy. S1P interacts with intracellular targets (in rectangles) or at S1P-specific GPCR, S1PRs after export to act in an autocrine and/or paracrine manner [Adapted from (Maceyka et al., 2012)]. HDAC, histone deacetylases; NF- κ B, nuclear factor kappa B; PHB2, Prohibitin 2; PKC δ , protein kinase C delta, S1P, sphingosine 1-phosphate; S1PR, sphingosine 1-phosphate receptor; TRAF2, TNF receptor-associated factor 2; α , alpha; β , beta; γ , gamma.

1.4 Sphingolipid metabolising enzymes

Many of the sphingolipid metabolising enzymes, including SMS, SMase, CDase, GCase, GCerS, CerS, S1PP, SPL, SPT and CERK have been introduced to in earlier sections. However, it is beyond the scope of this thesis to discuss all of these in detail, for details refer to the following recent reviews (Lewis *et al.*, 2018; Hannun and Obeid, 2018). In the context of this study, it is appropriate to focus upon dihydroceramide desaturase (Degs1) and the sphingosine kinases (SKs) – see below.

1.4.1 Dihydroceramide desaturase 1 (Degs1)

Two distinct dihydroceramide desaturases, Degs1 and Degs2, catalyse the desaturation of dhCers to Cers, the final step in the *de novo* pathway of Cer synthesis (Ternes *et al.*, 2002). In 1997, Degs1 was first identified as a Δ^4 desaturase, i.e. converting dhCer into Cer through desaturation at the C4 – C5 bond to generate a 4,5 *trans* double bond in the sphingoid moiety (Michel *et al.*, 1997). In contrast, Degs2 has both Δ^4 desaturase and c-4 hydroxylase activities, which control the synthesis of phytoceramides and dhCers, to a lesser extent (Omae *et al.*, 2004a; Omae *et al.*, 2004b). The two enzymes have different tissue distribution profiles. Degs1 is ubiquitously expressed and accounts for the Cer synthesis in most body tissues, especially the liver, kidneys, Harderian gland, and lungs (Omae *et al.*, 2004b; Causeret *et al.*, 2000). Moreover, Degs1 has been shown to play a unique role in spermatogenesis (Endo *et al.*, 1996). Basu and Li reported that lethal alleles of the Degs1 gene, which are associated with the contractile ring in the anaphase and telophase of meiosis in the spermatocyte, lead to male sterility as a result of its protein dysfunction (Basu and Li, 1998). On the other hand, the expression of Degs2

is mainly restricted to the skin, kidneys, and intestines, where phytoceramides are essential (Omae *et al.*, 2004a; Mizutani *et al.*, 2004).

Degs1 is a trans-membrane protein residing in the endoplasmic reticulum (ER) membrane, which contains three conserved histidine-based motifs typical for membrane lipid desaturases and membrane hydrocarbon hydroxylases (Ternes *et al.*, 2002). The active site of Degs1 is likely located at the cytosolic face of the membrane, as deduced from mild proteolytic susceptibility measurements and further predicted by the requirement of cytochrome b5, which is also located at the cytosolic face of the membrane for the reaction (Michel and van Echten-Deckert, 1997; Yamaji and Hanada, 2015). Degs1 has also been shown to have some substrate preferences; with regard to the sphingoid base stereochemistry, *D-erythro*-dihydroceramides are more readily used than *L-threo*-dihydroceramides while there is a preference for C18 > C12 > C8 within the head group. The highest activity of Degs1 is observed with dhCer as a substrate and dhSM to a lesser extent (20%) (Rodriguez-Cuenca *et al.*, 2015).

Degs1 is an emerging important enzyme which regulates essential biological functions, including hypoxia, autophagy, and proliferation, now implicated in the aetiology, diagnosis, and/or treatment of cancer, diabetes, neurodegenerative diseases, and ischemia/reperfusion injury (Siddique *et al.*, 2015). However, it is unclear whether Degs1 is a pro-survival or pro-apoptotic enzyme as there are conflicting results within the literature. Degs1 could act as a stress sensor to protect cells by initiating autophagy or growth arrest/senescence in order to apoptose or

adapt cells (Gagliostro *et al.*, 2012; Hernández-Tiedra *et al.*, 2016). Degr1 is sensitive to thiols (i.e., GSH); thiol accumulation leads to the inhibition of Degr1 that would result in the accumulation of dhCer and the activation of downstream adaptive or protective mechanisms, including the induction of autophagy and/or the delaying of the cell cycle in gastric cancer cells (Gagliostro *et al.*, 2012). This was recapitulated by Siddique *et al.* who showed that Degr1 ablation in mouse embryonic fibroblasts promoted autophagy and inhibited proliferation (Siddique *et al.*, 2013) as well as resistance to chemotherapeutic agents through the activation of defensive pro-survival pathways (Siddique *et al.*, 2012). Moreover, recent studies have suggested that the inhibition of Degr1 and consequent dhCer accumulation might be mainly responsible for the anticancer properties of some SK inhibitors (Aurelio *et al.*, 2016).

Degr1 is also a biosensor for oxidative stress in cells where it requires O₂ and NADPH for its enzymatic function (Fabrias *et al.*, 2012). Degr1 activity is inhibited by oxidative stress, resulting in the accumulation of dhCers in HEK293, A549, MCF7, and SMS-KCNR cells (Idkowiak-Baldys *et al.*, 2010). Similarly, Degr1 acts as an oxygen biosensor in colon and lung cancer cell lines (Devlin *et al.*, 2011). Furthermore, Azzam *et al.* showed that Degr1 mediated adaption to chronic hypoxia cardiomyocytes in a hypoxic mouse heart model, where the accumulation of dhCer with hypoxia caused Degr1 mRNA levels to be down-regulated over time (Azzam *et al.*, 2013). Moreover, the siRNA knockdown of Degr1 in normoxia recapitulated the effects of hypoxia on cell proliferation. On the other hand, the over expression of Degr1 or Degr2 promoted proliferation in hypoxic MCF7 cells (Devlin *et al.*, 2011).

1.4.2 Sphingosine kinases (SKs)

Sphingosine kinases catalyse the ATP-dependent phosphorylation of Sph and dhSph to generate S1P and dihydrosphingosine-1-phosphate (dhS1P), respectively (Kohama *et al.*, 1998; Olivera *et al.*, 1998). There are two mammalian isoforms, SK1 and SK2, which are transcribed from two different genes, *SPHK1* on chromosome 17 (17q25.2) and *SPHK2* on chromosome 19 (19q13.2). They differ in their amino acid sequences, functions, physiological roles, biochemical characteristics, tissue distributions, catalytic properties, and subcellular localisations (Liu *et al.*, 2000; Taha *et al.*, 2006a; Pyne *et al.*, 2016b). Three splice variants of SK1 (SK1a, SK1b, and SK1c) and three splice variants of SK2 (SK2a, SK2b, and SK2c) have been discovered in human cells; these differ in their N-terminal extensions (Pitson, 2011a). SK1 and SK2 share approximately 80% similarity with the amino acid sequence, although SK2 possesses a larger amino acid sequence (383 amino acids for human SK1 versus 618 for human SK2) with two N-terminal and central additional regions (Liu *et al.*, 2000). Five highly conserved regions (C1–C5) are identified in the sequence of all known eukaryotic SKs, with an ATP-binding domain (C2), a catalytic domain (C1–C3), and a sphingosine-binding domain (C4) (Liu *et al.*, 2000; Kohama *et al.*, 1998; Pitson *et al.*, 2002). New insights into the structural features and mechanistic functioning of SK1 have been aided when human SK1 was crystallised by different groups (Wang *et al.*, 2013b; Wang *et al.*, 2014). It is now proposed that SK1 exhibits a dimeric quaternary structure in which it can dimerise through interactions of the N-terminal domain (NTD) of two protomers creating a head-to-head homodimer complex (Adams *et al.*, 2016). Recently, Bayraktar *et al.* used computational analysis to better understand how SK1 might dimerise and

suggested a putative dimerisation interface which overlaps with the proposed mechanism of Adams, Pyne, and Pyne (Bayraktar *et al.*, 2017). Interestingly, a dimerisation through the NTDs of two SK1 protomers allows alignment of the interface, curvature sensing of SK1, and the strengthening of the interaction between SK1 and membranes (Pulkoski-Gross *et al.*, 2018). Similarly, Shen *et al.* proposed that SK1 can sense the negative curvature of membranes (Shen *et al.*, 2014). For example, SK1 activates in the presence of certain anionic phospholipids, such as phosphatidylserine (PS) and phosphatidic acid (PA) (Olivera *et al.*, 1996). This finding is important when considering how SK1 associates with the plasma membrane where a positive charged region at the dimer interface interacts with negative charged lipids on the membrane resulting in opening of a lipid-binding loop (LBL-1) to allow Sph into the catalytic site (Adams *et al.*, 2016). Whereas there is no crystal structure available till date for SK2 to allow for comparisons between the two SKs (Pitson, 2011a; Neubauer and Pitson, 2013).

SK1 is mainly expressed in the spleen, lungs, brain, heart, thymus and immune system whereas SK2 is mostly expressed in the liver and kidneys (Neubauer and Pitson, 2013). Therefore, these enzymes likely have different physiological roles. SK1 is largely located in the cytoplasm and, upon stimulation, can be phosphorylated on Ser225 by ERK1/2 and in turn translocates to the plasma membrane where it is most active (Pitson *et al.*, 2003; Wattenberg, 2010). Currently, three proposed mechanisms that explain translocation of SK1 and interaction with membranes. Two of the mechanisms recognise specific residues that mediate membrane localisation (Stahelin *et al.*, 2005; Shen *et al.*, 2014), whereas the third mechanism explains

localisation of SK1 to be dependent on another protein known as calcium/integrin binding protein 1 (CIB1) (Jarman *et al.*, 2010; Zhu *et al.*, 2017a). Indeed, the protein-protein interaction between SK1 and CIB1 occurs at a hydrophobic site on SK1 that was identified by Stahelin *et al.* for membrane interaction where Thr54 and Asn89 residues were proposed to interact with PS in the membrane (Stahelin *et al.*, 2005). In contrast, Shen *et al.* identified residues that are part of a small hydrophobic patch on SK1 surface and these residues have been implicated to mediate endocytosis and neurotransmission (Shen *et al.*, 2014). Similarly, Pulkoski-Gross *et al.* (2018) showed that SK1 interacts with membrane-associated anionic phospholipids through a single contiguous interface, consisting of an electrostatic site and a hydrophobic site. This describes that SK1 has a multifactorial domain that controls intrinsic binding ability to membranes, which is crucial for proper SK1 function (Pulkoski-Gross *et al.*, 2018). Recently, Zhu *et al.* (2017) showed that calcium and integrin-binding protein 2 (CIB2) negatively regulates SK1 plasma membrane redistribution. Although CIB2 binds SK1 at the same location as CIB1, it lacks the Ca²⁺-myristoyl switch function thus it inhibits the interaction of SK1 at the plasma membrane. This results in inhibition of SK1 oncogenic signalling in ovarian cancer cells *in vitro* while reducing *in vivo* tumour growth (Zhu *et al.*, 2017b). This shows that redistribution of SK1 rather than phosphorylation is responsible for increase of SK activity. Indeed, induction of SK1-related cell growth has been blocked when SK1 translocation to the plasma membrane but not SK1 phosphorylation was blocked (Pitson *et al.*, 2005; Jarman *et al.*, 2010). These studies demonstrate that sub-cellular localisation of SK1 is important for its activation and consequent oncogenic actions. This is due to the fact that the SK1 substrate Sph is

mostly abundant at the plasma membrane and that S1P produced by SK1 at the plasma membrane is in an optimal location for export and subsequent action at S1PRs. Additionally, S1P stimulates ERK1/2 that phosphorylates SK1 which leads to propagation of translocated-SK1 in a positive feedback loop. Moreover, breakdown or de-phosphorylation of S1P by ER bound SPL or S1PP is minimal in relation to S1P formed at the plasma membrane (Gault *et al.*, 2010). Deactivation of SK1 occurs through de-phosphorylation on Ser225 by PPA2, an effector of Cer (Barr *et al.*, 2008). Since PP2A belongs to serine/threonine phosphatases family, it also de-phosphorylates other pro-survival signals including p-Akt, β -catenin, p-ERK1/2, BAD and Bcl-2 (Kuo *et al.*, 2008). In addition, negative regulation of SK1 occurs through degradation with the ubiquitin-proteasomal and lysosomal systems (Ren *et al.*, 2010).

Similarly, SK2 is a cytoplasmic enzyme but has a nuclear export region that can facilitate nuclear-cytoplasmic shuttling (Ding *et al.*, 2007; Wattenberg, 2010). Like SK1, SK2 is activated through ERK1/2-mediated phosphorylation (Hait *et al.*, 2007). SK1 and SK2 differences in sequence and structure likely account for the different kinetic properties (Liu *et al.*, 2000; Pitson, 2011a). For example, human SK2 phosphorylates a wider range of substrates than human SK1, including the Sph analogue FTY720 (Paugh *et al.*, 2003; Billich *et al.*, 2003). Although both enzymes catalyse the same reaction, they may possess opposing functions when co-expressed (Maceyka *et al.*, 2005). Indeed, whereas SK1 mainly promotes cell proliferation and survival (Olivera *et al.*, 1999; Xia *et al.*, 1999), SK2 was reported to be involved in the suppression of cellular growth and activation of apoptosis without the

involvement of S1P receptors (Liu *et al.*, 2003). The opposing effects of SK1 and SK2 on cell survival were suggested to be due to their different effects on levels of Cer, due to their differing subcellular localisations (Maceyka *et al.*, 2005). However, other evidence supports a pro-survival role for SK2 in some cell types; hence, the down-regulation of SK2 decreased cell proliferation and induced apoptosis both *in vitro* and *in vivo* (Gao and Smith, 2011; Sankala *et al.*, 2007; Weigert *et al.*, 2009). Therefore, although SK1 promotes cell proliferation and survival, the effects of SK2 are more complex and may be localisation-dependent and cell type specific (Maceyka *et al.*, 2005). Interestingly, SK1 and SK2 may play a compensatory role in the absence or down-regulation of one isoforms. As an example, Gao and Smith showed that knocking down SK2 resulted in higher SK1 activity (Gao and Smith, 2011). Moreover, SK1/SK2 double knockout mice die *in utero* due to severe developmental defects in both cardiovascular and central nervous systems whereas SK1 or SK2 single knockout mice appear phenotypically normal (Mizugishi *et al.*, 2005; Allende *et al.*, 2004).

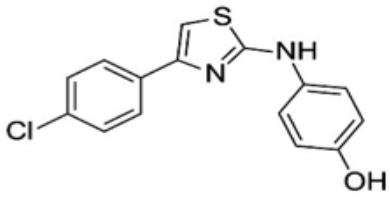
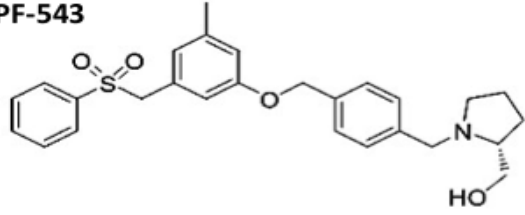
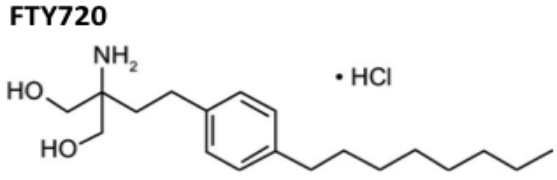
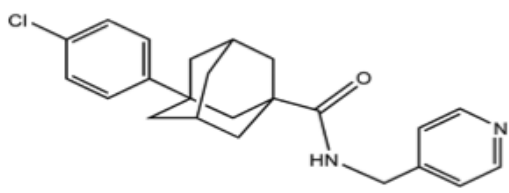
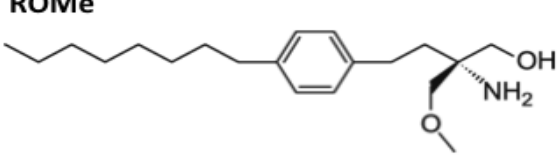
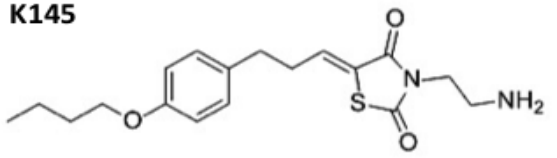
Various stimuli of their cognate receptors can stimulate the activity of both SK1 and SK2, including cytokines such as IL-1 β and TNF α (Mastrandrea *et al.*, 2005), ERK1/2, PKC and growth factors such as EGF (Hait *et al.*, 2005). In the absence of stimuli, both SK isoforms have a basal catalytic function to form 'housekeeping' S1P that sustains physiological levels of Sph and Cer (Chan and Pitson, 2013). Furthermore, SK1 and SK2 may exert non-catalytic activities unrelated to the formation of S1P. For example, Pyne *et al.* found that over-expression of either wild type or a dominant negative mutant form of SK1 inhibited EGF-stimulated ERK-1/2

in breast cancer cells whereas pharmacological inhibition of SK1 failed to exert this effect (Pyne *et al.*, 2009). On the other hand, although the pro-apoptotic function of SK2 is due to its enzymatic activity (Maceyka *et al.*, 2005), SK2-induced apoptosis may also partly be due to its non-catalytic activity through its putative BH3 domain (Liu *et al.*, 2003).

1.5 Sphingosine kinase inhibitors

Sphingosine kinases (SK1/SK2) inhibitors hold potential for the treatment of various diseases, including cancer, vascular disorders, and inflammatory diseases. Inhibiting the SK/S1P pathway reduce S1P and increase pro-apoptotic Cer, inhibits both intra- and extracellular S1P effects, inhibits growth factors and hypoxia-related effects, and sensitises cancer cells to therapeutics (Kunkel *et al.*, 2013). SK inhibitors have been classified into non-selective SK inhibitors, selective SK1 inhibitors, and selective SK2 inhibitors as recently reviewed in details by Pyne *et al.* (Pyne *et al.*, 2018); only the inhibitors used experimentally in this study will be introduced in the following section. A summary of SK inhibitors employed here, with their chemical structures, is provided in Table 1.1.

Table 1.1 Structures and potencies of SK inhibitors. [Adapted from (Gandy and Obeid, 2013; Pitman et al., 2016)].

Type	Name and structure of inhibitors	Ki	
		SK1	SK2
SK1/2-Dual	SKi 	16 μ M	8 μ M
SK1-Selective	PF-543 	4 nM	--
	FTY720 	2 μ M	--
SK2-Selective	ABC294640 	--	10 μ M
	ROME 	--	17 μ M
	K145 	--	6 μ M

1.5.1 Non-selective SK inhibitor [SKI-II inhibitor (SKi)]

SKI-II ([2-(*p*-hydroxyanilino)-4-(*p*-chlorophenyl)thiazole]; also known as SKi) is the first non-lipid small molecule SK inhibitor to be reported; it failed to inhibit extracellular signal-regulated kinase 2 (ERK2), protein kinase C (PKC), and phosphatidylinositol 3-kinase (PI3K) (French *et al.*, 2003). SKi inhibits both SK1 (French *et al.*, 2003) and SK2 (Aurelio *et al.*, 2016) with an IC₅₀ of 35 and 25 μM for SK1 and SK2, respectively, which suggests that it has a slightly higher inhibition potency for SK2 over SK1 (Gao *et al.*, 2012). SKi is a dual SK1/SK2 mixed inhibitor with a competitive inhibition constant (K_i) whose value is 17 μM towards Sph and an uncompetitive inhibition constant (K_{iu}) whose value is 48 μM towards ATP in relation to SK1 (Lim *et al.*, 2012).

SKi has been shown to degrade SK1 that, in turn, reduces cellular S1P levels and inhibits proliferation; in addition, SKi increases cellular levels of Sph and C22:0 Cers, leading to the apoptosis of LNCaP prostate cancer cells (Loveridge *et al.*, 2010). Similar changes in sphingolipids and the induction of apoptosis has been reported in several other cancer cell lines (Gao *et al.*, 2012). SK1 degradation induced by SKi occurs through activation of the ubiquitin proteasomal pathway (Loveridge *et al.*, 2010; Lim *et al.*, 2012), however, in some cell lines, the lysosomal pathway has been implicated (Ren *et al.*, 2010). In addition, Watson *et al.* (2013) reported that SKi induced the proteasomal degradation of the master transcription factor (c-Myc), leading to an indirect antagonism of the Warburg effect. In contrast, the SK2-selective inhibitor, (R)-FTY720-OMe (ROME), was without effect on SK1 or Myc, but did reduce SK2 levels independently of the proteasome (Watson *et al.*,

2013). Recent studies discovered that SKi indirectly inhibits the enzyme Dggs1 through the inhibition of an upstream Dggs1 activator, NADH-cytochrome B5 reductase (Cingolani *et al.*, 2014). Alternatively, SKi could inhibit redox-sensitive Dggs1 through the induction of cellular oxidative stress (McNaughton *et al.*, 2016; Idkowiak-Baldys *et al.*, 2010). Regardless of the mechanism of Dggs1 inhibition, this inhibition leads to a substantial reduction in cellular S1P and an elevation in dihydroceramides (Illuzzi *et al.*, 2010; Loveridge *et al.*, 2010; Cingolani *et al.*, 2014), leading to cell cycle arrest (Siddique *et al.*, 2015). Moreover, Aurelio *et al.* demonstrated that the SKi anticancer activity is mainly due to the inhibition of Dggs1 rather than SK (Aurelio *et al.*, 2016).

SKi has also been shown to stabilise the nuclear factor erythroid 2-related factor 2 (Nrf2) through the de-stabilisation of its negative regulator, Keap1 (Mercado *et al.*, 2014). However, this effect is independent of SK inhibition or changes in levels of Sph/dhSph or S1P/dhS1P and results in cellular protection against oxidative stress. Thus, SKi could play a protective role in diseases that involve oxidative stress, such as neurodegenerative diseases, chronic obstructive pulmonary disease (COPD), and cancer (Barnes, 2015). SKi has also been shown to enhance the efficiency of other anti-cancer agents on different cell lines, such as sensitising glioblastoma cell lines resistant to temozolomide (Noack *et al.*, 2014), chemo-resistant MCF7-TN-R breast cancer cells to doxorubicin (Antoon *et al.*, 2012), head and neck squamous cell carcinoma cell lines to Cetuximab (Schiefner *et al.*, 2014), and MDA-MB-468 breast cancer xenografts to Gefitinib (Martin *et al.*, 2014).

1.5.2 Selective SK1 inhibitors

1.5.2.1 PF-543

PF-543 [(*R*)-(1-(4-((3-methyl-5-(phenylsulfonylmethyl) phenoxy) methyl) benzyl) pyrrolidin-2-yl) methanol] is a potent SK1 selective Sph competitive inhibitor with a K_i of 4 nM. It exhibits 130-fold selectivity for SK1 over SK2, making it the most selective commercially available inhibitor for SK1 with nano-molar potency (Schnute *et al.*, 2012). PF-543 induces proteasomal degradation of SK1, similar to many other Sph-competitive inhibitors, reduces cellular S1P levels, and increases levels of Sph (Byun *et al.*, 2013; Aurelio *et al.*, 2016). However, although PF-543 effectively reduces S1P, it fails to induce apoptosis in a range of cancer cell lines (Schnute *et al.*, 2012; Schrecengost *et al.*, 2015), unless incubated with Sph although an assessment of apoptosis under these conditions was not made (Schnute *et al.*, 2012). PF-543 has been shown to be a potential therapeutic in inflammatory disorders as it reduces S1P levels without leading to apoptosis. Indeed, PF-543 proved to be efficient at blocking sickling, inflammation, and haemolysis in a sickle-cell anaemia mouse model (Zhang *et al.*, 2014), promoted cardio protection in a hypoxic mouse model of pulmonary arterial hypertension (MacRitchie *et al.*, 2016) and reduced cardiac remodelling and dysfunction in a myocardial infarction model (Zhang *et al.*, 2016). In addition, pre-treatment with PF-543 has been shown to reduce inflammatory responses in a cerebral ischemia rat model (Lv *et al.*, 2016). However, PF-543 exacerbated symptoms in the experimental autoimmune encephalomyelitis (EAE) murine model of multiple sclerosis (Pyne *et al.*, 2016a).

1.5.2.2 FTY720

FTY720 [2-amino-2-[2-(4-octylphenyl) ethyl] propane-1,3-diol], known as Fingolimod or the trade name Gilenya™ is a Sph analogue derived from the immunosuppressive natural product ISP-I (myriocin) (Adachi and Chiba, 2007). FTY720 is a SK1 Sph competitive inhibitor with a K_i of $\sim 2 \mu\text{M}$ that induces proteasomal degradation of the SK1a splice variant (Lim *et al.*, 2011b). Fingolimod is a pro-drug used clinically to slow the progression and suppress symptoms of multiple sclerosis (MS) (Groves *et al.*, 2013). Indeed, FTY720 is phosphorylated by SK2 to FTY720-phosphate (FTY720-P), which is subsequently released and acts as an agonist at four of the five S1P receptor types (i.e., S1P₁, S1P₃, S1P₄, and S1P₅) (Chun and Hartung, 2010). Chun and Hartung illustrated the primary mode of action of Fingolimod to be as a T-lymphocyte-specific immunosuppressant. This occurs since activation and the subsequent proteasomal degradation of the S1P₁ receptor after ligation by FTY720-P, results in T-cell sequestration to the lymph nodes as they are no longer able to sense the S1P gradient between the lymph nodes and efferent lymph (Chun and Hartung, 2010). Emerging research for over a decade have indicated that Fingolimod can access the central nervous system (CNS) where its active metabolite, FTY720-P, has pleotropic neuroprotective effects in CNS inflammatory disease states. Geffin *et al.* showed that Fingolimod affects expression of neuronal genes in inflammatory viral-infected microenvironments, with the potential for neuroprotective effects (Geffin *et al.*, 2017). Others demonstrated that Fingolimod provides neuroprotection against excitotoxic neuronal cell death *in vitro* through direct action on neuronal S1P₁ receptors that promotes survival of neurons via intracellular pathways (Di Menna *et al.*, 2013). Additionally, the *in vivo* S1P₁-

mediated effects of fingolimod were tested successfully in two Parkinsonian neurodegeneration mouse models (Zhao *et al.*, 2016). Moreover, Fingolimod has been shown to elicit a neuronal gene expression response in rodent neuronal cell cultures, which modulated the morphology of actin-rich neuronal growth cones and promoted *in vitro* neurite growth (Anastasiadou and Knöll, 2016). Furthermore, there is some available evidence in relation to Fingolimod in favor of neurotrophic activity (Groves *et al.*, 2013) and neurorestorative effects (Hemmati *et al.*, 2013) as well as attenuation of β -amyloid peptide accumulation that impairs spatial learning and memory, in Alzheimer's disease rat models (Asle-Rousta *et al.*, 2013). Due to FTY720's clinical success, several pharmaceutical companies have sought to identify FTY720 chemical derivatives that have shown increased specificity and potency. For example, the discovery of Siponimod (BAF312), a selective modulator of S1P₁ and S1P₅ receptors, which exerts anti-inflammatory and neuroprotective effects in secondary progressive MS patients without the FTY720-related cardiovascular side effects (Behrangi *et al.*, 2019).

1.5.3 Selective SK2 inhibitors

1.5.3.1 ABC294640

ABC294640 [3-(4-chlorophenyl)-adamantane-1-carboxylic acid (pyridin-4-ylmethyl)amide] is a non-lipid small molecule analogue of SKi reported to selectively inhibit SK2 with a K_i of ~ 10 μ M with respect to Sph; it was shown to have dose-dependent antitumor activity in *in vivo* mice studies (French *et al.*, 2010). ABC294640 (YELIVA[™]) is currently in phase I clinical trials for advanced solid

tumours (Britten *et al.*, 2017) and in phase II clinical trials for cholangiocarcinoma and hepatocellular carcinoma (HCC) (Beljanski *et al.*, 2011; Ding *et al.*, 2016; Mahipal *et al.*, 2018). ABC294640 reduces S1P levels and proliferation through limiting S1P-driven activation of Akt and MAPK pathways. At the same time, ABC294640 increases intracellular Sph and Cer species that attribute to either autophagy, through LC3-II and Beclin-1, or apoptosis depending on cellular type (French *et al.*, 2010; Beljanski *et al.*, 2010). ABC294640 acts as a weak antagonist of estrogen receptor (ER α), with low micromolar affinity (100-fold greater than estrogen and 200-fold greater than tamoxifen) (Antoon *et al.*, 2010), and inhibits NF κ B-mediated chemo-resistance in breast cancer (Antoon *et al.*, 2011). Significantly, ABC294640 also inhibits Degr1 through its proteasomal degradation, leading to a 3-fold increase in levels of dihydroceramide (Venant *et al.*, 2015; McNaughton *et al.*, 2016). In addition, ABC294640 degrades SK1 through the proteasome in LNCaP AI prostate cancer cells; thus, its absolute selectivity as a SK2 inhibitor is questionable when used under chronic conditions (McNaughton *et al.*, 2016). ABC294640 has also been shown to down-regulate several onco-proteins, such as c-Myc, P-Akt, and androgen receptors, which inhibit cellular growth in LNCaP cells (Schrecengost *et al.*, 2015). Furthermore, ABC294640 was found to sensitise cancer cells to chemotherapy (Beljanski *et al.*, 2011), Bcl-2 inhibitors (Venkata *et al.*, 2014), the proteasome inhibitor Bortezomib (Wallington-Beddoe *et al.*, 2017), and the Bcr-Abl inhibitor Imatinib (Wallington-Beddoe *et al.*, 2014). Various *in vivo* studies have demonstrated the efficacy of ABC294640 in animal models of blood cancers (Wallington-Beddoe *et al.*, 2014), solid tumours (Schrecengost *et al.*, 2015; Beljanski *et al.*, 2011), osteoarthritis (Xu *et al.*, 2014),

and stroke/ischemia (Yung *et al.*, 2012).

1.5.3.2 ROME [(R)-FTY720-OMe]

ROME [(R)-FTY720-methyl ether], a derivative of the clinically successful FTY720 (in which the hydroxyl group of FTY720 is replaced with a methoxy group), is a SK2 selective Sph competitive inhibitor with a K_i of $\sim 17 \mu\text{M}$ (Lim *et al.*, 2011a). As ROME is an analogue of FTY720, it shares similar molecular targets (Pitman *et al.*, 2012). In HEK293 cells, ROME induced cellular apoptosis and stimulated focal adhesion assembly; in MCF-7 breast cancer cells, ROME inhibited DNA synthesis and prevented the S1P-stimulated rearrangement of actin (Lim *et al.*, 2011a; Lim *et al.*, 2011b). In T cell leukaemia cell lines, ROME appears to induce autophagy with EC_{50} values of $\sim 10 \mu\text{M}$ while reducing c-Myc and p-Akt (Evangelisti *et al.*, 2014). In LNCaP prostate cancer cells, ROME increased levels of Sph and reduced S1P levels, but had no observed effects on levels of C22:0 Cer, so it did not induce apoptosis (Watson *et al.*, 2013); this finding suggests a possible effect on the enzyme ceramide synthase, a recognised FTY720 target (Berdyshev *et al.*, 2009). Subsequently, Tonelli *et al.* showed that ROME increased levels of lysophosphatidylinositol (Lyso-PI) (produced by phospholipase A (PLA₁ and PLA₂)), and lysophosphatidic acid (LPA) (produced by autotaxin) in LNCaP prostate cancer cells (Tonelli *et al.*, 2013). However, both Lyso-PI and LPA were inhibited by FTY720 (Pitman *et al.*, 2012). Moreover, in MDA-MB-231 breast cancer cells, ROME reduced cellular growth by blocking the action of SK2-derived S1P on S1P₄ and S1P₂ that promotes growth effects (Ohotski *et al.*, 2014). ROME was also shown

to modulate the signalling of the S1P₁ receptor to the same extent as FTY720, resulting in improved pulmonary endothelial vascular integrity (Camp *et al.*, 2016).

1.5.3.3 K145

K145 [3-(2-amino-ethyl)-5-[3-(4-butoxyphenyl)-propylidene]-thiazolidine-2,4-dione] is a Sph-competitive inhibitor of SK2 with K_i of 6.4 μM and an IC_{50} of 4.3 μM ; it is selective for SK2 at concentrations up to 10 μM as no SK1 or CERK inhibition was observed at this concentration (Liu *et al.*, 2013). K145 reduced total levels of cellular S1P without affecting levels of Cer (Liu *et al.*, 2013); this result was consistent with that of Sanchez *et al.* who showed that inhibition of SK2 by K145 led to blockade of FTY720 phosphorylation in vascular endothelial cells (Sanchez *et al.*, 2003). Liu *et al.* demonstrated that K145 reduced proliferation and promoted apoptosis through the inhibition of ERK-1/2 and Akt phosphorylation in U937 cells at low concentrations (4 μM) (Liu *et al.*, 2013). K145 also inhibited tumour growth *in vivo* and reduced levels of S1P in U937 xenograft tumours in nude mice when administered orally. Similarly, K145 inhibited tumour growth in JC murine mammary adenocarcinoma allografts when injected into immunocompetent BALB/c mice (Liu *et al.*, 2013).

1.6 Post-translational modification and ubiquitination of proteins

Protein post-translational modifications (PTMs) are enzymatic, covalent chemical modifications of proteins that usually occur after mRNA translation; PTMs often change a protein's properties and play crucial roles in regulating cell biology (Farley and Link, 2009). More than 400 protein modifications have been recognised (Creasy and Cottrell, 2004). The most common PTMs include ubiquitination, sumoylation, phosphorylation, nitrosylation, acetylation, methylation, glycosylation, sulfation, and acylation (Farley and Link, 2009). Ubiquitination involves the PTM of target proteins through the formation of covalent attachments with ubiquitin (Ub), a highly preserved 76-amino acid protein with an extraordinary property of creating stable chemical bonds with other proteins. Ubiquitin forms an isopeptide bond in the carboxyl group of the carboxy-terminal glycine with the ϵ -amino group of target lysine residues and sometimes with the amino group at the amino terminus of targeted protein (Hershko and Ciechanover, 1998; Hochstrasser, 2006). Ubiquitin conjugation occurs through a three-step reaction catalysed by three enzymes, which involves the activation of ubiquitin by a ubiquitin-activating enzyme (E1), followed by ubiquitin conjugation with a ubiquitin-conjugating enzyme (E2), and finally the transfer of ubiquitin to the target substrate by a ubiquitin ligase (E3), as shown in Figure 1.6 (Ye and Rape, 2009).

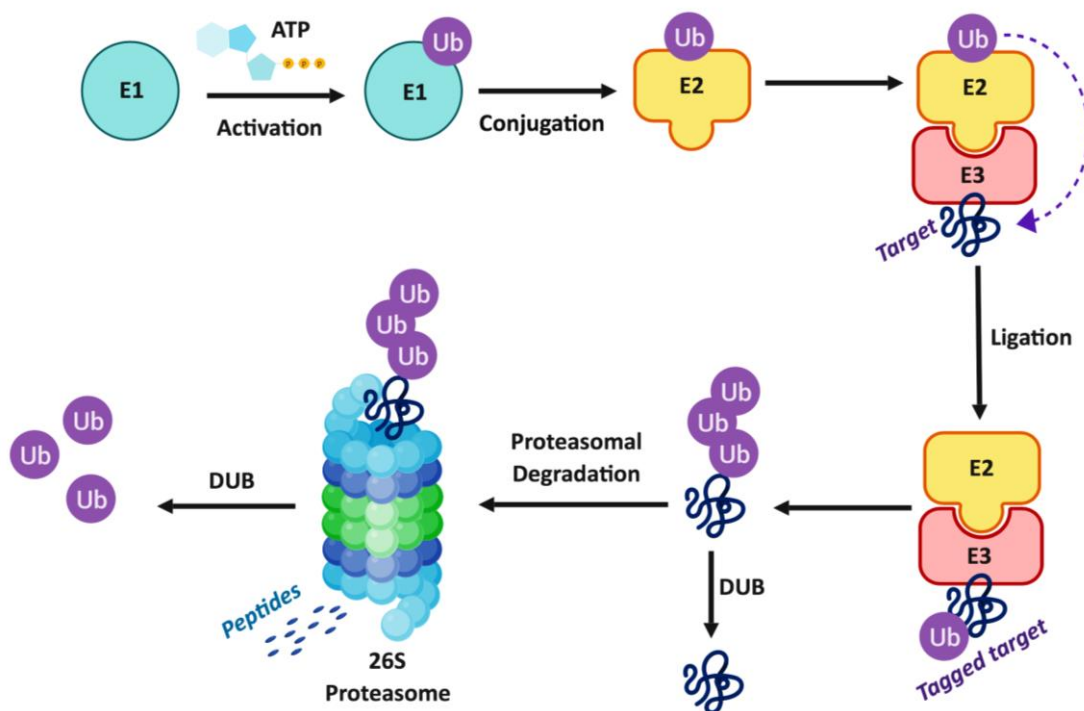


Figure 1.6 The ubiquitin proteasome system. Ubiquitin gets conjugated to the target protein via an organised milieu of E1, E2, and E3 enzymes which promote ligation of ubiquitin molecules. Tagged proteins (only K48-linked polyubiquitin chains) are recognised by the 26S proteasome and therefore get degraded. Deubiquitination (DUB) involves removal of polyubiquitin chains resulting in a free target [Adapted from (Hershko et al., 1983; Suresh et al., 2016)].

The ubiquitin sequence consists of seven lysines which could be selected for the formation of ubiquitin chains (Fang and Weissman, 2004). Therefore, the biological significance of this modification is determined according to the chosen internal lysines within ubiquitin for further ubiquitination. For example, ubiquitin chains linked to K48 signal the attached protein for degradation by the 26S proteasome, called the ubiquitin–proteasome system (UPS), while K63 linkages are associated in protein trafficking, DNA damage responses, and signal transduction in NF- κ B signalling, as shown in Figure 1.7 (Ikeda and Dikic, 2008; Pickart and Fushman, 2004).

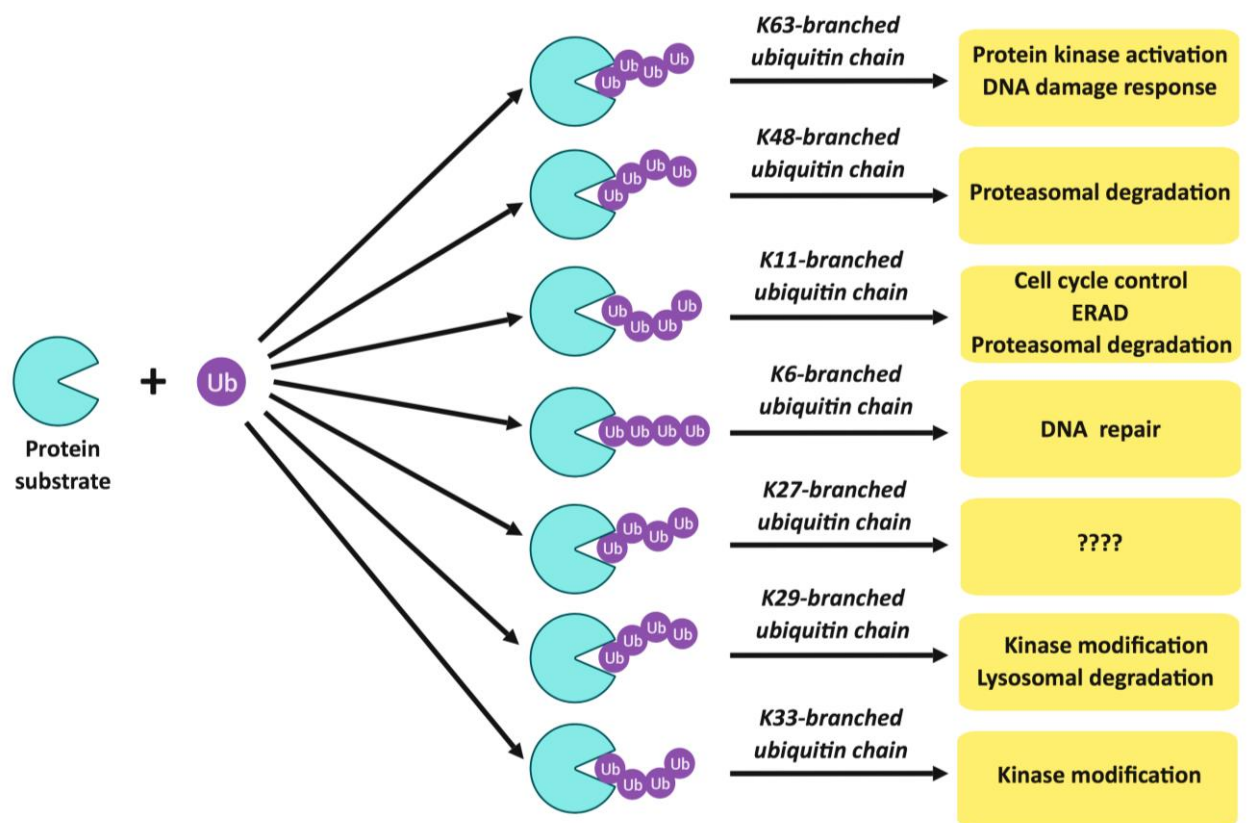


Figure 1.7 Ubiquitin modifications and related diverse cellular functions. Different types of polyubiquitin chains associated with different cellular functions according to their differential links to the lysine residues on the protein substrate [Adapted from (Suresh et al., 2016)].

The ubiquitination of proteins can occur by attaching a single ubiquitin moiety (monoubiquitin), modifying several target lysines with a single ubiquitin (multiple monoubiquitination), or attaching four or more ubiquitin moieties (polyubiquitination) (Figure 1.8) (Weissman, 2001). Each type of ubiquitin conjugate regulates specific cellular processes. Polyubiquitination is usually responsible for the degradation of substrates, while adding fewer ubiquitin moieties could change the protein function or target the protein to endosomes (Zhang *et al.*, 2004).

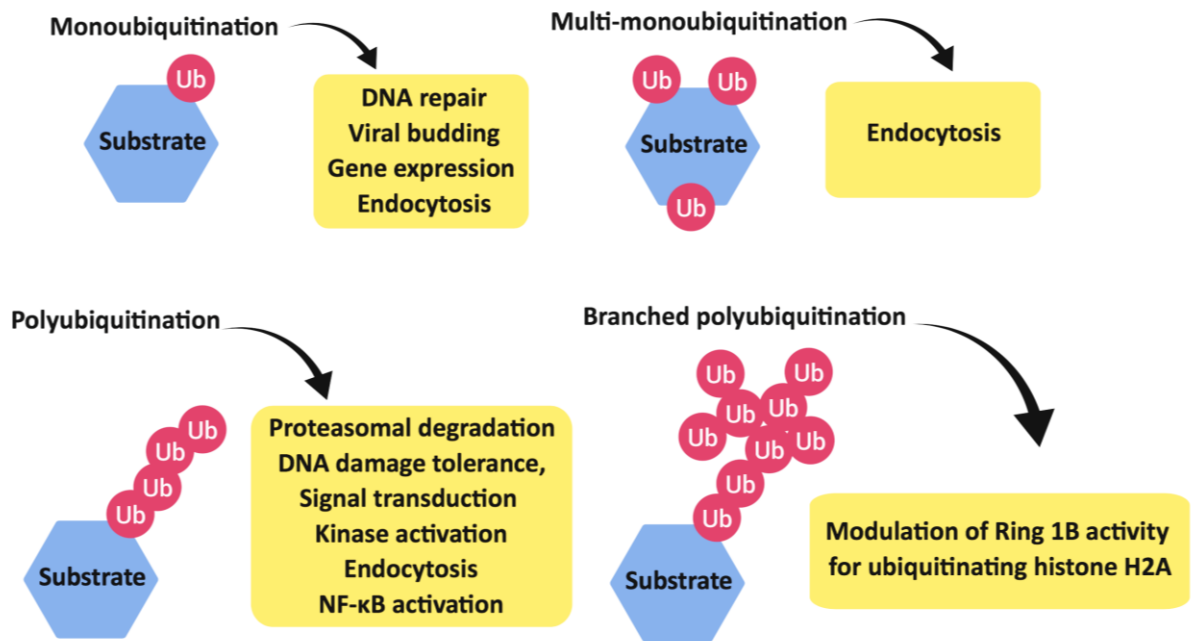


Figure 1.8 Types of ubiquitination. Different modes of ubiquitination result in different substrate fates [Adapted from (Sadowski *et al.*, 2012)].

PTMs by ubiquitin and ubiquitin-like proteins are critical regulatory events that affect various cellular processes, including inflammation, gene transcription, cell cycle progression, DNA repair, membrane trafficking, and autophagy (Pickart, 2001; Hershko and Ciechanover, 1998; Haglund *et al.*, 2003; Mukhopadhyay and Riezman, 2007; Chen and Sun, 2009; Kirkin *et al.*, 2009). Therefore, depending on the type of ubiquitin chains and how they are linked, PTMs of cellular proteins result in different cellular events. Ubiquitination usually targets proteins involved in numerous cellular processes, where their ubiquitination acts as a recognition signal by a ubiquitin-binding protein (UBP). A rapid turnover of ubiquitinated proteins occurs, resulting in low steady-state levels of this PTM (Peng *et al.*, 2003). Ubiquitination is a reversible process; ubiquitin cleavage from substrates could occur through certain deubiquitination enzymes (DUBs) by a process called deubiquitination (Hochstrasser *et al.*, 1995). Target proteins' activity and their cellular localisation are modulated

through ubiquitination in various ways, including proteasomal degradation of some target proteins, whereas deubiquitination results in the prevention of protein degradation and the stabilisation of other proteins, thereby playing a critical role in the regulation of the proteasomal pathway (Mei *et al.*, 2011). DUBs play an essential role in various cellular functions, including the processing of ubiquitin precursors, editing of ubiquitin chains, recycling of ubiquitin molecules during ubiquitination, reversal of ubiquitin conjugation, apoptosis, cell cycle progression, gene expression, DNA repair, kinase activation, and localisation and degradation of signalling intermediates (Amerik and Hochstrasser, 2004; Ramakrishna *et al.*, 2014; Ramakrishna *et al.*, 2011; Ramakrishna *et al.*, 2015; Reyes-Turcu *et al.*, 2009). However, the activity and specificity of DUBs are affected by protein–protein interactions with DUBs, subcellular localisation, changes in their expression levels, and their varying activities in the different phases of the cell cycle (Amerik and Hochstrasser, 2004; Reyes-Turcu *et al.*, 2009).

1.7 Endoplasmic reticulum (ER) stress pathway

The endoplasmic reticulum (ER) is a multifunctional organelle that extends from the perinuclear space throughout the cytoplasm and is responsible for a variety of important cellular housekeeping functions. There is both rough and smooth ER. The rough ER assembled with membrane-bound ribosomes play an essential role in the synthesis, folding, transport, post-translational modification, and processing of secretory and transmembrane proteins. Meanwhile, the smooth ER plays a significant role in lipids and steroids biosynthesis, the assembly of lipid bilayers, the regulation of calcium intracellular homeostasis, and the metabolism of carbohydrates

and drugs (Alberts *et al.*, 2008). ER homeostasis is important for proper protein folding and stresses, such as the elevation of protein synthesis, perturbations in calcium homeostasis, expression of misfolded or mutant proteins, the overload of cellular cholesterol, and the reduction of glucose or nutrients, which could lead to protein aggregates or the accumulation of unfolded proteins (Kaufman *et al.*, 2002). When unfolded proteins accumulate, the ER activates the unfolded protein response (UPR) system in order to prevent the accumulation of misfolded and unfolded proteins, a condition known as ER stress. UPR increases the capacity of protein folding, reduces newly translated proteins entering into the ER, and promotes the degradation of misfolded proteins to restore homeostasis. However, if the UPR fails to achieve ER normality, it signals for cell apoptosis in order to protect the adjacent normal cells (Ma and Hendershot, 2001; Kim *et al.*, 2008). An overview of the ER stress pathway and UPR is illustrated in Figure 1.9 that will be further explained in the following section. Recent evidence indicates that cellular dysfunction or death associated with ER stress is a major cause in the pathogenesis of some human disorders such as cancer, diabetes, cardiovascular, and neurodegenerative diseases (Ron and Walter, 2007).

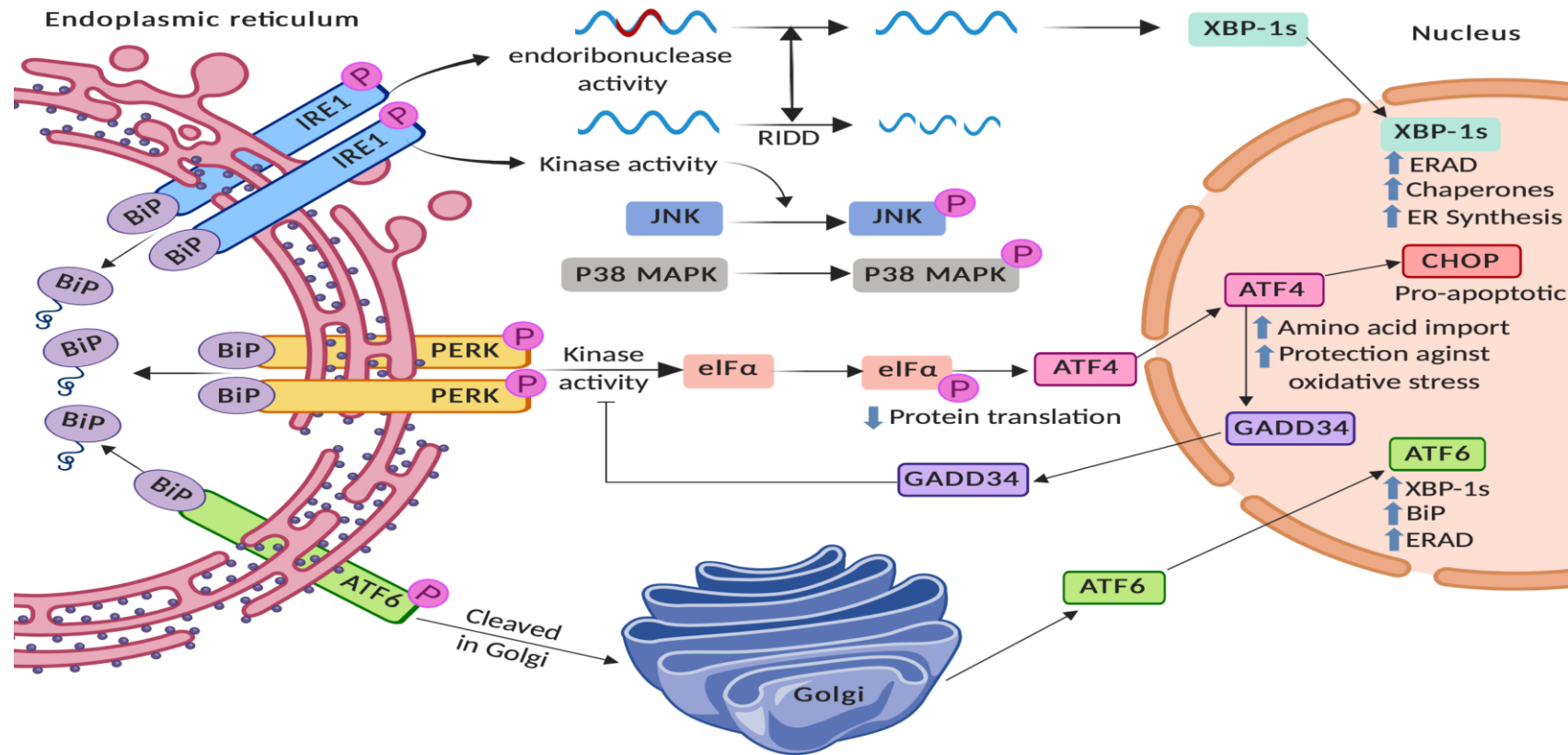


Figure 1.9 ER stress and UPR. Accumulation of unfolded proteins promotes dissociation of BiP from the luminal domain of the ER stress sensors IRE1, PERK and ATF6, resulting in their activation. Both IRE1 and PERK oligomerise and autophosphorylate, while ATF6 gets cleaved in the Golgi to form active ATF6. Activated form of IRE1 has both endoribonuclease activity that produce XBP-1s, and kinase activity that phosphorylates several targets, including JNK and p38 MAPK. Activated form of PERK phosphorylates eIF2 α leading to a decrease in cap-dependent translation and the production of the transcription factor ATF4. Since cleaved ATF6 is an active transcription factor it relocates to the nucleus where it can upregulate several genes including XBP-1s and BiP [Adapted from (Bennett et al., 2019)]. ATF4, activating transcription factor 4; ATF6, activating transcription factor 6; BiP, binding Ig protein; CHOP, CCAAT-enhancer-binding protein homologous protein; eIF α , eukaryotic initiation factor 2 alpha; ER, endoplasmic reticulum; ERAD, ER-associated degradation; GADD34, growth arrest and DNA-damage-inducible protein 34; IRE1, inositol requiring 1; JNK, c-JUN N-terminal kinase; MAPK, mitogen activated protein kinase; PERK, protein kinase r-like endoplasmic reticulum kinase; RIDD, regulated IRE1-dependent decay; XBP-1s, X-box DNA-binding protein-1s.

1.7.1 ER stress sensors

The ER contains a series of molecular chaperones and foldases that retain the newly synthesised polypeptide in a soluble form in order to promote its appropriate folding into a thermodynamically specific structure (Luoma, 2013). A Ca^{2+} -dependent molecular chaperone available in ER lumen is the Binding Ig Protein (BiP), also known as Glucose Regulated Protein 78 (GRP78), which transiently binds to newly synthesised proteins (Harding *et al.*, 2002; Zhang and Kaufman, 2004). Under normal conditions, BiP is also bound to the luminal domains of three ER transmembrane proteins—namely, Inositol Requiring 1 (IRE1), Protein kinase r-like Endoplasmic Reticulum Kinase (PERK), and Activating Transcription Factor 6 (ATF6)—keeping them inactive. However, upon ER stress with higher unfolded proteins, BiP will dissociate from these sensors and bind to the misfolded proteins, leading to their activation to regulate downstream effectors to perform their functions, including feedback control, adaptive response, and regulation of cell fate (Osowski and Urano, 2010).

Two homologues of IRE1 are found in mammals: IRE1 α is expressed in most cell types and has been extensively studied whereas IRE1 β is expressed in gastrointestinal epithelial cells (Ma and Hendershot, 2001). When BiP is released upon sensing the presence of unfolded or misfolded proteins, IRE1 α/β dimerises and autophosphorylates to stimulate its cytosolic RNase domain, which in turn splices a 26-nucleotide intron sequence from X-box DNA-binding protein (XBP1) mRNA (Figure 1) (Zhang and Kaufman, 2004). XBP1 then migrates to the nucleus and binds the upstream DNA UPR element (UPRE); as a result, it is considered a potent

activator of UPR genes, which are responsible for the regulation of protein maturation, folding, and degradation (Yoshida *et al.*, 2003). Zhang *et al.* showed that, in hyperhomocysteinaemia, homocysteine induces vascular endothelial cell apoptosis through the activation of IRE1 suppressed by overexpression of the point mutants of IRE1 with defective RNase. This suggests that high homocysteine levels indirectly activate UPR through the false stimulation of XBP1 (Zhang *et al.*, 2001). Furthermore, IRE1 is also responsible for regulating the transcription of proteins needed in the ER-associated degradation (ERAD) system signalling in order to degrade misfolded proteins (Yoshida *et al.*, 2003; Travers *et al.*, 2000). One of these proteins is the ER degradation-enhancing α -mannosidase-like protein (EDE1), a membrane protein that interacts with calnexin (CNX) to assist in the retro-translocation of irreparably misfolded proteins from ER back to cytoplasm, where they get ubiquitinated and subjected to proteasomal degradation (Kaufman *et al.*, 2002; Yoshida *et al.*, 2003; Oda *et al.*, 2003). Moreover, insoluble misfolded proteins could assemble with other cell debris into aggresomes, a highly regulated process that forms juxtannuclear complexes for the sequestration of toxic accumulated proteins, which get recycled through autophagy (Nakatsukasa and Brodsky, 2008; Clarke *et al.*, 2012).

PERK is also a type I ER transmembrane kinase and has a similar luminal domain of double stranded RNA of IRE1. When PERK is activated by ER stress, it oligomerizes, autophosphorylates, and then directly phosphorylates the α -subunit of eIF2 α which prevents the formation of ribosomal complexes and, thus, transiently attenuates mRNA translation and protein synthesis (Harding *et al.*, 1999; Harding *et*

al., 2000b). Therefore, when ER workload is reduced, it protects cells from apoptosis related to ER stress (Harding *et al.*, 2000b). On the other hand, some mRNAs, such as the mRNA encoding activating transcription factor 4 (ATF4), a b-ZIP transcription factor, require the phosphorylation of eIF2 α for translation. ATF4 regulates numerous UPR target genes, including those involved in ER stress-mediated apoptosis, such as C/EBP homologous protein (CHOP) (Harding *et al.*, 2000a). CHOP is associated with both growth arrest and cellular apoptosis. CHOP expression is activated by IRE1- and PERK-mediated signalling, which in turn stimulate ATF4 and ATF6 transcription factors (Schönthal, 2012). Therefore, when UPR is activated for a prolonged time, ATF4 can stimulate CHOP expression, leading to the activation of caspase-3 and cell death (Ma *et al.*, 2002). Otherwise, under prolonged UPR, calcium homeostasis in the ER could be disrupted, leading to the activation of caspase-12, an ER-associated effector of caspase activity which promotes apoptosis through the activation of caspases 9 and 3 (Zhang and Kaufman, 2004).

Similarly, two forms of ATF6 are available in the ER of mammalian cells, ATF6 α and ATF6 β , which upon release of BiP can move to the Golgi compartment (Kaufman *et al.*, 2002). The cytosolic region of ATF6 α/β is cleaved by site-1 and site-2 proteases (S1P/S2P) in the Golgi to produce an ATF6 active domain which is transferred to the nucleus to bind to the ER stress response element (ERSE) with CCAAT-binding factor (CBF) in order to activate the transcription of molecular chaperones and other associate-folding enzymes (Ye *et al.*, 2000; Kaufman *et al.*, 2002; Yoshida *et al.*, 2003). ATF6 could be working with XBP1 to stimulate

proteins required in the folding of unfolded proteins in the ER (Zhang and Kaufman, 2004).

1.7.2 Pharmaceutical ER stress inducers

The induction of ER stress and activation of UPR in cellular tissue can be achieved through numerous chemicals, including tunicamycin, MG132, dithiothreitol (DTT), Brefedin A, and thapsigargin. The treatment duration and concentration are essential in inducing ER stress; usually ER stress is induced with only a few hours of cell treatment, while extended exposures often lead to ER stress-mediated cellular death (Osowski and Urano, 2010). Tunicamycin is a naturally occurring antibiotic and a UDP-N-acetylglucosamine-dolichol phosphate N-acetylglucosamine-1-phosphate transferase (GPT) inhibitor which blocks glycoprotein biosynthesis's initial step (N-linked glycans) in the ER, leading to the accumulation of unfolded glycoproteins in the ER and, hence, to ER stress (Banerjee *et al.*, 2011). Treating cells with 2.5–5 µg/ml of tunicamycin for 5 hours is usually required to induce ER stress in many cell types (Duksin and Mahoney, 1982; Osowski and Urano, 2010). Some studies have proposed that tunicamycin could be a therapeutic drug used in cancer cells because it sensitises human prostate and colon cancer cells to TRAIL-induced apoptosis (de-Freitas- Junior *et al.*, 2012; Jung *et al.*, 2012). A second ER stress inducer used in this study is MG132, a specific and cell-permeable proteasome inhibitor which stimulates ER stress indirectly by blocking ERAD that leads to the accumulation of unfolded/misfolded proteins (Osowski and Urano, 2010).

1.8 Tumour suppressor protein (p53)

1.8.1 p53

In 1979, six independently working groups of investigators discovered p53, a 53 kDa protein present in mouse and human cells (DeLeo *et al.*, 1979; Kress *et al.*, 1979; Lane and Crawford, 1979; Linzer and Levine, 1979; Melero *et al.*, 1979; Smith *et al.*, 1979). Five of these studies discovered this protein due to its interaction with the oncogenic large T-antigen in SV40-infected cells that were co-immunoprecipitated with specific antibodies produced against the viral protein. In 1989, p53 changed from being a potential oncogene to a product of vital tumour-suppressor gene (TP53) in mammals whose inactivation by mutation or interaction with overexpressed cellular proteins or viruses occurs in almost all human cancers (Baker *et al.*, 1989; Oren, 2003). p53, “the guardian of cellular genome” has been known as a cellular sensor for DNA damage that responds to cellular genotoxic stresses in order to avoid genetic alterations in cells and maintain genome integrity (Vogelstein *et al.*, 2000; Lengauer *et al.*, 1998). Cells undergo either cell cycle arrest or apoptosis depending on the type and degree of DNA damage in cells (Rich *et al.*, 2000; Zhou and Elledge, 2000). These effects are mainly due to the ability of p53 to bind to DNA by a p53-responsive element (p53RE) and regulate the transcription of genes involved in this process (Lane, 1992; El-Deiry *et al.*, 1992) or through the non-transcriptional regulation of tumour suppression through the overexpression of p53 that induces cellular apoptosis without binding to DNA (Green and Kroemer, 2009; Haupt *et al.*, 1995; Kakudo *et al.*, 2005). Transcriptional and non-transcriptional activities of p53 involve the stimulation of p21 (cell cycle arrest) (El-Deiry *et al.*, 1993), Scotin

(apoptosis) (Bourdon *et al.*, 2002), caspase 6 (MacLachlan and El-Deiry, 2002), extrinsic apoptosis cascade FAS/FASL (Müller *et al.*, 1998; Li *et al.*, 2015), death receptor 5 (DR5) (Wu *et al.*, 1997), and pro-apoptotic “Bax/Bak” which directly stimulate oligomerisation or indirectly suppress pro-survival members “Bcl-2 and Bcl-xL” (Wei *et al.*, 2001). Moreover, p53 promotes apoptosis by targeting members of BH3-only proteins, including PUMA (Nakano and Vousden, 2001) and NOXA (Oda *et al.*, 2000). The role of p53 as a tumour suppressor has been established through various investigations and studies. For example, p53-null mice showed increased tumorigenesis (Donehower *et al.*, 1992; Jacks *et al.*, 1994). Moreover, patients with p53 mutations were more susceptible to the development of cancer (Malkin *et al.*, 1990; Srivastava *et al.*, 1990). In addition, the overexpression of p53 resulted in cellular growth arrest as well as the induction of apoptosis in myeloid leukemic cells and human colon cancer cells (Yonish-Rouach *et al.*, 1991; Shaw *et al.*, 1992).

1.8.1.1 Mdm2 and p53

In the absence of stress, p53 is expressed in very low steady-state basal levels that prevent it from exerting profound changes on cellular phenotype. Under these conditions, p53 regulation is performed by the ubiquitin proteasomal pathway through the Mdm2 protein (Michael and Oren, 2002; Deb, 2002; Daujat *et al.*, 2001; Momand *et al.*, 2000), a product of a proto-oncogene overexpressed in a many human cancers that tightly binds to p53, rendering it inactive. Two different molecular mechanisms govern this inactivation (Figure 1.1). The first mechanism involves direct binding of Mdm2 to the N-terminal transactivation domain of p53, which interferes with p53 transcriptional activity and blocks essential protein

interactions necessary for the p53-dependent regulation of gene expression. The second mechanism involves p53 degradation achieved through the binding of Mdm2 to p53 and acting as a p53-specific E3 ubiquitin ligase by attaching to p53 ubiquitin moieties that, in turn, target p53 for rapid degradation by the 26S proteasome (Honda *et al.*, 1997; Oren, 2003). Therefore, high Mdm2 levels affect p53 activity even under normal p53 functional conditions. It should also be mentioned that other mechanisms have been discovered by different investigators for p53 degradation unrelated to Mdm2, which contribute to the maintenance of low steady-state p53 levels (Asher *et al.*, 2002; Benetti *et al.*, 2001; Fuchs *et al.*, 1998; Kubbutat and Vousden, 1997). The Mdm2 gene is a major target for p53 because it has two adjacent p53 binding sites (p53BS) within its first intron. p53 can therefore bind to these p53BS and activate the expression of Mdm2. As a result, a negative auto-regulatory feedback loop is established, where stimulation of Mdm2 synthesis by p53 would in turn switch off p53 synthesis (Figure 1.8) (Michael and Oren, 2002). p53 is a leading transcription factor which regulates the expression of various signalling molecules involved in apoptosis, senescence, cell cycle regulation, DNA metabolism, cell differentiation, angiogenesis, immune response, motility and migration, and cell–cell interaction (Menendez *et al.*, 2009).

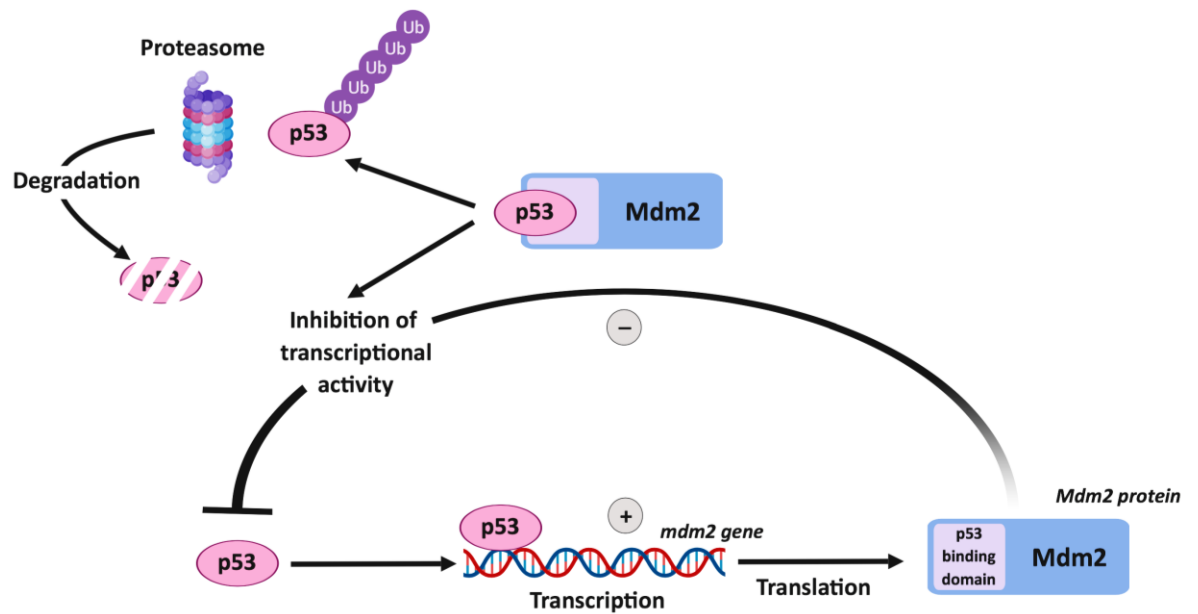


Figure 1.10 *p53-Mdm2 auto-regulatory loop.* Mdm2 protein inactivates p53 through physical blocking of p53 transcriptional activity or promoting ubiquitination of p53 and consequent degradation via the proteasome. Similarly, expression of Mdm2 can be positively regulated through p53 when it binds to p53 binding sites within mdm2 gene promoter [Adapted from (Oren, 2003)].

1.8.2 p63, p73, and p90

In 1997, almost two decades after p53 discovery, two genes named p63 and p73 were discovered that have significant structural and functional similarities to the well-studied p53 (Kaghad *et al.*, 1997; Augustin *et al.*, 1998; Yang *et al.*, 1998). p63 and p73 share hallmark features of the tumour-suppressor protein p53 which includes an acidic, amino-terminal transactivation (TA) domain, a core domain for DNA binding (DBD), and a carboxy-terminal oligomerisation domain, as shown in Figure 1.11 (Dötsch *et al.*, 2010; Yang and McKeon, 2000). Both p63 and p73 are available as numerous protein variants, exhibiting similar or opposed activities due to different splicing that occurs at the carboxy-terminal end as well as the presence of an alternative promoter located in the third intron (Dötsch *et al.*, 2010). The full-length

isoforms of p63 and p73 (TAp63 and TAp73), with a transactivation domain (TAD), usually have similar behaviours as p53 in target promoters and biological functions; however, different splicing events produce different transactivation capacity proteins among the TA variants. Therefore, using an alternative promoter creates amino-terminally truncated DN isoforms which lack TAD and, thus, are transcriptionally inactive, thereby inhibiting the active p53 family members (Dötsch *et al.*, 2010; Murray-Zmijewski *et al.*, 2006). Hence, p53 family members possess structural complexity with molecular flexibility that affects functional diversity. As p63 and p73 share similar sequence identity and domain architecture with p53, they can form oligomers and bind DNA which allows for the transactivation of p53-responsive genes in response to DNA damage leading to cell cycle arrest, cellular senescence, or apoptosis (Yang *et al.*, 1998; Melino *et al.*, 2003; Keyes *et al.*, 2005). Indeed, both p63 and p73 display unique and distinct biological functions; p63 plays a significant role in the development of squamous epithelia and their derivatives whereas p73 is vital in the differentiation of neurons and the development of olfactory and nervous systems. p63 and p73 knockout mice have consistently shown severe limb truncations and the absence of hair, skin, teeth, and lachrymal, mammary, and salivary glands (Yang *et al.*, 1999; Mills *et al.*, 1999) as well as neuronal development abnormalities (Pozniak *et al.*, 2000; Yang *et al.*, 2000), respectively. Consequently, an imbalance in the members of the p53 family results in a substantial amount of congenital developmental abnormalities in humans.

p90, also known as coiled-coil domain-containing protein 8 (CCDC8), is a 538–amino acid protein that contains 2 coiled-coil domains (Hanson *et al.*, 2011), and the

proteins contained within this domain are involved in various biological processes, such as the regulation of cell division, gene expression, and membrane fusion (Burkhard *et al.*, 2001; Woolfson, 2005). p90 is evolutionarily conserved, and p90 mutation leads to the development of 3M syndrome in humans, a primordial growth disorder, through interacting with p53, CUL7 (Cullin 7), and OBSL1 (Obscurin-Like 1) (Dai *et al.*, 2011; Hanson *et al.*, 2011; Hanson *et al.*, 2012a). p90 is a unique regulator of p53 and has been shown to interact with p53 both in vitro and in vivo (Dai *et al.*, 2011). Knockdown of p90 has no obvious effect on p53-mediated activation of p21 but specifically abrogates its effect on p53 upregulated modulator of apoptosis, also known as Bbc3 (PUMA) activation. Moreover, p90 has also been shown to interact with Tip60 and promote Tip60-dependent Lys120 acetylation of p53, therefore enhancing the apoptotic response of p53 (Dai, 2014). This demonstrates that p90 acts as an upstream regulator of the Tip60-p53 interaction and is specifically required for p53-mediated apoptosis upon DNA damage. Low-level or no expression of p90 was shown to be related to the development of some tumors, such as multiple myeloma (Zhan *et al.*, 2007), renal cell carcinoma (Morris *et al.*, 2011), prostate cancer (Law *et al.*, 2010), and breast cancer (Pangeni *et al.*, 2015). However, the roles and possible mechanisms of action of p90 in other tumors are yet to be elucidated. In addition, it was primarily demonstrated that inhibition of p90 affects cancer cell proliferation; however, roles of p90 in cancer metastasis have not been completely understood.

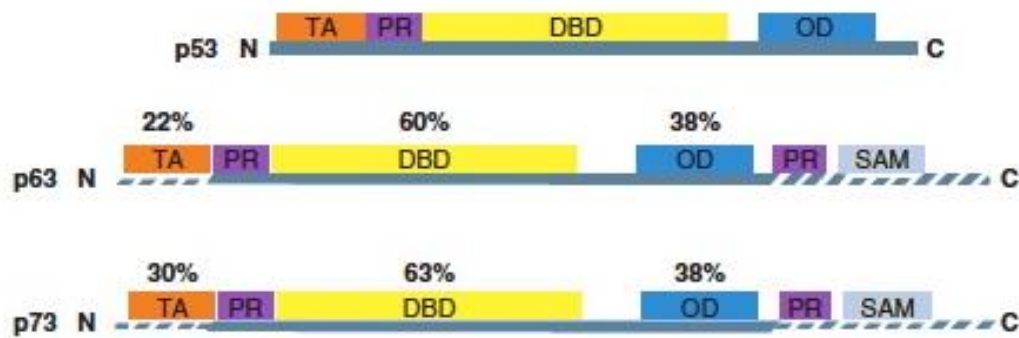


Figure 1.11 *Modular structure of the p53 family members [Adapted from (Dötsch et al., 2010)].*

1.9 Nuclear factor kappa B (NF- κ B)

Nuclear factor kappa B (NF- κ B) is a master transcription factor initially discovered by David Baltimore in 1986 as a nuclear activity with a specific binding toward a ten-base-pair DNA sequence 5'-GGGACTTCC-3' present within the immunoglobulin kappa light chain in mature antibody-producing B lymphocytes (Sen and Baltimore, 1986). Since this initial identification, NF- κ B has also been shown to be a ubiquitously expressed cytoplasmic signalling molecule; once activated, it can undergo nuclear translocation and consequently regulate transcription of selective target genes. NF- κ B activates the expression of stress response genes in response to multiple stimuli, including growth factors, cytokines, engagement of the T-cell receptor, and bacterial and viral products (Hayden and Ghosh, 2008). NF- κ B controls important cellular processes, including cell proliferation, growth, survival, inflammation, immunity, and apoptosis (Bours *et al.*, 2000; Karin *et al.*, 2002). Dysregulation of NF- κ B pathways results in severe diseases, such as immunodeficiency, arthritis, autoimmunity, and cancer (Courtois and Gilmore, 2006).

1.9.1 The NF- κ B family

The NF- κ B family of transcription factors consists of five members that have been identified in eukaryotic cells, known as p50, p52, p65 (RelA), c-Rel, and RelB, encoded by NFKB1, NFKB2, RELA, REL, and RELB, respectively (Ghosh *et al.*, 1998; Ghosh and Hayden, 2008). p65 (Rel A), Rel B, and c-Rel proteins are synthesised as fully functional proteins and possess a transcription activation domain (TAD) necessary for the positive regulation of gene expression. p50 and p52 proteins are produced *in vivo* as their precursor proteins, p105 and p100, and require proteolytic cleavage in order to generate the active molecules; since p50 and p52 lack TADs, they could suppress transcription unless associated with a TAD-containing NF- κ B family member or other proteins with the ability of coactivator recruitment (Perkins and Gilmore, 2006). The TAD is divided into two distinct transactivation domains, TA1 and TA2. TA1 is found in the C-terminal portion (residues 521–551) of the TAD while TA2 is located within the adjacent 90 amino acids (residues 428–521). The transcriptional activation of RelA has been found to be regulated by the two TADs (Schmitz and Baeuerle, 1991; O'Shea and Perkins, 2008). Published evidence has proposed that RelA phosphorylation in the TAD regions functions as a method of post-translational modification to regulate transcriptional activation (Viatour *et al.*, 2005). The NF- κ B family shares an N-terminal Rel homology domain (RHD) responsible for DNA-binding, homo-/hetero-dimerisation, nuclear translocation, as well as interaction with I κ Bs as the family is regulated by eight I κ B family members (Ghosh *et al.*, 1998; Ghosh and Hayden, 2008). The nuclear localisation sequence (NLS) was found within the RHD that becomes apparent upon proteasomal degradation of I κ B- α (Ghosh and Hayden,

2008).

1.9.2 Inhibitory kappa B (I κ B)

In unstimulated cells, NF- κ B is located in the cytoplasm where it is physically sequestered by the inhibitory kappa B (I κ B) proteins because they mask the NLS, thereby preventing translocation of the NF- κ B to the nucleus (Beg *et al.*, 1992). The I κ B protein family consists of three functional groups: the typical I κ B proteins I κ B- α , I κ B- β , and I κ B- ϵ , which are present in the cytoplasm of unstimulated cells and upon stimulation can get degraded and re-synthesised; the atypical I κ B proteins I κ B- ζ (encoded by NFKBIZ), BCL-3 (B-cell lymphoma 3), and I κ BNS (encoded by NFKBID), which are expressed following activation and mediate their effects in the nucleus; and the precursor p100 and p105 NF- κ B members which could be processed to produce p52 and p50 NF- κ B family members, respectively, or get degraded (Ghosh and Hayden, 2008). The first I κ B protein identified—and probably the most well characterised within this family—is I κ B- α (Ishikawa *et al.*, 1995). Upon stimulation, I κ B- α undergoes phosphorylation followed by rapid ubiquitin-mediated proteasomal degradation that results in the release of the cytoplasmic-bound NF- κ B dimers which then translocates to the nucleus to initiate gene expression (Hayden and Ghosh, 2008).

1.9.3 The Inhibitory kappa B kinases (IKKs)

The inhibitory kappa B kinase (IKK) complex is the major regulatory kinase complex within the NF- κ B pathway and consists of two homologous kinase subunits,

IKK α (IKK1) and IKK β (IKK2), as well as a regulatory subunit, IKK γ (NEMO) (Scheidereit, 2006; Häcker and Karin, 2006). IKK α and IKK β are catalytically active and share 52% of their protein sequence identity; they have an N-terminal kinase domain, a C-terminal helix-loop-helix (HLH) domain that controls the kinase activity, and a leucine-zipper (LZ) region that facilitates the kinases dimerisation (Mercurio *et al.*, 1997). Although IKK γ is a non-catalytic enzyme that lacks kinase activity, it plays a major regulatory function in the canonical NF- κ B pathway (Rothwarf *et al.*, 1998). The N-terminal region of NEMO is responsible for interaction with the carboxyl terminus of the IKK α and IKK β subunits required for the activation of the IKK complex (May *et al.*, 2002). In most canonical NF- κ B signalling pathways, IKK β is necessary in the phosphorylation of I κ B- α following its activation by the pro-inflammatory cytokines TNF, interleukin-1 (IL-1), or several microbial products, although there is increasing evidence of a role for IKK α in this process (Hayden and Ghosh, 2008). IKK α has been shown to function as a significant regulator of the NF- κ B-dependent transcriptional response by non-I κ B substrates, including transcriptional co-activator, transcriptional co-repressors, and NF- κ B itself. In addition, the non-canonical NF- κ B pathway mainly depends on IKK α (Scheidereit, 2006; Hayden and Ghosh, 2008) whereas IKK γ is essential for all canonical NF- κ B signalling pathways, including those catalysed by IKK α (Häcker and Karin, 2006). I κ B- α expression induced by the signalling of NF- κ B provides a dominant and robust negative feedback loop directed against NF- κ B-dependent transcriptional activity. Therefore, recent evidence has proposed an analogous role for the post-translational ubiquitylation of signalling intermediates (Liu *et al.*, 2005).

1.9.4 Three distinctive pathways of NF- κ B activation

Three intracellular mechanisms have been shown to activate the NF- κ B pathway: the classical (canonical), alternative (non-canonical), and atypical pathways (Figure 1.12).

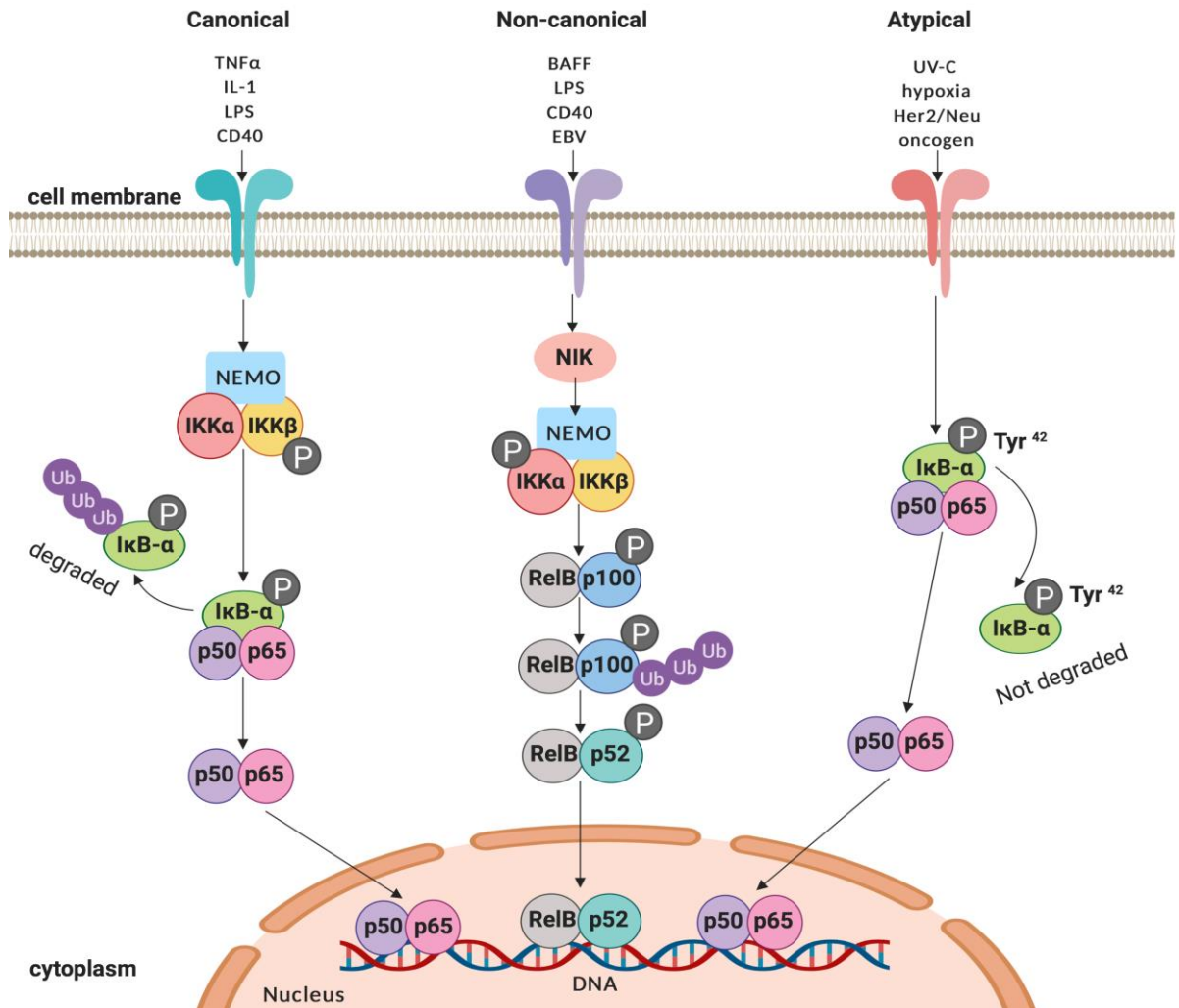


Figure 1.12 *The three distinctive NF- κ B pathways.* The canonical NF- κ B pathway (left) when activated through different stimuli it activates and phosphorylates the IKK β subunit of the IKK complex. That phosphorylates I κ B proteins bound to NF- κ B dimers such as p50-p65 results in ubiquitination (Ub) of I κ B and proteasome-induced degradation, which allows NF- κ B to enter the nucleus where it binds specific DNA sequences. The non-canonical pathway (middle) when activated it requires NIK to activate IKK α , which then phosphorylates p100 (NF- κ B2), triggering its proteosomal processing needed for the activation of p52-RelB dimers. Whereas the atypical pathway (right) when activated it results in tyrosine 42

phosphorylation of IκB-α that results in NF-κB translocation without degradation of the IκB-α protein [Adapted from (Gerondakis et al., 2014)]. BAFF, B-cell-activating factor of the TNF family; EBV, Epstein–Barr virus; IKK, IκB kinase; IL-1, Interleukin-1; IκB-α, inhibitory kappa B alpha; LPS, lipopolysaccharides; NEMO, IKKγ; NIK, NF-κB-inducing kinase; P, phosphorylation; TNF-α, tumour necrosis factor alpha Ub, ubiquitination; UV-C, ultraviolet.

1.9.4.1 Classical (canonical) pathway

The classical (canonical) pathway is the initial pathway to be characterised, and it involves the rapid activation and nuclear translocation of cytoplasmic NF-κB that leads to the degradation of its inhibitor IκB-α, as a result of IκB-α phosphorylation by the activated IκB kinase (IKK) complex through inflammatory mediators, such as LPS, IL-1, and TNF-α (Soloff *et al.*, 2006; Hayden and Ghosh, 2008). Cytokine receptors including TNFR1, the IL-1β receptor, and toll-like receptors (TLRs) have been shown to activate the canonical NF-κB pathway in a number of cell types (Plotnikov *et al.*, 2011). For example, TNFα activates NF-κB by binding a trimerised TNF protein to one of two cell surface receptors, known as p55 (TNFR-1, TNFRSF1A) or p75 (TNFR-2, TNFRSF1B) (Ding and Yin, 2004). Once the TNF receptor is activated, it results in the recruitment of the TNF receptor-associated death domain (TRADD), which in turn recruits TRAF-2 along with a serine/threonine kinase known as the ring-finger interacting protein (RIP). TRAF-2 is the protein responsible for the binding and recruiting of IKKβ, thereby facilitating its activation, which in turn mediates the IKKβ-dependent phosphorylation of IκB-α at serine 32 and 36 (Häcker and Karin, 2006; Karin and Ben-Neriah, 2000). Consequently, IκB-α gets ubiquitinated and undergoes proteasomal degradation;

thus, the NF- κ B member translocates to the nucleus, where it initiates the transcription of its target genes (Mercurio and Manning, 1999).

1.9.4.2 Alternative (non-canonical) pathway

The alternative (non-canonical) pathway involves the stimulation of the B-cell-activating factor of the TNF family (BAFF), LPS, CD40 and lymphotoxin-b receptors, and latent membrane protein (LMP)-1 of the Epstein–Barr virus (EBV). The non-canonical pathway proceeds through the activation of TRAF, which stimulates the activation of the NF- κ B-inducing kinase (NIK); this action in turn activates an IKK α dimer, which mediates a site-specific phosphorylation of C-terminus of the precursor protein of the p100 (NF- κ B2) NF- κ B subunit and stimulation of its proteolytic processing to p52 (Hayden and Ghosh, 2004; Bonizzi and Karin, 2004). The processing of p100 to p52 results in the activation of complexes containing this subunit, which in most circumstances consists of p52/RelB heterodimers translocating to the nucleus in order to regulate gene transcription (Bonizzi and Karin, 2004; Bonizzi *et al.*, 2004).

1.9.4.3 Atypical pathway

The atypical pathway involves IKK-independent mechanisms as well as the use of IKK activity in a different manner than that found in the canonical and non-canonical pathways, resulting in the tyrosine phosphorylation of I κ B- α on tyrosine 42 as opposed to the classical residues serine 32 and 36, such as the casein kinase II (CK2)-dependent phosphorylation and degradation of I κ B- α as a result of either short

wavelength ultraviolet (UV-C) light or the expression of the Her2/Neu oncogene (Kato Jr *et al.*, 2003; Romieu-Mourez *et al.*, 2002). Interestingly, the phosphorylation of I κ B- α at Tyr42 results in NF- κ B translocation without degradation of the I κ B- α protein (Sethi *et al.*, 2007).

1.10 Activator protein-1 (AP-1)

Activator protein-1 (AP-1), one of the first mammalian transcriptional factors to be identified, regulates a broad range of cellular processes, including cellular growth, survival, differentiation, proliferation, cell migration, transformation, and apoptosis (Angel *et al.*, 1987; Shaulian and Karin, 2002). Various studies have shown that AP-1 plays an essential role in many disorders including fibrosis, cancer, and organ injury, as well as inflammatory disorders such as psoriasis, asthma, and rheumatoid arthritis (Palanki, 2002; Shaulian and Karin, 2002; Eferl and Wagner, 2003); therefore, in the past two decades AP-1 has emerged as a pursued drug discovery target, with a resurgence of attention in recent years.

AP-1 is a dimeric complex composed of homodimers and heterodimers members from the JUN (v-JUN, c-JUN, JUNB, and JUND), FOS (v-FOS, c-FOS, FOSB, FRA-1, and FRA-2), ATF (ATF-2, ATF-3, ATF-4, ATF-5, ATF-6, ATF-6B, ATF-7, BATF, BATF-2, BATF-3, JDP1, and JDP2), or MAF (c-MAF, MAFA, MAFB, MAFF, MAFG, MAFK, and NRL) protein families (Shaulian and Karin, 2002; Eferl and Wagner, 2003). All active AP-1 members are characterised by the possession of basic leucine-zipper (bZIP) domains, which are essential for DNA binding and dimerization as they recognise different response elements (REs) in genomic

regulatory regions. The bZIP domain, together with its adjacent basic domain, forms a unique and flexible “scissor-shaped” α -helix structure; the carboxy-terminal regions of the α -helices align to form parallel “coiled coils”, whereas the amino-terminal regions provide base-specific contacts with DNA in the main groove (c-FOS/c-JUN, PDB code 1FOS) (Glover and Harrison, 1995). AP-1 is activated by phorbol 12-myristate 13-acetate (PMA), the tumour-promoting agent 12-O-tetradecanoylphorbol-13-acetate (TPA), allowing its binding to the TPA-response element (TRE) with the consensus sequence 5'-TGAG/CTCA-3' (Hess *et al.*, 2004). AP-1 activity is stimulated by a plethora of physiological and environmental stimuli, such as growth factors, cytokines, onco-proteins, neurotransmitters, cell–matrix interactions, polypeptide hormones, UV irradiation, and bacterial or viral infections (Shaulian and Karin, 2002; Suto and Ransone, 1997; Wang *et al.*, 2013a).

The AP-1 transcription factor family is ruled under strict transcriptional, translational, and post-translational regulations specific to cellular type and context except in the case of cancer cells. AP-1 is mainly regulated by the transcriptional levels of both JUN and FOS that involves activation of mitogen-activated protein kinase (MAPK) pathways and by post-translational modification through phosphorylation and de-phosphorylation (Suto and Ransone, 1997). The MAPK cascade is activated by a MAPK kinase (MAPKK), which is activated by a MAPK kinase kinase (MAPKKK) that is either directly stimulated by a small G-protein such as Ras or through another upstream kinase (Fanger *et al.*, 1997). The MAPK pathway consists of three separate groups of c-JUN N-terminal kinases (JNKs), also referred to as stress-activated kinases (SAPKs), extracellular signal-regulated kinases

(ERKs), and the later discovered p38s. JNKs have three alternative forms of proteins (JNK1, JNK2, JNK3) with different abilities to bind and phosphorylate family members of AP-1 (Gupta *et al.*, 1996). JNKs are activated by the MAPKKs MKK4, and MKK7, whereas the ERKs are activated by MEK1 and MEK2, and p38 is activated by MKK3 and MKK6. Once the MAPK pathway is activated, it regulates downstream transcription factors that promote the transcription of FOS and JUN genes, thereby increasing the expression of AP-1 complexes. FOS expression is stimulated by TCFs, which are activated through phosphorylation by the p38, JNKs, and ERKs, whereas JUN expression is induced by MEF2C, ATF2, and JUN, which are activated through phosphorylation by the p38 and JNK (Eferl and Wagner, 2003). AP-1 activity could also be regulated through various kinases via post-translational phosphorylation that regulate AP-1 DNA-binding capacity, transactivating potential, and the stability of AP-1 components, such as glycogen synthase kinase-3 β (GSK-3 β), casein kinase II (CKII), and ribosomal S6 kinase 2 (RSK2). AP-1 was recently shown to be regulated through other mechanisms, including genetic interaction with other oncoproteins, mRNA turnover, and protein stability (Shaulian and Karin, 2002).

AP-1 family members are controlled through rapid degradation by the proteasome (Salvat *et al.*, 1998); interestingly, c-FOS has been shown to be degraded via the proteasome independently of its own ubiquitination (Bossis *et al.*, 2003) whereas c-JUN is degraded through the proteasome in a ubiquitin-dependent manner (Treier *et al.*, 1994). It was recently suggested that c-JUN/c-FOS dimers are degraded through the SUMO pathway (Bossis *et al.*, 2005). In addition, reversible protein acetylation

has been shown to be involved in the regulation of AP-1 as well, because osmotic stress down-regulates c-JUN via the histone deacetylase, HDAC3-dependent transcriptional repression (Xia *et al.*, 2007). Moreover, HDAC inhibitors have been shown to suppress c-JUN binding to Cyclooxygenase-2 (COX-2), Collagenase-1, and Cyclin D1 promoter regions, resulting in the blocking of transcription (Yamaguchi *et al.*, 2005).

1.11 Project aims

As SKs represent a promising target for the development of novel therapeutics, the main aim of this research is to add knowledge to the role of Degs1, SK1 and SK2 in regulating cell survival/apoptosis pathways to help identify novel signalling networks and therapeutic targets that advance treatment options for various disorders, including cancer, T2D, metabolic disorders, and inflammatory skin disease. The specific aims of the thesis include the following:

- i.** To investigate the controversy concerning the role of dihydroceramide desaturase (Degs1) in regulating cell survival/apoptosis. A molecular and pharmacological approach was taken and the role of Degs1 polyubiquitination was further investigated.
- ii.** To evaluate the role of SK1 and SK2 in relation to the downstream effectors p53, p38 MAPK, JNK, and XBP-1s as these kinases are involved in survival/apoptosis fates.
- iii.** To examine the role of SK1 and SK2 in inflammation-based transcriptional regulation in keratinocytes in relation to NF- κ B/AP-1 as the role of SKs in inflammation is controversial.

CHAPTER 2:
MATERIALS AND METHODS

CHAPTER2: MATERIALS AND METHODS

2.1 Materials

2.1.1 General reagents

All general biochemical materials and reagents were purchased from Sigma-Aldrich (Poole, UK) unless otherwise indicated.

Bio-Rad (UK)

1.0 mm integrated spacer plate for Mini-PROTEAN® 3 Multi-Casting Chamber (Cat No. 165-3311); short plate for Mini-PROTEAN® 3 (Cat No. 165-3308).

Christiansen-Linhart (Munich)

CEA RP New X-ray film (Cat No. C011824); KODAK RP X-OMAT developer (Cat No. KK17E2); KODAK RP X-OMAT fixer (Cat No. KK17F1).

Fisher Scientific (Leicestershire, England)

Amersham nitrocellulose blotting membrane (Cat No. 15259794); Bovine Serum Albumin (Cat No. 11413164); Geneticin G-418 Sulphate (Cat No. 10463982); Pierce™ BCA Protein Assay Kit (Cat No. 10678484); Pierce™ D-Luciferin Monosodium Salt (Cat No. 88291); Scintsafe2 scintillation cocktail (Cat No. 10659633); UltraPure DNase/RNase-Free Distilled Water (Cat No. 11538646); Western Blotting Filter Papers (Cat No. 10675935).

Vector Laboratories (Peterborough, UK)

VECTASHIELD HardSet Antifade Mounting Medium with DAPI (Cat No. H1500).

2.1.2 Cell culture

All cell culture materials and reagents were purchased from Fisher Scientific (Leicestershire, England) unless otherwise indicated. HEK293 cells were purchased from European Collection of Animal Cell Cultures, supplied through Public Health England (Salisbury, UK) and HEK293T cells were gifted from Professor Anthony Futerman (Weizmann Institute, Israel); while NCTC-NF- κ B and NCTC-API reporter keratinocytes were gifted from Dr Andrew Paul (SIPBS, Glasgow, UK).

VWR (Leicestershire, UK)

96-well Black plates with clear bottom for fluorescent and luminescent (Cat No. 734-2327).

Sera Labs (UK)

Foetal Bovine Serum (Cat No. EU-000-F).

2.1.3 Antibodies

Abcam (UK)

Anti-Degs1 (EPR9680) monoclonal antibody (Cat No. ab185237); anti-SK1 antibody (lab reference number 48:2) was custom made by Abcam using antigens detailed in (Huwiler *et al.*, 2006).

Insight Biotechnology LTD (Wembley, UK)

Anti-P-ERK-1/2 monoclonal antibody (Cat No. sc-7383); anti-GAPDH (0411) monoclonal antibody (Cat No. sc-47724).

New England Biolabs Ltd. (Hitchin, UK)

Anti-CHOP (D46F1) monoclonal antibody (Cat No. 5554); anti-I κ B- α polyclonal antibody (Cat No. 9242); anti-LC3B polyclonal antibody (Cat No. 2775); anti-P-AKT (Thr308) (C31E5E) monoclonal antibody (Cat No. 2965); anti-PARP polyclonal antibody (Cat No. 9542); anti-PERK (D11A8) monoclonal antibody (Cat no. 5683); anti-P-p38 MAPK (Thr180/Tyr182) polyclonal antibody (Cat No. 9211); anti-P-SAPK/JNK (Thr183/Tyr185) (98F2) monoclonal antibody (Cat No. 4671); anti-XBP-1s (D2C1F) monoclonal antibody (Cat No. 12782).

Sigma-Aldrich (Poole, UK)

Anti-actin polyclonal antibody (Cat No. A2066); anti-p53 (DO-7) monoclonal antibody (Cat No. P8999); anti-Mouse IgG-tetramethyl rhodamine isothiocyanate (TRITC) antibody (Cat No. T5393); anti-Mouse IgG-reporter horseradish peroxidase (HRP) antibody (Cat No. A9044); anti-Rabbit IgG-tetramethyl rhodamine isothiocyanate (TRITC) antibody (Cat No. T6778); anti-Rabbit IgG-reporter horseradish peroxidase (HRP) antibody (Cat No. A0545); protein A-Sepharose® 4B, Fast Flow (Cat No. P9424); protein G Sepharose®, Fast Flow (Cat No. P3296).

2.1.4 Agonists and inhibitors

Cambridge Bioscience (Cambridge, UK)

BMS345541 (IKK inhibitor) (N¹-(1,8-dimethylimidazo[1,2-a]quinoxalin-4-yl)-1,2-ethanediamine) (trifluoroacetate salt) (Cat No. CAY16667).

Enzo Life Sciences (UK)

SB203580 (p38 MAPK inhibitor) (4-(4-Fluorophenyl)-2-(4-methylsulfinylphenyl)-5-(4-pyridyl)1H-imidazole) (Cat No. BML-EI286); SP600125 (JNK inhibitor) (Anthra(1,9-cd)pyrazol-6(2H)-one, 1,9-Pyrazoloanthrone) (Cat No. BML-EI305).

Merck Biosciences (Nottingham, UK)

PF-543 (Cat No. 567741); SKi (2-(p-Hydroxyanilino)-4-(p-chlorophenyl)thiazole) (Cat No. 567731).

R & D Systems (Bio-Techne) (UK)

Recombinant Human TNF α (Cat No. 210-TA/CF).

Insight Biotechnology LTD (UK)

Bortezomib (Cat No. sc-217785); Fenretenide (Cat No. HY-15373).

Sigma-Aldrich (Poole, UK)

FTY720 (2-amino-2-[2-(4-octylphenyl)ethyl]propane-1,3-diol) (Cat No. SML0700); K145 hydrochloride ((Z)-3-(2-Aminoethyl)-5-(3-(4-butoxyphenyl) propylidene) thiazolidine-2,4-dione Hydrochloride) (Cat No. SML1003); MG132 (Z-Leu-Leu-

Leu-al) (Cat No. C2211); N-acetyl-L-cysteine (NAC) (Cat No. A7250); Nutlin (Cat No. N6287); PMA (Phorbol 12-Myristate 13-Acetate) (Cat No. P8139); Tunicamycin (Cat No. T7765).

Stratech Scientific (UK)

ABC294640 (3-(4-chlorophenyl)-adamantane-1-carboxylic acid(pyridin-4-ylmethyl) amide) (Cat No. S7174).

(*R*)-FTY720 methylether (ROME) was synthesised as described previously in (Lim *et al.*, 2011a) and gifted by Professor Robert Bittman (City University of New York, USA).

2.1.5 Molecular biology

Addgene (Teddington, UK)

HA-Ubiquitin plasmid construct (Cat No. 18712).

BD Biosciences (UK)

Bacto™ Agar (Cat No. 214010); Bacto™ Tryptone pancreatic digest of casein (Cat No. 211705); Bacto™ Yeast Extract of autolysed yeast cells (Cat No. 212750).

Dharmacon (Cromlington, UK)

DharmaFECT™2 reagent (Cat No. T-2002); ON-TARGETplus SMARTpool® DEGS1 siRNA (Cat No. L-006675-00-0005); ON-TARGETplus SMARTpool® SK1 siRNA (Cat No. L-004172-00-0005); ON-TARGETplus SMARTpool® SK2 siRNA

(Cat No. L-004831-00-0005); ON-TARGETplus SMARTpool® TP53 siRNA (Cat No. L-003329-00-0005).

Fisher Scientific (Leicestershire, England)

Lipofectamine™ 2000 Transfection Reagent (Cat No. 11668019); plasmid construct (pcDNA3.1) (Cat No. V79020); PureLink™ HiPure Plasmid Maxiprep Kit (Cat No. K210006).

Qiagen (Crawley, UK)

Scrambled siRNA (ALLSTARS Negative control) (Cat No. 1027310); QIAGEN Plasmid plus Kits (Cat No. 12943).

2.1.6 Radioisotopes

PerkinElmer (UK)

[Methyl-³H] thymidine (25 Ci/mmol; 37 MBq/ml) (Cat No. NET027A)

2.2 Methods

2.2.1 Cell culture

All cell culture work was carried out in a class II cell culture hood under aseptic conditions. Human embryonic kidney (HEK293 and HEK293T) cells and keratinocytes reporter cells (NCTC-NF- κ B and NCTC-AP-1) were cultivated in 75 cm² cell culture flasks (T-75) containing DMEM/Glutamax supplemented with 100 U/ml penicillin, 100 μ g/ml streptomycin, and 10 % (v/v) foetal bovine serum in a humidified atmosphere at 37°C with 5 % CO₂. Once per month, 400 μ g/ml Genitacin (G-418 Sulfate) was added to NCTC-NF- κ B/NCTC-AP-1 reporter keratinocytes culture media in the absence of antibiotics to ensure continued selection of the reporter construct-containing cells.

Cells were replenished with complete fresh medium every 2–3 days until confluent. Confluent cells were detached from the flask surface by incubating them in a trypsin/EDTA solution for 2–3 minutes at 37°C after washing the cells' surface gently with a serum-free DMEM/Glutamax medium. The complete medium was then added to dilute the cell/trypsin suspension at ratios of 1:8 to 1:10 before transferring it to a new flask. Cells between passages 1 and 20 were used for the experiments stated in the current study. Figure 2.1 shows the typical phenotype of HEK293T cells and NCTC-NF- κ B or NCTC-AP-1 reporter keratinocytes under the TMS inverted phase contrast microscope.

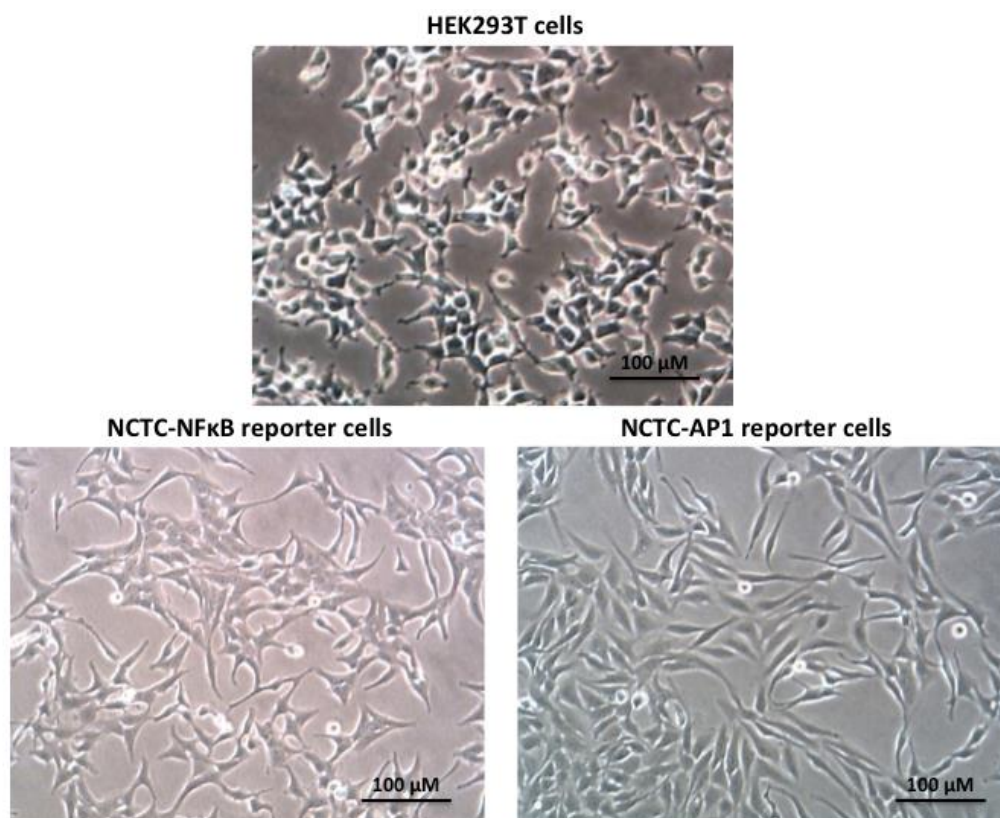


Figure 2.1 Cells' morphology. Phase contrast images of healthy HEK293T cells and NCTC- $\text{NF-}\kappa\text{B}$ /NCTC-AP-1 reporter keratinocytes. Images were taken using a Nikon TMS inverted phase contrast microscope connected to Motic Images Plus 2.0 software. Objective lens is 20x. Scale bar represents 100 μm for all images. Images are from an individual experiment, typical of 2 others.

2.2.2 Treatment protocol

For experiments, cells were plated on 12-well plates or 6-well plates, as required, and grown to approximately 70% confluence before being treated as described in each figure legend in the Results chapters. NCTC- $\text{NF-}\kappa\text{B}$ /NCTC-AP-1 reporter cells were quiesced with serum-free medium for 24 hours before the addition of compounds, whereas HEK293/HEK293T cells were not quiesced.

SKi, ABC294640, K145, ROME, PF-543, FTY720, MG132, nutlin, fenretinide, bortezomib, tunicamycin, SP600125, SB203580, BMS345541, and PMA (used at the final concentrations indicated in the Figure legends) were reconstituted in DMSO before being added to the culture medium for cell stimulation/inhibition at a final concentration of 0.1–0.2% DMSO. TNF α was reconstituted in sterile distilled H₂O whereas NAC was dissolved to the required final concentration in sterile DMEM/Glutamax supplemented with 100 U/ml penicillin, 100 μ g/ml streptomycin, and 10% (v/v) foetal bovine serum and incubated overnight at 37°C with 5% CO₂ before being used for experimentation.

2.2.3 Plasmid DNA transformation and purification

A sterile loop was dabbed onto HA-Ubiquitin plasmid-containing agar supplied, then stirred in a vial containing 5 ml of sterilised L-Broth media (1% (w/v) Bacto-Tryptone, 0.5% (w/v) Bacto-yeast extract, and 1% (w/v) NaCl) and 5 μ l of ampicillin (1:1000) added into the miniprep culture. The vial was left to shake in a shaking incubator at 200 rpm overnight at 37°C. Then, the overnight culture was added to a sterile centrifuge tube before being pelleted for 3 minutes at 120 g. Plasmid DNA from the resulting pellet was purified using the PureLink™ HiPure Plasmid Maxiprep Kit, as per the manufacturer's instructions. The DNA yield was determined by measuring absorbance at 260 nm using the Nanodrop 2000 UV-Vis Spectrophotometer and Nanodrop 2000/2000 c Software.

2.2.4 Cell transfections

2.2.4.1 siRNA transfections

HEK293T cells were transiently transfected with siRNA constructs or scrambled siRNA (as a negative control) at a final concentration of 100 nM. Cells were grown to approximately 70% confluence, and for three wells a mixture of 1 μ M siRNA in 175 μ l of antibiotic-free DMEM/Glutamax medium and 2.8 μ l of DharmaFECT® 2 transfection reagent in 172.2 μ l of antibiotic-free DMEM/Glutamax medium was prepared. These preparations were incubated for 5 minutes at room temperature to mix and then combined and incubated for 20 minutes at room temperature to allow for the formation of siRNA and DharmaFECT® 2 transfection reagent complexes. Next, 1.4 ml of antibiotic-free DMEM/Glutamax medium supplemented with 10% (v/v) foetal bovine serum was added to the 350 μ l transfection mixture and mixed gently. Then 500 μ l of the transfection mixture was used to replace the cell culture medium of each well, and the cells were incubated at 37°C in 5% CO₂ for 48 hours.

2.2.4.2 Transient plasmid transfection

HEK293T cells were transiently transfected with plasmid constructs or vector plasmid (pcDNA3.1) as a control. For each well of cells to be transfected, 1 μ g of the appropriate plasmid DNA and 1.5 μ l of Lipofectamine™ 2000 were diluted separately in 200 μ l of serum-free media and incubated at room temperature for 20 minutes before 800 μ l of DMEM/Glutamax antibiotic-free media supplemented with 1% (v/v) of foetal bovine serum was added to the DNA complexes and then used to replace the medium in relevant wells. Cells were incubated at 37°C in 5% CO₂ for 8

hours. The medium was then replaced with DMEM/Glutamax supplemented with 10% (v/v) of foetal bovine serum before being treated with compounds (as indicated in Figure legends) for a further 24 hours and harvested.

2.2.5 Immunoprecipitation

Cells were placed in an ice-cold lysis buffer (500 μ l/3 wells) containing 137 mM NaCl, 2.7 mM KCl, 1 mM MgCl₂, 1 mM CaCl₂, 1% (w/v) Na deoxycolate, 10% (v/v) Glycerol, 20 mM Tris-Base, 1 mg/ml BSA, 0.5 mM Na₃VO₄, 0.2 mM PMSF, and 10 μ g/ml of both leupeptin and aprotinin (pH 8.0). The samples were homogenised using a 0.24 mm gauge needle and syringe and left to shake at 4°C for 60 minutes. After centrifugation to remove cell debris, 250 μ l of supernatant was pre-cleared with 20 μ l of protein A or G Sepharose beads (1:1 with lysis buffer; 20 minutes at 4°C) for rabbit/mouse, depending on the antibody used, before subsequent immunoprecipitation was achieved by adding 2 μ l of the anti-Degs1 or anti-p53 antibody and 20 μ l protein A or G Sepharose beads, respectively (mixed by rotation; 2 hours at 4°C). Immunoprecipitates were collected by centrifugation and washed three times with Buffer A (10 mM HEPES, 100 mM NaCl, 0.5% (v/v) NP-40, and 0.2 mM PMSF; pH 7.0) and three times with Buffer B (Buffer A without NP-40). The beads were then sedimented by centrifugation, the supernatant removed, and 20 μ l of Laemmli buffer (0.125 M Tris-HCl, 10% (v/v) 2-mercaptoethanol, 20% (v/v) glycerol, 4% (w/v) SDS and 0.004% (w/v) bromophenol blue; pH 6.7) added to the beads, which were then heated at 100°C for 3 minutes. The samples were then subjected to SDS-PAGE.

2.2.6 Preparation of the pellet and supernatant fractions:

Cells were first treated as previously described and lysed with either a sucrose-based isotonic buffer containing [10 mM Tris, pH 7.4, 1 mM EDTA and 0.25 M sucrose] or an ionic detergent lysis buffer containing [137 mM NaCl, 2.7 mM KCl, 1 mM MgCl₂, 1 mM CaCl₂, 1% (w/v) Na deoxycolate, 10% (v/v) Glycerol, 20 mM Tris-Base, 1 mg/ml BSA, 0.5 mM Na₃VO₄, 0.2 mM PMSF, and 10 µg/ml of both leupeptin and aprotinin (pH 8.0)] before being transferred to microcentrifuge tubes and centrifuged at high speed 22000 g at 4°C for 10 minutes. The pellet and supernatant fractions were carefully separated in different microcentrifuge tubes and lysed with a sample buffer containing [62.5 mM Tris-base (pH 6.7), 0.5 mM sodium pyrophosphate, 1.25 mM EDTA, 1.25% (w/v) sodium dodecyl sulphate (SDS), 0.06% (w/v) bromophenol blue, 12.5% (v/v) glycerol, and 50 mM dithiothreitol (DTT)]. Cell lysates fractions were homogenised by repeated passages (10 x) through a 0.24 mm gauge needle and syringe and kept at -20°C if not used immediately for SDS-PAGE and western blotting analysis.

2.2.7 Preparation of cell lysates for western blotting analysis of protein expression

Any floating cells present in different proportions depending on the treatment used were transferred to microcentrifuge tubes and pelleted by centrifugation at 1000 rpm for 5 minutes before being combined and lysed with the scraped adherent cells in a sample buffer containing 62.5 mM Tris-base (pH 6.7), 0.5 mM sodium pyrophosphate, 1.25 mM EDTA, 1.25% (w/v) sodium dodecyl sulphate (SDS),

0.06% (w/v) bromophenol blue, 12.5% (v/v) glycerol, and 50 mM dithiothreitol (DTT). Cell lysates were homogenised by repeated passages (10 x) through a 0.24 mm gauge needle and syringe and kept at -20°C if not used immediately for SDS-PAGE and western blotting analysis.

2.2.8 SDS-PAGE and western blotting

2.2.8.1 Preparation of polyacrylamide gels

Proteins were resolved by electrophoresis using polyacrylamide gels consisting of two layers: the resolving gel (lower layer), made of 10% (v/v) acrylamide:bis-acrylamide (29:1), 0.375 M Tris-Base (pH 8.8), 0.1% (w/v) SDS, 0.05% (w/v) ammonium persulfate (APS), and 0.025% (w/v) tetramethylethylenediamine (TEMED), and the stacking gel (upper layer) made of 4.5% (v/v) acrylamide-bis-acrylamide (29:1), 0.125 M Tris-Base (pH 6.7), 0.1% (w/v) SDS, 0.05% (w/v) APS, and 0.1% (v/v) TEMED. The resolution of proteins by electrophoresis occurs in the resolving (separating) lower layer while the stacking upper layer allows the proteins to concentrate before entering the separating layer.

2.2.8.2 Polyacrylamide gel electrophoresis (SDS-PAGE)

The Bio-Rad Mini-Protean II electrophoresis kit was used to carry out polyacrylamide gel electrophoresis of samples (typically 15 µl) loaded into the gel using a Hamilton syringe. Pre-stained molecular weight markers with known molecular weights (Table 2.1) were also loaded (typically 5 µl) into one well of the gel in order to identify the band related to the protein of interest. Electrophoresis

was carried out at a voltage of 120 V and a current limit of 1.0 mA for around 2 hours using a running buffer containing 25 mM Tris-Base, 0.21 M glycine, and 0.1% (w/v) SDS.

Table 2.1 *Pre-stained molecular weight marker standards. Molecular weight marker with known molecular weights used for comparison with bands of immunoreactive proteins of interest.*

Pre-stained Protein	Molecular weight (kDa)
α_2-Macroglobulin from equine serum	180
β-galactosidase from <i>E.coli</i>	116
Lactoferrin From human milk	90
Pyruvate kinase From rabbit muscle	58
Fumarase From porcine heart	48.5
Lactic dehydrogenase From rabbit muscle	36.5
Triosephosphate isomerase From rabbit muscle	26.6

2.2.8.3 Transfer to nitrocellulose membranes

A Bio-Rad Mini Trans-Blot kit filled with a buffer containing 25 mM Tris-Base, 0.21 M glycine, and 20% (v/v) methanol was used to carry out the electrophoretic transfer of the resolved proteins from the gel to a nitrocellulose membrane. A voltage of 100 V with a current limit of 0.6 mA for 60 minutes was applied for the transfer to occur.

2.2.8.4 Western blotting

Nitrocellulose membranes were incubated for 60 minutes at room temperature in a blocking solution consisting of 3% (w/v) non-fat dry milk in TBST (10 mM Tris-Base, 100 mM NaCl, 0.1% (v/v) Tween-20; pH 7.4) or 5% (w/v) bovine serum albumin (BSA), depending on the primary antibody to be used. Membranes were then incubated with the antibody specific for the protein of interest to be detected (typically diluted at 1:1000 in 1% (w/v) BSA) in TBST overnight with gentle agitation at 4°C. Nitrocellulose membranes were then washed 3 times (7 minutes each) with TBST to remove any unbound antibody. Membranes were then incubated in horseradish peroxidase-conjugated secondary antibody (anti-mouse or anti-rabbit IgG, depending on the primary antibody origin) diluted at a ratio of 1:26,000 in 1% (w/v) non-fat dry milk or 1% (w/v) BSA in TBST for 60 minutes at room temperature. Membranes were washed with 3 further washes (7 minutes each) to remove any excess antibody. Membranes were then incubated in enhanced chemiluminescence (ECL) reagent (developing solution) that provides the substrate for the peroxidase, thereby allowing the detection of immunoreactive proteins. The developing solution was freshly prepared each time by mixing equal volumes of a solution containing 0.04% (w/v) luminol, 0.1 M Tris-Base (pH 8.5), and 0.016% (w/v) *p*-coumaric acid and a solution containing 2% (v/v) H₂O₂ and 0.1 M Tris-Base (pH 8.5).

Membranes were incubated for 2 minutes in the ECL mixture at room temperature, placed between two transparent plastic sheets in a radiography cassette, and exposed to X-ray film before being developed through an X-ray film developing machine (X-

OMAT or JP-33). Immunoreactive proteins appeared as dark bands on the film, and their molecular weights were estimated by comparing their mobility on SDS-PAGE to that of pre-stained molecular weight markers with known molecular weights.

2.2.8.5 Stripping and re-probing nitrocellulose membranes

Bound antibodies were removed by incubating membranes at 70°C for 1 hour with gentle agitation in a buffer containing 62.5 mM Tris-HCl (pH 6.7), 2% (w/v) SDS, and 100 mM β -mercaptoethanol. Membranes were washed three times with TBST (10 minutes each) in gentle agitation before being incubated overnight with the specific primary antibody for the protein of interest. In each experiment, blots were stripped and re-probed with an antibody known to be unaffected with treatments (such as anti-actin or anti-GAPDH) to ensure comparable protein loading between samples.

2.2.8.6 Quantification and statistical analysis of western blots

Protein bands' densities were determined using Image J software program (Scion Corporation, Frederick, MD) and expressed as the ratio of protein of interest versus GAPDH (or actin) and represented as mean ratio \pm SEM for fold changes of three separate experiments. Statistical analysis was undertaken using Unpaired *t*-test or one way ANOVA Dunnet's or Bonferroni's multiple comparisons test and considered significant when $*p < 0.05$.

2.2.9 [³H]-Thymidine incorporation assay

The thymidine incorporation assay measures the amount of a radioactive nucleoside, [³H]-thymidine, incorporation into new strands of chromosomal DNA during mitotic cell division. This gives a measure of the extent of cell division and proliferation in response to a test agent (Haugland, 2005). HEK293T cells were seeded in 24-well plates and maintained overnight in 1 ml of complete DMEM medium. Once the cells reached 60%–70% confluency, they were treated with compounds as indicated in the Figure legends or a vehicle control (0.1% DMSO) for 24 hours. Five hours before the end of the incubation period, [³H] thymidine (37 kBq) was added to each well. Cells were then washed (three 10-minute washes) on ice with 1 ml of ice-cold 10% (w/v) trichloroacetic acid (TCA). Residual nuclear material, including newly synthesised DNA, was dissolved in 0.25 ml of 0.1% (w/v) SDS/0.3M NaOH. Samples were transferred to scintillation vials and mixed with 2 ml of a Scintisafe 2 scintillation cocktail before measuring the radioactivity incorporated using a liquid scintillation counter.

2.2.10 Luciferase reporter assay

The luciferase reporter assay is commonly used to study gene expression at the transcriptional level. Luciferases are oxidative enzymes originating from different species, which enable the organisms to “bioluminesce”, or emit light when expressed. Firefly luciferase is the most famous enzyme catalysing a chemical reaction that converts luciferin to oxyluciferin, leading to light emission (Figure 2.2). This chemical reaction is highly efficient as nearly all the energy put into the reaction

is promptly converted to light, making it a great tool for studying transcriptional activity (Allard and Kopish, 2008).

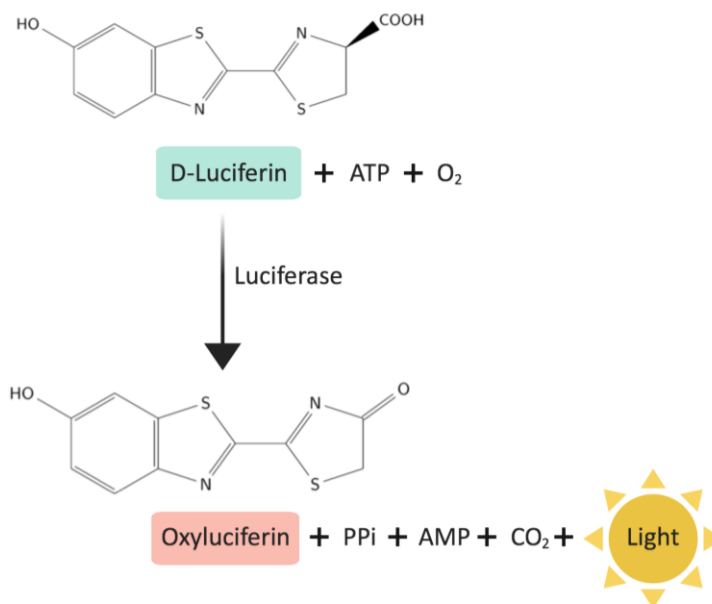


Figure 2.2 Luciferase reaction. Bioluminescent reaction scheme which involves luciferase enzyme that uses ATP to catalyse the two-step oxidation of luciferin to oxyluciferin that, in turn, generates the light bioluminescence signal.

NCTC-NF- κ B and NCTC-AP-1 reporter cells were separately seeded in a 96-well plate at a density of 10,000 cells per well in 200 μ L of complete DMEM medium (50,000 cells/ml) and incubated overnight for 24 hours. Cells were quiesced with 40 μ L/well of serum-free phenol red-free DMEM medium for another 24 hours. NCTC-NF- κ B and NCTC-AP-1 reporter cells were then pre-treated with inhibitors at the indicated concentration for 10 minutes before the addition of TNF (15 ng/ml) or PMA (100 nM), respectively, and incubated for 4 hours. The medium was then removed, and 100 μ L of complete lysis buffer containing 25 mM Tris Base (pH7.8), 8 mM MgCl₂, 1% Triton X 100, 15% (v/v) Glycerol with 1 mM ATP, 1% BSA, 1

mM DTT, and 0.2 mM Luciferin were added to each well and incubated at room temperature in the dark for 5 minutes before luminescence was measured using a Wallac 1420 Victor plate reader (Perkin-Elmer, UK) using Iso96lum. GraphPad Prism 8 software was used to analyse data, and results were expressed as means with SEM.

2.2.11 Immunofluorescence microscopy

Immunofluorescence microscopy is a powerful technique used extensively by researchers to measure both the localisation and endogenous expression levels of a target protein of interest. This method uses specific antibodies that are conjugated (directly or indirectly) to a fluorescent dye to visualise the distribution of the protein of interest throughout the sample (Miller and Shakes, 1995). Cells were plated on autoclaved glass coverslips, each of which was placed in one well of a 12-well plate, and treated or transfected as previously described. Cells were fixed by a 10-minute incubation in 3.7% (v/v) formaldehyde in phosphate-buffered saline (PBS) [0.01 M phosphate buffer, 0.0027 M potassium chloride and 0.137 M sodium chloride, pH 7.4] then kept at 4°C overnight in PBS to enhance the cells' sticking down on coverslips. Cells were permeabilised using 0.1% (v/v) Triton X-100 in PBS for 1 minute. Cells were then incubated with a blocking solution (5% (v/v) FCS and 1% (w/v) BSA in PBS) for 30 minutes at room temperature, followed by 60 minutes of incubation at room temperature with the primary (anti-p53) antibody (1:100 dilution in the blocking solution). Coverslips were then washed three times with PBS and incubated for another 60 minutes at room temperature with the secondary antibody (TRITC-conjugated anti-mouse IgG according to primary antibody used) at 1:100

dilution in the blocking solution. The coverslips were then washed three times with PBS and mounted on glass slides using Vectashield® hard set mounting medium containing 4',6-Diamidino-2-phenylindole (DAPI) to stain the nuclei. Fluorescence was visualised using a Leica SP5 confocal microscope through HC PL APO CS2 20x/0.75 DRY lense with 20x magnification using Velocity software.

2.2.12 Lipidomics (Cell pellet preparation for mass spectrometry for sphingolipid analysis)

Lipidomics refers to the large-scale study of pathways and networks of diversified cellular lipids (lipidomes) in a biological system that describes a complete lipid profile within a cell. It requires advanced and complementary analytical techniques as well as multiple statistical tools (Wenk, 2005). HEK293T cells were treated with a vehicle—namely, DMSO (0.1% v/v final), ABC294640 (25 μ M), or SKI (10 μ M)—for 24 hours, then carefully rinsed twice with 1 ml of ice-cold PBS before being scraped into ice-cold PBS. Cells were pelleted by centrifugation (180 g, 4°C, 3 minutes), and the supernatant was carefully removed. The cell pellet was snap frozen in liquid nitrogen for 5 seconds before being stored in -80°C for sphingolipid analysis, which was conducted by Samuel L. Kelly and Alfred H. Merrill in School of Biological Sciences and Petit Institute for Bioengineering and Bioscience (Georgia Institute of Technology, Atlanta, Georgia, USA) as previously described in (Shaner *et al.*, 2009; Sullards *et al.*, 2011), using liquid chromatography, electrospray-ionization tandem mass spectrometry, and multiple reaction monitoring for quantitation.

2.2.13 Statistical analysis

Experiments were repeated at least three times, unless otherwise stated. GraphPad Prism 8 software was used to analyse data, and results were expressed as mean \pm standard error of the mean (SEM), unless otherwise stated. Statistical analysis was performed using Unpaired *t*-test or one way ANOVA with Dunnet's post-hoc multiple comparisons test and considered significant when $p < 0.05$.

CHAPTER 3:

**THE ROLE OF DIHYDROCERAMIDE
DESATURASE IN REGULATING THE
SURVIVAL OF HUMAN EMBRYONIC
KIDNEY CELLS**

CHAPTER 3: THE ROLE OF DIHYDROCERAMIDE DESATURASE IN REGULATING THE SURVIVAL OF HUMAN EMBRYONIC KIDNEY CELLS

3.1 INTRODUCTION

Dihydroceramides were primarily considered as a biologically inactive intermediate in the *de novo* ceramide (Cer) biosynthesis. However, they are now regarded as eliciting essential cellular responses, including autophagy, apoptosis, and cell proliferation, that play vital roles in health and the aetiology of several human diseases (Siddique *et al.*, 2015). Dihydroceramide desaturase (Dggs1) is the last enzyme in the *de novo* synthesis of Cer. Blocking this enzyme, which increases levels of dihydroceramides (dhCers), can be achieved by several drugs, including fenretinide (Fabrias *et al.*, 2012). Many studies have shown that cells treated with fenretinide produce high levels of dhCers (Rahmaniyan *et al.*, 2011; Apraiz *et al.*, 2011; Bikman *et al.*, 2012; Yasuo *et al.*, 2013), resulting in autophagy (Zheng *et al.*, 2006; Holliday Jr *et al.*, 2013). Gagliostro *et al.* (2012), demonstrated that the accumulation of dhCers in response to the exogenous addition of dhCers or Dggs1 inhibitors led to autophagy and endoplasmic reticulum (ER) stress (Gagliostro *et al.*, 2012). However, effects of some Dggs1 inhibitors on autophagy appear to be unrelated to dhCers (Casasampere *et al.*, 2017).

The literature details significant controversy regarding the involvement of dhCers in autophagy related to either cell survival or cell death. On one hand, cells deficient in

Degs1 exhibit anti-apoptotic effects through the stimulation of Akt and autophagy (Siddique *et al.*, 2013), while other reports have demonstrated that Degs1 inhibition leads to cellular death through the activation of autophagy or apoptosis (Gagliostro *et al.*, 2012; Hernández-Tiedra *et al.*, 2016). There might be some functional interaction between Degs1 and SK, as SK inhibitors including DMS [D-erythro-N,N-dimethylsphingosine] and SKi [2-(phydroxyanilino)-4-(p-chlorophenyl) thiazole] have been shown to abolish fenretinide resistance or synergise with fenretinide to promote cancer cellular death (Wang *et al.*, 2008; Illuzzi *et al.*, 2010; Apraiz *et al.*, 2011). Furthermore, Illuzzi *et al.* (2010) used the dual SK inhibitor SKi to establish a connection between SK1 and A2780 ovary cancer cell resistance to fenretinide (Illuzzi *et al.*, 2010). Treating fenretinide-resistant cells with SKi efficiently lowered the production of S1P and sensitised cells to fenretinide cytotoxic effects, while a combination treatment of fenretinide/SKi resulted in a dramatic rise in dhCer and sphinganine (dhSph) levels in cells. Of note, cells treated with SKi alone raised dhCer cellular levels, but not Cer levels, although this increase was much less than that observed with fenretinide alone or the fenretinide/SKi combination. Furthermore, Gao *et al.* (2012) demonstrated that SKi increased N-hexadecanoyldihydrosphingosine (C16 dhCer) in A498 kidney adenocarcinoma cells (Gao *et al.*, 2012). Unexpectedly, none of the referenced studies discussed or addressed the molecular mechanisms underlying these effects. In addition, Degs1 inhibitors have been shown to reverse fenretinide-apoptotic effects in endothelial cells (Erdreich-Epstein *et al.*, 2002; Wu *et al.*, 2001), suggesting that fenretinide might induce a 'gain of function' in Degs1 that can be blocked by Degs1 inhibitors. In contrast, other studies using different cell types failed to discover a role for

sphingolipids in fenretinide-induced apoptosis (Uyama *et al.*, 2005). Moreover, Dggs1 inhibition using siRNA to deplete the enzyme, or other pharmacological agents results in strong cellular resistance to apoptosis induced by various stimuli (Gagliostro *et al.*, 2012; Siddique *et al.*, 2013; Siddique *et al.*, 2012; Breen *et al.*, 2013). Our research group found that the sphingosine kinase inhibitors SKi and ABC294640 [3-(4-chlorophenyl)-adamantane-1-carboxylic acid (pyridin-4-ylmethyl)amide] affected Dggs1 activity (McNaughton *et al.*, 2016). ABC294640 induced proteasomal degradation of SK1 and Dggs1 while increasing expression of p53 and p21 and this resulted in the senescence of androgen-independent LNCaP-AI prostate cancer cells (McNaughton *et al.*, 2016). In addition, Venant *et al.* (2015) demonstrated that inhibitory effects of SKi and ABC294640 on Dggs1 resulted in higher levels of dhCer in prostate cancer cells (Venant *et al.*, 2015). Furthermore, SKi has been proposed to indirectly inhibit Dggs1 activity through a cytochrome B5 reductase dependent mechanism (Cingolani *et al.*, 2014) which results in higher levels of dhCer in ovarian and prostate cancer cells (Illuzzi *et al.*, 2010; Loveridge *et al.*, 2010).

The homeostasis of folding proteins in the ER lumen is protected by the unfolded protein response (UPR) in cases where an imbalance occurs between levels of unfolded proteins (Volmer and Ron, 2015). This homeostatic response is regulated by three known ER stress sensors: IRE1, PERK, and ATF6 (Volmer and Ron, 2015). The process involves detachment of the ER chaperone BiP from the luminal domains of ER stress sensors (Volmer *et al.*, 2013). The human homolog IRE1 α is responsible for splicing XBP-1 mRNA that converts XBP-1 from a full length XBP-

1u isoform to the spliced XBP-1s isoform, the latter of which is a potent transcriptional activator promoting the expression of various UPR responsive genes (Lee *et al.*, 2002). PERK is a kinase that phosphorylates eukaryotic eIF2 α to repress protein translation, resulting in the inhibition of protein synthesis (Harding *et al.*, 1999). ER stress also up-regulates components of the ERAD pathway that enhance the clearance of misfolded proteins from the ER (Travers *et al.*, 2000). Previous studies have shown that changes in ER lipid composition, especially Cer/dhCer, regulated through Degr1, is responsible for the activation of ER stress which contributes to cell survival/apoptosis (Volmer *et al.*, 2013; Gagliostro *et al.*, 2012; Spassieva *et al.*, 2009; Volmer and Ron, 2015). The activation of ER stress leads to cell survival through the promotion of UPR, while a sustained activation of UPR appears to result in apoptosis (White-Gilbertson *et al.*, 2013). A recent study by Wallington-Beddoe *et al.* (2017) demonstrated that SK2 inhibitors, ABC294640 and K145 [3-(2-amino-ethyl)-5-[3-(4-butoxyphenyl)-propylidene]-thiazolidine-2,4-dione] promote the induction of ER stress. In this case, K145 induced expressions of ER stress sensors XBP-1s and p-eIF2 α (Wallington-Beddoe *et al.*, 2017). Moreover, synergistic cell apoptosis was seen in myeloma cells treated with K145 and bortezomib, the latter of which activated ER stress and promoted UPR through the stimulation of the IRE1, JNK, and p38 MAPK pathways (Wallington-Beddoe *et al.*, 2017). In addition, Evangelisti *et al.* (2014) reported that treatment of T-cell lymphoblastic leukemic (T-ALL) cells with SKi promoted ER stress/UPR, leading to survival of these cells through autophagy (Evangelisti *et al.*, 2014). Therefore, ABC294640 and SKi could be involved in both “apoptotic”-promoting UPR or “survival” UPR related to the regulation of Degr1. In this study, we investigated the

controversial role of Degr1 in both cell survival/apoptosis by using Degr1 inhibitors, and certain sphingosine kinase inhibitors, known to modulate the activity of Degr1.

3.2 RESULTS

3.2.1 Effect on Degr1 expression in HEK293T and parental

HEK293 cells

The study initially focused on investigating the mechanism by which the SK1/SK2 inhibitor SKi and the SK2 inhibitor ABC294640 regulate the survival of HEK293T. Previous studies have shown that ABC294640 induces the proteasomal degradation of Degr1 in androgen-independent LNCaP-AI cells (McNaughton *et al.*, 2016) to produce a senescent response in these cells. Therefore, the effect of these SK inhibitors on Degr1 expression levels in HEK293T cells was investigated.

3.2.2 Effect of SKi and ABC294640 on Degr1 expression in

HEK293T cells

Degr1 is expressed as a 32 kDa native band identified with an anti-Degr1 antibody on western blots in HEK293T cells (Figure 3.1). Interestingly, when treating these cells with the SK1/SK2 inhibitor SKi (10 μ M, 24 hours), there is an induction of a ladder of higher protein bands with molecular masses ranging from M_r = 40–130 kDa that cross-react with the anti-Degr1 antibody (Figure 3.1). These higher molecular mass protein bands appear to be post-translationally modified forms of Degr1. Degr1 siRNA was used to verify the identity of ladderized proteins that cross-reacted with the anti-Degr1 antibody. Thus, HEK293T cells were transfected with Degr1 siRNA (100 nM, 48 hours), which decreased the immunoreactivity of the native 32 kDa protein band as well as ladderized proteins formed in response to SKi (Figure

3.2A), resulting in an 80% reduction in the expression of the 46 kDa protein (Figure 3.2B). The significant reduction of the higher molecular mass protein bands in response to Degr1 siRNA confirms their identity of being post-translationally modified forms of Degr1. In contrast, treatment with the SK2 inhibitor ABC294640 (25 μ M, 24 hours) alone did not induce the Degr1 ladder (Figure 3.1).

The second method used to confirm the identity of the proteins in the ladder was to immunoprecipitate post-translationally modified forms of Degr1 with the anti-Degr1 antibody. The isotonic lysis buffer containing [10 mM Tris, pH 7.4, 1 mM EDTA and 0.25 M sucrose] failed to release Degr1 from the pellet fraction into the high-speed supernatant (Figure 3.3A). Therefore, the isotonic-sucrose-based lysis buffer was replaced with an ionic detergent lysis buffer containing [137 mM NaCl, 2.7 mM KCl, 1 mM MgCl₂, 1 mM CaCl₂, 1% (w/v) Na deoxycolate, 10% (v/v) Glycerol, 20 mM Tris-Base, 1 mg/ml BSA, 0.5 mM Na₃VO₄, 0.2 mM PMSF, and 10 μ g/ml of both leupeptin and aprotinin (pH 8.0)] (Heckelman *et al.*, 1996), which successfully solubilised native Degr1 and those proteins constituting the ladder, such that they are released into a high-speed supernatant fraction (Figure 3.3B). Therefore, Degr1 appears to be localised to non-ionic detergent-resistant membranes in HEK293T cells. Thus, this method was used to carry out the immunoprecipitation of the post-translationally modified forms of Degr1 by the anti-Degr1 antibody. The native Degr1 and ladder proteins were solubilised into the supernatant fraction and immunoprecipitated while resulting immunoprecipitates were resolved by western blotting in the presence and absence (negative controls) of Degr1 antibody to avoid any false positive results (Figure 3.4). Results showed that Degr1 and the ladder

proteins were immunoprecipitated with the Degr1 antibody providing an additional confirmation to the identity of the Degr1 ladder proteins (Figure 3.4).

The ladder of immunoreactive Degr1 bands induced by SKi might suggest that this enzyme undergoes polyubiquitination in response to SKi. Polyubiquitination is catalysed by a family of enzymes called E3 ligases (Zheng and Shabek, 2017). One member of this family, Mdm2, regulates the polyubiquitination of p53 (Moll and Petrenko, 2003). As SK inhibitors have been linked to p53 regulation (Lima *et al.*, 2018), we tested the effect of nutlin, an E3 ligase inhibitor, on the formation of the Degr1 ladder. HEK293T cells were pre-treated with the E3 ligase inhibitor of Mdm2, nutlin (10 μ M, 30 minutes), before the addition of SKi (for 24 hours), and this reduced the formation of the Degr1 ladder (Figure 3.1). Additional studies in the laboratory by others using HA-ubiquitin-transfected HEK293T cells and the immunoprecipitation of HA-ubiquitin have confirmed that SKi promotes the polyubiquitination of Degr1 (Alsanafi *et al.*, 2018).

To establish whether agents that affect the activity of Degr1 also induce the formation of polyubiquitinated Degr1, fenretinide was used. This potential anti-cancer drug has been shown to regulate the activity of Degr1 and stimulates oxidative stress through the accumulation of reactive oxygen species (ROS) (Wu *et al.*, 2001). The treatment of cells with fenretinide also induced the appearance of polyubiquitinated forms of Degr1 (Figure 3.1).

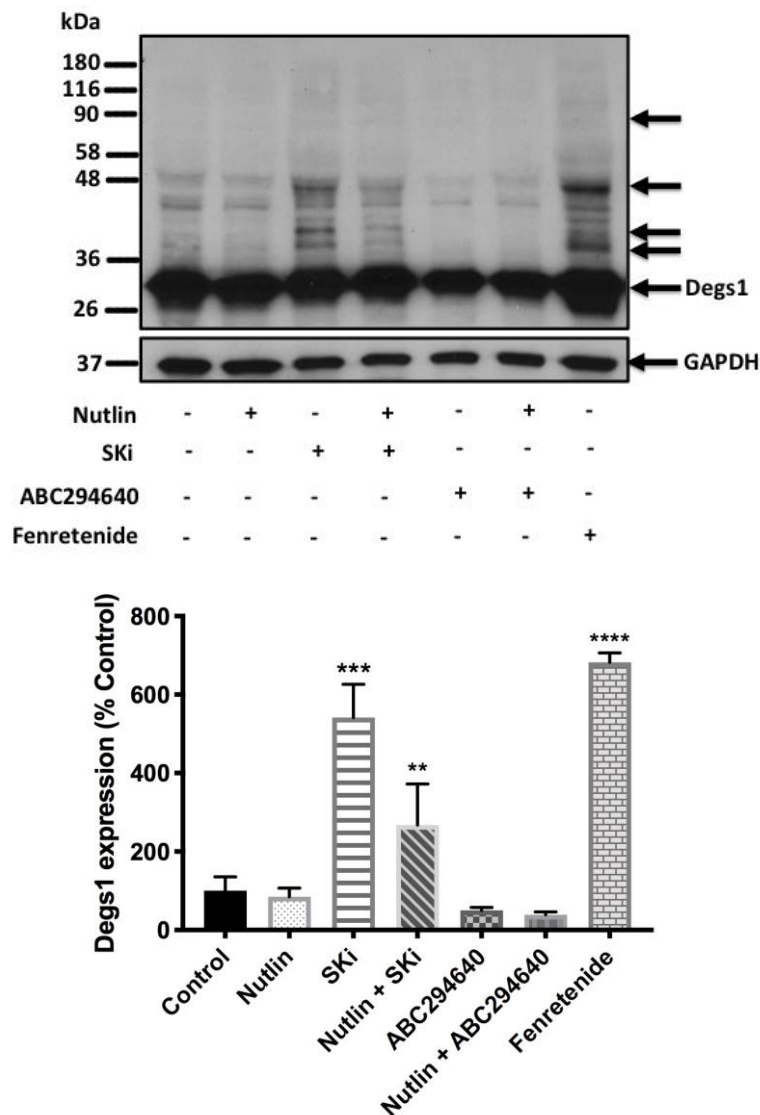


Figure 3.1 *Effect of SKi and ABC294640 on Degr1 protein expression in HEK293T cells.* HEK293T cells were cultured in complete medium containing 10% FCS until ~70% confluent. Cells were pre-treated with Nutlins (10 μ M, 30 minutes) with and without addition of SKi (10 μ M) or ABC294640 (25 μ M) or Fenretenide (1 μ M) or with the vehicle alone (DMSO 0.1% v/v) for 24 hours. Degr1 expression was detected using SDS PAGE and western blotting probed with anti-Degr1 antibody. Blots were stripped and re-probed with anti-GAPDH antibody to ensure comparable protein loading. A representative western blot is shown of an experiment performed at least three independent times. Also shown is the densitometric quantification of post-translationally modified Degr1/GAPDH ratio immunoreactivity of (Mr 46 kDa), expressed as a percentage of the control (Control=100%). The data was expressed as means \pm SEM for n=3 experiments and analysed by one-way ANOVA multiple comparisons tests, **p<0.01 for Nutlin/SKi vs SKi, ***p<0.001 for SKi vs control, and ****p<0.0001 for Fenretenide vs control.

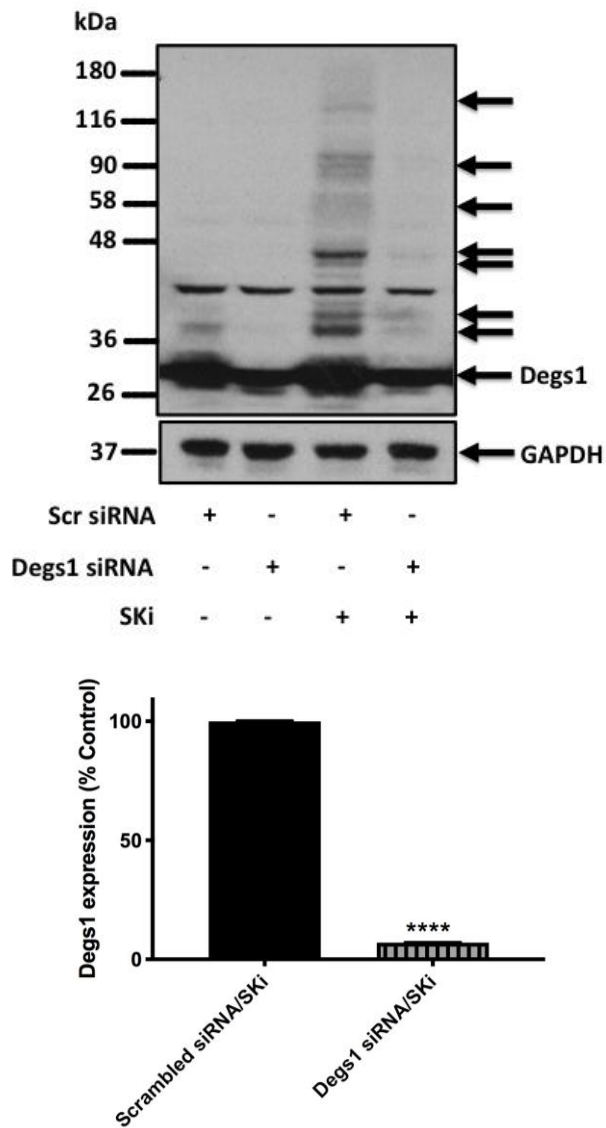


Figure 3.2 Confirmation of SKi-induced Degr1 ladder identity using siRNA in HEK293T cells. HEK293T cells were cultured in complete medium containing 10% FCS until ~70% confluent. Cells were transiently transfected with Degr1 siRNA or scrambled siRNA at a final concentration of 100 nM in antibiotic free medium for 48 hrs before being treated with and without SKi (10 μ M) or with the vehicle alone (DMSO 0.1% v/v) for further 24 hours. Degr1 expression was detected using SDS PAGE and western blotting with anti-Degr1 antibody. Blots were stripped and re-probed with anti-GAPDH antibody to ensure comparable protein loading. A representative western blot is shown of an experiment performed at least three independent times. Also shown is the densitometric quantification of post-translationally modified Degr1/GAPDH ratio immunoreactivity of (Mr 46 kDa), expressed as a percentage of the control (Scrambled siRNA/SKi) (Control=100%). The data was expressed as means \pm SEM for n=3 experiments and analysed by Unpaired t-test, **** $p < 0.0001$ for Degr1 siRNA/SKi vs Scrambled siRNA/SKi.

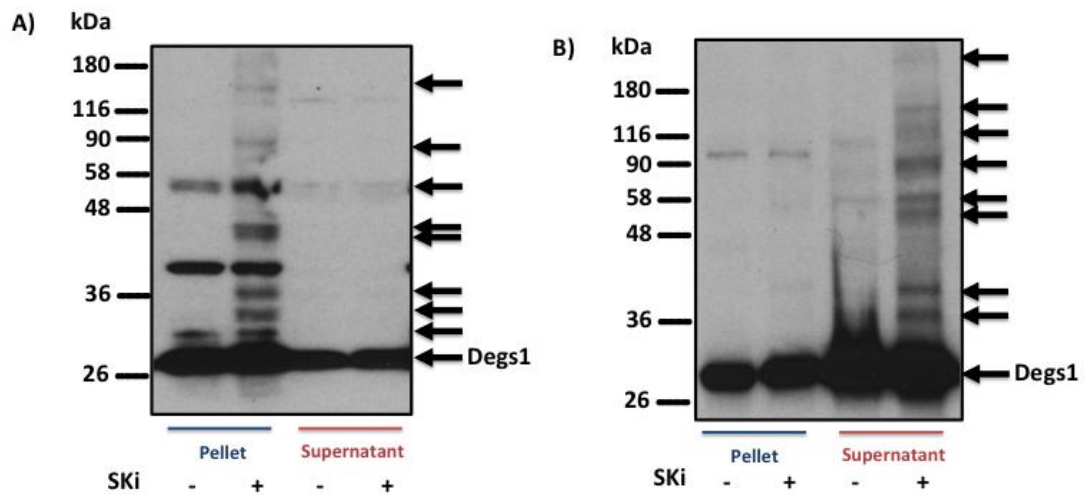


Figure 3.3 *Degr1* location change according to cell harvesting method in **HEK293T** cells. **HEK293T** cells were cultured in complete medium containing 10% FCS until ~70% confluent. Cells were treated with SKi (10 μ M) or with the vehicle alone (DMSO 0.1% v/v) for 24 hours. A) Cells were lysed with a sucrose-based isotonic buffer and *Degr1* was present in the high-speed pellet fraction. A representative western blot is shown of an experiment performed at least three independent times. B) Cells were lysed in 1% deoxycholate lysis buffer and *Degr1* was located in the high-speed supernatant fraction. *Degr1* expression was detected using SDS PAGE and western blotting with anti-*Degr1* antibody. A representative western blot is shown of an experiment performed at least three independent times.

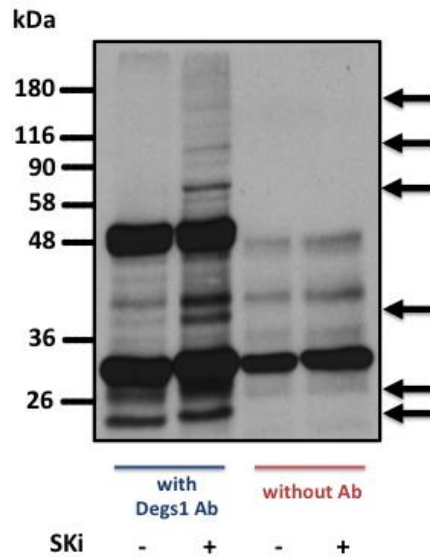


Figure 3.4 *Degr1* immunoprecipitation in HEK293T cells. HEK293T cells were cultured in complete medium containing 10% FCS until ~70% confluent. Cells were treated with SKi (10 μ M) or with the vehicle alone (DMSO 0.1% v/v) for 24 hours. *Degr1* was immunoprecipitated using 1% deoxycholate lysis buffer with/without *Degr1* antibody. The resulting immunoprecipitate were resolved by SDS PAGE and western blotted with anti-*Degr1* antibody. A representative western blot is shown of an experiment performed at least three independent times.

3.2.3 Effect of proteasome inhibitors on the polyubiquitination of Degr1 in HEK293T cells

The polyubiquitination of proteins targets them for proteasomal degradation (Schrader *et al.*, 2009); therefore, we assessed the effect of proteasome inhibitors on the formation of the Degr1 ladder. HEK293T cells were treated with the proteasome inhibitor MG132 (10 μ M, 24 hours), which induced the formation of a Degr1 ladder similar to that induced with the SK1/SK2 inhibitor SKi (Figures 3.5 and 3.6). However, additional lower molecular mass bands below 32 kDa ($M_r=16-130$ kDa) (Figures 3.5 and 3.6) were also detected on western blots with the anti-Degr1 antibody. The additional lower immunoreactive protein bands might represent proteasomal degradation products that are trapped from being further processed due to proteasome inhibition. Next, we pre-treated cells with the proteasome inhibitor MG132 (10 μ M, 30 mins) prior to treatment with SKi, and this resulted in an increased formation of the Degr1 ladder forms, with a $M_r > 50$ kDa (Figures 3.5 and 3.6). In contrast, the combination of the proteasome inhibitor MG132 with the SK2 inhibitor ABC294640 reduced the formation of this ladder (Figure 3.5), suggesting that ABC29460 (at 25 μ M) prevents the polyubiquitination of Degr1.

The Degr1 siRNA transfection (100 nM, 48 hours) of HEK293T cells was used to confirm the identity of ladderized proteins that cross-reacted with the anti-Degr1 antibody, which decreased the intensity of the native 32 kDa protein band as well as ladderized proteins produced in response to either SKi or MG132 (Figure 3.6). Another (therapeutic) proteasome inhibitor, bortezomib (5 nM–10 μ M, 24 hours), was assessed in HEK293T cells and it induced a similar effect compared with

MG132 (Figure 3.7). These outcomes suggest that Degr1 is subject to ubiquitin-proteasomal degradation in HEK293T cells and that this can be modulated by SKI and MG132/bortezomib.

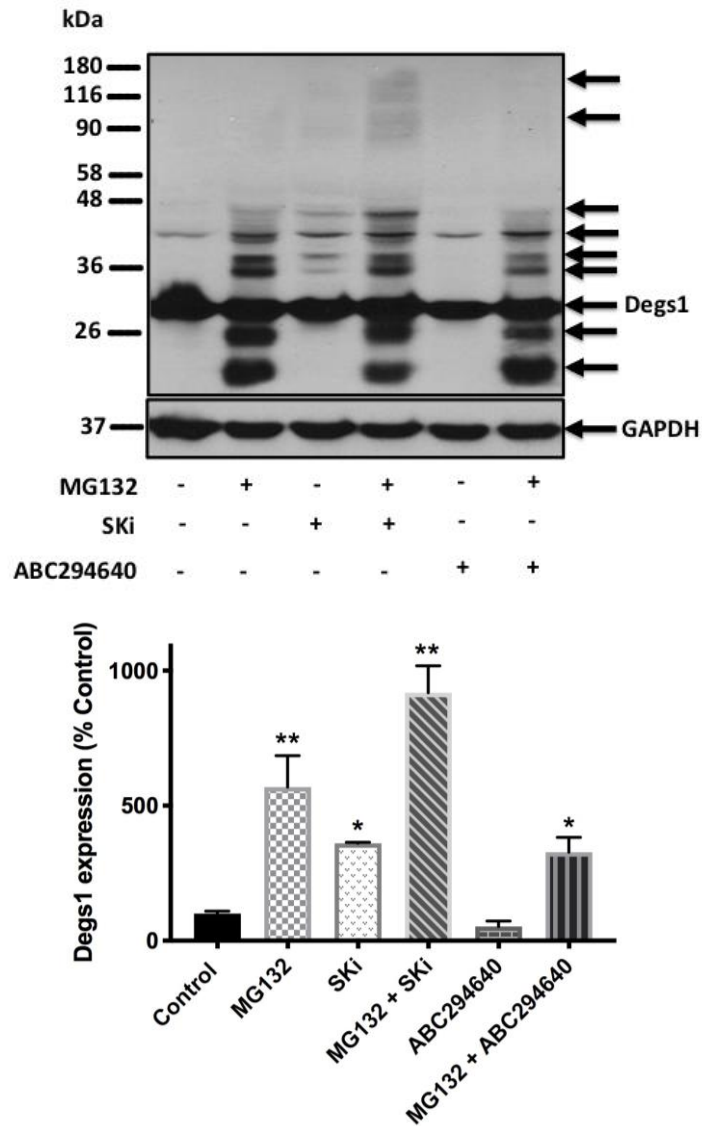


Figure 3.5 Effect of MG132 on Degr1 protein expression in HEK293T cells. HEK293T cells were cultured in complete medium containing 10% FCS until ~70% confluent. Cells were pre-treated with MG132 (10 μ M, 30 minutes) before addition of SKi (10 μ M) or ABC294640 (25 μ M) or with the vehicle alone (DMSO 0.1% v/v) for 24 hours. Degr1 expression was detected using SDS PAGE and western blotting with anti-Degr1 antibody. Blots were stripped and re-probed with anti-GAPDH antibody to ensure comparable protein loading. A representative western blot is shown of an experiment performed at least three independent times. Also shown is the densitometric quantification of post-translationally modified Degr1/GAPDH ratio immunoreactivity of (Mr 36 kDa), expressed as a percentage of the control (Control=100%). The data was expressed as means \pm SEM for n=3 experiments and analysed by one-way ANOVA multiple comparisons test, * p <0.05 for SKi vs control or MG132/ABC294640 vs MG132 and ** p <0.01 for MG132 vs control or MG132/SKi vs MG132.

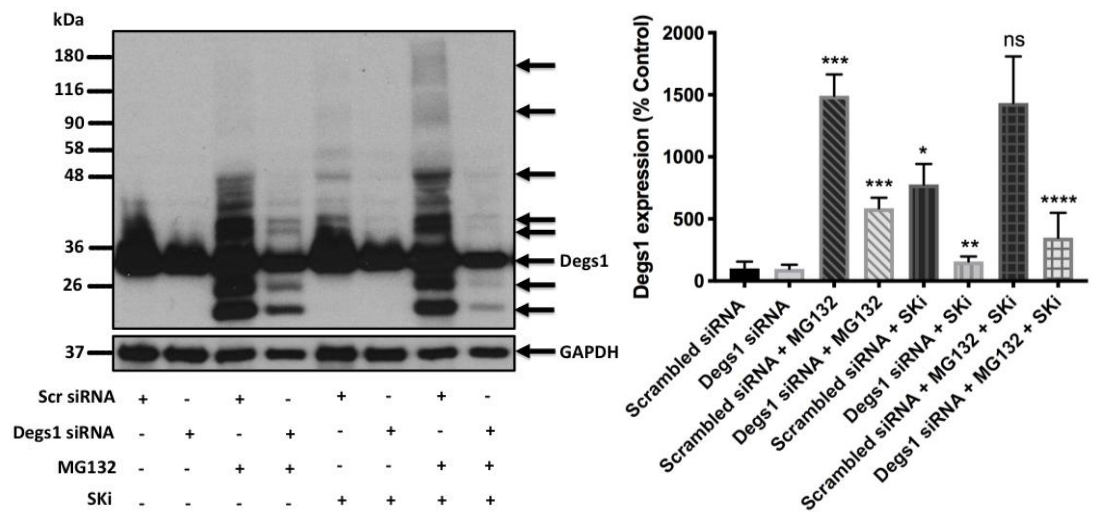


Figure 3.6 Confirmation of MG132 and MG132/SKi-induced Degr1 ladder identity using siRNA. HEK293T cells were cultured in complete medium containing 10% FCS until ~70% confluent. Cells were transiently transfected with Degr1 siRNA or scrambled siRNA at a final concentration of 100 nM in antibiotic free medium for 48 hrs. Cells were then pre-treated with MG132 (10 μ M, 30 minutes) before addition of SKi (10 μ M) or with the vehicle alone (DMSO 0.1% v/v) for further 24 hours. Degr1 expression was detected using SDS PAGE and western blotting with anti-Degr1 antibody. Blots were stripped and re-probed with anti-GAPDH antibody to ensure comparable protein loading. A representative western blot is shown of an experiment performed at least three independent times. Also shown is the densitometric quantification of post-translationally modified Degr1/GAPDH ratio immunoreactivity of (Mr 36 kDa), expressed as a percentage of the control (Control=100%). The data was expressed as means \pm SEM for n=3 experiments and analysed by one-way ANOVA multiple comparisons test, * p <0.05 Scrambled siRNA/SKi vs Scrambled siRNA, ** p <0.01 for Degr1 siRNA/SKi vs Scrambled siRNA/SKi, *** p <0.001 for Scrambled siRNA/MG132 vs Scrambled siRNA or Degr1 siRNA/MG132 vs Scrambled siRNA/MG132, **** p <0.0001 for Degr1 siRNA/MG132/SKi vs Scrambled siRNA/MG132/SKi, and ns denotes not statistically significant (p value >0.05) for Scrambled siRNA/MG132/SKi vs Scrambled siRNA/MG132.

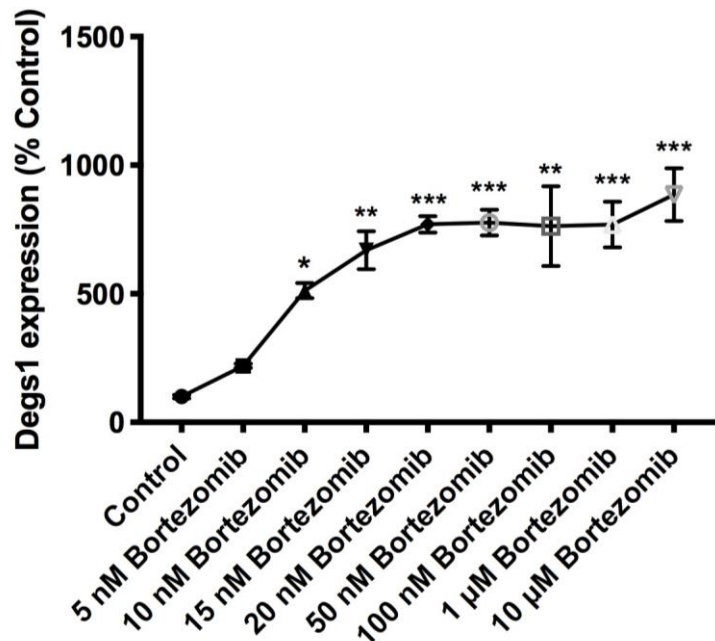
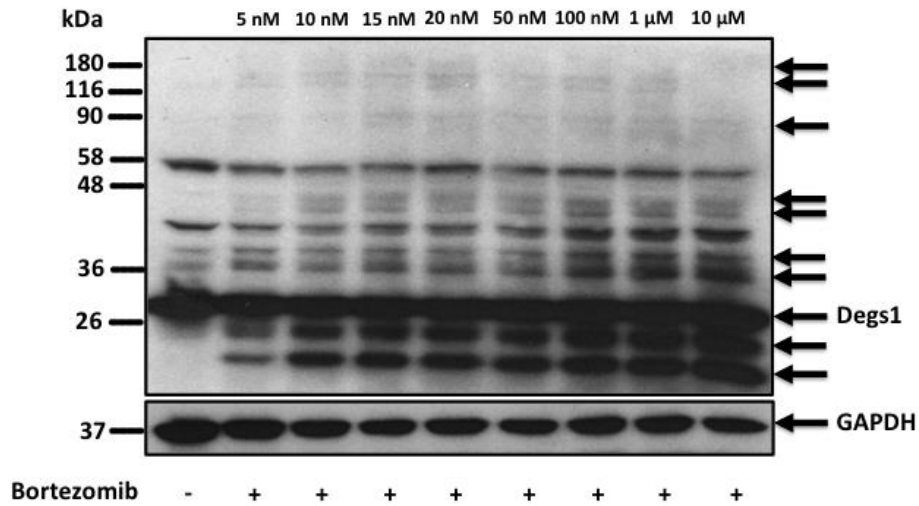


Figure 3.7 Effect of Bortezomib on Degr1 protein expression in HEK293T cells. HEK293T cells were cultured in complete medium containing 10% FCS until ~70% confluent. Cells were treated with Bortezomib (5 nM-10 μM) or with the vehicle alone (DMSO 0.1% v/v) for 24 hours. Degr1 expression was detected using SDS PAGE and western blotting with anti-Degr1 antibody. Blots were stripped and re-probed with anti-GAPDH antibody to ensure comparable protein loading. A representative western blot is shown of an experiment performed two independent times. Also shown is the densitometric quantification of post-translationally modified Degr1/GAPDH ratio immunoreactivity of (Mr 46 kDa), expressed as a percentage of the control (Control=100%). The data was expressed as means \pm SEM for n=3 experiments and analysed by one-way ANOVA Dunnett's multiple comparisons test, * $p < 0.05$ vs control, ** $p < 0.01$ vs control, and *** $p < 0.001$ vs control.

3.2.4 Effect of SKi, ABC294640, and MG132 on Degr1 expression in parental HEK293 cells

Similar results were achieved with the parental HEK293 cells treated with SKi, ABC294640, or MG132 in terms of the Degr1 ladder formation, as shown in Figure 3.8.

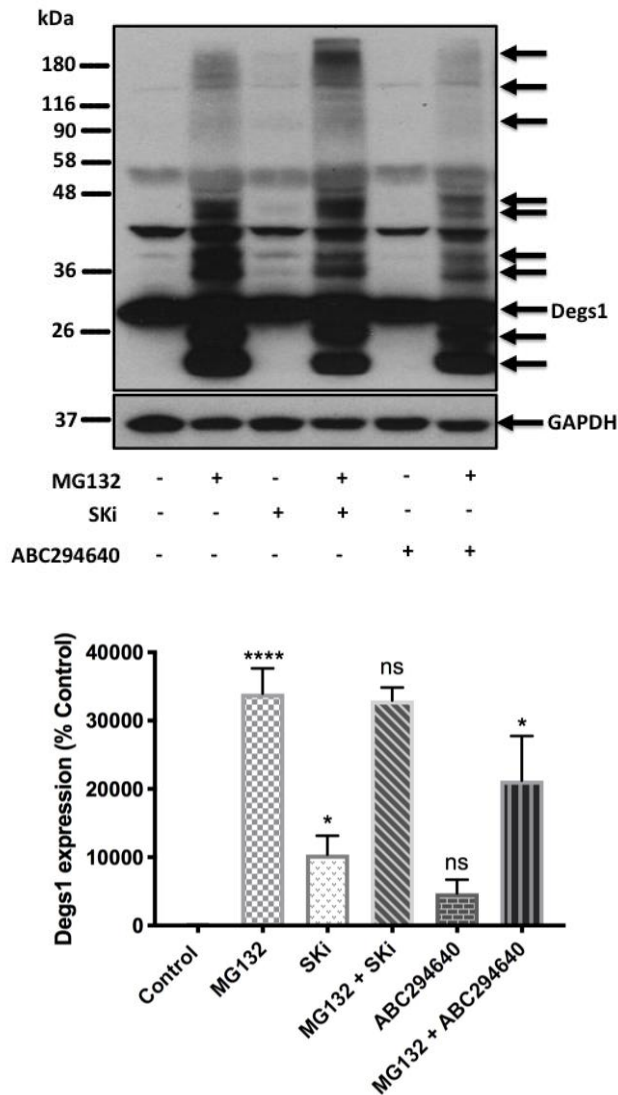


Figure 3.8 *SKi and MG132 induce post-translational modification of Degr1 in parental HEK293 cells. HEK293 cells were cultured in complete medium containing 10% FCS until ~70% confluent. Cells were pre-treated with MG132 (10 μ M, 30 minutes) before addition of SKi (10 μ M) or ABC294640 (25 μ M) or with the vehicle alone (DMSO 0.1% v/v) for 24 hours. Degr1 expression was detected using SDS PAGE and western blotting with anti-Degr1 antibody. Blots were stripped and re-probed with anti-GAPDH antibody to ensure comparable protein loading. A representative western blot is shown of an experiment performed at least three independent times. Also shown is the densitometric quantification of post-translationally modified Degr1/GAPDH ratio immunoreactivity of (Mr 36 kDa), expressed as a percentage of the control (Control=100%). The data was expressed as means \pm SEM for $n=3$ experiments and analysed by one-way ANOVA multiple comparisons test, * $p<0.05$ for SKi vs control or MG132/ABC294640 vs MG132, **** $p<0.0001$ for MG132 vs control, and ns denotes not statistically significant (p value >0.05) for MG132/SKi vs MG132 or ABC294640 vs control.*

3.2.5 Effect of NAC on Degs1 expression in HEK293T cells

Cingolani et al. (2014) suggested that the dual SK1/SK2 inhibitor, SKi, indirectly decreased the activity of Degs1 through the inhibition of oxidative stress and NADH-cytochrome B5 reductase (Cingolani *et al.*, 2014). Likewise, many studies have demonstrated that fenretinide inhibits Degs1 activity and promotes oxidative stress (Zheng *et al.*, 2006; Wang *et al.*, 2008; Rahmaniyan *et al.*, 2011). Thus, we tested whether the antioxidant N-acetylcysteine (NAC) could modulate the formation of the Degs1 ladder in response to SKi or fenretinide. HEK293T cells were pre-treated with NAC before the addition of SKi (Figure 3.9) or fenretinide (Figure 3.10) or MG132 (Figure 3.10), and NAC was shown to reduce Degs1 ladder formation in response to SKi or MG132 or fenretinide.

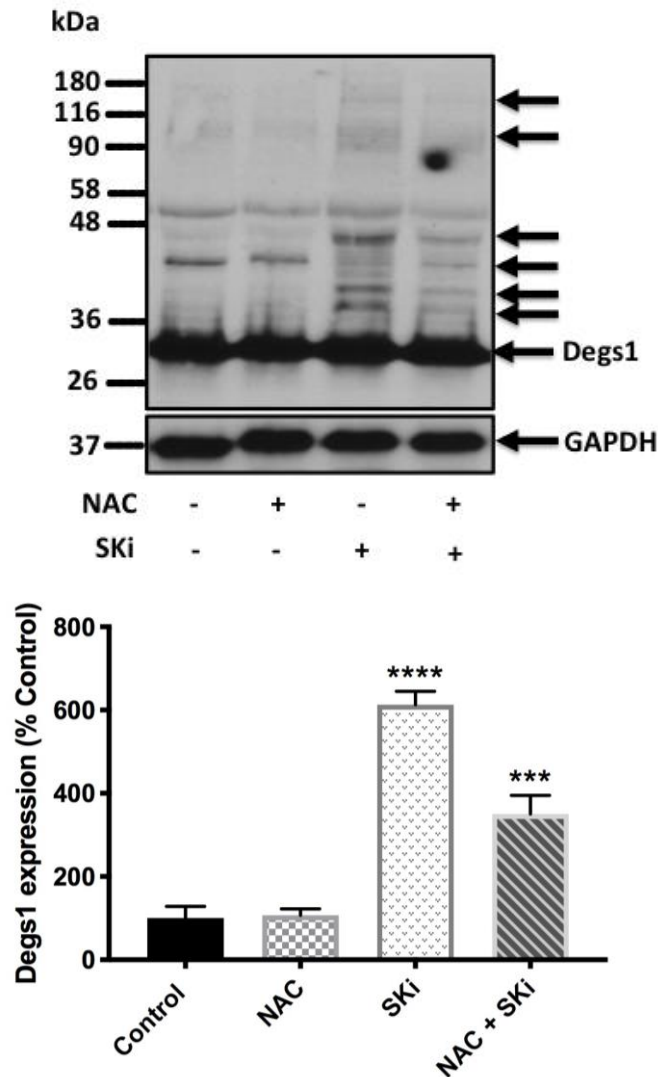


Figure 3.9 Effect of NAC on the SKi-induced formation of the Degr1 ladder in HEK293T cells. HEK293T cells were cultured in complete medium containing 10% FCS until ~70% confluent. Cells were pre-treated with NAC (10 mM, 30 minutes) before addition of SKi (10 μ M) or with the vehicle alone (DMSO 0.1% v/v) for 24 hours. Degr1 expression was detected using SDS PAGE and western blotting with anti-Degr1 antibody. Blots were stripped and re-probed with anti-GAPDH antibody to ensure comparable protein loading. A representative western blot is shown of an experiment performed at least three independent times. Also shown is the densitometric quantification of post-translationally modified Degr1/GAPDH ratio immunoreactivity of (Mr 46 kDa), expressed as a percentage of the control (Control=100%). The data was expressed as means \pm SEM for n=3 experiments and analysed by one-way ANOVA multiple comparisons test, *** p <0.001 for NAC/SKi vs SKi and **** p <0.0001 for SKi vs control.

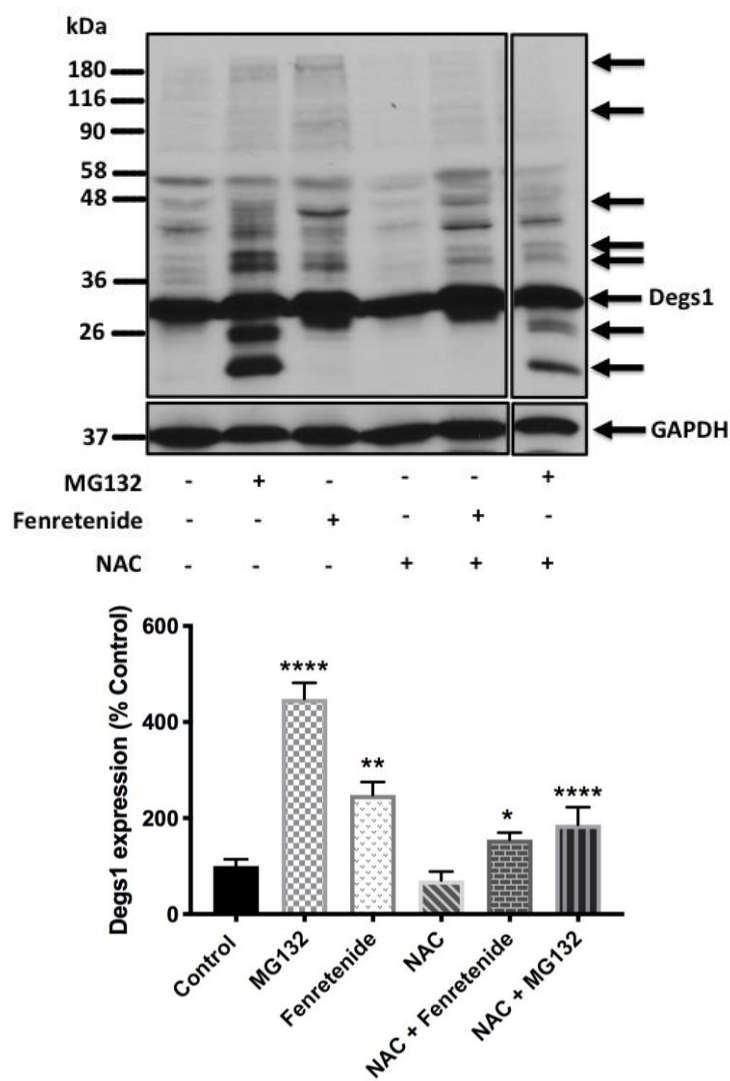


Figure 3.10 *The effect of NAC on Fenretinide- and MG132-induced formation of the Degr1 ladder in HEK293T cells. HEK293T cells were cultured in complete medium containing 10% FCS until ~70% confluent. Cells were pre-treated with NAC (10 mM, 30 minutes) before addition of MG132 (10 μ M) or Fenretinide (1 μ M) or with the vehicle alone (DMSO 0.1% v/v) for 24 hours. Degr1 expression was detected using SDS PAGE and western blotting with anti-Degr1 antibody. Blots were stripped and re-probed with anti-GAPDH antibody to ensure comparable protein loading. A representative western blot is shown of an experiment performed at least three independent times. Also shown is the densitometric quantification of post-translationally modified Degr1/GAPDH ratio immunoreactivity of (Mr 36 kDa), expressed as a percentage of the control (Control=100%). The data was expressed as means \pm SEM for n=3 experiments and analysed by one-way ANOVA multiple comparisons test, * p <0.05 for NAC/Fenretinide vs Fenretinide, ** p <0.01 for Fenretinide vs control, and **** p <0.0001 for MG132 vs control or NAC/MG132 vs MG132.*

3.2.6 Assessment of the role of SK1 and SK2 in regulating Degr1 ladder formation in HEK293T cells

Since SKi and ABC294640 are SK inhibitors, it is important to establish the role of these enzymes in regulating the formation of the Degr1 ladder. Previous studies have demonstrated that SKi or ABC294640 induces the proteasomal degradation of SK1 in cancer cells (McNaughton *et al.*, 2016; Loveridge *et al.*, 2010), resulting in its elimination from these cells. Thus, we tested whether SKi or ABC294640 induce the same effect in HEK293T cells. In this regard, both inhibitors induced proteasomal degradation of SK1, and which was reversed by pre-treatment with the proteasome inhibitor, MG132 (10 μ M, 24 hours) (Figure 3.11). SKi or ABC294640 induced an approximately 80% reduction in the expression of SK1 (Figure 3.11).

An indication that SK1 has no role in regulating the formation of the Degr1 ladder was suggested by the finding that NAC, which inhibits the formation of the Degr1 ladder, had no effect on the proteasomal degradation of SK1 (Figure 3.11). In addition, it is very unlikely that SK1 or SK2 plays a role in regulating the formation of the Degr1 ladder as ABC294640, which inhibits SK2 activity (Gao *et al.*, 2012) and, as shown here, stimulates the proteasomal degradation of SK1, failed to induce the Degr1 ladder at this concentration. Nevertheless, to provide additional evidence for this, HEK293T cells were treated with gene-specific siRNA to knock down of the SK1 or SK2 expression. The treatment of cells with SK1 siRNA reduced SK1 expression by approximately 70% (Figure 3.12). However, siRNA knock down of SK1 neither induced the formation of the Degr1 ladder nor modified the response to SKi (Figure 3.13). Additional proof for this emerged when HEK293T cells were

treated with the potent and specific SK1 inhibitor PF-543 (100 nM, 24 hours) that has a K_i of 4 nM (Schnute *et al.*, 2012); PF-543 failed to produce the Degr1 ladder (Figure 3.14). SK2 siRNA reduced SK2 mRNA transcript by approximately 50% (Figure 3.15) but did not promote the formation of the Degr1 ladder and had no effects on the formation of the SKi-induced Degr1 ladder (Figure 3.16).

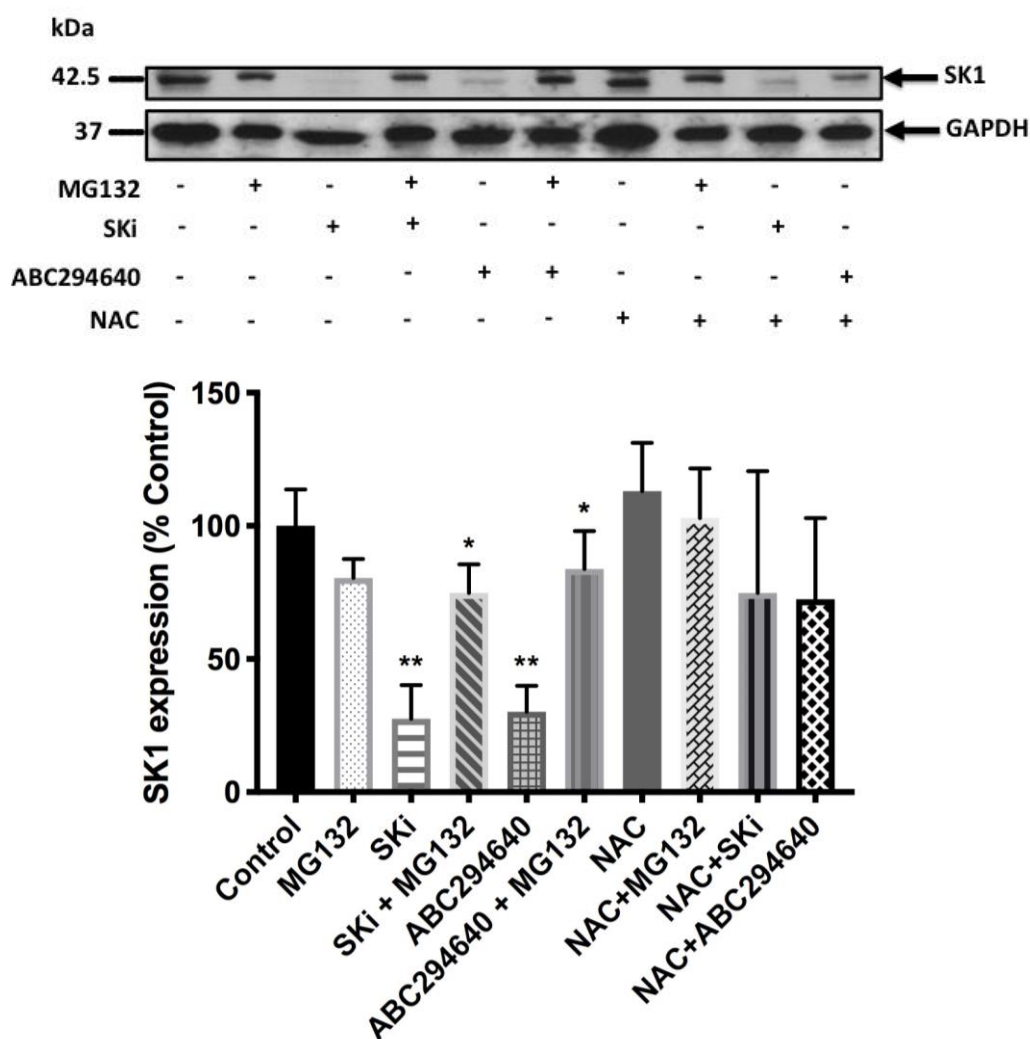


Figure 3.11 *Effect of SKi or ABC294640 on SK1 protein expression in HEK293T cells and role of oxidative stress. HEK293T cells were cultured in complete medium containing 10% FCS until ~70% confluent. Cells were pre-treated with MG132 (10 μ M, 30 minutes) or NAC (10 mM, 30 minutes) before addition of SKi (10 μ M) or ABC294640 (25 μ M) or with the vehicle alone (DMSO 0.1% v/v) for 24 hours. SK1 expression was detected using SDS PAGE and western blotting with anti-SK1 antibody. Blots were stripped and re-probed with anti-GAPDH antibody to ensure comparable protein loading. A representative western blot is shown of an experiment performed at least three independent times. Also shown is the densitometric quantification of SK1/GAPDH ratio immunoreactivity of (Mr 42.5 kDa), expressed as a percentage of the control (Control=100%). The data was expressed as means \pm SEM for $n=3$ experiments and analysed by one-way ANOVA multiple comparisons test, $*p<0.05$ for SKi/MG132 vs SKi or ABC294640/MG132 vs ABC294640 and $**p<0.01$ for SKi or ABC294640 vs control.*

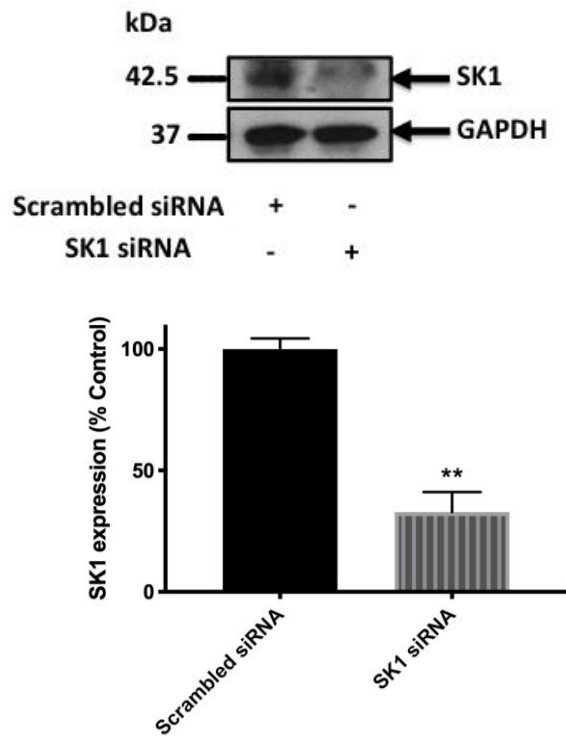


Figure 3.12 *siRNA knockdown of SK1 expression in HEK293T cells.* HEK293T cells were cultured in complete medium containing 10% FCS until ~70% confluent. Cells were transiently transfected with SK1 siRNA or scrambled siRNA at a final concentration of 100 nM in antibiotic free medium for 48 hrs. SK1 expression was detected using SDS PAGE and western blotting with anti-SK1 antibody. Blots were stripped and re-probed with anti-GAPDH antibody to ensure comparable protein loading. A representative western blot is shown of an experiment performed at least three independent times. Also shown is the densitometric quantification of SK1/GAPDH ratio immunoreactivity of (Mr 42.5 kDa), expressed as a percentage of the control (Scrambled siRNA) (Control=100%). The data was expressed as means \pm SEM for $n=3$ experiments and analysed by Unpaired t -test, $**p<0.01$ for SK1 siRNA vs Scrambled siRNA.

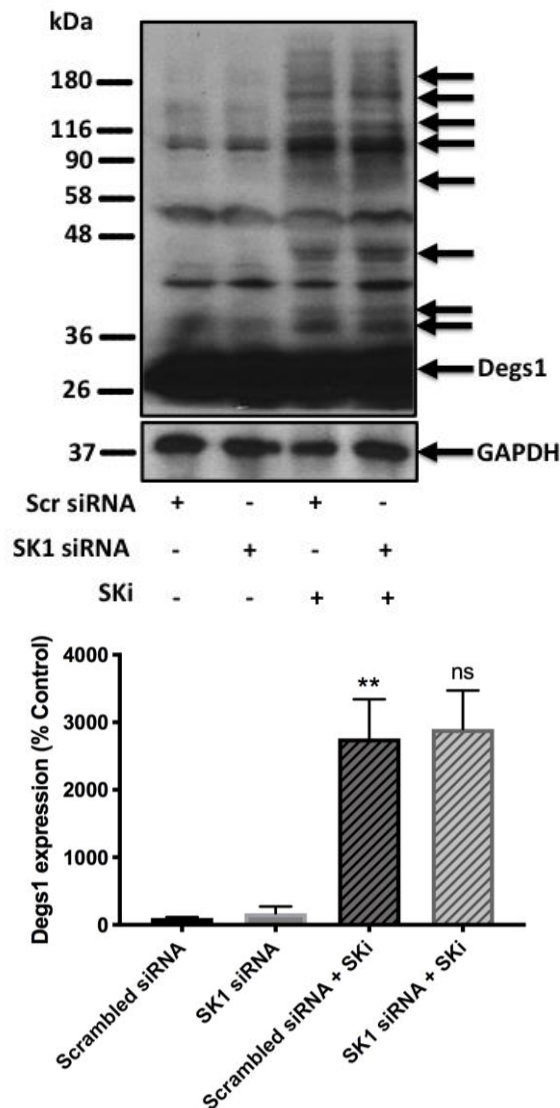


Figure 3.13 *Effect of SK1 siRNA on the Degr1 ladder in HEK293T cells.* HEK293T cells were cultured in complete medium containing 10% FCS until ~70% confluent. Cells were transiently transfected with SK1 siRNA or scrambled siRNA at a final concentration of 100 nM in antibiotic free medium for 48 hrs before being treated with SKi (10 μ M) or with the vehicle alone (DMSO 0.1% v/v) for further 24 hours. Degr1 expression was detected using SDS PAGE and western blotting with anti-Degr1 antibody. Blots were stripped and re-probed with anti-GAPDH antibody to ensure comparable protein loading. A representative western blot is shown of an experiment performed at least three independent times. Also shown is the densitometric quantification of post-translationally modified Degr1/GAPDH ratio immunoreactivity of (Mr 46 kDa), expressed as a percentage of the control (Control=100%). The data was expressed as means \pm SEM for n=3 experiments and analysed by one-way ANOVA multiple comparisons test, ** $p < 0.01$ for Scrambled siRNA/SKi vs Scrambled siRNA and ns denotes not statistically significant (p value > 0.05) for SK1 siRNA/SKi vs Scrambled siRNA/SKi.

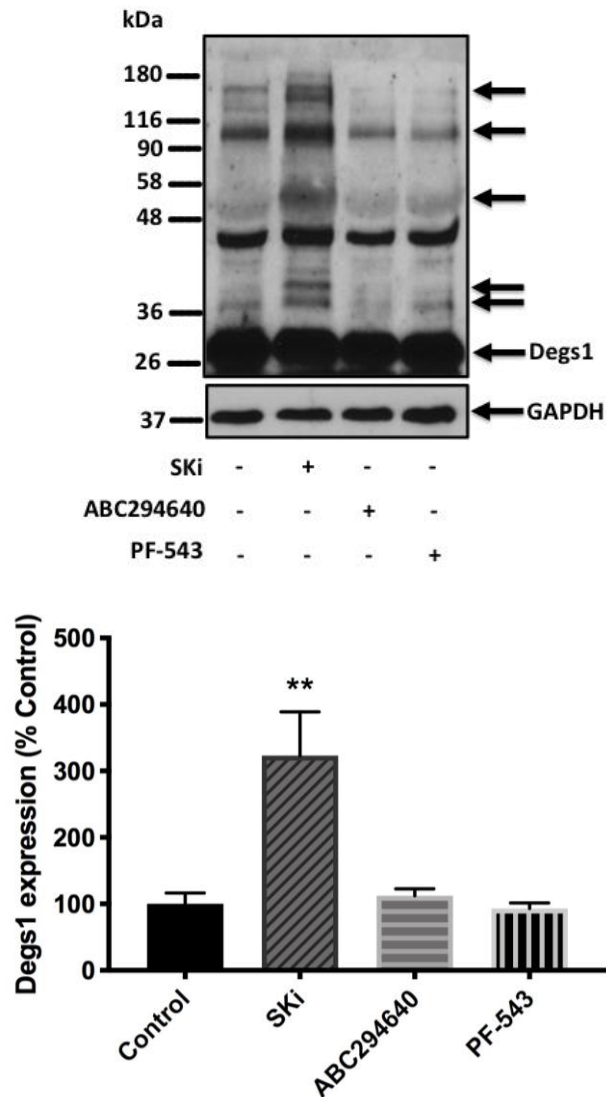


Figure 3.14 *Effect of PF-543 on formation of Degr1 ladder in HEK293T cells. HEK293T cells were cultured in complete medium containing 10% FCS until ~70% confluent. Cells were treated with SKi (10 μ M) or ABC294640 (25 μ M) or PF-543 (100 nM) or with the vehicle alone (DMSO 0.1% v/v) for 24 hours. Degr1 expression was detected using SDS PAGE and western blotting with anti-Degr1 antibody. Blots were stripped and re-probed with anti-GAPDH antibody to ensure comparable protein loading. A representative western blot is shown of an experiment performed at least three independent times. Also shown is the densitometric quantification of post-translationally modified Degr1/GAPDH ratio immunoreactivity of (Mr 46 kDa), expressed as a percentage of the control (Control=100%). The data was expressed as means \pm SEM for $n=3$ experiments and analysed by one-way ANOVA Dunnett's multiple comparisons test, $**p<0.01$ for SKi vs control.*

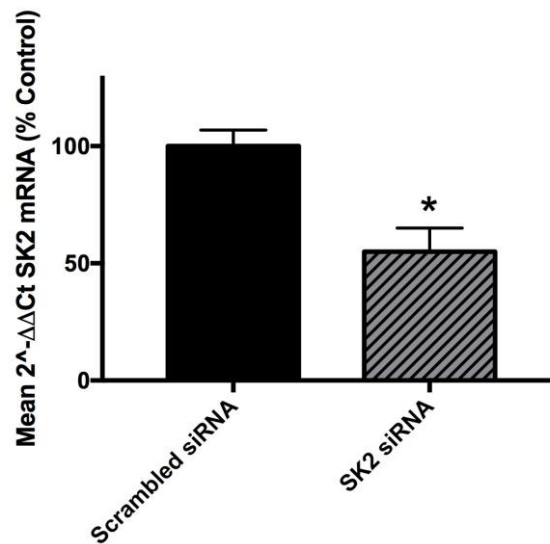


Figure 3.15 *RT-qPCR analysis of mRNA transcript levels of SK2 in HEK293T cells.* SK2 mRNA levels were examined by RT-qPCR using gene-specific primers, followed by agarose gel electrophoresis of the amplification products. The expression of the housekeeping gene GAPDH was analysed using gene-specific primers to ensure that comparable amounts of cDNA template were used for the two cell lines. The optical density of each band (amplification product) was quantified using densitometry, expressed as a percentage of the control (Control=100%). The data was expressed as means \pm SEM for $n=3$ experiments and analysed by Unpaired *t*-test, $*p < 0.01$ for SK2 siRNA versus scrambled siRNA.

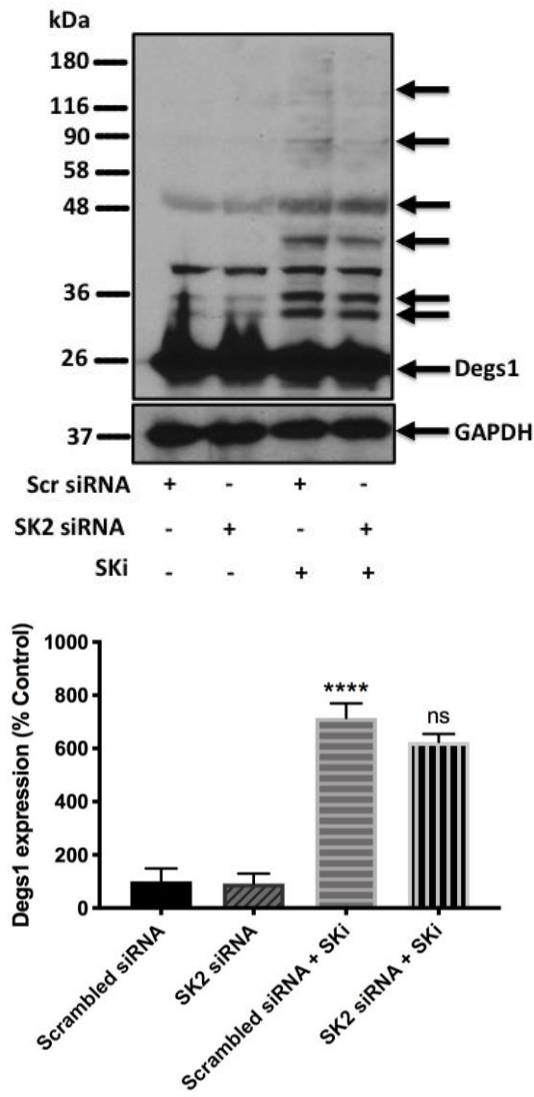


Figure 3.16 Effect of SK2 siRNA on the Degr1 ladder in HEK293T cells. HEK293T cells were cultured in complete medium containing 10% FCS until ~70% confluent. Cells were transiently transfected with SK2 siRNA or scrambled siRNA at a final concentration of 100 nM in antibiotic free medium for 48 hrs before being treated with SKi (10 μ M) or with the vehicle alone (DMSO 0.1% v/v) for further 24 hours. Degr1 expression was detected using SDS PAGE and western blotting with anti-Degr1 antibody. Blots were stripped and re-probed with anti-GAPDH antibody to ensure comparable protein loading. A representative western blot is shown of an experiment performed at least three independent times. Also shown is the densitometric quantification of post-translationally modified Degr1/GAPDH ratio immunoreactivity of (Mr 46 kDa), expressed as a percentage of the control (Control=100%). The data was expressed as means \pm SEM for n=3 experiments and analysed by one-way ANOVA multiple comparisons test, ****p<0.0001 for Scrambled siRNA/SKi vs Scrambled siRNA and ns denotes not statistically significant (p value >0.05) for SK2 siRNA/SKi vs Scrambled siRNA/SKi.

3.2.7 Effect of SKi and ABC294640 on apoptosis and DNA synthesis in HEK293T cells

Much controversy has emerged regarding the role of Degr1 in regulating cell survival. Some reports (e.g., Siddique et al., 2015) have reviewed that it can act to both protect against and promote apoptosis (Siddique *et al.*, 2015). The conversion of native Degr1 into polyubiquitinated forms with opposing functions on apoptosis could potentially provide an explanation for this controversy. Therefore, the effect of SKi or ABC294640 on the growth and apoptosis of HEK293T cells was assessed. PARP cleavage and CCAAT-enhancer-binding protein homologous protein (CHOP) expression were measured as markers for apoptosis whereas [³H]-thymidine incorporation assay into DNA was used to assess DNA synthesis/growth of HEK293T cells. Cells treated with ABC294640 (25 μM, 24 hours) produced cleavage of PARP (Figure 3.17), induced CHOP expression (Figure 3.18), and decreased DNA synthesis (Figure 3.19) whereas SKi (10 μM, 24 hours) failed to induce any of these effects. Therefore, the polyubiquitination of Degr1 might be associated with a prosurvival/growth response in these cells, while native Degr1 (Mr=32 kDa) is associated with apoptosis and inhibition of growth (This finding will be discussed in greater depth later in the discussion Section 3.3).

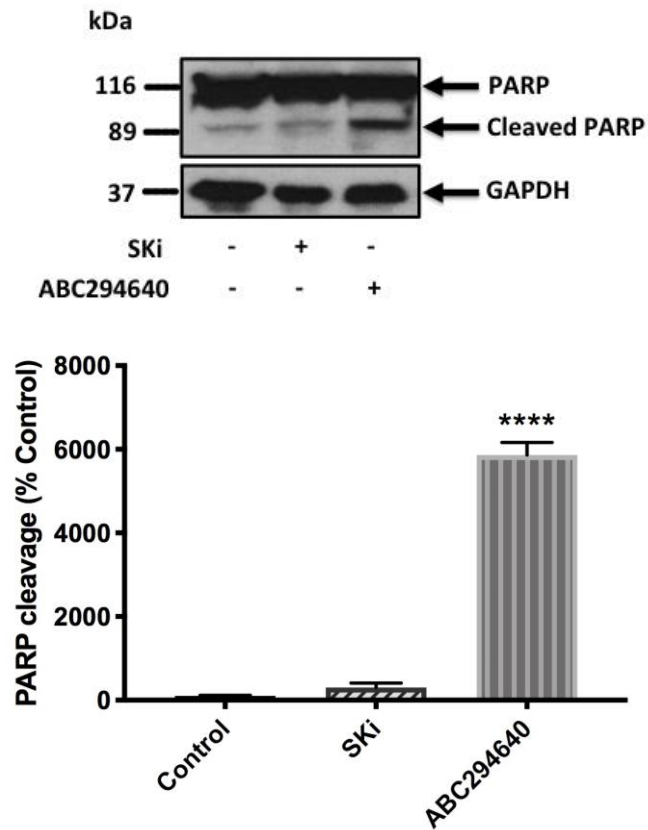


Figure 3.17 *Effect of SKi or ABC294640 on PARP cleavage in HEK293T cells. HEK293T cells were cultured in complete medium containing 10% FCS until ~70% confluent. Cells were treated with SKi (10 μ M) or ABC294640 (25 μ M) or with the vehicle alone (DMSO 0.1% v/v) for 24 hours. PARP cleavage was detected using SDS PAGE and western blotting with anti-PARP antibody. Blots were stripped and re-probed with anti-GAPDH antibody to ensure comparable protein loading. A representative western blot is shown of an experiment performed at least three independent times. Also shown is the densitometric quantification of cleaved PARP/GAPDH ratio immunoreactivity of (Mr 89 kDa), expressed as a percentage of the control (Control=100%). The data was expressed as means \pm SEM for n=3 experiments and analysed by one-way ANOVA Dunnett's multiple comparisons test, **** p <0.0001 for ABC294640 vs control.*

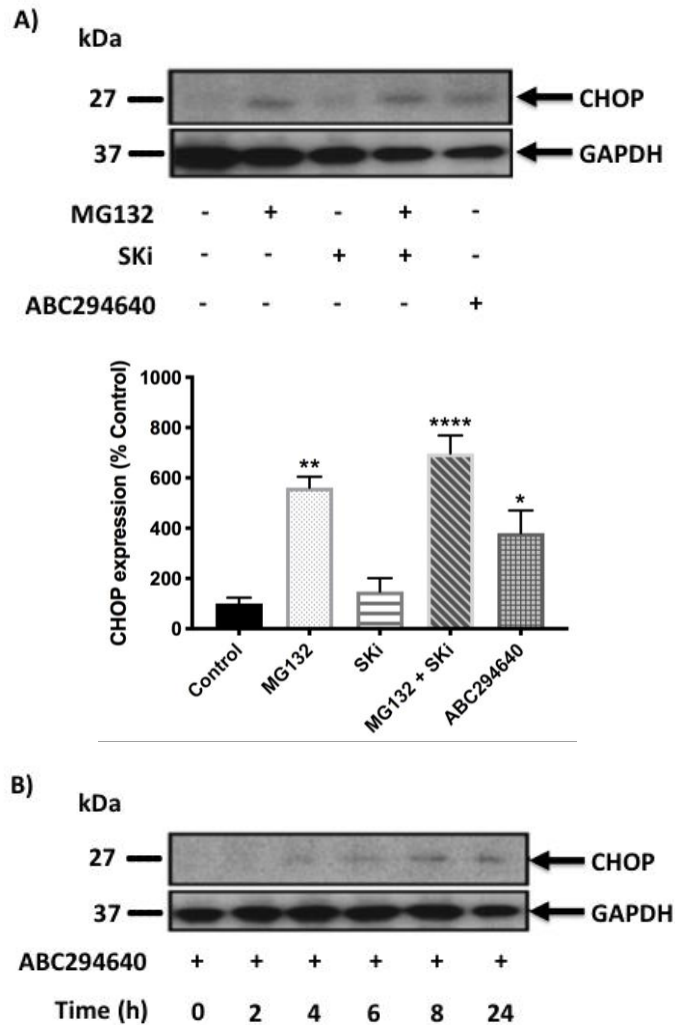


Figure 3.18 *Effect of SKi, ABC294640, or MG132 on CHOP expression in HEK293T cells. HEK293T cells were cultured in complete medium containing 10% FCS until ~70% confluent. A) Cells were pre-treated with MG132 (10 μ M, 30 minutes) before addition of SKi (10 μ M) or ABC294640 (25 μ M) or with the vehicle alone (DMSO 0.1% v/v) for 24 hours. B) Cells were treated with ABC294640 (25 μ M) for a time course (0-24 hours). CHOP expression was detected using SDS PAGE and western blotting with anti-CHOP antibody. Blots were stripped and re-probed with anti-GAPDH antibody to ensure comparable protein loading. A) A representative western blot is shown of an experiment performed at least three independent times. Also shown is the densitometric quantification of CHOP/GAPDH ratio immunoreactivity of (Mr 27 kDa), expressed as a percentage of the control (Control=100%). The data was expressed as means \pm SEM for $n=3$ experiments and analysed by one-way ANOVA multiple comparisons test, * $p<0.05$ for ABC294640 vs control, ** $p<0.01$ for MG132 vs control, and **** $p<0.0001$ for MG132/SKi vs SKi. B) A representative western blot is shown of an experiment performed two independent times.*

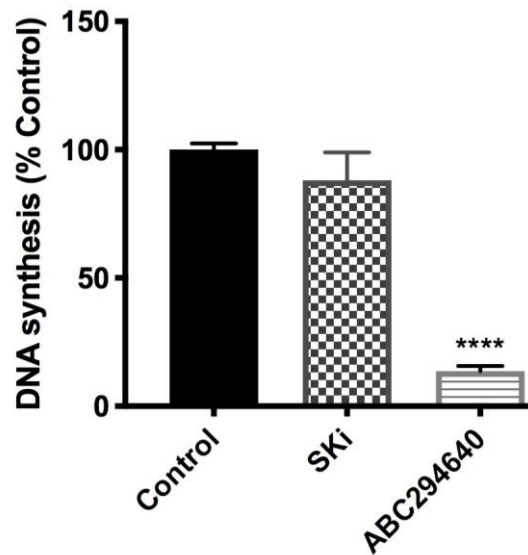


Figure 3.19 *Effect of SKi or ABC294640 on DNA synthesis in HEK293T cells. HEK293T cells were cultured in complete medium containing 10% FCS until ~70% confluent. Cells were then treated with SKi (10 μ M) or ABC294640 (25 μ M) or with the vehicle alone (DMSO 0.1% v/v) for 24 hours. [3 H] Thymidine was added for the last 5 hours then nuclear material was precipitated with 1ml of 10% (w/v) ice cold TCA and then dissolved in 0.1% SDS/0.3M NaOH. [3 H] Thymidine uptake was quantified by liquid scintillation counting. Data are expressed as a % of control \pm SEM for n=3 experiments. The data was analysed by one-way ANOVA Dunnett's multiple comparisons test, ****p<0.0001 for ABC294640 vs control.*

Next, we investigated whether the effect of ABC294640 on apoptosis or DNA synthesis involved the native Degr1. This was achieved by assessing the effect of knocking down the expression of Degr1 with gene-specific siRNA. HEK293T cells were transfected with Degr1 siRNA, which reversed the ABC294640-induced PARP cleavage (Figure 3.20). The reduction in DNA synthesis with ABC294640 was also reversed (Figure 3.21) indicating the involvement of native Degr1 (polyubiquitinated forms of Degr1 are not formed in response to ABC294640) in apoptosis and DNA synthesis. As SK1 and ABC294640 inhibit SK1 and SK2 activity, these enzymes were assessed for their role in regulating apoptosis and DNA synthesis. No effect was observed with SK1 siRNA alone or on ABC294640-induced PARP cleavage and DNA synthesis (Figures 3.22 and 3.23), although SK2 siRNA reduced PARP cleavage in response to ABC294640 (Figure 3.24). This functional interaction between the native Degr1 and SK2 might therefore contribute to apoptosis in HEK293T cells.

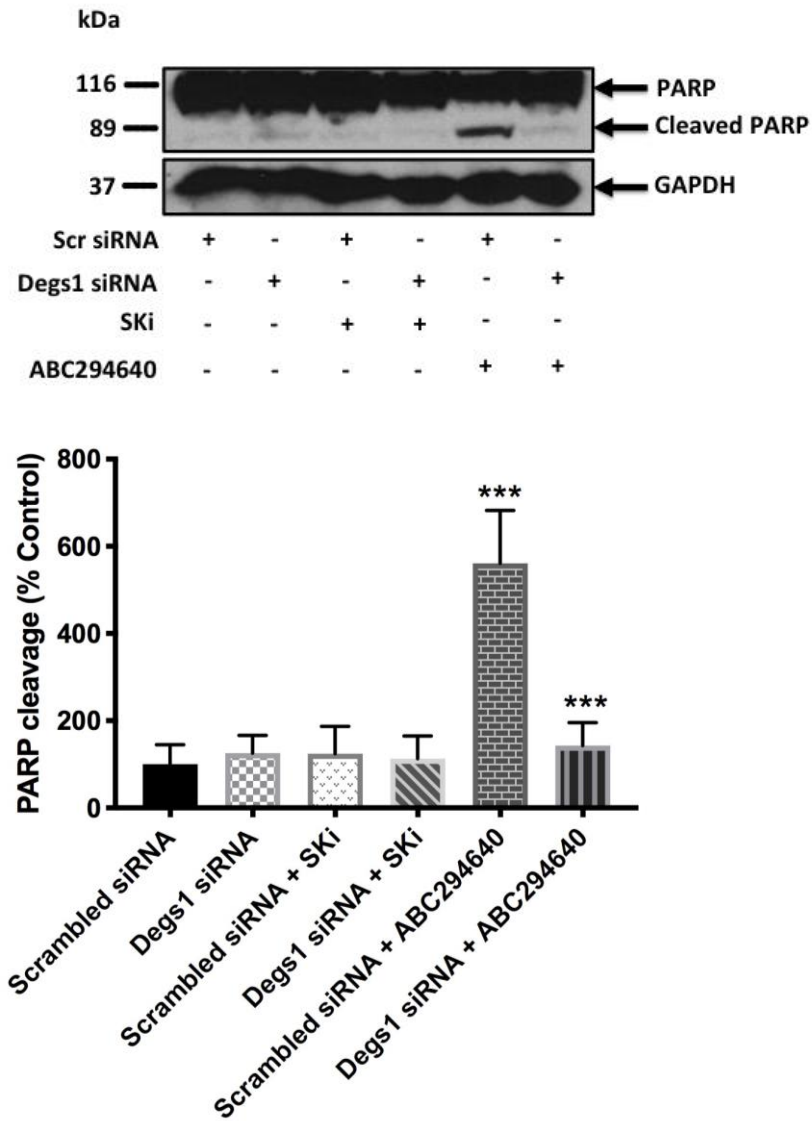


Figure 3.20 *Effect of Degr1 siRNA on ABC294640-induced PARP cleavage in HEK293T cells.* HEK293T cells were cultured in complete medium containing 10% FCS until ~70% confluent. Cells were transiently transfected with Degr1 siRNA or scrambled siRNA at a final concentration of 100 nM in antibiotic free medium for 48 hrs before being treated with SKi (10 μ M) or ABC294640 (25 μ M) or with the vehicle alone (DMSO 0.1% v/v) for further 24 hours. PARP cleavage was detected using SDS PAGE and western blotting with anti-PARP antibody. Blots were stripped and re-probed with anti-GAPDH antibody to ensure comparable protein loading. A representative western blot is shown of an experiment performed at least three independent times. Also shown is the densitometric quantification of cleaved PARP/GAPDH ratio immunoreactivity of (Mr 89 kDa), expressed as a percentage of the control (Control=100%). The data was expressed as means \pm SEM for n=3 experiments and analysed by one-way ANOVA multiple comparisons test, *** p <0.001 for Scrambled siRNA/ABC294640 vs Scrambled siRNA or Degr1 siRNA/ABC294640 vs Scrambled siRNA/ABC294640.

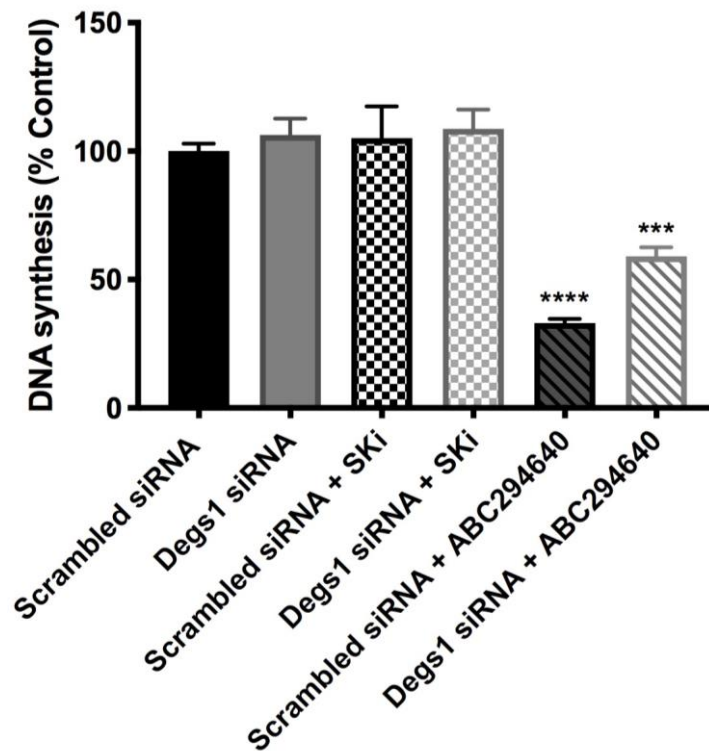


Figure 3.21 *Effect of Degr1 siRNA on DNA synthesis in HEK293T cells.* HEK293T cells were cultured in complete medium containing 10% FCS until ~70% confluent. Cells were transiently transfected with Degr1 siRNA or scrambled siRNA at a final concentration of 100 nM in antibiotic free medium for 48 hrs before being treated with SKi (10 μ M) or ABC294640 (25 μ M) or with the vehicle alone (DMSO 0.1% v/v) for further 24 hours. [3 H] thymidine was added for the last 5 hours then nuclear material was precipitated with 1ml of 10% (w/v) ice cold TCA and then dissolved in 0.1% SDS/0.3M NaOH. [3 H] thymidine uptake was quantified by liquid scintillation counting. Data are expressed as a % of control \pm S.E.M for n=3 experiments. The data was analysed by one-way ANOVA multiple comparisons, *** p <0.001 for Degr1 siRNA/ABC294640 vs Scrambled siRNA/ABC294640 and **** p <0.0001 for Scrambled siRNA/ABC294640 vs Scrambled siRNA.

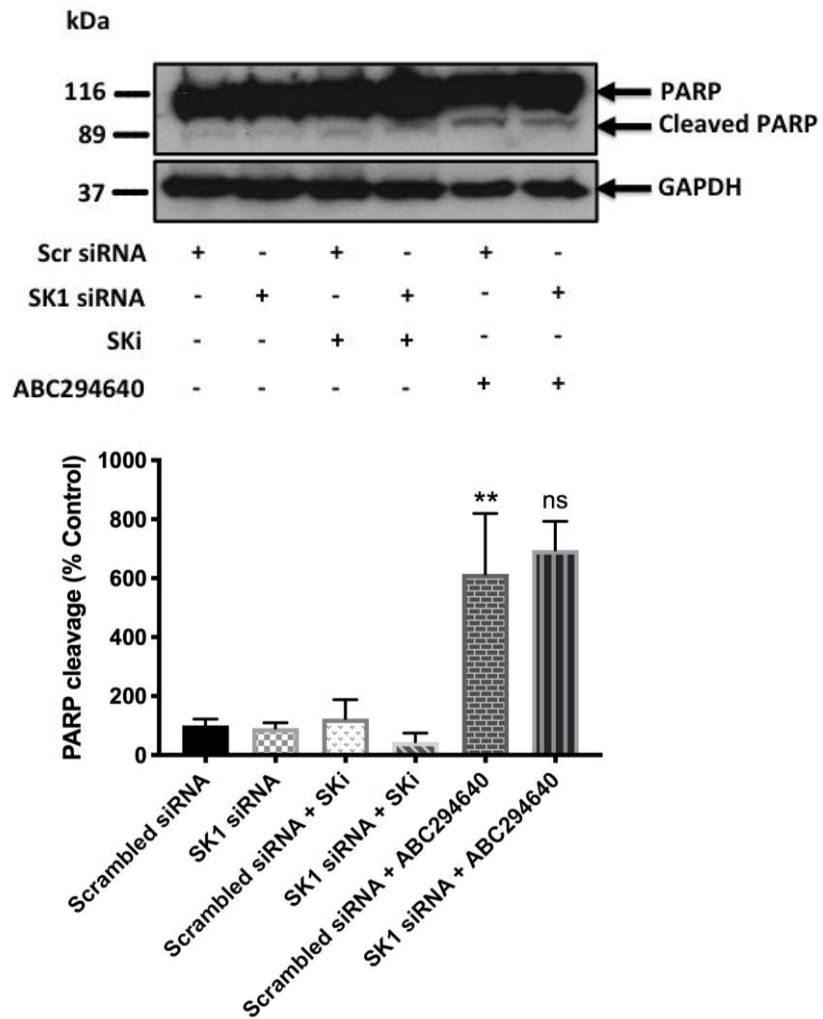


Figure 3.22 *Effect of SK1 siRNA on ABC294640-induced PARP cleavage in HEK293T cells.* HEK293T cells were cultured in complete medium containing 10% FCS until ~70% confluent. Cells were transiently transfected with SK1 siRNA or scrambled siRNA at a final concentration of 100 nM in antibiotic free medium for 48 hrs before being treated with SKi (10 μ M) or ABC294640 (25 μ M) or with the vehicle alone (DMSO 0.1% v/v) for further 24 hours. PARP cleavage was detected using SDS PAGE and western blotting with anti-PARP antibody. Blots were stripped and re-probed with anti-GAPDH antibody to ensure comparable protein loading. A representative western blot is shown of an experiment performed at least three independent times. Also shown is the densitometric quantification of cleaved PARP/GAPDH ratio immunoreactivity of (Mr 89 kDa), expressed as a percentage of the control (Control=100%). The data was expressed as means \pm SEM for n=3 experiments and analysed by one-way ANOVA multiple comparisons test, ** p <0.01 for Scrambled siRNA/ABC294640 vs Scrambled siRNA and ns denotes not statistically significant (p value >0.05) for SK1 siRNA/ABC294640 vs Scrambled siRNA/ABC294640.

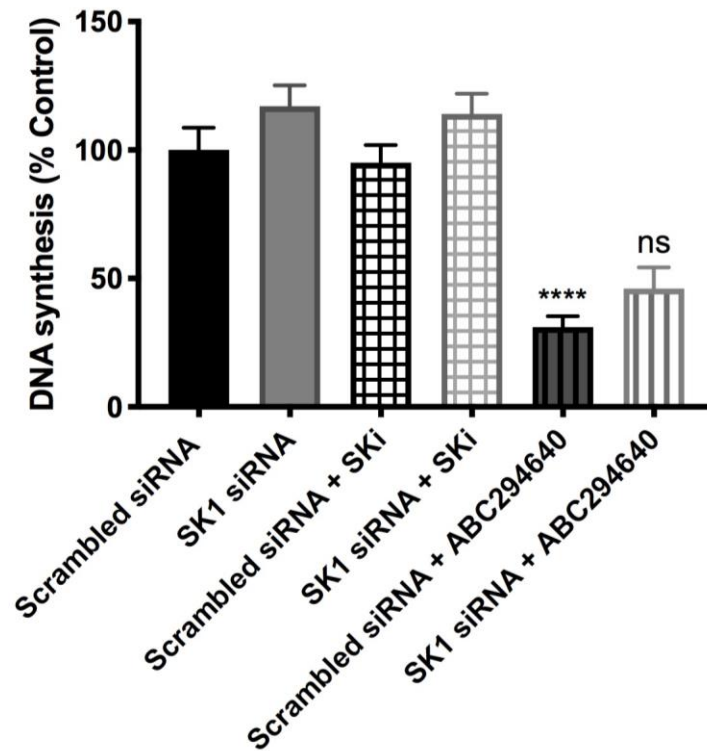


Figure 3.23 *Effect of SK1 siRNA on DNA synthesis in HEK293T cells.* HEK293T cells were cultured in complete medium containing 10% FCS until ~70% confluent. Cells were transiently transfected with SK1 siRNA or scrambled siRNA at a final concentration of 100 nM in antibiotic free medium for 48 hrs before being treated with SKi (10 μ M) or ABC294640 (25 μ M) or with the vehicle alone (DMSO 0.1% v/v) for further 24 hours. [3 H] Thymidine was added for the last 5 hours then nuclear material was precipitated with 1ml of 10% (w/v) ice cold TCA and then dissolved in 0.1% SDS/0.3M NaOH. [3 H] Thymidine uptake was quantified by liquid scintillation counting. Data are expressed as a % of control \pm SEM for n=3 experiments. The data was analysed by one-way ANOVA multiple comparisons test, ****p<0.0001 for Scrambled siRNA/ABC294640 vs Scrambled siRNA and ns denotes not statistically significant (p value >0.05) for SK1 siRNA/ABC294640 vs Scrambled siRNA/ABC294640.

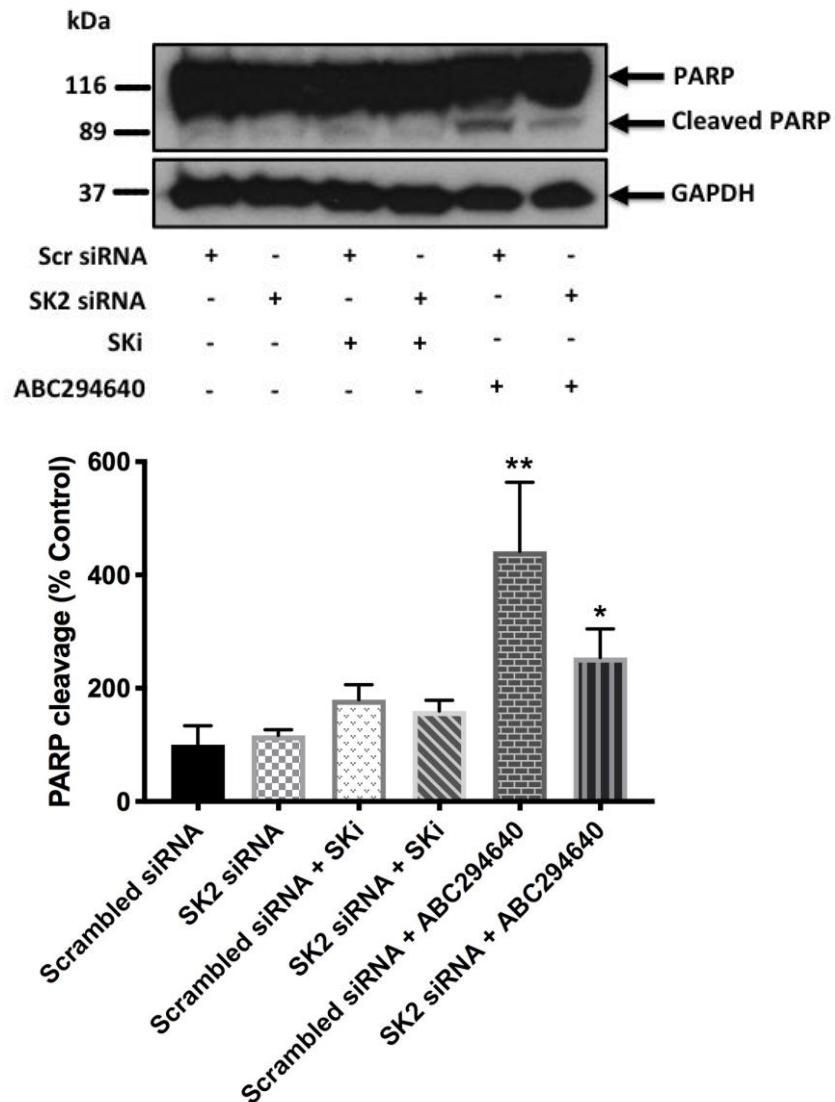


Figure 3.24 *Effect of SK2 siRNA on ABC294640-induced PARP cleavage in HEK293T cells. HEK293T cells were cultured in complete medium containing 10% FCS until ~70% confluent. Cells were transiently transfected with SK2 siRNA or scrambled siRNA at a final concentration of 100 nM in antibiotic free medium for 48 hrs before being treated with SKi (10 μ M) or ABC294640 (25 μ M) or with the vehicle alone (DMSO 0.1% v/v) for further 24 hours. PARP cleavage was detected using SDS PAGE and western blotting with anti-PARP antibody. Blots were stripped and re-probed with anti-GAPDH antibody to ensure comparable protein loading. A representative western blot is shown of an experiment performed at least three independent times. Also shown is the densitometric quantification of cleaved PARP/GAPDH ratio immunoreactivity of (Mr 89 kDa), expressed as a percentage of the control (Control=100%). The data was expressed as means \pm SEM for n=3 experiments and analysed by one-way ANOVA multiple comparisons, * p <0.05 for SK2 siRNA/ABC294640 vs Scrambled siRNA/ABC294640 and ** p <0.01 for Scrambled siRNA/ABC294640 vs Scrambled siRNA.*

We next assessed whether the Akt pathway was involved as activation of this pathway contributes to cell survival and growth (Osaki *et al.*, 2004). Treatment of HEK293T cells with ABC294640 (25 μ M, 24 hours) or MG132 (10 μ M, 24 hours) reduced the phosphorylation of Akt whereas SKi (10 μ M, 24 hours) had no effect (Figure 3.25).

LC3B was also analysed to see whether autophagy was involved. Autophagy is a catabolic process for the autophagosomic-lysosomal degradation of bulk cytoplasmic contents (Reggiori and Klionsky, 2002). Autophagy is generally activated by conditions of nutrient deprivation, but it has also been associated with a number of physiological processes, including development, differentiation, neurodegenerative diseases, infection, and cancer (Levine and Yuan, 2005). During autophagy, LC3-I is converted to LC3-II through lipidation by a ubiquitin-like system involving Apg7 and Apg3 that allows for LC3 to become associated with autophagic vesicles (Tanida *et al.*, 2004; Ichimura *et al.*, 2000). Thus, the presence of LC3 in autophagosomes as well as the conversion of LC3 to the faster migrating form LC3-II has been used as indicators of autophagy that can lead to apoptosis. Treating HEK293T cells with SKi inhibited conversion of LC3B-I to LC3B-II and, hence, autophagy. In contrast, ABC294640 stimulated autophagy through the extensive removal of both LC3B-I and LC3B-II (Figure 3.26). MG132 alone promoted autophagy through the conversion of LC3B-I to LC3B-II; pretreatment with MG132 to SKi/ABC294640 did not affect the MG132 results (Figure 3.26).

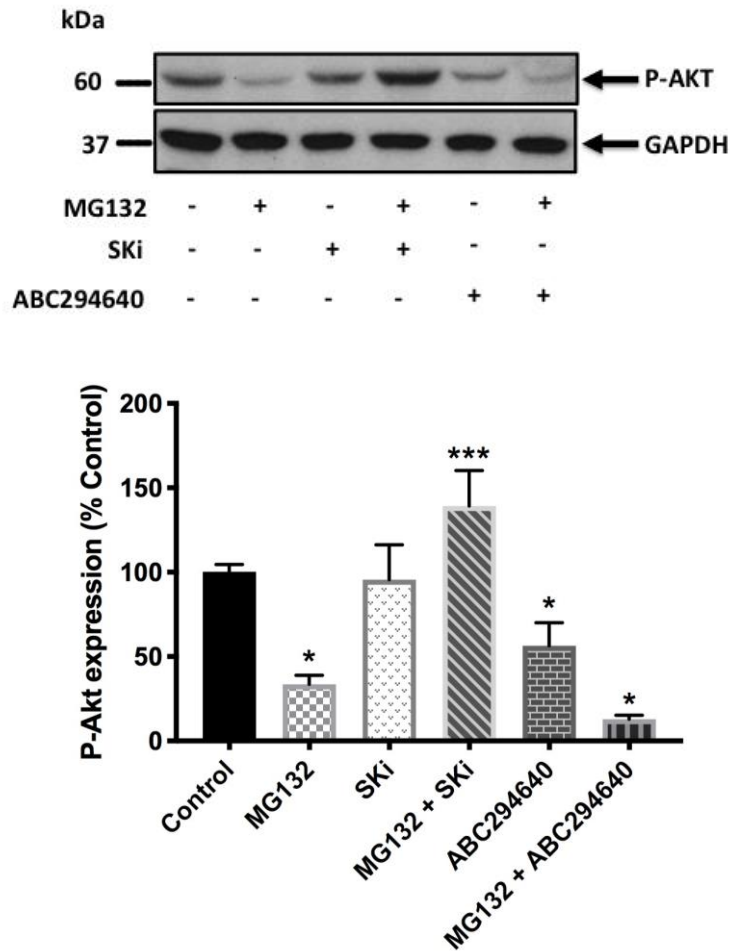


Figure 3.25 *Effect of SKi and ABC294640 on P-Akt expression in HEK293T cells.* HEK293T cells were cultured in complete medium containing 10% FCS until ~70% confluent. Cells were pre-treated with MG132 (10 μ M, 30 minutes) before being treated with or without SKi (10 μ M) or ABC294640 (25 μ M) or with the vehicle alone (DMSO 0.1% v/v) for 24 hours. P-Akt expression was detected using SDS PAGE and western blotting with anti-P-Akt antibody. Blots were stripped and re-probed with anti-GAPDH antibody to ensure comparable protein loading. A representative western blot is shown of an experiment performed at least three independent times. Also shown is the densitometric quantification of P-Akt/GAPDH ratio immunoreactivity of (Mr 60 kDa), expressed as a percentage of the control (Control=100%). The data was expressed as means \pm SEM for $n=3$ experiments and analysed by one-way ANOVA multiple comparisons test, * $p<0.05$ for MG132 vs control or ABC294640 vs control or MG132/ABC294640 vs ABC294640 and *** $p<0.001$ for MG132/SKi vs MG132.

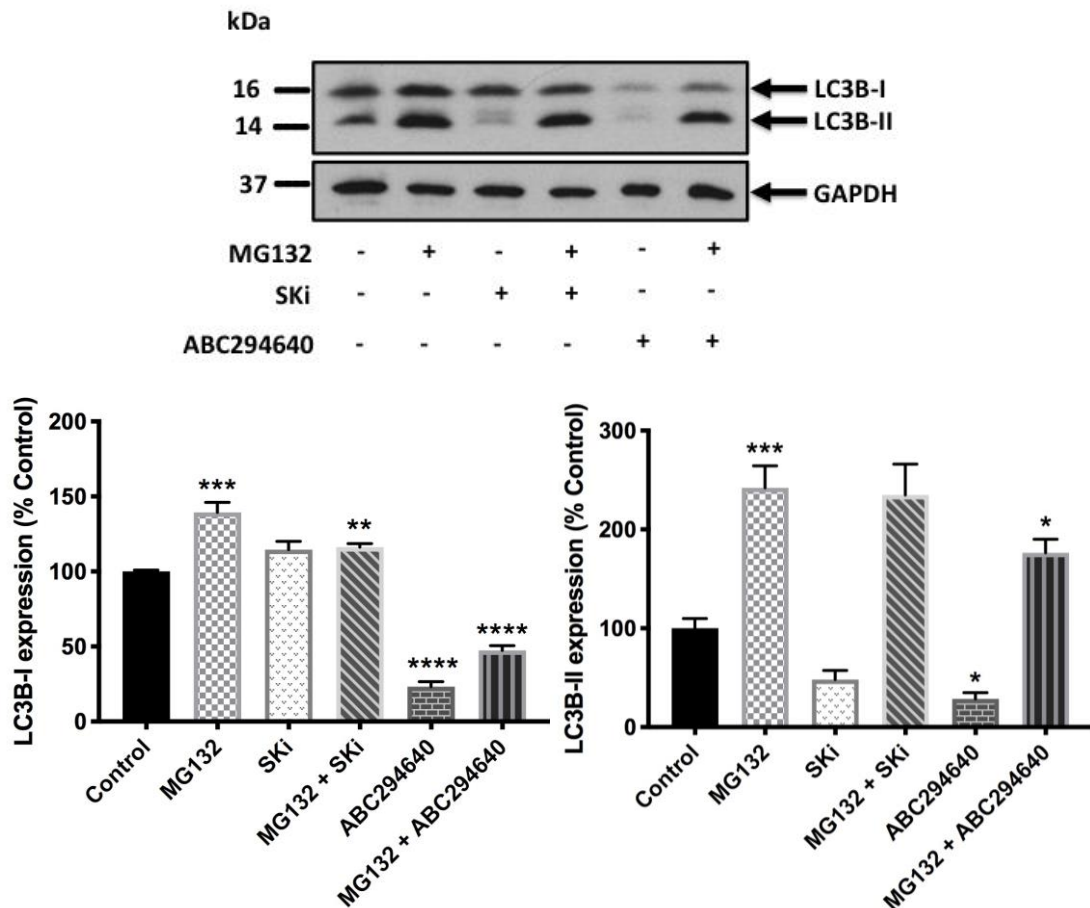


Figure 3.26 Effect of SKi and ABC294640 on LC3B expression in HEK293T cells. HEK293T cells were cultured in complete medium containing 10% FCS until ~70% confluent. Cells were pre-treated with MG132 (10 μ M, 30 minutes) before being treated with and without SKi (10 μ M) or ABC294640 (25 μ M) or with the vehicle alone (DMSO 0.1% v/v) for 24 hours. LC3B-I/II expression was detected using SDS PAGE and western blotting. Blots were stripped and re-probed with anti-GAPDH antibody to ensure comparable protein loading. A representative western blot is shown of an experiment performed at least three independent times. Also shown is the densitometric quantification of LC3B-I/GAPDH and LC3B-II/GAPDH ratios immunoreactivities of (Mr 16 and 14 kDa, respectively), expressed as a percentage of the control (Control=100%). The data was expressed as means \pm SEM for $n=3$ experiments and analysed by one-way ANOVA multiple comparisons test, in LC3B-I **** $p < 0.0001$ for ABC294640 vs control or MG132/ABC294640 vs MG132, *** $p < 0.001$ for MG132 vs control, and ** $p < 0.01$ for MG132/SKi vs MG132 while in LC3B-II *** $p < 0.001$ for MG132 vs control and * $p < 0.05$ for ABC294640 vs control or MG132/ABC294640 vs MG132.

3.2.8 Effect of SKi and ABC294640 on p38 MAPK and JNK

activation in HEK293T cells

The involvement of phosphorylated p38 MAPK and JNK pro-survival signalling pathways was assessed in terms of the regulation of the Degr1 ladder. These are known as “alarm signals” which might reduce UPR-induced cell death, thereby increasing cell growth and survival (Wang and Ron, 1996; Deng *et al.*, 2001; Svensson *et al.*, 2011). Both SKi and ABC294640 have been assessed in terms of whether they modulate the activation of p38 MAPK and JNK in HEK293T cells. SKi increased the phosphorylated p38 MAPK and JNK levels in HEK293T cells in a dose- and time-dependent manner (Figure 3.27). In contrast, ABC294640 failed to induce the phosphorylation of p38 MAPK and JNK at 24 hours, but did activate these kinases in lower doses and at earlier times (Figure 3.28).

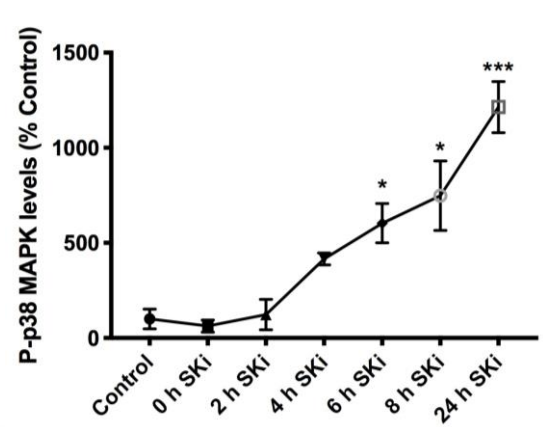
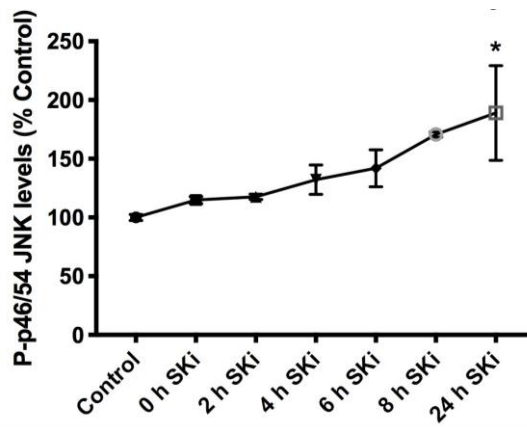
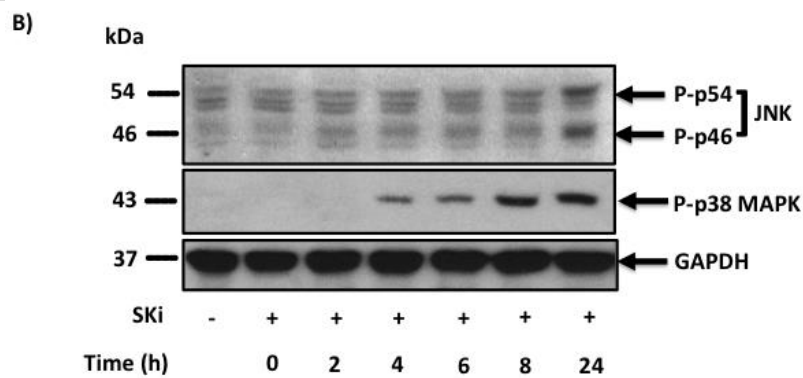
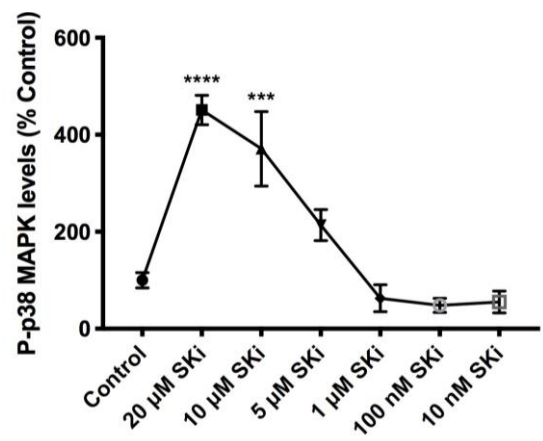
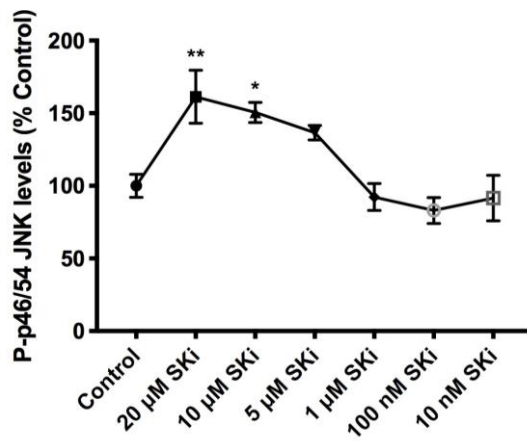
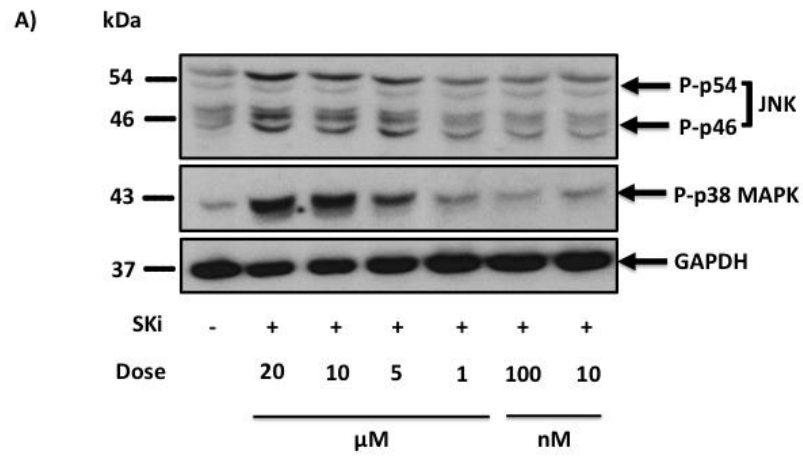


Figure 3.27 *Effect of SKi on levels of phosphorylated p38 and JNK protein expressions in HEK293T cells. HEK293T cells were cultured in complete medium containing 10% FCS until ~70% confluent. A) Cells were treated with SKi (10 nM-20 μ M) or with the vehicle alone (DMSO 0.1% v/v) for 24 hours. B) Cells were treated with SKi (10 μ M) or with the vehicle alone (DMSO 0.1% v/v) for a time course (0-24 hours). P-JNK and P-p38 MAPK levels were detected using SDS PAGE and western blotting with respective antibodies. Blots were stripped and re-probed with anti-GAPDH antibody to ensure comparable protein loading. Two representative western blots are shown each of an experiment performed at least three independent times. Also shown is the densitometric quantification of P-JNK/GAPDH and P-p38 MAPK/GAPDH ratios immunoreactivities of (Mr 46-54 and 43 kDa, respectively), expressed as a percentage of the control (Control=100%). The data was expressed as means \pm SEM for n=3 experiments and analysed by one-way ANOVA Dunnett's multiple comparisons test, * p <0.05 vs control, ** p <0.01 vs control, *** p <0.001 vs control, and **** p <0.0001 vs control.*

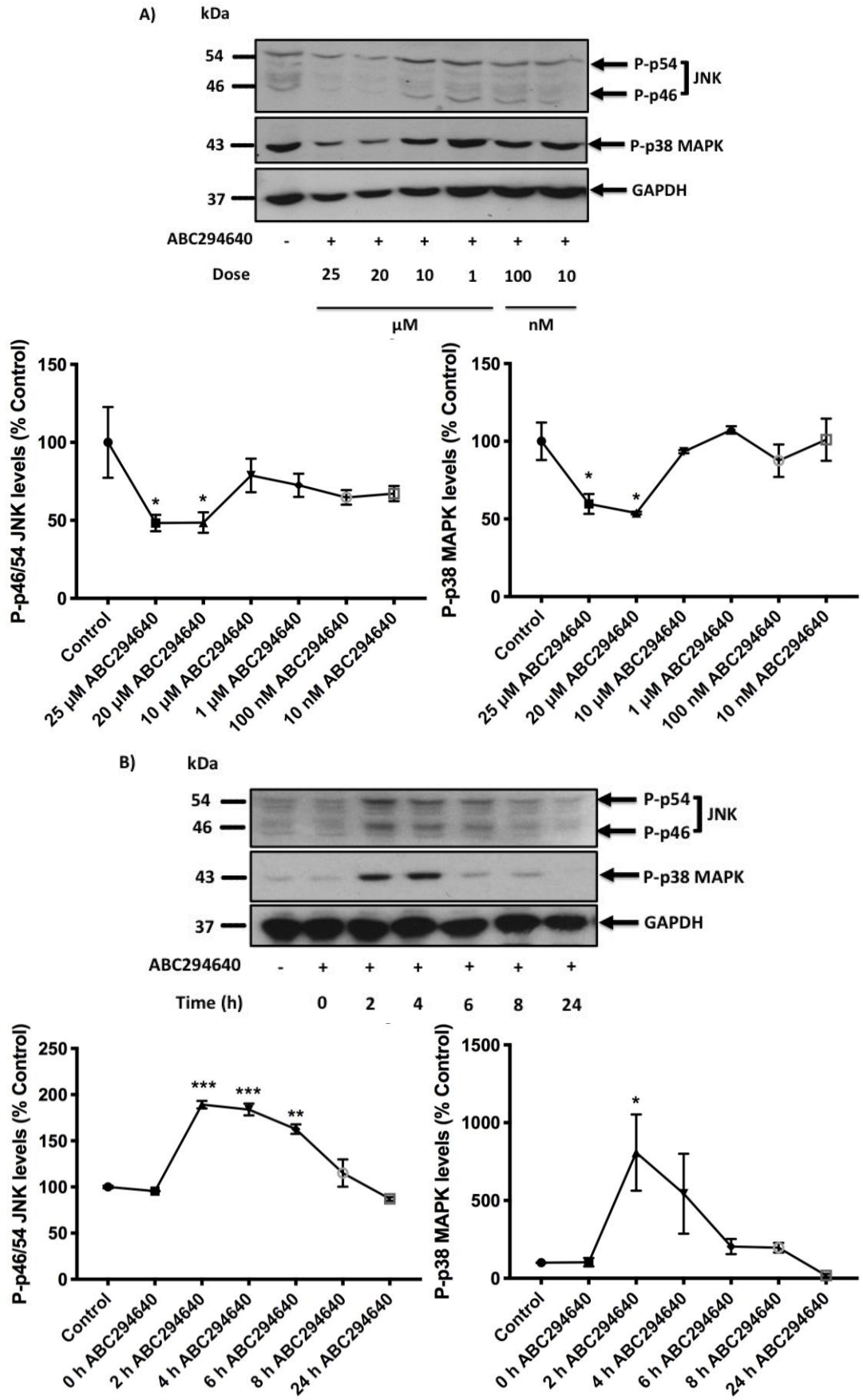


Figure 3.28 *Effect of ABC294640 on levels of phosphorylated p38 and JNK protein expression in HEK293T cells. HEK293T cells were cultured in complete medium containing 10% FCS until ~70% confluent. A) Cells were treated with ABC294640 in different concentrations (10 nM-25 μ M) or with the vehicle alone (DMSO 0.1% v/v) for 24 hours. B) Cells were treated with ABC294640 (25 μ M) or with the vehicle alone (DMSO 0.1% v/v) for a time course (0-24 hours). P-JNK and P-p38 MAPK levels were detected using SDS PAGE and western blotting with respective antibodies. Blots were stripped and re-probed with anti-GAPDH antibody to ensure comparable protein loading. Two representative western blots are shown each of an experiment performed at least three independent times. Also shown is the densitometric quantification of P-JNK/GAPDH and P-p38 MAPK/GAPDH ratios immunoreactivities of (Mr 46-54 and 43 kDa, respectively), expressed as a percentage of the control (Control=100%). The data was expressed as means \pm SEM for n=3 experiments and analysed by one-way ANOVA Dunnett's multiple comparisons test, * p <0.05 vs control, ** p <0.01 vs control, and *** p <0.001 vs control.*

To further test the relationship of activating phosphorylated p38 MAPK and JNK to cell survival/growth, cells were treated with the JNK inhibitor (SP600125) and the p38 MAPK inhibitor (SB203580). Their effect on cell survival/growth was tested. In this regard, the JNK inhibitor (SP600125) but not the p38 MAPK inhibitor (SB203580) induced the formation of cleaved PARP (Figure 3.29). However, SB203580 reduced DNA synthesis (Figure 3.30). These findings suggest that JNK protects against apoptosis whereas p38 MAPK stimulates DNA synthesis. Moreover, although SKi alone did not affect DNA synthesis, pre-treatment with the p38 MAPK inhibitor SB203580 enhanced the inhibitory effect of SB203580 (Figure 3.30). Therefore, although SKi might promote survival via p38 MAPK, the compound can be converted to an inhibitor of DNA synthesis when p38 MAPK is blocked by SB203580.

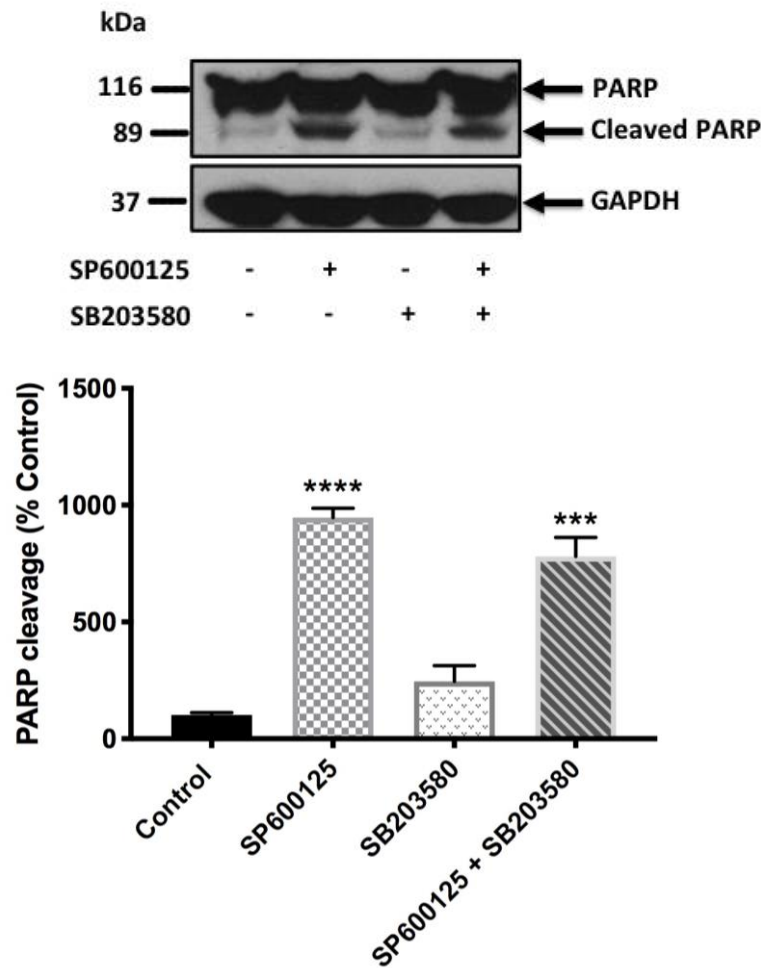


Figure 3.29 Effect of JNK inhibitor (SP600125) and the p38 MAPK inhibitor (SB203580) on PARP cleavage in HEK293T cells. HEK293T cells were cultured in complete medium containing 10% FCS until ~70% confluent. Cells were treated with inhibitors SP600125 (20 μ M) or SB203580 (10 μ M) or both or with the vehicle alone (DMSO 0.1% v/v) for 24 hours. PARP cleavage was detected using SDS PAGE and western blotting with anti-PARP antibody. Blots were stripped and re-probed with anti-GAPDH antibody to ensure comparable protein loading. A representative western blot is shown of an experiment performed at least three independent times. Also shown is the densitometric quantification of cleaved PARP/GAPDH ratio immunoreactivity of (Mr 89 kDa), expressed as a percentage of the control (Control=100%). The data was expressed as means \pm SEM for $n=3$ experiments and analysed by one-way ANOVA multiple comparisons test, *** $p<0.001$ for SP600125/SB203580 vs SB203580 and **** $p<0.0001$ for SP600125 vs control.

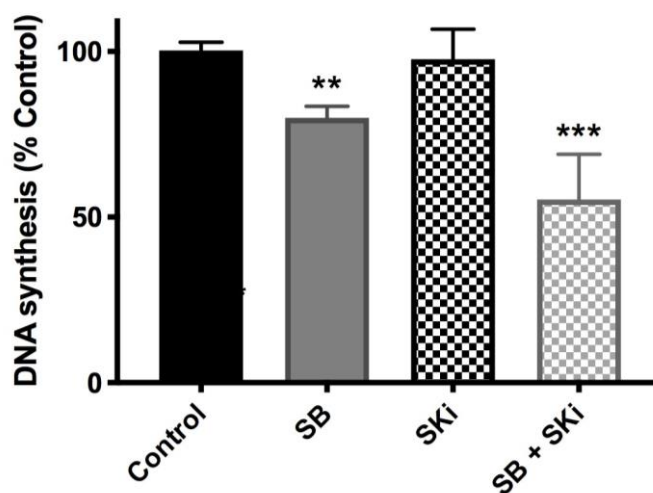


Figure 3.30 Effect of the p38 MAPK inhibitor (SB203580) pre-treatment to SKi on DNA synthesis in HEK293T cells. HEK293T cells were cultured in complete medium containing 10% FCS until ~70% confluent. Cells were pre-treated with SB203580 (10 μ M, 30 min) before addition of SKi (10 μ M) or with the vehicle alone (DMSO 0.1% v/v) for 24 hours. [3 H] Thymidine was added for the last 5 hours then nuclear material was precipitated with 1ml of 10% (w/v) ice cold TCA and then dissolved in 0.1% SDS/0.3M NaOH. [3 H] Thymidine uptake was quantified by liquid scintillation counting. Data are expressed as a % of control \pm S.E.M for n=3 experiments. The data was analysed by one-way ANOVA multiple comparisons test, ** p <0.01 for SB203580 vs control and *** p <0.001 for SB203580/SKi vs SKi.

We next assessed the functional relationship among Degr1, SK1, and SK2 in terms of regulating the p38 MAPK and JNK pathways, which we have demonstrated are pro-survival/growth pathways in HEK293T cells. Interestingly, knocking down Degr1 with Degr1 siRNA reversed the SKi-induced activation of p38 MAPK and JNK (Figure 3.31). As previously shown in Figure 3.2, knocking down Degr1 reduced the native (32 kDa) and the polyubiquitinated forms of Degr1. Since Degr1 siRNA alone had no effect on the phosphorylation of JNK or p38 MAPK (Figure 3.31) it is likely that this form does not regulate JNK/p38 MAPK. These findings suggest that the polyubiquitinated forms are responsible for the regulation of JNK and p38 MAPK. Furthermore, phosphorylated p38 MAPK and JNK survival signals are activated in response to SKi treatment and not ABC294640 at 24 hours, where polyubiquitinated forms of Degr1 are formed in response to SKi and not ABC294640.

The next step was to evaluate whether SK1 and SK2 were involved in SKi-induced p38 MAPK and JNK effects. Knocking down SK1 using SK1 siRNA reduced the basal levels of phosphorylated p38 MAPK and phosphorylated JNK (Figure 3.32), and therefore does not recapitulate the effect of SKi, thereby excluding it from promoting formation of polyubiquitinated Degr1. As additional proof that SK1 is not involved in JNK/p38 MAPK activation, both SKi and ABC294640 induced the proteasomal degradation of SK1 (Figure 3.11), but only SKi activated JNK/p38 MAPK at 24 hours (Figure 3.27). The siRNA knockdown of SK2 had no effect on the phosphorylation levels of p38 MAPK and JNK (Figure 3.33), thereby also excluding this kinase. Moreover, ABC294640 failed to persistently activate

JNK/p38 MAPK at 24 hours.

As p38 MAPK has been shown to regulate Mdm2 (Zhu *et al.*, 2002; Héron-Milhavel and Le Roith, 2002), the E3 ligase responsible for the polyubiquitination of Degr1, we assessed whether there might be a feedback loop from p38 MAPK that enhances the polyubiquitination of Degr1. In this respect the treatment of HEK293T cells with the p38 MAPK inhibitor SB203580 (10 μ M, 24 hours) prior to the addition of SKI reduced the formation of the Degr1 ladder (Figure 3.34). There appears to be specificity for p38 MAPK, as the JNK inhibitor SP600125 had no effect on the ability of SKI to promote the formation of the Degr1 ladder (Data not shown).

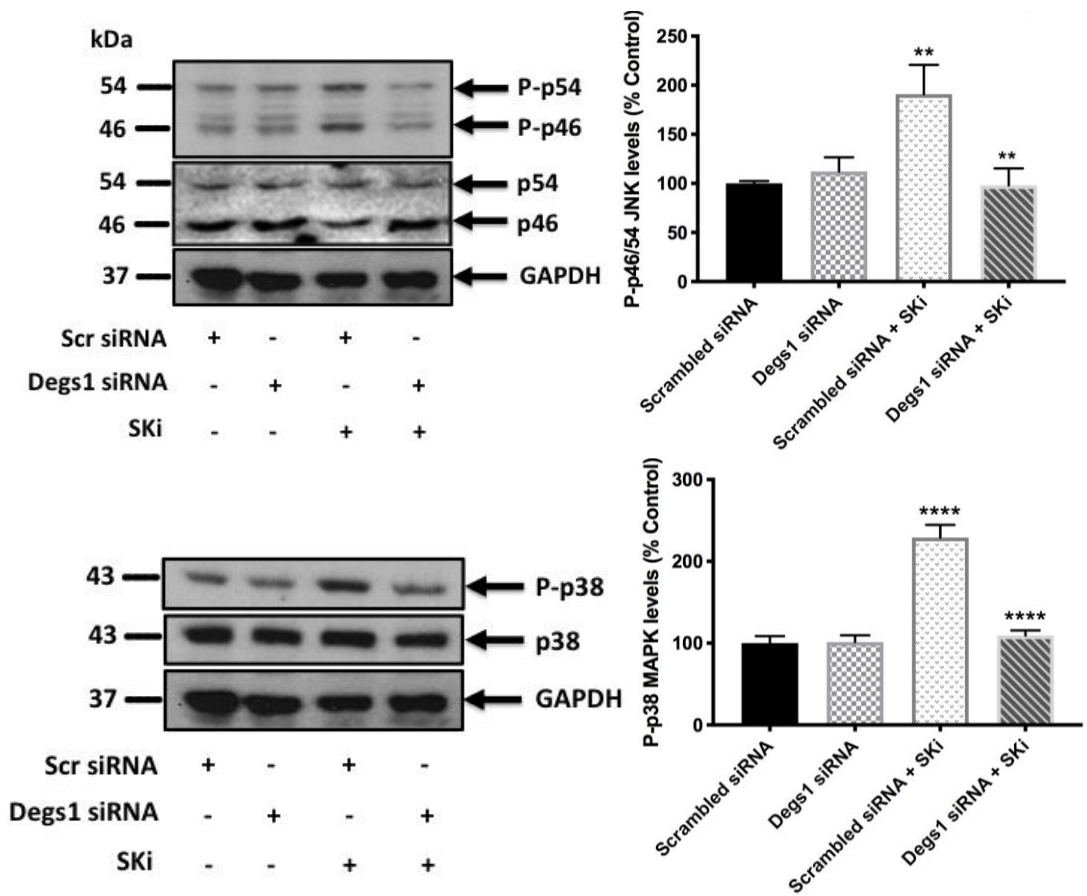


Figure 3.31 *Effect of Degr1 siRNA on SKI-induced p38 MAPK and JNK pathways in HEK293T cells.* HEK293T cells were cultured in complete medium containing 10% FCS until ~70% confluent. Cells were transiently transfected with Degr1 siRNA or scrambled siRNA at a final concentration of 100 nM in antibiotic free medium for 48 hrs before being treated with SKi (10 μ M) or with the vehicle alone (DMSO 0.1% v/v) for further 24 hours. P-JNK and P-p38 MAPK levels were detected using SDS PAGE and western blotting with respective antibodies. Blots were stripped and re-probed with anti-GAPDH or anti-p38 MAPK or anti-JNK antibodies to ensure comparable protein loading. Two representative western blots are shown each of an experiment performed at least three independent times. Also shown is the densitometric quantification of P-JNK/GAPDH and P-p38 MAPK/GAPDH ratios immunoreactivities of (Mr 46-54 and 43 kDa, respectively), expressed as a percentage of the control (Control=100%). The data was expressed as means \pm SEM for $n=3$ experiments and analysed by one-way ANOVA multiple comparisons test, in P-JNK ** $p < 0.01$ for Scrambled siRNA/SKi vs Scrambled siRNA or Degr1 siRNA/SKi vs Scrambled siRNA/SKi while in P-p38 MAPK **** $p < 0.0001$ for Scrambled siRNA/SKi vs Scrambled siRNA or Degr1 siRNA/SKi vs Scrambled siRNA/SKi.

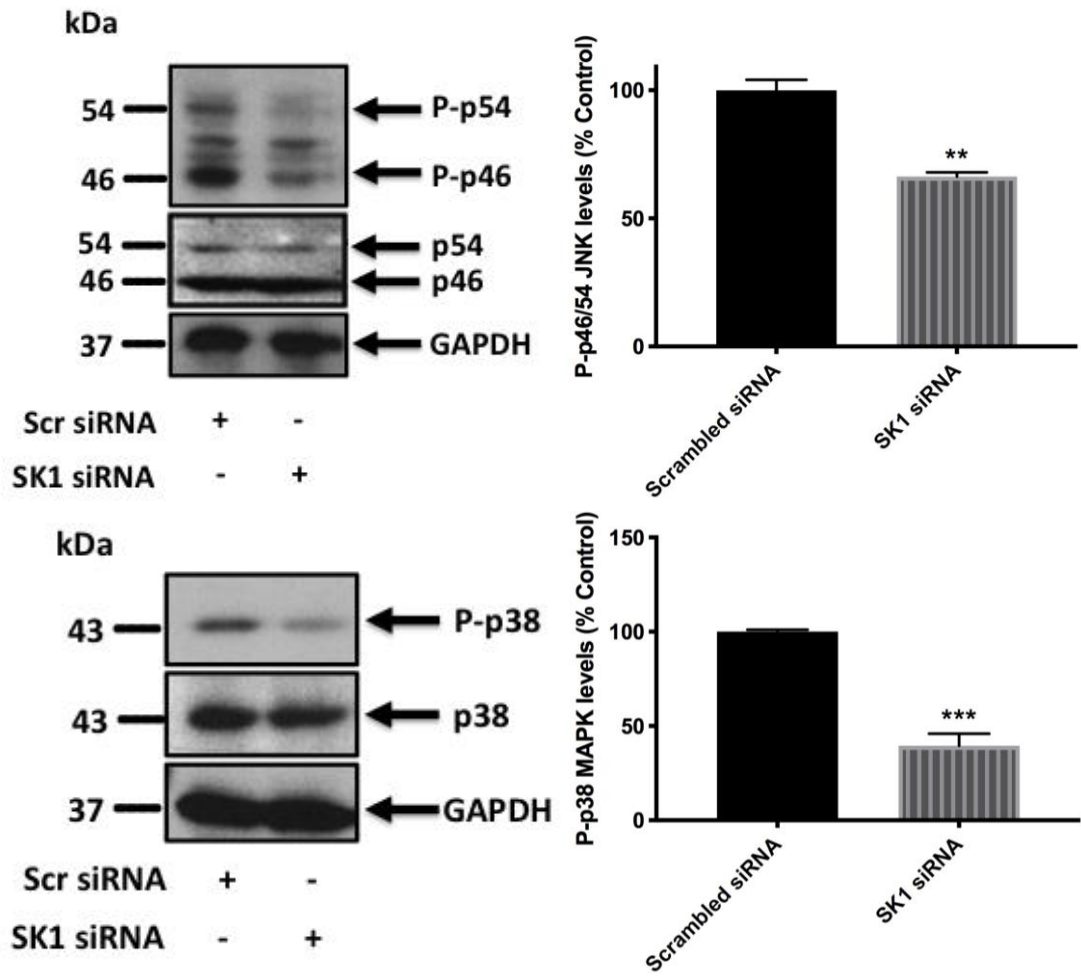


Figure 3.32 *Effect of SK1 siRNA on p38 MAPK and JNK pathways in HEK293T cells.* HEK293T cells were cultured in complete medium containing 10% FCS until ~70% confluent. Cells were transiently transfected with SK1 siRNA or scrambled siRNA at a final concentration of 100 nM in antibiotic free medium for 48 hrs. P-JNK and P-p38 MAPK levels were detected using SDS PAGE and western blotting with respective antibodies. Blots were stripped and re-probed with anti-GAPDH or anti-p38 MAPK or anti-JNK antibodies to ensure comparable protein loading. Two representative western blots are shown each of an experiment performed at least three independent times. Also shown is the densitometric quantification of P-JNK/GAPDH and P-p38 MAPK/GAPDH ratios immunoreactivities of (Mr 46-54 and 43 kDa, respectively), expressed as a percentage of the control (Control=100%). The data was expressed as means \pm SEM for $n=3$ experiments and analysed by Unpaired *t*-test, in P-JNK $**p<0.01$ for SK1 siRNA vs Scrambled siRNA while in P-p38 MAPK $***p<0.001$ for SK1 siRNA vs Scrambled siRNA

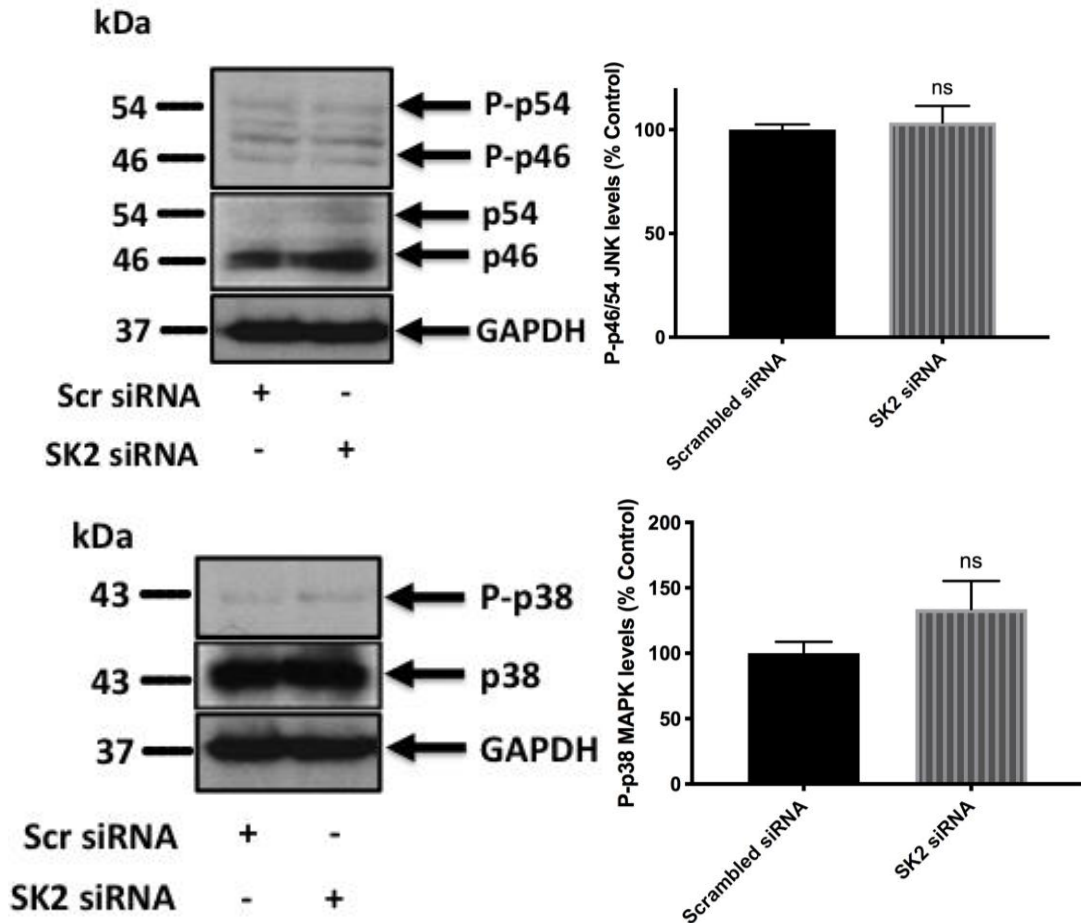


Figure 3.33 *Effect of SK2 siRNA p38 MAPK and JNK pathways in HEK293T cells.* HEK293T cells were cultured in complete medium containing 10% FCS until ~70% confluent. Cells were transiently transfected with SK2 siRNA or scrambled siRNA at a final concentration of 100 nM in antibiotic free medium for 48 hrs. P-JNK and P-p38 MAPK levels were detected using SDS PAGE and western blotting with respective antibodies. Blots were stripped and re-probed with anti-GAPDH or anti-p38 MAPK or anti-JNK antibodies to ensure comparable protein loading. Two representative western blots are shown each of an experiment performed at least three independent times. Also shown is the densitometric quantification of P-JNK/GAPDH and P-p38 MAPK/GAPDH ratios immunoreactivities of (Mr 46-54 and 43 kDa, respectively), expressed as a percentage of the control (Control=100%). The data was expressed as means \pm SEM for $n=3$ experiments and analysed by Unpaired *t*-test, in both P-JNK and P-p38 MAPK ns denotes not statistically significant (p value >0.05) for SK2 siRNA vs Scrambled siRNA.

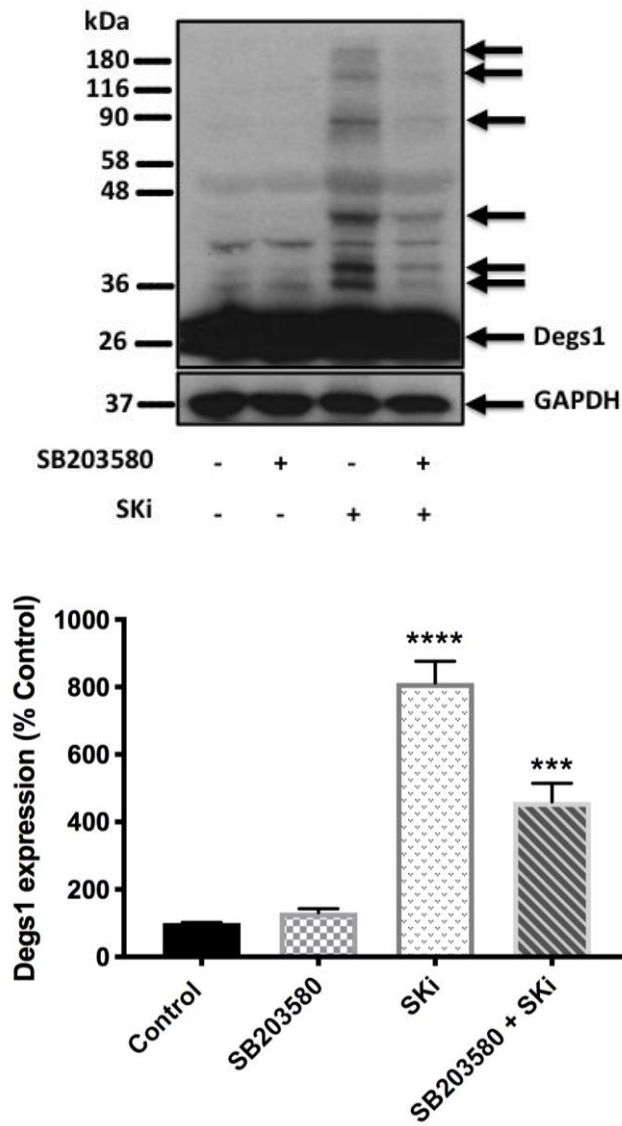


Figure 3.34 Effect of p38 MAPK inhibitor (SB203580) on the polyubiquitination of Degr1 in response to SKi in HEK293T cells. HEK293T cells were cultured in complete medium containing 10% FCS until ~70% confluent. Cells were pre-treated with SB203580 (10 μ M, 30 minutes) before addition of SKi (10 μ M) or with the vehicle alone (DMSO 0.1% v/v) for 24 hours. Degr1 expression was detected using SDS PAGE and western blotting with anti-Degr1 antibody. Blots were stripped and re-probed with anti-GAPDH antibody to ensure comparable protein loading. A representative western blot is shown of an experiment performed at least three independent times. Also shown is the densitometric quantification of post-translationally modified Degr1/GAPDH ratio immunoreactivity of (Mr 46 kDa), expressed as a percentage of the control (Control=100%). The data was expressed as means \pm SEM for n=3 experiments and analysed by one-way ANOVA multiple comparisons test, *** p <0.001 for SB203580/SKi vs SKi and **** p <0.0001 for SKi vs control.

3.2.9 Effect of SKi, ABC294640, and tunicamycin on PERK and XBP-1s levels in HEK293T cells

The homeostasis of folding proteins in the ER lumen is protected by the UPR in cases where an imbalance occurs between levels of unfolded proteins regulated by the ER stress sensors IRE1, PERK, and ATF6 (Volmer and Ron, 2015). Therefore, Degr1 might regulate cell survival/apoptosis through the activation of ER stress as changes in the levels of Cer/dhCer in ER could activate ER cellular stress responses (Gagliostro *et al.*, 2012; Spassieva *et al.*, 2009; Volmer and Ron, 2015). Therefore, SKi and ABC294640 were used to assess the involvement of this pathway and its regulation by Degr1. Two ER stress sensors were chosen for this study: PERK and XBP-1s.

HEK293T cells were treated with SKi (10 μ M, 24 hours), producing a mobility shift in PERK on SDS-PAGE (Figure 3.35A) which was previously described as a result of phosphorylation (Koumenis *et al.*, 2002). However, the mobility shift was not reversed when pre-treated with NAC excluding the role of oxidative stress (Figure 3.35A). On the other hand, the SK2 inhibitor ABC294640 (25 μ M, 24 hours) failed to induce the mobility shift in PERK (Figure 3.35B). HEK293T cells were also treated with the ER stress activator tunicamycin (5 μ g/ml) (known for preventing the formation of N-acetylglucosamine lipid intermediates and the glycosylation of newly synthesised glycoproteins to induce unfolded protein response (Chan and Egan, 2005; Elbein, 1981)), which resulted in a mobility shift in PERK (Figure 3.35C).

Next, we assessed the involvement of Degr1, SK1, and SK2 in the SKi-induced PERK shift using siRNA transfections. Knocking down Degr1 (Figure 3.36), SK1 (Figure 3.37), or SK2 (Figure 3.38) using specific siRNAs did not reverse the SKi-induced mobility shift in PERK, thereby excluding their role in regulating PERK. The lack of effect of NAC is consistent with the finding that Degr1 is unlikely to have a role in regulating PERK as the formation of the Degr1 ladder in response to SKi was reduced by NAC (see Figure 3.9).

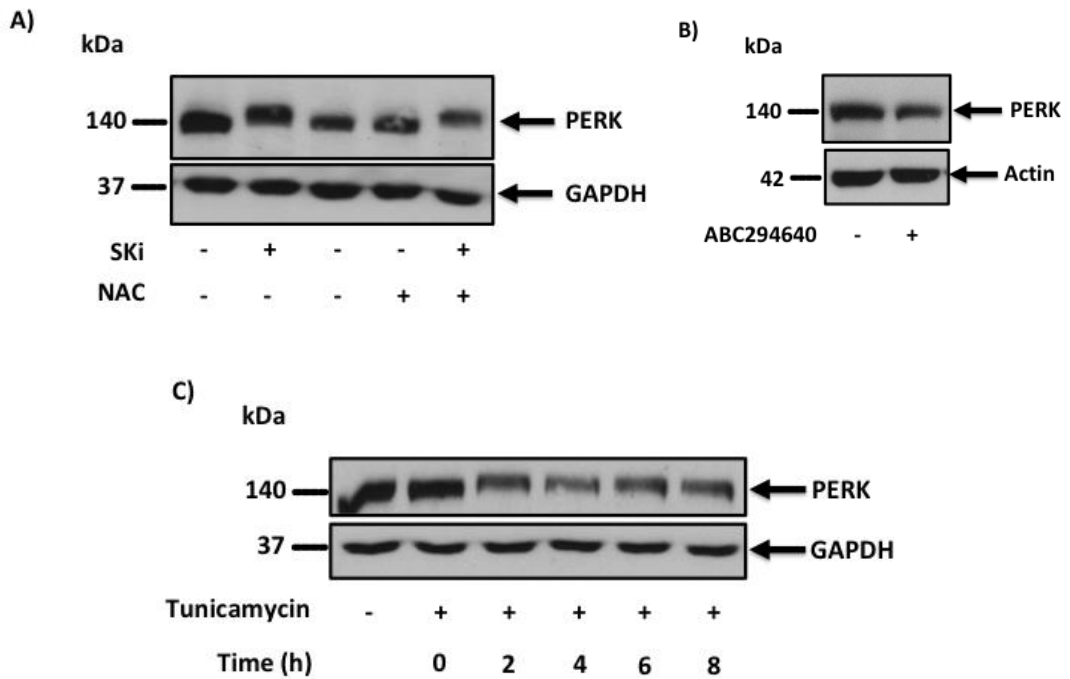


Figure 3.35 *Effect of SKi, ABC294640, or Tunicamycin on PERK mobility shift in HEK293T cells.* HEK293T cells were cultured in complete medium containing 10% FCS until ~70% confluent. A) Cells were pre-treated with NAC (10 mM, 30 minutes) before addition of SKi (10 μ M) or with the vehicle alone (DMSO 0.1% v/v) for 24 hours. B) Cells were treated with ABC204640 (25 μ M) or with the vehicle alone (DMSO 0.1% v/v) for 24 hours. C) Cells were treated with tunicamycin (5 μ g/ml) or with the vehicle alone (DMSO 0.1% v/v) for a time course (0-8 hours). PERK levels were detected using SDS PAGE and western blotting with anti-PERK antibody. Blots were stripped and re-probed with anti-GAPDH or anti-actin antibodies to ensure comparable protein loading. Three representative western blots are shown each of an experiment performed at least three independent times.

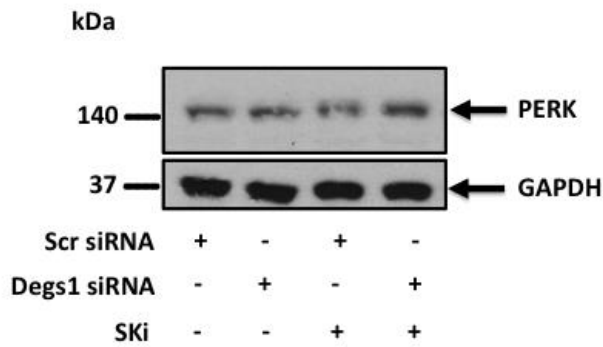


Figure 3.36 *Lack of effect of Degr1 siRNA on PERK mobility shift in HEK293T cells.* HEK293T cells were cultured in complete medium containing 10% FCS until ~70% confluent. Cells were transiently transfected with Degr1 siRNA or scrambled siRNA at a final concentration of 100 nM in antibiotic free medium for 48 hrs before being treated with SKi (10 μ M) or with the vehicle alone (DMSO 0.1% v/v) for further 24 hours. PERK levels were detected using SDS PAGE and western blotting with anti-PERK antibody. Blots were stripped and re-probed with anti-GAPDH antibody to ensure comparable protein loading. A representative western blot is shown of an experiment performed at least three independent times.

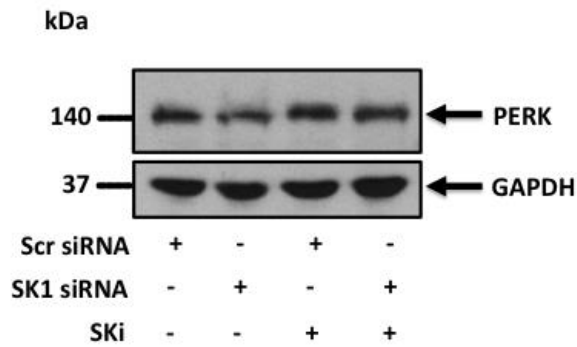


Figure 3.37 *Lack of effect of SK1 siRNA on PERK mobility shift in HEK293T cells.* HEK293T cells were cultured in complete medium containing 10% FCS until ~70% confluent. Cells were transiently transfected with SK1 siRNA or scrambled siRNA at a final concentration of 100 nM in antibiotic free medium for 48 hrs before being treated with or without SKi (10 μ M) or with the vehicle alone (DMSO 0.1% v/v) for further 24 hours. PERK levels were detected using SDS PAGE and western blotting with anti-PERK antibody. Blots were stripped and re-probed with anti-GAPDH antibody to ensure comparable protein loading. A representative western blot is shown of an experiment performed at least three independent times.

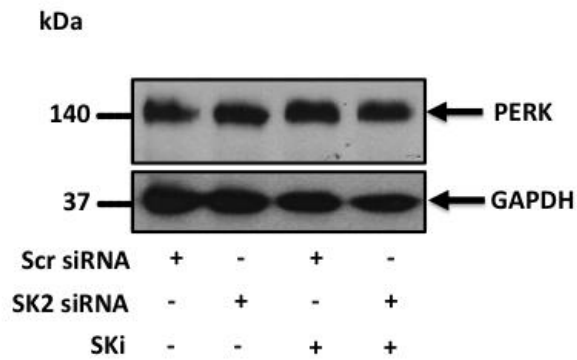


Figure 3.38 *Lack of effect of SK2 siRNA on PERK mobility shift in HEK293T cells.* HEK293T cells were cultured in complete medium containing 10% FCS until ~70% confluent. Cells were transiently transfected with SK2 siRNA or scrambled siRNA at a final concentration of 100 nM in antibiotic free medium for 48 hrs before being treated with or without SKi (10 μ M) or with the vehicle alone (DMSO 0.1% v/v) for further 24 hours. PERK levels were detected using SDS PAGE and western blotting with anti-PERK antibody. Blots were stripped and re-probed with anti-GAPDH antibody to ensure comparable protein loading. A representative western blot is shown of an experiment performed at least three independent times.

The second ER stress sensor we investigated was XBP-1s. The proteasome inhibitor MG132 (10 μ M, 24 hours) alone induced an increase in XBP-1s expression and this was enhanced by SKi (Figure 3.39). We previously demonstrated that a combination of MG132 and SKi enhanced the formation of the Degr1 ladder with a $M_r > 50$ kDa (Figure 3.5). Thus, it is considered an important finding and suggests that the post-translationally modified forms of Degr1 are positively linked with the increase in the XBP-1s pro-survival expression. On the other hand, ABC294640 (25 μ M, 24 hours) reduced the MG132-induced increase in XBP-1s levels (Figure 3.39). Similarly, as previously shown, the combination of MG132 and ABC294640 reduced the MG132-induced Degr1 ladder (Figure 3.5), suggesting that this might account for the reduction in XBP-1s expression (32 kDa). To confirm the involvement of Degr1 in this pathway, we knocked down Degr1 using Degr1 siRNA; indeed, this reduced the MG132/SKi-induced increase in XBP-1s expression (Figure 3.40).

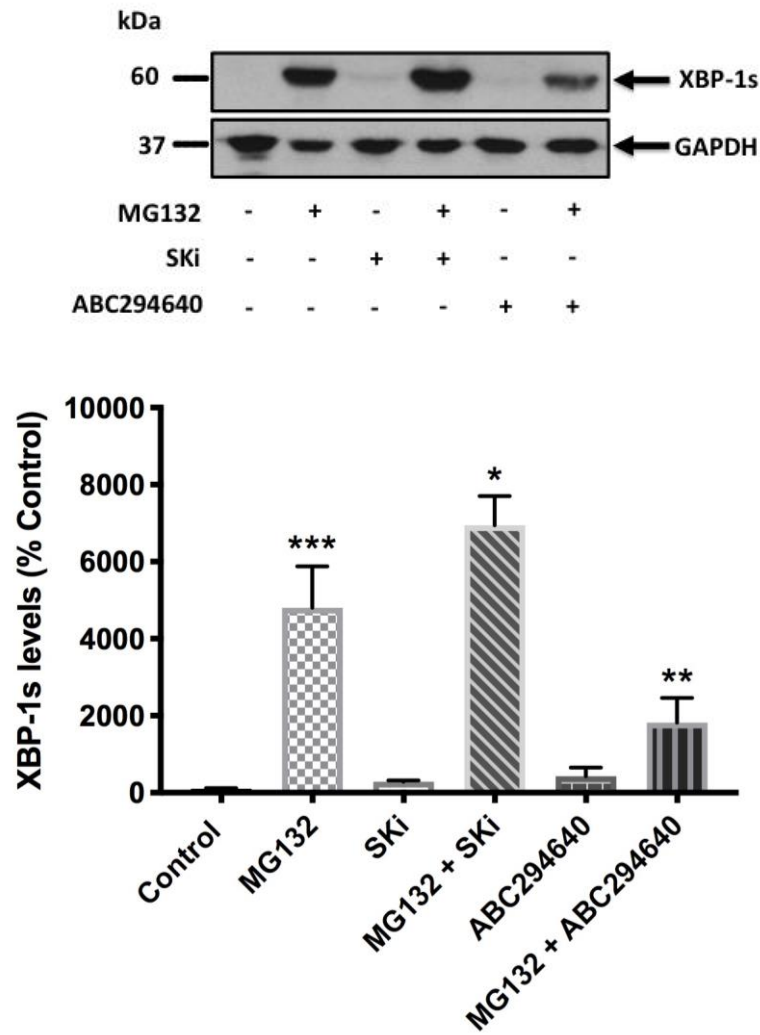


Figure 3.39 Effect of SKi or ABC294640 in combination with MG132 to XBP-1s levels in HEK293T cells. HEK293T cells were cultured in complete medium containing 10% FCS until ~70% confluent. Cells were pre-treated with MG132 (10 μ M, 30 minutes) before addition of SKi (10 μ M) or ABC294640 (25 μ M) or with the vehicle alone (DMSO 0.1% v/v) for 24 hours. XBP-1s levels were detected using SDS PAGE and western blotting with anti-XBP-1s antibody. Blots were stripped and re-probed with anti-GAPDH antibody to ensure comparable protein loading. A representative western blot is shown of an experiment performed at least three independent times. Also shown is the densitometric quantification of XBP-1s/GAPDH ratio immunoreactivity of (Mr 60 kDa), expressed as a percentage of the control (Control=100%). The data was expressed as means \pm SEM for n=3 experiments and analysed by one-way ANOVA multiple comparisons test, * p <0.05 for MG132/SKi vs MG132, ** p <0.001 for MG132/ABC294640 vs MG132, and *** p <0.001 for MG132 vs control.

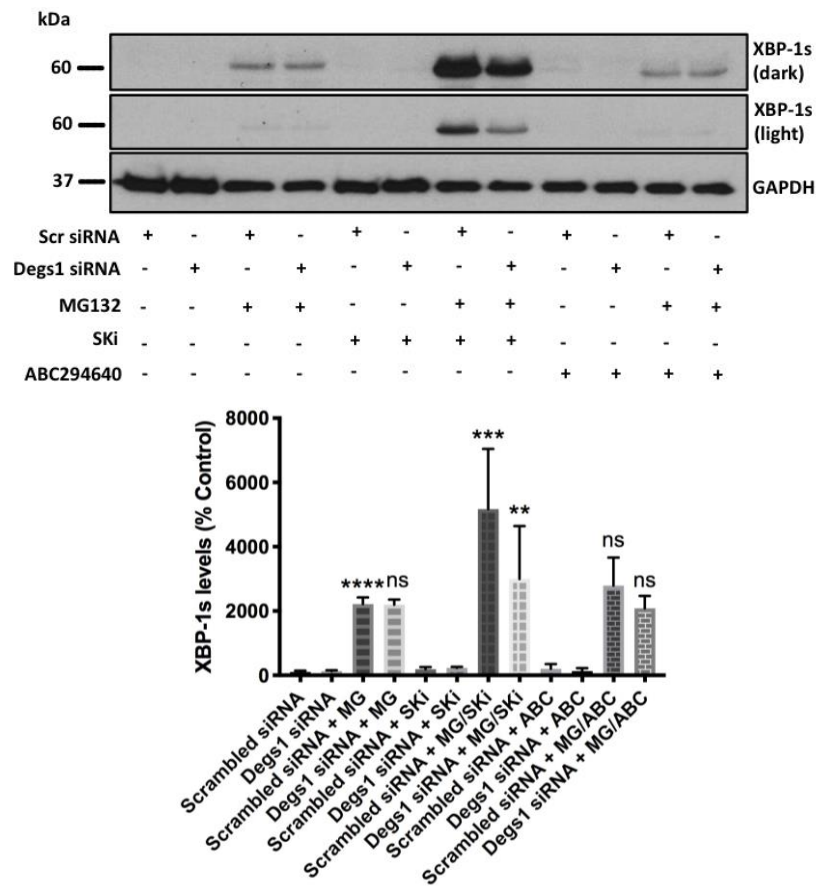


Figure 3.40 Effect of *Degs1* siRNA on *XBP-1s* levels in *HEK293T* cells. *HEK293T* cells were cultured in complete medium containing 10% FCS until ~70% confluent. Cells were transiently transfected with *Degs1* siRNA or scrambled siRNA at a final concentration of 100 nM in antibiotic free medium for 48 hours. Cells were then pre-treated with MG132 (10 μ M, 30 minutes) before addition of SKi (10 μ M) or ABC294640 (25 μ M) or with the vehicle alone (DMSO 0.1% v/v) for further 24 hours. *XBP-1s* levels were detected using SDS PAGE and western blotting with anti-*XBP-1s* antibody. Blots were stripped and re-probed with anti-GAPDH antibody to ensure comparable protein loading. A representative western blot is shown of an experiment performed at least three independent times. A lighter version of *XBP-1s* levels is also shown. Also shown is the densitometric quantification of *XBP-1s*/GAPDH ratio immunoreactivity of (Mr 60 kDa), expressed as a percentage of the control (Control=100%). The data was expressed as means \pm SEM for $n=3$ experiments and analysed by one-way ANOVA multiple comparisons test, $**p<0.01$ for *Degs1* siRNA/MG132/SKi vs Scrambled siRNA/MG132/SKi, $***p<0.001$ for Scrambled siRNA/MG132/SKi vs Scrambled siRNA/MG132, $****p<0.0001$ for Scrambled siRNA/MG132 vs Scrambled siRNA, and ns denotes not statistically significant (p value >0.05) for *Degs1* siRNA/MG132 vs Scrambled siRNA/MG132 or Scrambled siRNA/MG132/ABC294640 vs Scrambled siRNA/MG132 or *Degs1* siRNA/MG132/ABC294640 vs Scrambled siRNA/MG132/ABC294640.

3.2.10 Effect of SKi and ABC294640 on sphingolipid levels in

HEK293T cells

Changes in sphingolipid levels in response to SKi (10 μ M, 24 hours) and ABC294640 (25 μ M, 24 hours) were measured. The first sphingolipid analysed was levels of dihydroceramide; both SKi and ABC294640 stimulated increases in dihydroceramide levels. SKi elevated C24:1 dihydroceramide levels, with a significant increase in C16:0 and C24:0 dihydroceramides (Appendix, Figure S1). ABC294640 significantly increased C16:0, C22:0, C24:1, C24:0, C26:1, and C18:1 dihydroceramide levels, with slight increase in C18:0, C20:0, C:26:0, and C14 dihydroceramides (Appendix, Figure S1). Very low levels of hexosyl dihydroceramide were detected, but it was difficult to establish any consistent changes (data not shown).

We then investigated the effect of SKi and ABC294640 on long chain sphingoid bases as both compounds are considered to be dual SK1/SK2 inhibitors. SKi reduced sphinganine 1-phosphate levels, with a reduction in S1P approaching significance ($p=0.06$; Appendix, Figure S2), which was consistent with its characteristic as a dual SK1 and SK2 inhibitor. Moreover, SKi reduced Sph levels without affecting levels of sphinganine. On the other hand, ABC294640 increased Sph, sphinganine, and S1P levels, which could suggest the increasing of uptake and/or *de novo* synthesis whilst reducing levels of sphinganine 1-phosphate, which is a characteristic of SK inhibitors (Appendix, Figure S2). In addition, ABC294640 elevated Cer levels, which could also be due to *de novo* biosynthesis and/or uptake from the medium (Appendix, Figure S3). Furthermore, ABC294640 increased many

Cers levels (including C14:0, C16:0, C18:0, C18:1, C20:0, C22:0, C24:1, C24:0, C26:0, and C26:1; Appendix, Figure S4), which could account for the ABC294640-induced apoptosis. In contrast, SKi decreased C18:0 and C20:0 Cers, but increased levels of C24:1 and C14:0 Cers (Appendix, Figure S3). SKi had a slight effect on total Cers assuming that it failed to stimulate “apoptotic” Cers; thus, it did not induce cleavage of PARP or the expression of CHOP, nor did it inhibit DNA synthesis (Figures 3.17, 3.18, and 3.19).

Sphingomyelin levels were also analysed. ABC294640 appears to increase C20:0, C22:0, 24:0, 24:1, and C26:1 Cers, with a significant increase in C18:0, but SKi had no effect (Appendix, Figure S4). Dihydro sphingomyelin levels were also significantly elevated by ABC294640 (including C18:0, C22:0, C24:0, C26:1, and C24:1; $p=0.054$), whereas SKi increased only C16:0 dihydro sphingomyelin levels (Appendix, Figure S5).

3.3 DISCUSSION

The main finding of this study is to demonstrate that Degr1 is subject to regulation by the ubiquitin-proteasomal degradation pathway and that this can be induced by SKi. Confirmation that Degr1 is subject to polyubiquitination was based on the following:

- (1) formation of the Degr1 ladder was reduced by knocking down Degr1 with Degr1 siRNA.
- (2) immunoprecipitation of the Degr1 ladder proteins with the anti-Degr1 antibody.
- (3) reduction in the formation of the Degr1 ladder by pre-treatment of cells with the E3 ligase Mdm2 inhibitor, nutlin.
- (4) induction of the Degr1 ladder upon treatment of cells with proteasome inhibitors, MG132 or bortezomib.

The native and polyubiquitinated forms of Degr1 were found to produce completely different effects on HEK293T cell fate. The native Degr1, modulated by substrate induction by ABC294640, promoted cell death. In contrast, the polyubiquitinated forms that accumulate in response to SKi, promoted cell survival through the activation of P-JNK/P-p38 MAPK and XBP-1s (Figures 3.27 and 3.39). The formation of the polyubiquitinated forms of Degr1 increased when cells were treated with a combination of either MG132 or bortezomib and SKi, thereby indicating that Degr1 is subject to a dynamic ubiquitin-proteasomal turnover. Since these forms accumulate when SKi is combined with a proteasome inhibitor, an explanation might be that some compounds force degradation of Degr1 in cells through the ubiquitin-proteasomal pathway that, in turn, may lead to senescence cell death (as opposed to

apoptotic cell death). This is based on a previous study which showed that removal of Degr1 by siRNA knockdown induced markers of senescence, p53 and p21, in prostate cancer cells (McNaughton *et al.*, 2016). This removal of Degr1 through the ubiquitin-proteasomal system could account for cell death produced by these compounds, which has been reported in the previous literature (Hernández-Tiedra *et al.*, 2016; Wu *et al.*, 2001; Erdreich-Epstein *et al.*, 2002; Hail *et al.*, 2006; Gagliostro *et al.*, 2012). Therefore, the polyubiquitinated forms of Degr1 might predominate when the degradation rate is low, leading to cell survival (Zheng *et al.*, 2006; Signorelli *et al.*, 2009; Gagliostro *et al.*, 2012; Siddique *et al.*, 2012; Siddique *et al.*, 2013; Breen *et al.*, 2013), while complete removal of the protein might lead to senescent death (not apoptotic) (McNaughton *et al.*, 2016).

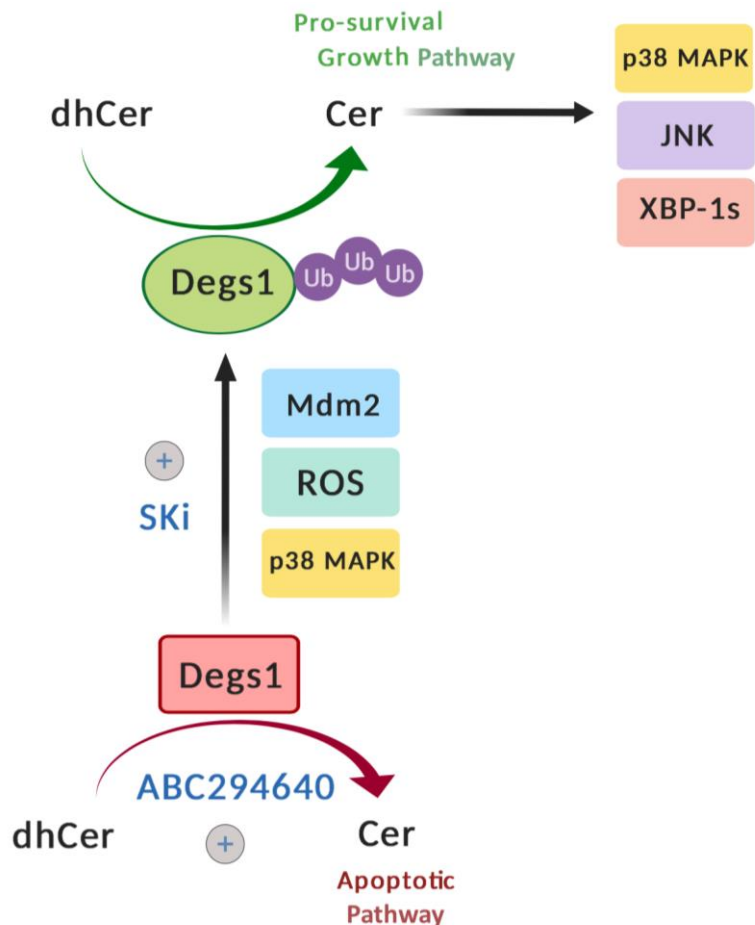


Figure 3.41 *Different roles of native and polyubiquitinated Dsgs1 forms.* An illustrative scheme shows that the native and polyubiquitinated forms of Dsgs1 produce different effects on cell fate. Native Dsgs1 activated through ABC294640 regulates formation of Cer species responsible for apoptosis, while polyubiquitinated Dsgs1 activated through SKi regulates formation of prosurvival/growth Cer species [Adapted from (Alsanafi et al., 2018)].

In addition, since ABC294640, but not SKi, has been shown to induce PARP cleavage, CHOP expression, and decreased DNA synthesis, the native Dsgs1 is likely associated with apoptosis and growth inhibition. This was supported by evidence showing that gene-specific Dsgs1 siRNA reversed the ABC294640-induced PARP cleavage as well as the reduction in DNA synthesis, thereby indicating the involvement of native Dsgs1. Moreover, reduction of phosphorylated

Akt, which is involved in cell survival and growth (Osaki *et al.*, 2004), when cells were treated with ABC294640, but not SKi, provides additional evidence that the native enzyme functions to reduce cell survival. Sphingolipids measurements also showed that ABC294640 induced increases in the levels of Cer species that are known to inhibit Akt phosphorylation (Schubert *et al.*, 2000; Bourbon *et al.*, 2002). This was consistent with studies by French *et al.* (2010), who showed ABC294640 markedly shifted the sphingolipid rheostat in favour of ceramide with C16, C22, C24, and C24:1 ceramide species elevated concomitant with S1P levels being reduced (French *et al.*, 2010). In addition, the current study, shows that ABC294640 stimulated autophagy through the extensive removal of both LC3B-I and LC3B-II, while SKi inhibited conversion of LC3B-I to LC3B-II and, hence, appears to block autophagy. This finding was consistent with previous literature which showed that ABC294640 is an inducer of autophagy in pancreatic and kidney cancer cells (Beljanski *et al.*, 2010). Moreover, Tonelli *et al.* (2013) reported that SKi inhibits autophagy in LNCaP AI cells through the accumulation of the non-lipidated inactive form LC3 (LC3-I) (Tonelli *et al.*, 2013). The ability of SKi to inhibit autophagy in HEK293T cells might be related to oxidative stress, since mitochondria are the chief endogenous producers of cellular ROS and when defective they are subjected to degradation through the autophagic pathway. Therefore, inhibition of autophagy could result in accumulation of defective mitochondria that might lead to abnormal ROS production (Jin and White, 2008). This is of particular interest as the SKi-induced polyubiquitination of Degr1 is inhibited by the ROS scavenger, NAC.

Autophagy is known as a double-edged sword that can either promote apoptosis (Maiuri *et al.*, 2007) or protect cells from apoptosis (Li *et al.*, 2013) depending on the cell type, triggering stimuli, intracellular metabolic activity, and extracellular nutrient supply. In this study, it is apparent that stimulation of autophagy in either ABC294640- or MG132-treated HEK293T cells was linked with apoptotic cell death. The concept that ABC294640 could lead to apoptotic cellular death was shown in previous literature. A recent study by Xu *et al.* (2018) reported that ABC294640 induced G1-S arrest and apoptosis in cervical carcinoma cells (Xu *et al.*, 2018). In addition, ABC294640 was recently shown by Ding *et al.* (2019) to inhibit proliferation and induce apoptosis of RBE and HCCC9810 cells (Ding *et al.*, 2019). Moreover, Song *et al.* (2019) reported that ABC294640 induced cell cycle arrest in S phase and increased apoptosis in EOC cells (Song *et al.*, 2019). Furthermore, various recent studies reported that ABC294640 can synergise with different compounds, such as agents that block bone marrow kinase in chromosome X (BMX), chemotherapeutic agents (e.g. doxorubicin) and the Bcl-2 inhibitor, ABT-199 to enhance cellular apoptosis (Jin *et al.*, 2018; Leili *et al.*, 2018; Sundaramoorthy *et al.*, 2018). Recent advances in the study of cell death have shown that apoptosis and autophagy are interconnected signalling pathways that can cross-talk with each other under various cellular stress responses (Chen *et al.*, 2018). For example, Kulkarni *et al.* (2016) showed that a novel digitoxin analogue was able to promote autophagy-induced apoptosis in lung cancer cells (Kulkarni *et al.*, 2016). In addition, Cheng *et al.* (2018) showed that autophagy enhances apatinib-induced apoptosis through ER stress in human colorectal cancer (CRC) cells (Cheng *et al.*, 2018). Recently others have reported that apoptosis regulated through autophagy is

linked to targeting NOXA for degradation (Wang *et al.*, 2018). Therefore, if autophagy is linked with apoptosis then SKi inhibition of autophagy will contribute to a cell survival function enhanced through the formation of polyubiquitinated Degr1 forms. Overall, the native form of Degr1 might be accountable for the synthesis of Cer species which can block Akt signalling, whereas the polyubiquitinated forms of Degr1 are linked with p38 MAPK signalling that functions to reduce autophagy through phosphorylation of Unc-51-like autophagy-activating kinase 1 (ULK1) (He *et al.*, 2018). Indeed, certain Degr1 inhibitors/modulators promote autophagy (Signorelli *et al.*, 2009; Gagliostro *et al.*, 2012) possibly as a consequence of proteasomal degradation and loss of Degr1 from cells. However, results showed that ABC294640 induces autophagy without removal of Degr1 in HEK293T cells. This finding was consistent with Casasampere *et al.* (2017) who reported that autophagy can be induced through both dihydroceramide-dependent and independent pathways and the balance between these two pathways affects the final cell fate (Casasampere *et al.*, 2017).

The results from this current study demonstrate that oxidative stress, p38 MAPK, and Mdm2 are involved in regulating the ubiquitin-proteasomal degradation of Degr1 in response to SKi. Cingolani *et al.* (2014) suggested that the dual SK1/SK2 inhibitor, SKi, indirectly decreased the activity of Degr1 and increased the levels of dhCers through the inhibition of oxidative stress and NADH-cytochrome B5 reductase (Cingolani *et al.*, 2014). Likewise, many studies have demonstrated that fenretinide inhibits Degr1 activity and promotes oxidative stress (Zheng *et al.*, 2006; Wang *et al.*, 2008; Rahmaniyan *et al.*, 2011). An explanation might be that Degr1 is only

partially and not fully removed from cells through the proteasomal degradation pathway in response to fenretinide. Thus, SKi or fenretinide are not considered as catalytic inhibitors but induce proteasomal degradation mediated by oxidative stress. Additional evidence that supports this mode of regulation and linkage between Mdm2 and p38 MAPK was obtained by Li *et al.*, who demonstrated that TNF α stimulated the ubiquitin ligase atrogin1/MAFbx via a mechanism involving p38 MAPK pathway in skeletal muscle (Li *et al.*, 2005). In addition, Zhu *et al.* (2002) reported that p38 MAPK inhibitors and a dominant-interfering mutant of the p38-activating kinase mitogen-activated protein kinase kinase 3 reduced the hypoxia down-regulation of Mdm2 (Zhu *et al.*, 2002).

The effect of SKi and ABC294640 on sphingolipid levels has also provided information on the functional relationship between Degs1, SK1, and SK2 in terms of regulating the survival of HEK293T cells. For example, SKi induced a modest increase C16:0 and C24:0 dihydroceramides levels that are consistent with the loss of Degs1 via the ubiquitin-proteasomal degradation route. While Degs1 catalyses the desaturation of various molecular species of dihydroceramide, the effect of SKi was selective to two dihydroceramide species, suggesting that the polyubiquitinated forms of Degs 1 either have altered substrate specificity (compared with the native form) for certain dihydroceramide species or that there is a change in localisation of Degs1 to a specialised lipid microdomain where access is restricted to C16:0 and C24:0 dihydroceramides.

The rate of loss of Degr1 in response to SKi is thought to be slow, thereby allowing for the accumulation of intermediate polyubiquitinated forms that promote cell survival. Furthermore, SKi treatment increased C14:0 and C24:1 Cers, which might be endowed with pro-survival functions in terms of regulation of p38 MAPK/JNK and XBP-1s signalling. These findings are supported by the studies of Beauchamp et al. (2009) who demonstrated that the sub-cellular localisation of Degr1 can be regulated by N-myristoylation, which promotes redistribution of Degr1 from the ER to the mitochondria. However, it is likely that the polyubiquitinated forms of Degr1 are localised to the ER because of the link with the activation of ER stress effectors (e.g. JNK and p38 MAPK).

Degr1 appears to be localised to non-ionic detergent-resistant membranes in HEK293T cells since the ionic detergent lysis buffer successfully solubilised native and polyubiquitinated Degr1 forms. Karsai et al. (2019) reported that Degr1 was found mainly co-localised with the ER marker protein disulfide isomerase (PDI) with minimal co-localisation with the mitochondrial marker Tim23 (Karsai *et al.*, 2019). The post-translationally modified forms of Degr1 is positively linked with the increase in the XBP-1s pro-survival expression since SKi but not ABC294640 enhanced the MG132-induced XBP-1s levels and Degr1 siRNA reduced this response. The concept of sphingolipids being able to directly activate UPR and ER stress sensors is consistent with various previous studies recently reviewed in Bennett et al. (2019) (Bennett *et al.*, 2019).

On the other hand, ABC294640 induced an increase in levels of both dihydroceramide and Cer, thereby indicating a general increase in flux through the *de novo* Cer pathway and/or cellular uptake. High levels of dihydroceramides would provide “gain of function” to the native form of Degs1 through the mechanism of substrate induction in order to promote the formation of Cers that induce the apoptotic response. The observed changes in dihydroceramide levels with SKi and ABC294640 are consistent with McNaughton et al. (2016), who reported that SKi and ABC294640 induce senescence of androgen-independent LNCaP-AI prostate cancer cells concomitant with the proteasomal degradation of SK1 and Degs1 as well as increased expression of p53 and p21 (McNaughton *et al.*, 2016). Other studies have also demonstrated that SKi and ABC294640 elevate dihydroceramide levels through apparent inhibition of Degs1 activity in prostate cancer cells (Loveridge *et al.*, 2010; Venant *et al.*, 2015). Furthermore, SKi has been shown to induce an increase in the levels of dihydroceramide in ovarian cancer cells (Illuzzi *et al.*, 2010). In the current study, ABC294640 increased the levels of both Sph and S1P, which was an unpredicted finding as this compound is a SK2 inhibitor and induces the proteasomal degradation of SK1. However, ABC294640 is considered a weak SK2 inhibitor ($IC_{50} = 50 \mu M$) (French *et al.*, 2010), thereby possibly leaving sufficient residual SK2 activity to drive the formation of S1P as a result of the accumulated high Sph levels in response to ABC294640. ABC294640 also lowered levels of sphinganine 1-phosphate, which was consistent with its ability to promote the proteasomal degradation of SK1 in HEK293T cells. This result might suggest that SK1, more than SK2, is involved in catalysing the formation of sphinganine 1-phosphate in these cells. In addition, the moderate reduction of S1P upon treatment

with SKi could be explained by the fact that SKi has stronger SK2 inhibition activity ($IC_{50} = 2 \mu M$) (unpublished data) compared to ABC294640; thus, S1P levels might be regulated primarily through SK2 in HEK293T cells.

The findings of this study reveal that Degr1 is a versatile enzyme, and the polyubiquitination of this enzyme appears to change its function from being pro-apoptotic to pro-survival. This result could explain the contradictory reports on Degr1 in promoting cell survival, such as through autophagy or apoptosis, as reviewed in Siddique et al. (2015). Sridevi et al. (2010) showed that cellular stress in HEK293 cells promoted translocation of CerS1 from the ER to Golgi and proteasomal degradation (Sridevi *et al.*, 2010). In addition, Min et al. (2007) reported that over-expression of CerS1 in HEK293 cells induced activation of p38 MAPK in response to cisplatin (Min *et al.*, 2007). Taken together with the current findings, it is conceivable that CerS1 and polyubiquitinated Degr1 could function together to regulate the p38 MAPK pathway.

The lifespan of polyubiquitinated forms of Degr1 might govern the pro-survival function of Degr1 in diverse cellular systems. This finding could have a significant benefit in validating Degr1 as a drug target in different cancer cells. For instance, the drug-induced prevention of the formation of polyubiquitinated forms of Degr1, in addition to increasing *de novo* biosynthesis of apoptotic Cers, might be usefully exploited to induce apoptotic cell death of cancer cells. In addition, accelerating the proteasomal degradation of Degr1 and reducing the levels of the polyubiquitinated forms might result in the senescent-induced death of cancer cells.

CHAPTER 4:

**THE ROLE OF SPHINGOSINE KINASES 1
AND 2 IN REGULATING p53, p38 MAPK,
JNK AND XBP-1s SIGNALLING IN HUMAN
EMBRYONIC KIDNEY CELLS**

CHAPTER 4: THE ROLE OF SPHINGOSINE KINASES 1 AND 2 IN REGULATING p53, p38 MAPK, JNK AND XBP-1s SIGNALLING IN HUMAN EMBRYONIC KIDNEY CELLS

4.1 INTRODUCTION

The p53 tumour-suppressor gene, a cellular stress sensor, is often mutated in most human cancers (Vousden and Lu, 2002). Many cellular stresses induce and promote phosphorylation of p53, including UV radiation, γ -irradiation, DNA cross-linking, hypoxia, oxidative stress, and nucleotide depletion (Sharpless and DePinho, 2002; Wahl and Carr, 2001; Vousden and Lu, 2002). Once p53 is activated, it functions as a transcription factor and stimulates the expression of various downstream genes associated with DNA repair, cell cycle arrest, or apoptosis (Vousden and Lu, 2002). p53 is strictly regulated by cofactor binding, post-translational modifications, and subcellular localisation in order for it to function properly. Mdm2, an E3 ubiquitin ligase, tightly regulates p53 functions through the acceleration of p53 nuclear export and degradation by the 26S proteasome, resulting in the inactivation of its tumour suppressor activity (Michael and Oren, 2002). Meanwhile, p53 phosphorylation within its amino-terminal domain stabilises p53 through the disruption of the p53–Mdm2 interaction (Michael and Oren, 2002; Wahl and Carr, 2001) and the prevention of its nucleo-cytoplasmic export (Zhang and Xiong, 2001).

Various studies have demonstrated that sphingosine kinase inhibitors promote cellular apoptosis through the activation of p53. For example, Lima et al. (2018)

showed that SK1-I [(2R, 3S, 4E)-N-methyl-5-(4'-pentylphenyl)-2-aminopent-4-ene-1,3-diol], an SK1 selective inhibitor, promotes the phosphorylation of p53 on Ser15 and induces the expression of pro-apoptotic members of the Bcl-2 family, including BAX, BAK1 and BID, leading to the suppression of cancer cell growth. In addition, SK1-I promoted the accumulation of dilated intracellular vacuoles and enhanced BECN- and ATG5-dependent autophagy and cell death in a p53-dependant manner (Lima *et al.*, 2018). Carroll *et al.* (2018) also reported that p53 stimulates SK1 proteolysis via a mechanism involving caspase-2 activation to induce apoptosis. These authors also identified mutations in p53 in various cancers, including triple-negative breast cancer cells (TNBC) that impaired caspase 2 activation and degradation of SK1 (Carroll *et al.*, 2018). Interestingly, a recently identified caspase-2-dependent apoptotic pathway has been shown to suppress cell cycle kinase (CHK1), thereby leading to an independent activation of caspase-2-mediated apoptosis as a response to DNA damage in p53-mutant cells (Sidi *et al.*, 2008). Components of this apoptotic pathway and essential downstream targets are still to be identified (Sidi *et al.*, 2008; Ando *et al.*, 2012; Thompson *et al.*, 2015).

McNaughton *et al.* (2016) reported that the sphingosine kinase inhibitors SKi and ABC294640 promote the proteasomal degradation of SK1 and Degr1 and increase expression of p53 and p21 that results in cellular senescence in androgen-independent prostate cancer cells. While knocking down SK1 or SK2 failed to promote expressions of p53 and p21, SK1 siRNA reduced DNA synthesis in these cells. Moreover, Degr1 siRNA increased expression of p53 whereas a combination of Degr1/SK1 siRNA induced p21 expression. Hence, Degr1 and SK1 were shown

to be involved in regulating the growth of LNCaP-AI prostate cancer cell growth through p53/p21-dependent and -independent pathways (McNaughton *et al.*, 2016). Venant *et al.* (2015) also showed that ABC294640 induces suppression of Degr1 activity and accumulation of dhCers in prostate cancer cells (Venant *et al.*, 2015). SKi has been proposed to indirectly inhibit the activity of Degr1 through a mechanism that involves cytochrome B5 reductase (Cingolani *et al.*, 2014), resulting in higher levels of dhCer in ovarian and prostate cancer cells (Illuzzi *et al.*, 2010; Loveridge *et al.*, 2010). Therefore, both SKi and ABC294640 stimulate cellular senescence coupled with proteasomal degradation of SK1 and Degr1 and increased expression of p53 in cancer cells (McNaughton *et al.*, 2016).

The literature has various controversial reports regarding the role of SK1, SK2 and Degr1 in cell survival/apoptosis and we propose that these enzymes could functionally interact with each other in a cell context specific manner leading to either cell survival or cell apoptosis. The controversy regarding Degr1 was previously discussed in details in Chapter 3. For example, Siddique *et al.* (2013) reported that Degr1 ablation simultaneously activates anabolic and catabolic signalling pathways. Anabolic signalling pathway was regulated by Akt/protein kinase B (PKB) leading to an anti-apoptotic effect and cell survival while catabolic signalling pathway was regulated through AMP-activated protein kinase and stimulation of autophagosomes leading to cell autophagy and which is dissociated from the activated pro-survival pathway (Siddique *et al.*, 2013). Others reported that inhibition of Degr1 induces autophagic cell death (Gagliostro *et al.*, 2012; Hernández-Tiedra *et al.*, 2016). Moreover, fenretenide and resveratrol-induced

apoptosis was reported to be due to inhibition of Dggs1 (Wu *et al.*, 2001; Hail *et al.*, 2006) and blocking enzymes up-stream of Dggs1 in the *de novo* Cer synthesis pathway was shown to prevent apoptosis (Erdreich-Epstein *et al.*, 2002). SK1 is broadly associated with cell proliferation and survival (Olivera *et al.*, 1999; Xia *et al.*, 1999), whereas SK2 can be involved in the suppression of cellular growth and activation of apoptosis (without the involvement of S1P receptors) due to its putative BH3 domain that isolates the anti-apoptotic Bcl2 resulting in apoptosis (Liu *et al.*, 2003). However, various other reports showed that SK2 inhibition stimulates apoptosis in several cancer cells, as reviewed in (Pyne *et al.*, 2018).

In Chapter 3, SKi was found to induce polyubiquitination of Dggs1 that is linked with the activation of pro-survival pathways, including p38 MAPK, JNK, and XBP-1s in HEK293T cells. However, ABC294640 failed to induce these polyubiquitinated forms of Dggs1 leading to high *de novo* synthesis of ceramide and apoptosis through a native Dggs1-dependent mechanism (Alsanafi *et al.*, 2018). These novel findings support opposing functions of the native and polyubiquitinated forms of Dggs1 in relation to cell survival. Similarly, Sridevi *et al.* (2010) showed that CerS1 translocates from the ER to the Golgi in stressed HEK293 cells, leading to the stimulation of the ubiquitin–proteasome degradation pathway (Sridevi *et al.*, 2010). Therefore, in this Chapter, I have further investigated the effect of the sphingosine kinase inhibitors SKi and ABC294640 on HEK293T cells survival in terms of SK1, SK2, and Dggs1 as well as their regulation of downstream effectors p53, p38 MAPK, JNK, and XBP-1s.

4.2 RESULTS

4.2.1 Effect of SKi and ABC294640 on post-translational modification of p53 in HEK293T and parental HEK293 cells

The study investigated the role of SK1, SK2 and Degs1 in regulating p53 signalling in HEK293T cells, given that previous studies have shown that SK1 inhibitors promote p53-mediated cell death (Lima *et al.*, 2018). p53 is expressed as a 53 kDa protein in HEK293T cells. In addition, a minor protein species with a molecular mass of 63 kDa was detected with anti-p53 antibody on western blots. Treatment of HEK293T cells SKi (10 μ M, 24 hours) induced the expression of p63 and a protein with a molecular mass of 90 kDa, both of which cross-reacted with anti-p53 antibody (Figure 4.1A). In contrast, ABC294640 (25 μ M, 24 hours) (French *et al.*, 2010) only very weakly stimulated the formation of p63 and p90 in HEK293T cells (Figure 4.1A). Similar results were attained with the parental HEK293 cell line (Figure 4.1B).

p53 siRNA (100 nM, 48 hours) was used to confirm p53, p63, and p90 are related proteins. In this case, the siRNA treatment decreased the expression of p53 and removed both p63 and p90 in SKi-treated HEK293T cells (Figure 4.2). This suggests that these proteins are post-translational modified forms of p53. Immunoprecipitation with anti-p53 antibody was used to confirm the identities of the p53-related proteins. An isotonic lysis buffer failed to release p63 and p90 from the pellet fraction into the high-speed supernatant of SKi-treated cells (Figure 4.3A) and therefore, the isotonic sucrose-based lysis buffer was replaced with an ionic

detergent-containing (sodium deoxycholate) lysis buffer (Heckelman *et al.*, 1996). This successfully solubilised p53, p63 and p90 such that they were released into a high-speed supernatant fraction of SKi-treated cells (Figure 4.3B). Therefore, p53, p63 and p90 appear to be localised to non-ionic detergent-resistant membranes in HEK293T cells. Using this method, the post-translationally modified forms of p53 were then immunoprecipitated by the anti-p53 antibody (Figure 4.4). This confirms that p63 and p90 proteins are related to p53.

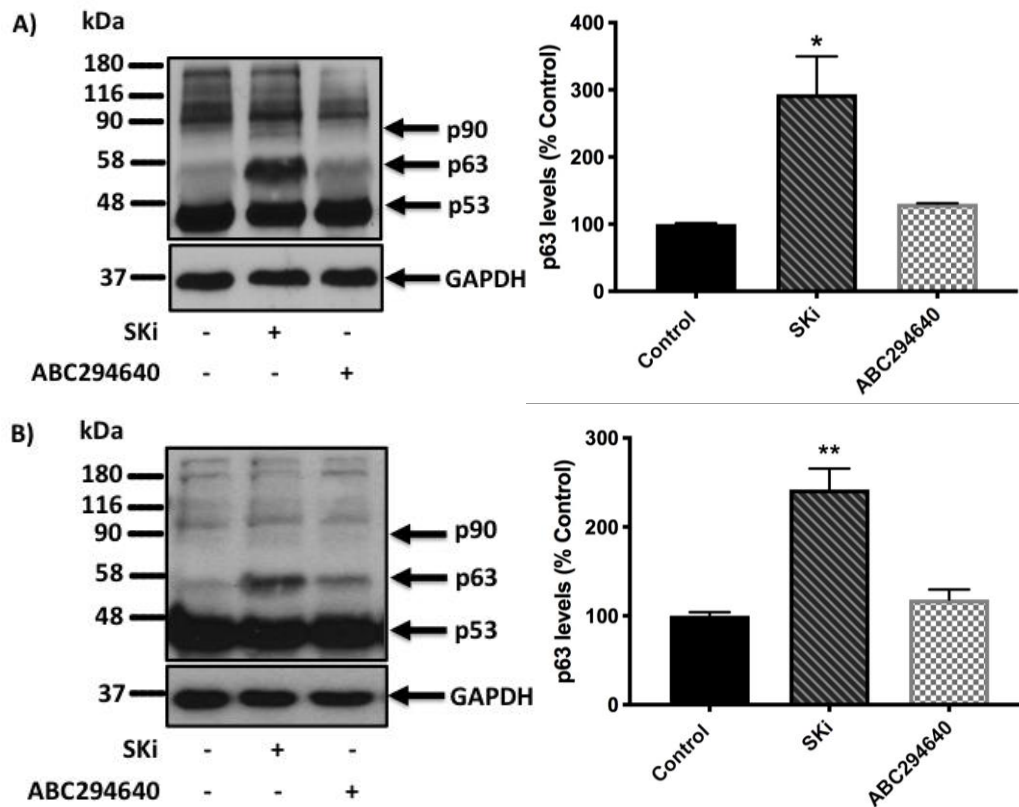


Figure 4.1 *Effect of SKi and ABC294640 on p53 in HEK293T and parental HEK293 cells.* A) HEK293T cells or B) Parental HEK293 cells were cultured in complete medium containing 10% FCS until ~70% confluent. Cells treated with SKi (10 μ M) or ABC294640 (25 μ M) or with the vehicle alone (DMSO 0.1% v/v) for 24 hours. p53, p63 and p90 levels were detected using SDS PAGE and western blotting probed with anti-p53 antibody. Blots were stripped and re-probed with anti-GAPDH antibody to ensure comparable protein loading. Two representative western blots are shown each of an experiment performed at least three independent times. Also shown is the densitometric quantification of p63/GAPDH ratio immunoreactivity of (Mr 63 kDa), expressed as a percentage of the control (Control=100%). The data was expressed as means \pm SEM for n=3 experiments and analysed by one-way ANOVA Dunnett's multiple comparisons test, * p <0.05 for SKi vs control and ** p <0.01 for SKi vs control.

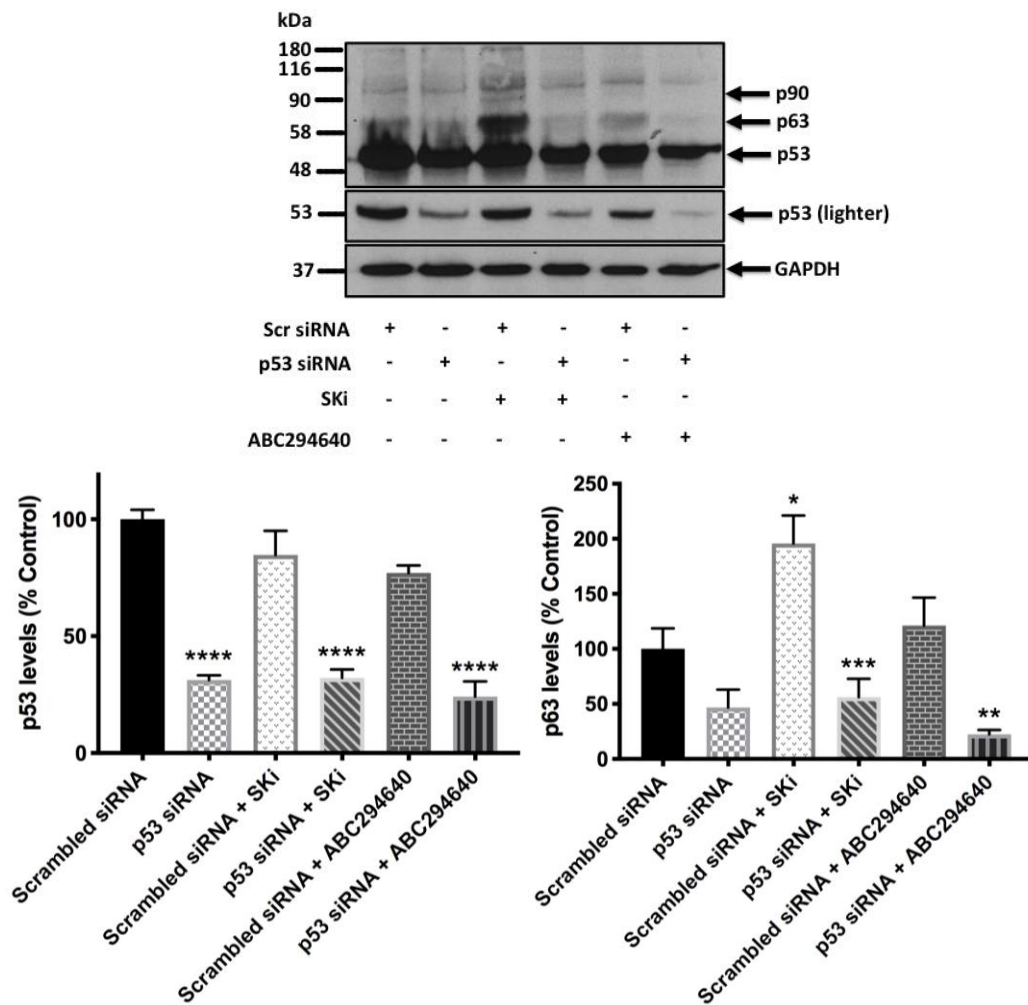


Figure 4.2 Confirmation of p53, p63 and p90 identities using siRNA in HEK293T cells. HEK293T cells were cultured in complete medium containing 10% FCS until ~70% confluent. Cells were transiently transfected with p53 siRNA or scrambled siRNA at a final concentration of 100 nM in antibiotic free medium for 48 hrs before being treated with SKi (10 μ M) or ABC294640 (25 μ M) or with the vehicle alone (DMSO 0.1% v/v) for further 24 hours. p53, p63 and p90 levels were detected using SDS PAGE and western blotting with anti-p53 antibody. Blots were stripped and re-probed with anti-GAPDH antibody to ensure comparable protein loading. A representative western blot is shown of an experiment performed at least three independent times. Also shown is the densitometric quantification of p53/GAPDH and p63/GAPDH ratios immunoreactivities of (Mr 53 and 63 kDa, respectively), expressed as a percentage of the control (Control=100%). The data was expressed as means \pm SEM for n=3 experiments and analysed by one-way ANOVA multiple comparisons test, in p53 levels **** p <0.0001 for p53 siRNA vs Scrambled siRNA or p53 siRNA/SKi vs Scrambled siRNA/SKi or p53 siRNA/ABC294640 vs Scrambled siRNA/ABC294640, and in p63 levels * p <0.05 for Scrambled siRNA/SKi vs Scrambled siRNA, ** p <0.01 for p53 siRNA/ABC294640 vs Scrambled siRNA/ABC294640, and *** p <0.001 for p53 siRNA/SKi vs Scrambled siRNA/SKi.

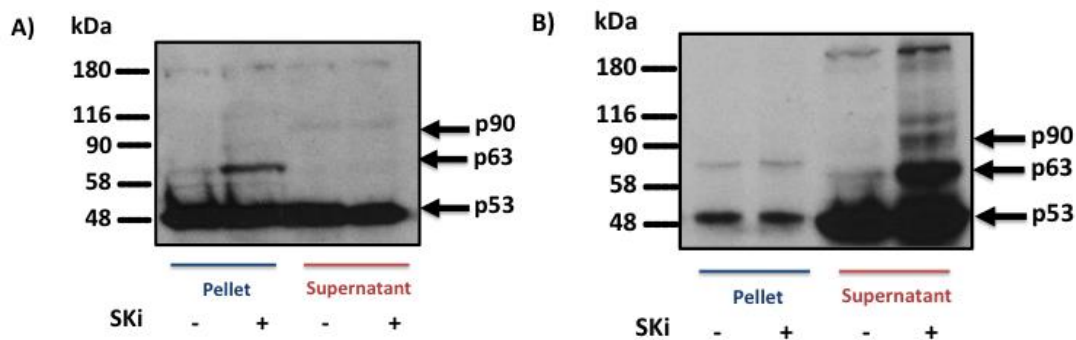


Figure 4.3 *p53 and location change according to cell harvesting method in HEK293T cells.* HEK293T cells were cultured in complete medium containing 10% FCS until ~70% confluent. Cells were treated with SKi (10 μ M) or with the vehicle alone (DMSO 0.1% v/v) for 24 hours. A) Cells were lysed with a sucrose-based isotonic buffer and p53, p63 and p90 were present in the high-speed pellet fraction. B) Cells were lysed in 1% deoxycolate lysis buffer and p53, p63 and p90 were located in the high-speed supernatant fraction. p53, p63 and p90 levels were detected using SDS PAGE and western blotting with anti-p53 antibody. Two representative western blots are shown each of an experiment performed at least three independent times.

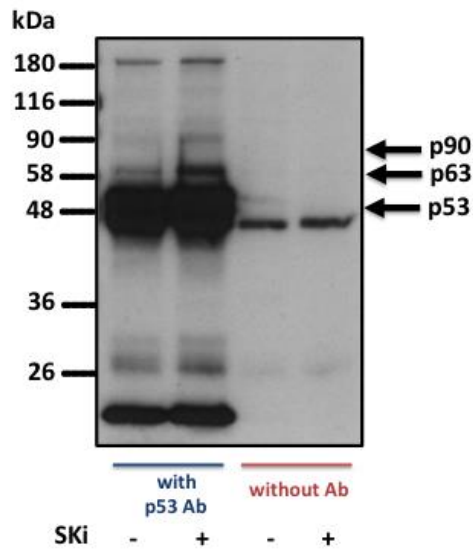


Figure 4.4 *p53 immunoprecipitation in HEK293T cells.* HEK293T cells were cultured in complete medium containing 10% FCS until ~70% confluent. Cells were treated with SKi (10 μ M) or with the vehicle alone (DMSO 0.1% v/v) for 24 hours. p53 was immunoprecipitated using 1% deoxycolate lysis buffer with/without p53 antibody. The resulting immunocomplexes were resolved by SDS PAGE and western blotted with anti-p53 antibody. A representative western blot is shown of an experiment performed at least three independent times.

The proteins p63 and p90 are post-translationally modified forms of p53 due to ubiquitination. This was established using HEK293T cells over-expressing an HA-tagged ubiquitin plasmid construct prior to treatment with SKi (10 μ M, 24 hours) and western blotting with the anti-p53 antibody. This experiment showed that over-expressed HA-tagged ubiquitin enhances the effect of SKi on p63 and p90 formation (Figure 4.5). As mentioned in Chapter 3, polyubiquitination is catalysed by a family of enzymes called E3 ligases (Zheng and Shabek, 2017). One member of this family, Mdm2, regulates the polyubiquitination of p53 (Moll and Petrenko, 2003) and might be responsible for regulating the conversion of p53 to p63 and p90, although this requires further investigation. Additional studies in the laboratory by others using the anti-phospho-p53 antibody with SKi-treated HEK293T cells failed to detect p63 and p90, thereby excluding the involvement of phosphorylation (data not shown).

Ubiquitination tags proteins for degradation by the proteasome. Therefore, it was expected that pre-treatment of cells with MG132 should enhance p63 and p90 formation in response to SKi due to the inhibition of proteasome activity. However, MG132 completely prevented the SKi-induced formation of p63 and p90 (Figure 4.6). These findings suggest that SKi induces the proteasomal degradation of an unidentified protein that function to suppress the formation of p63 and p90, i.e. proteasomal degradation of this protein in response to SKi facilitates p53 ubiquitination to p63 and p90. This protein could be SK1 because SKi induces the degradation of this enzyme and this is reversed by MG132 (Figure 3.11). To provide support for this possibility, HEK293T cells were transfected with SK1 siRNA (100

nM, 48 hours) to remove SK1 before being treated with SKi for another 24 hours. The results showed that combining SK1 siRNA and SKi treatment increased the formation of p63 and p90 compared with SKi alone (Figure 4.7A) and completely eliminated SK1 expression (Figure 4.7B). Since each agent alone decreased around 80% of SK1 expression while in combination achieved complete removal of SK1 (Figure 4.7B), this suggests that low level expression of SK1 can suppress formation of p63 and p90. The involvement of SK2 or Degr1 was also investigated because SKi has been shown to modulate these enzymes (as discussed in Chapter 3). However, knocking down SK2 or Degr1 with respective siRNAs did not affect the formation of p63 and p90 in response to SKi (Figures 4.8 and 4.9), thereby eliminating a role for these enzymes.

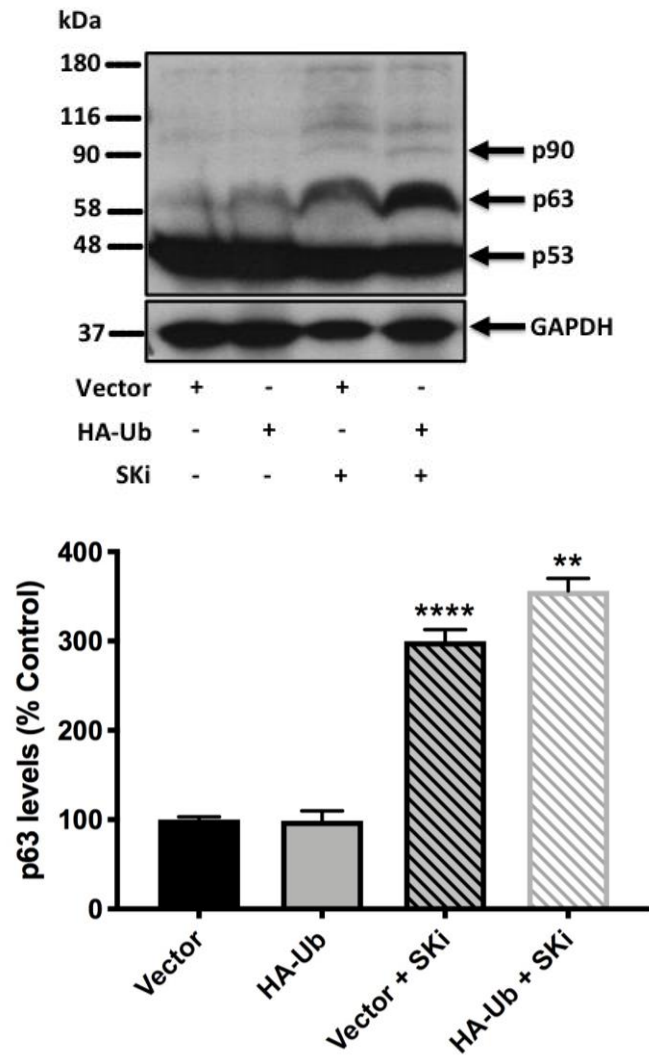


Figure 4.5 Effect of HA-tagged ubiquitin plasmid transfection on SKi-induced post-translationally modified forms of p53 in HEK293T cells. HEK293T cells were cultured in complete medium containing 10% FCS until ~70 % confluent. Cells were transiently transfected with HA-tagged ubiquitin plasmid construct or vector pcDNA 3.1 for 8 hrs before being treated with SKi (10 μ M) or with the vehicle alone (DMSO 0.1% v/v) for further 24 hours. p53, p63 and p90 levels were detected using SDS PAGE and western blotting with anti-p53 antibody. Blots were stripped and re-probed with anti-GAPDH antibody to ensure comparable protein loading. A representative western blot is shown of an experiment performed at least three independent times. Also shown is the densitometric quantification of p63/GAPDH ratio immunoreactivity of (Mr 63 kDa), expressed as a percentage of the control (Control=100%). The data was expressed as means \pm SEM for n=3 experiments and analysed by one-way ANOVA multiple comparisons test, ** p <0.01 for HA-Ub/SKi vs Vector/SKi and **** p <0.0001 for Vector/SKi vs Vector.

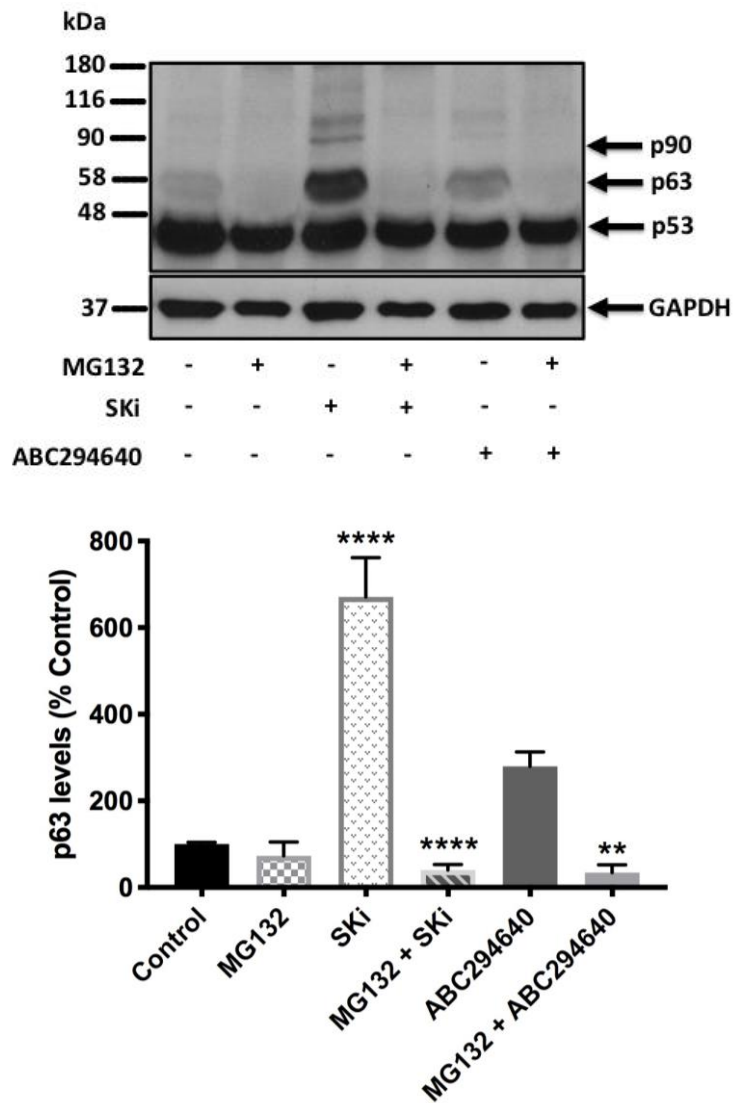


Figure 4.6 Effect of MG132 on p53 post-translationally modified forms in HEK293T cells. HEK293T cells were cultured in complete medium containing 10% FCS until ~70% confluent. Cells were pre-treated with MG132 (10 μ M, 30 minutes) before addition of inhibitors SKi (10 μ M) or ABC294640 (25 μ M) or with the vehicle alone (DMSO 0.1% v/v) for 24 hours. p53, p63 and p90 levels were detected using SDS PAGE and western blotting with anti-p53 antibody. Blots were stripped and re-probed with anti-GAPDH antibody to ensure comparable protein loading. A representative western blot is shown of an experiment performed at least three independent times. Also shown is the densitometric quantification of p63/GAPDH ratio immunoreactivity of (Mr 63 kDa), expressed as a percentage of the control (Control=100%). The data was expressed as means \pm SEM for n=3 experiments and analysed by one-way ANOVA multiple comparisons test, ** p <0.01 for MG132/ABC294640 vs ABC294640 and **** p <0.0001 for SKi vs control or MG132/SKi vs SKi.

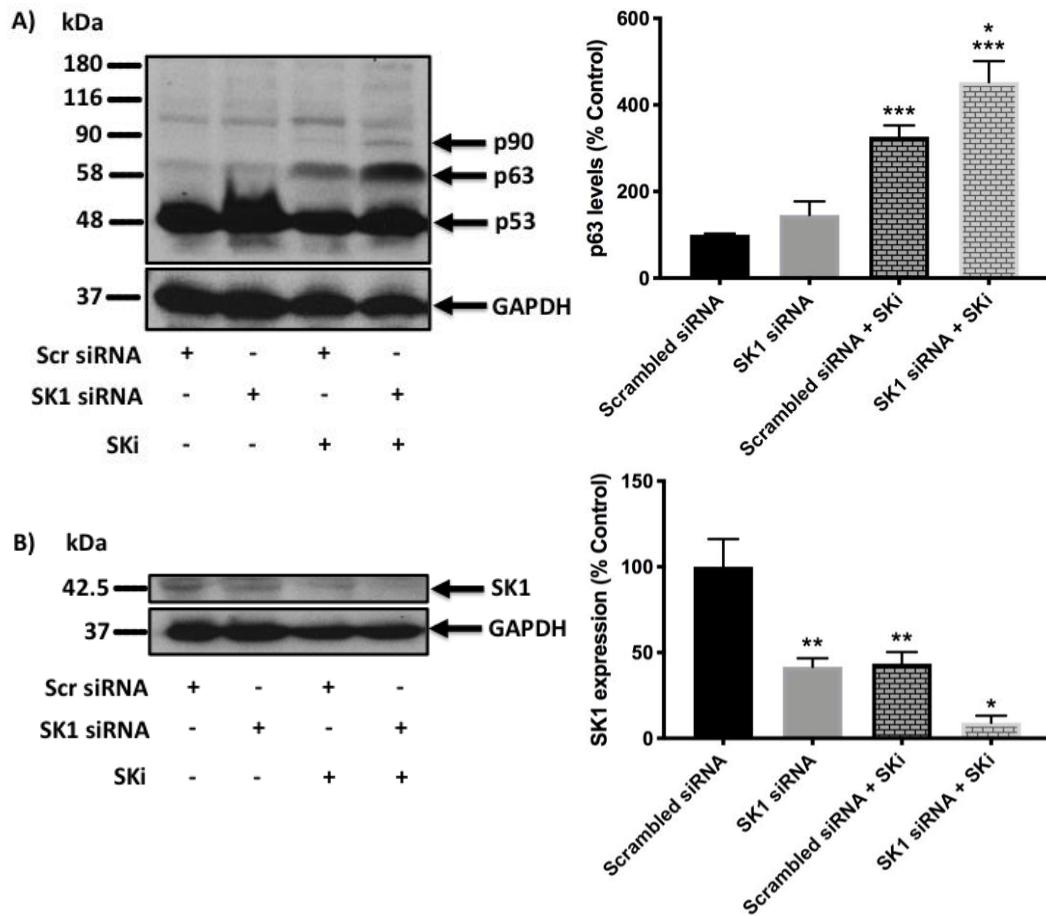


Figure 4.7 *Effect of SK1 siRNA on p53 post-translationally modified forms in HEK293T cells.* HEK293T cells were cultured in complete medium containing 10% FCS until ~70% confluent. Cells were transiently transfected with SK1 siRNA or scrambled siRNA at a final concentration of 100 nM in antibiotic free medium for 48 hrs before being treated with SKi (10 μ M) or with the vehicle alone (DMSO 0.1% v/v) for further 24 hours. A) p53, p63 and p90 levels were detected using SDS PAGE and western blotting with anti-p53 antibody or B) SK1 expression was detected using SDS PAGE and western blotting with anti-SK1 antibody. Blots were stripped and re-probed with anti-GAPDH antibody to ensure comparable protein loading. Two representative western blots are shown each of an experiment performed at least three independent times. Also shown is the densitometric quantification of p63/GAPDH and SK1/GAPDH ratios immunoreactivities of (Mr 63 and 42.5 kDa, respectively) expressed as a percentage of the control (Control=100%). The data was expressed as means \pm SEM for n=3 experiments and analysed by one-way ANOVA multiple comparisons test, A) * p <0.05 for SK1 siRNA/SKi vs Scrambled siRNA/SKi and *** p <0.001 for Scrambled siRNA/SKi vs Scrambled siRNA or SK1 siRNA/SKi vs SK1 siRNA B) * p <0.05 for SK1 siRNA/SKi vs SK1 siRNA or SK1 siRNA/SKi vs Scrambled siRNA/SKi and ** p <0.01 for SK1 siRNA vs Scrambled siRNA or Scrambled siRNA/SKi vs Scrambled siRNA.

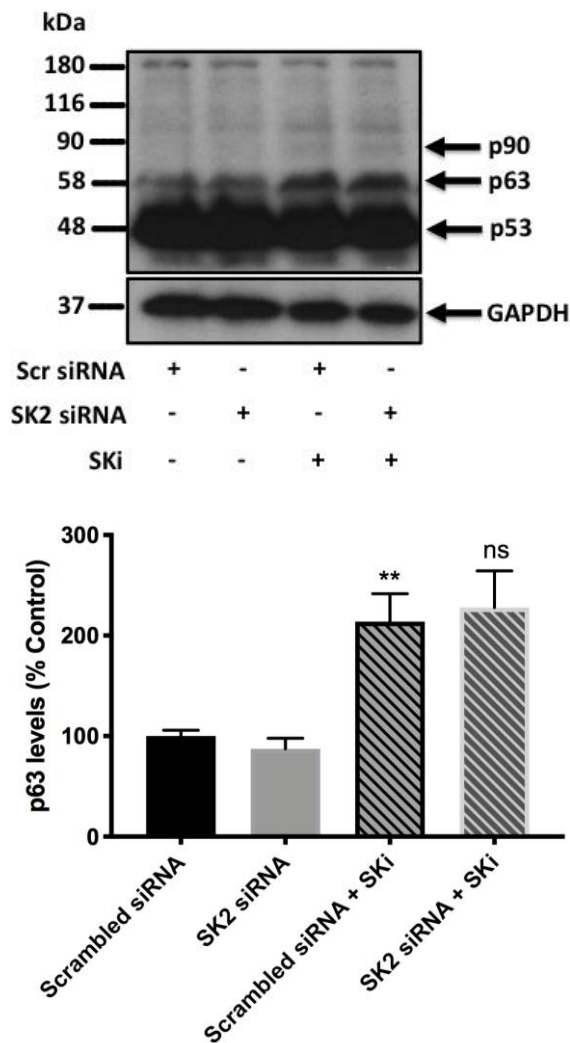


Figure 4.8 Effect of SK2 siRNA on p53 post-translationally modified forms in HEK293T cells. HEK293T cells were cultured in complete medium containing 10% FCS until ~70% confluent. Cells were transiently transfected with SK2 siRNA or scrambled siRNA at a final concentration of 100 nM in antibiotic free medium for 48 hrs before being treated with SKi (10 μ M) or with the vehicle alone (DMSO 0.1% v/v) for further 24 hours. p53, p63 and p90 levels were detected using SDS PAGE and western blotting with anti-p53 antibody. Blots were stripped and re-probed with anti-GAPDH antibody to ensure comparable protein loading. A representative western blot is shown of an experiment performed at least three independent times. Also shown is the densitometric quantification of p63/GAPDH ratio immunoreactivity of (Mr 63 kDa), expressed as a percentage of the control (Control=100%). The data was expressed as means \pm SEM for n=3 experiments and analysed by one-way ANOVA multiple comparisons test, **p<0.01 for Scrambled siRNA/SKi vs Scrambled siRNA and ns denotes not statistically significant (p value >0.05) for SK2 siRNA/SKi vs Scrambled siRNA/SKi.

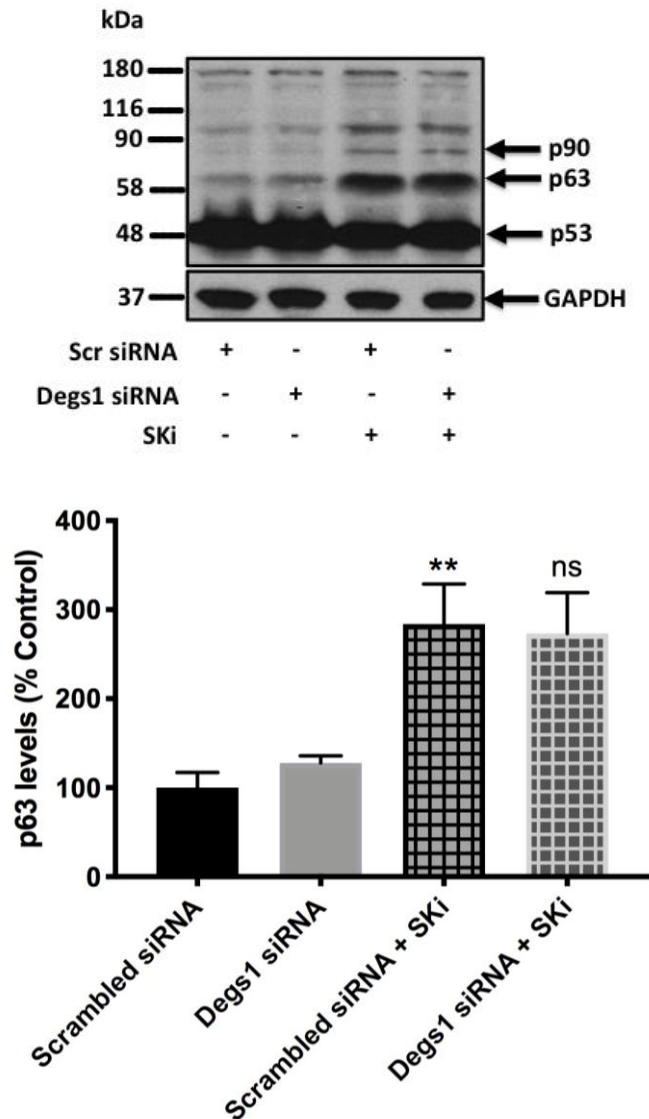


Figure 4.9 *Effect of Degs1 siRNA on p53 post-translationally modified forms in HEK293T cells.* HEK293T cells were cultured in complete medium containing 10% FCS until ~70% confluent. Cells were transiently transfected with Degs1 siRNA or scrambled siRNA at a final concentration of 100 nM in antibiotic free medium for 48 hrs before being treated with SKi (10 μ M) or with the vehicle alone (DMSO 0.1% v/v) for further 24 hours. p53, p63 and p90 levels were detected using SDS PAGE and western blotting with anti-p53 antibody. Blots were stripped and re-probed with anti-GAPDH antibody to ensure comparable protein loading. A representative western blot is shown of an experiment performed at least three independent times. Also shown is the densitometric quantification of p63/GAPDH immunoreactivity of (Mr 63 kDa), expressed as a percentage of the control (Control=100%). The data was expressed as means \pm SEM for n=3 experiments and analysed by one-way ANOVA multiple comparisons test, ** $p < 0.01$ for Scrambled siRNA/SKi vs Scrambled siRNA and ns denotes not statistically significant (p value > 0.05) for Degs1 siRNA/SKi vs Scrambled siRNA/SKi.

4.2.2 Effect of NAC on SKi-induced p63/p90 formation in

HEK293T cells

Vigneron and Vousden (2010) reviewed the importance of p53 in the regulation of senescence and longevity through its ability to both promote and inhibit oxidative stress and autophagy at different levels of ROS, which are highly dependent on collaborating factors, such as mTOR activity or oxidative stress (Vigneron and Vousden, 2010). Therefore, we investigated whether oxidative stress was involved in the ubiquitination of p53 using the antioxidant N-acetylcysteine (NAC). However, pre-treatment of cells with NAC did not affect the SKi-induced p63 and p90 formation, thereby eliminating the involvement of oxidative stress (Figure 4.10). This rules out a role for the formation of polyubiquitinated Degs1, which was inhibited by pre-treatment with NAC (Figure 3.9), and confirmed by use of Degs1 siRNA (Figure 3.6).

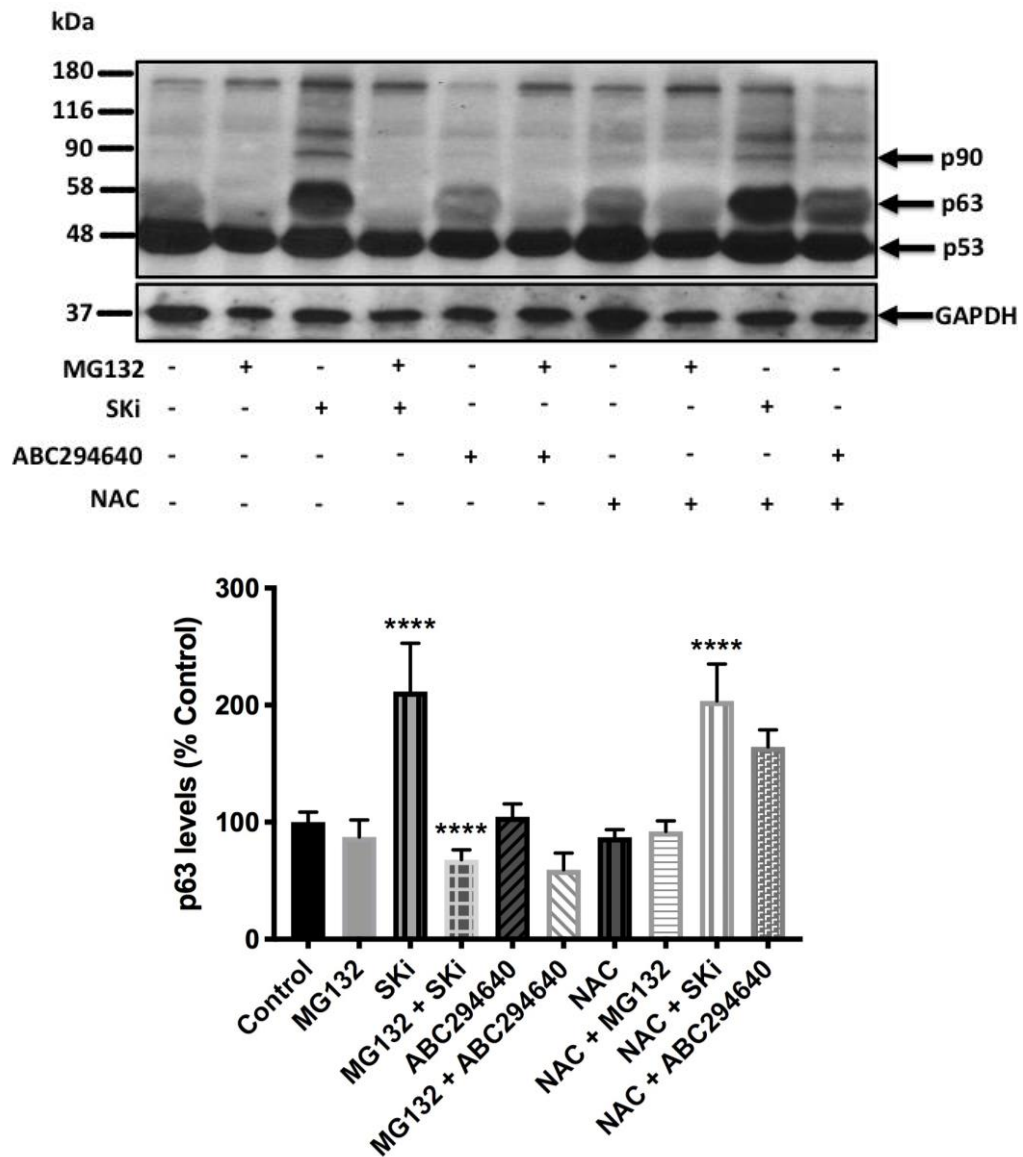


Figure 4.10 *The effect of NAC on post-translational modification of p53 in HEK293T cells. HEK293T cells were cultured in complete medium containing 10% FCS until ~70% confluent. Cells were pre-treated with NAC (10 mM, 30 minutes) or MG132 (10 μ M, 30 min) before addition of SKi (10 μ M) or ABC294640 (25 μ M) or with the vehicle alone (DMSO 0.1% v/v) for 24 hours. p53, p63 and p90 levels were detected using SDS PAGE and western blotting with anti-p53 antibody. Blots were stripped and re-probed with anti-GAPDH antibody to ensure comparable protein loading. A representative western blot is shown of an experiment performed at least three independent times. Also shown is the densitometric quantification of p63/GAPDH ratio immunoreactivity of (Mr 63 kDa), expressed as a percentage of the control (Control=100%). The data was expressed as means \pm SEM for n=3 experiments and analysed by one-way ANOVA multiple comparisons test, **** p <0.0001 for SKi vs control or MG132/SKi vs SKi or NAC/SKi vs NAC.*

4.2.3 Effect of SKi on p38 MAPK and JNK activation in HEK293T cells

As reported in Chapter 3, the polyubiquitinated forms of Degs1 positively regulate p38 MAPK and JNK pro-survival pathways in HEK293T cells. Indeed, p38 MAPK and JNK inhibitor were shown to inhibit HEK293T cells growth and induce cleavage of PARP respectively (Alsanafi *et al.*, 2018). Since dhCer, a Degs1 substrate, is produced from dhSph catalysed through the enzyme CerS, while SK is known to phosphorylate dhSph to form dhS1P, we tested involvement of SK1 and SK2 in regulation of p38 MAPK and JNK survival pathways in HEK293T cells. SK1 siRNA enhanced the formation of SKi-induced phosphorylated p38 MAPK and phosphorylated JNK levels in HEK293T cells (Figure 4.11). This finding suggests that SK1 opposes p38 MAPK and JNK survival pathways. Neither siRNA knock down of SK2 nor p53 in HEK293T cells affected basal or SKi-induced phosphorylation of pro-survival p38 MAPK and JNK proteins (Figures 4.12 and 4.13).

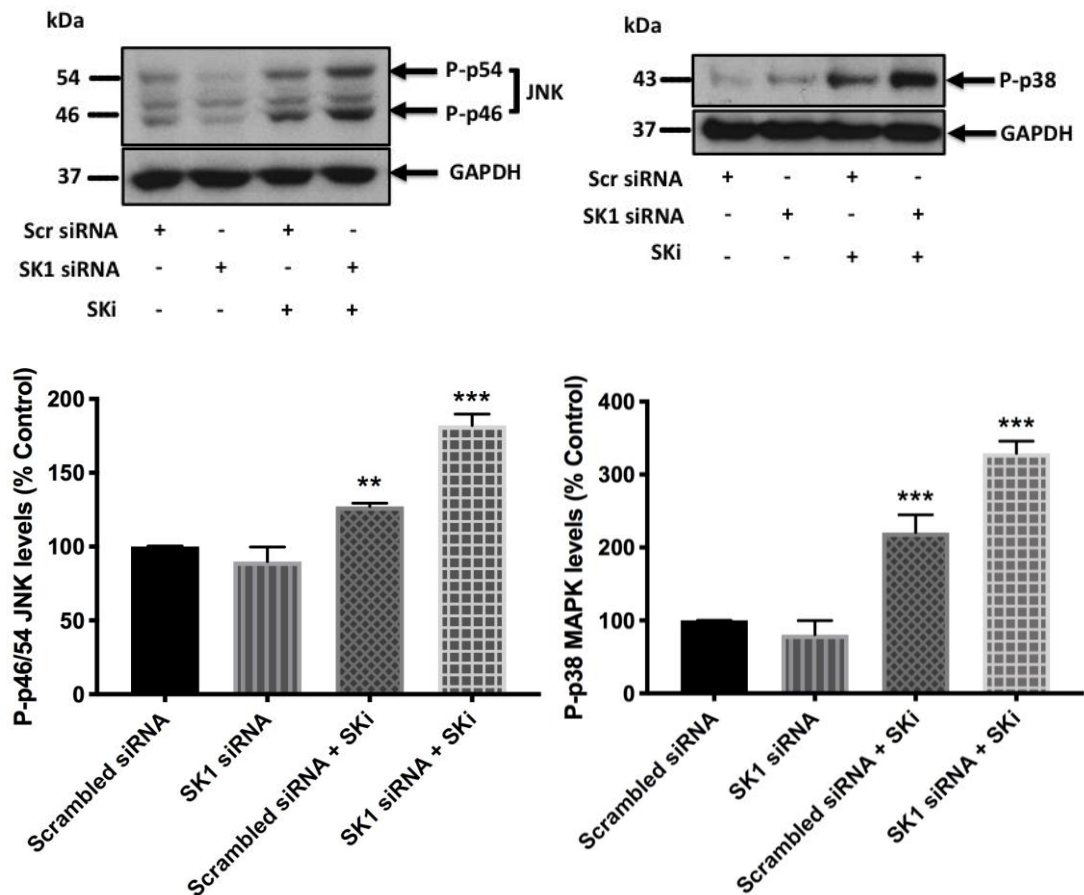


Figure 4.11 Effect of SK1 siRNA on SKi-induced p38 MAPK and JNK pathways in HEK293T cells. HEK293T cells were cultured in complete medium containing 10% FCS until ~70% confluent. Cells were transiently transfected with SK1 siRNA or scrambled siRNA at a final concentration of 100 nM in antibiotic free medium for 48 hrs before being treated with SKi (10 μ M) or with the vehicle alone (DMSO 0.1% v/v) for further 24 hours. P-JNK and P-p38 MAPK levels were detected using SDS PAGE and western blotting with respective antibodies. Blots were stripped and re-probed with anti-GAPDH antibody to ensure comparable protein loading. Two representative western blots are shown each of an experiment performed at least three independent times. Also shown is the densitometric quantification of P-JNK/GAPDH and P-p38 MAPK/GAPDH ratios immunoreactivities of (Mr 46-54 and 43 kDa, respectively), expressed as a percentage of the control (Control=100%). The data was expressed as means \pm SEM for $n=3$ experiments and analysed by one-way ANOVA multiple comparisons test, in P-JNK levels ** $p<0.01$ for Scrambled siRNA/SKi vs Scrambled siRNA and *** $p<0.001$ for SK1 siRNA/SKi vs Scrambled siRNA/SKi while in P-p38 levels MAPK *** $p<0.001$ for Scrambled siRNA/SKi vs Scrambled siRNA or SK1 siRNA/SKi vs Scrambled siRNA/SKi.

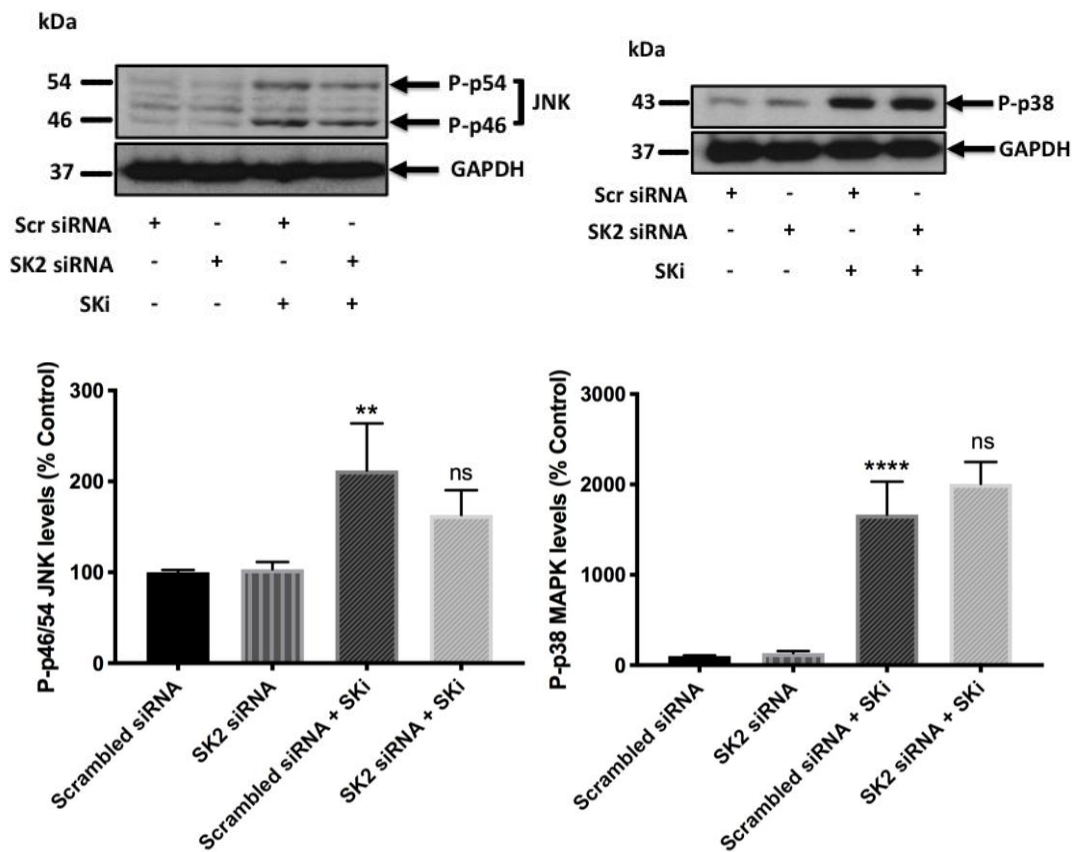


Figure 4.12 *Effect of SK2 siRNA on SKi-induced p38 MAPK and JNK pathways in HEK293T cells.* HEK293T cells were cultured in complete medium containing 10% FCS until ~70% confluent. Cells were transiently transfected with SK2 siRNA or scrambled siRNA at a final concentration of 100 nM in antibiotic free medium for 48 hrs before being treated with SKi (10 μ M) or with the vehicle alone (DMSO 0.1% v/v) for further 24 hours. P-JNK and P-p38 MAPK levels were detected using SDS PAGE and western blotting with respective antibodies. Blots were stripped and re-probed with anti-GAPDH antibody to ensure comparable protein loading. Two representative western blots are shown each of an experiment performed at least three independent times. Also shown is the densitometric quantification of P-JNK/GAPDH and P-p38 MAPK/GAPDH ratios immunoreactivities of (Mr 46-54 and 43 kDa, respectively), expressed as a percentage of the control (Control=100%). The data was expressed as means \pm SEM for $n=3$ experiments and analysed by one-way ANOVA multiple comparisons test, in P-JNK ** $p<0.01$ for Scrambled siRNA/SKi vs Scrambled siRNA and ns denotes not statistically significant (p value >0.05) for SK2 siRNA/SKi vs Scrambled siRNA/SKi; in P-p38 MAPK **** $p<0.0001$ for Scrambled siRNA/SKi vs Scrambled siRNA and ns denotes not statistically significant (p value >0.05) for SK2 siRNA/SKi vs Scrambled siRNA/SKi.

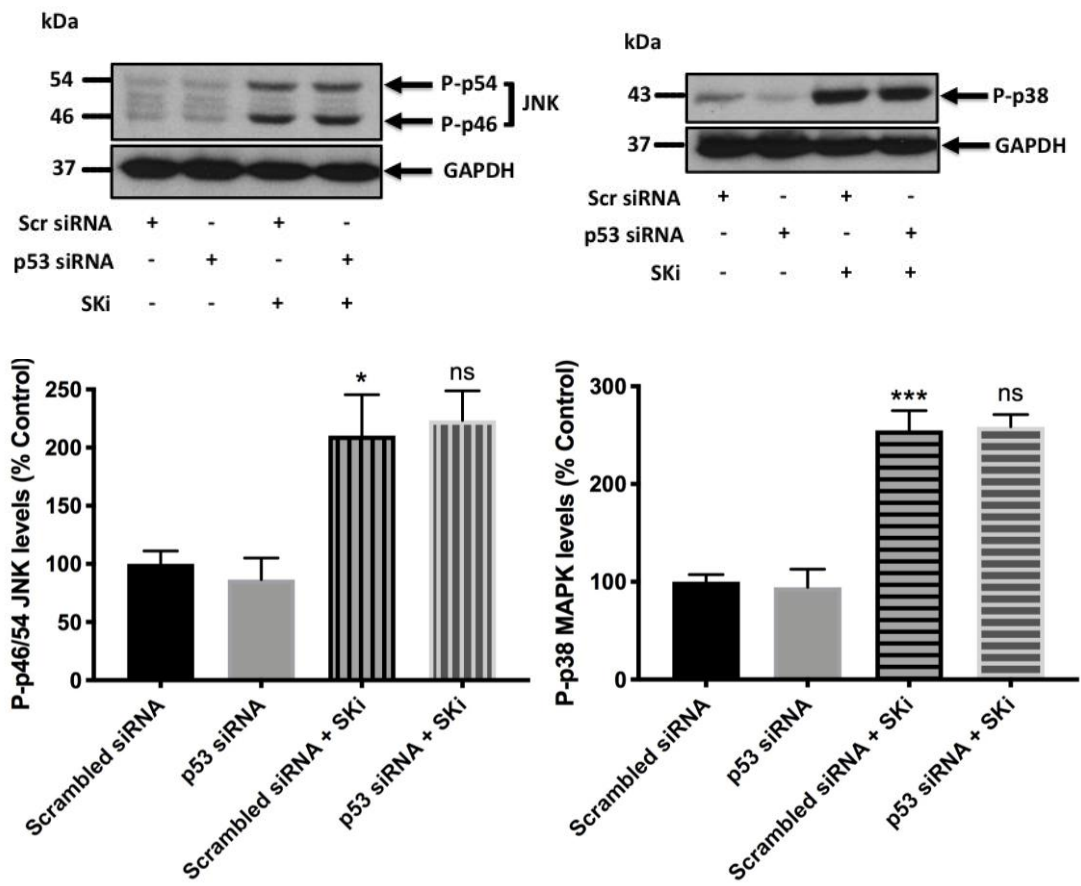


Figure 4.13 Effect of p53 siRNA on SKi-induced p38 MAPK and JNK pathways in HEK293T cells. HEK293T cells were cultured in complete medium containing 10% FCS until ~70% confluent. Cells were transiently transfected with p53 siRNA or scrambled siRNA at a final concentration of 100 nM in antibiotic free medium for 48 hrs before being treated with SKi (10 μ M) or with the vehicle alone (DMSO 0.1% v/v) for further 24 hours. P-JNK and P-p38 MAPK levels were detected using SDS PAGE and western blotting with respective antibodies. Blots were stripped and re-probed with anti-GAPDH antibody to ensure comparable protein loading. Two representative western blots are shown each of an experiment performed at least three independent times. Also shown is the densitometric quantification of P-JNK/GAPDH and P-p38 MAPK/GAPDH ratios immunoreactivities of (Mr 46-54 and 43 kDa, respectively), expressed as a percentage of the control (Control=100%). The data was expressed as means \pm SEM for $n=3$ experiments and analysed by one-way ANOVA multiple comparisons test, * $p<0.05$ for Scrambled siRNA/SKi vs Scrambled siRNA, *** $p<0.001$ for Scrambled siRNA/SKi vs Scrambled siRNA, and ns denotes not statistically significant (p value >0.05) for p53 siRNA/SKi vs Scrambled siRNA/SKi.

4.2.4 Role of p53 and apoptosis in HEK293T cells

We next assessed the role of p63 and p90 in regulating cell growth and apoptosis. As mentioned in Chapter 3, SKi did not induce cleavage of PARP or affect DNA synthesis (Figures 3.17 and 3.19), indicating that p63 and p90 might be inactive forms of p53 based on the finding that their formation is not associated with enhanced apoptosis. On the other hand, ABC294640 only weakly stimulated the formation of p63 and p90, if at all, but does stimulate the formation of Cer, the induction of PARP cleavage and the inhibition of DNA synthesis in HEK293T cells (Figures 3.17 and 3.19). Therefore, formation of p63 and p90 appears to be associated with an abrogation of p53 function. Indeed, knocking down p53 prevented ABC294640-induced PARP cleavage and reduced the inhibitory effect of ABC294640 on DNA synthesis, thereby confirming that ABC294640 promotes apoptosis through p53 (Figures 4.14 and 4.15).

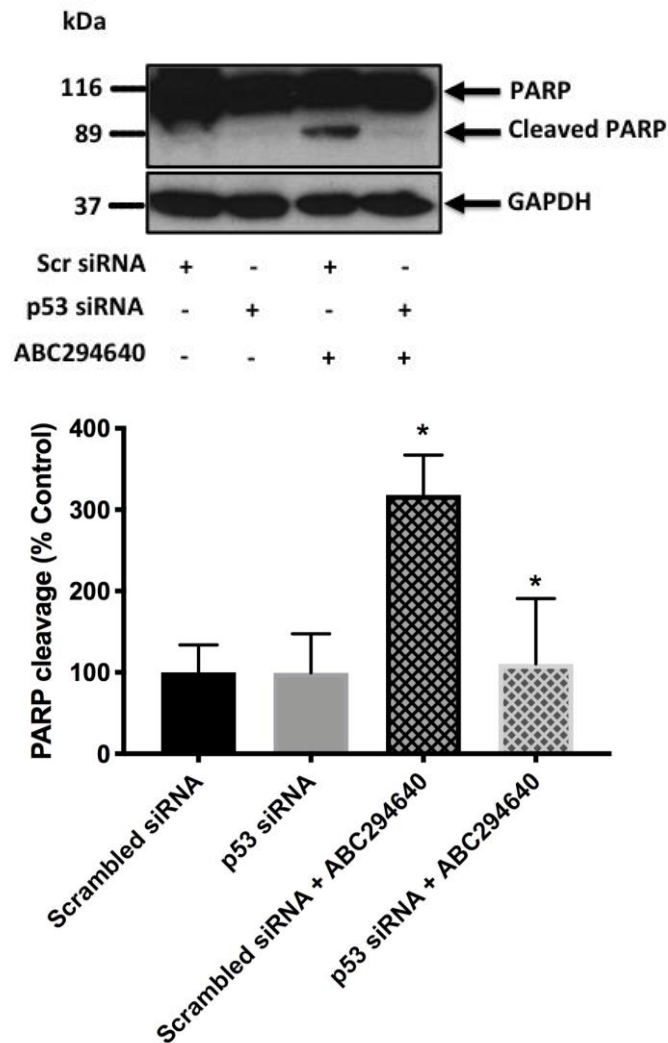


Figure 4.14 *Effect of p53 siRNA on ABC294640-induced PARP cleavage in HEK293T cells.* HEK293T cells were cultured in complete medium containing 10% FCS until ~70% confluent. Cells were transiently transfected with p53 siRNA or scrambled siRNA at a final concentration of 100 nM in antibiotic free medium for 48 hrs before being treated with ABC294640 (25 μ M) or with the vehicle alone (DMSO 0.1% v/v) for further 24 hours. PARP cleavage was detected using SDS PAGE and western blotting with anti-PARP antibody. Blots were stripped and re-probed with anti-GAPDH antibody to ensure comparable protein loading. A representative western blot is shown of an experiment performed at least three independent times. Also shown is the densitometric quantification of cleaved PARP/GAPDH ratio immunoreactivity of (Mr 89 kDa), expressed as a percentage of the control (Control=100%). The data was expressed as means \pm SEM for n=3 experiments and analysed by one-way ANOVA multiple comparisons test, * p <0.05 for Scrambled siRNA/ABC294640 vs Scrambled siRNA or p53 siRNA/ABC294640 vs Scrambled siRNA/ABC294640.

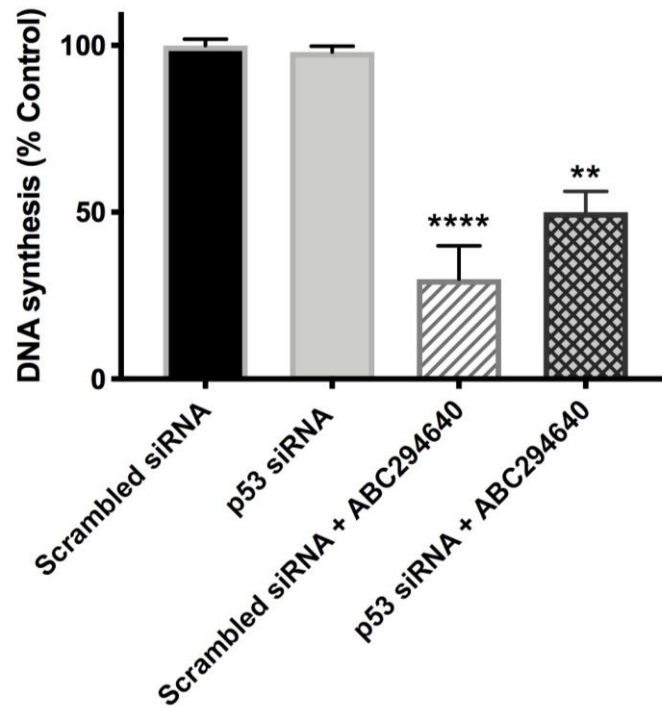


Figure 4.15 *Effect of p53 siRNA on DNA synthesis in HEK293T cells. HEK293T cells were cultured in complete medium containing 10% FCS until ~70% confluent. Cells were transiently transfected with p53 siRNA or scrambled siRNA at a final concentration of 100 nM in antibiotic free medium for 48 hrs before being treated with ABC294640 (25 μ M) or with the vehicle alone (DMSO 0.1% v/v) for further 24 hours. [3 H] Thymidine was added for the last 5 hours then nuclear material was precipitated with 1ml of 10% (w/v) ice cold TCA and then dissolved in 0.1% SDS/0.3M NaOH. [3 H] Thymidine uptake was quantified by liquid scintillation counting. Data are expressed as a % of control \pm S.E.M for n=3 experiments. The data was analysed by one-way ANOVA multiple comparisons test, ** p <0.01 for p53 siRNA/ABC294640 vs Scrambled siRNA/ABC294640 and **** p <0.0001 for Scrambled siRNA/ABC294640 vs Scrambled siRNA.*

4.2.5 Role of p53 in regulating XBP-1s levels in HEK293T cells

ER stress sensors including IRE1, PERK, and ATF6 regulate cell survival and homeostasis while sphingosine kinases are known to regulate cell survival through ER stress (Spassieva *et al.*, 2009; Gagliostro *et al.*, 2012; Volmer and Ron, 2015). Previous studies indicate a link between SK2 and ER stress by testing the SK2 inhibitors ABC294640 and K145 (Liu *et al.*, 2013); both induced ER stress while K145 increased XBP-1s and p-eIF2a expressions (Wallington-Beddoe *et al.*, 2017). In addition, inhibition of SK2 with K145 synergises with bortezomib in promoting ER stress through stimulation of IRE1, JNK and p38 MAPK pathways leading to a potent apoptotic response in myeloma cells (Wallington-Beddoe *et al.*, 2017). As previously mentioned in Chapter 3, SKi enhances the MG132-induced expression of XBP-1s in HEK293T cells that involves the polyubiquitinated forms of Degr1 (Figure 3.40) (Alsanafi *et al.*, 2018). Therefore, we assessed the involvement of SK1 and SK2 in this effect. Knocking down SK1 decreased the MG132-induced expression of XBP-1s with no effect on XBP-1s levels induced by the combination of SKi and MG132 (Figure 4.16). Meanwhile, knocking down SK2 reduced the induction of XBP-1s in response to combined treatment with SKi and MG132 (Figure 4.17). These findings suggest a relationship of both SK1 and SK2 with XBP-1s regulation. Moreover, p53 siRNA increased the effect of MG132 on XBP-1s expression (Figure 4.18), which is mediated through native p53 and not the polyubiquitinated p63/p90 forms because MG132 prevents the formation of these p63/p90 (Figure 4.6). We then linked these findings to apoptosis and noticed that p53 siRNA reduced the MG132-induced cleavage of PARP (Figure 4.21); however, knocking down SK1 or SK2 had no effect on the MG132-induced cleavage of PARP

(Figures 4.19 and 4.20), suggesting that the maximum PARP cleavage might be produced with MG132.

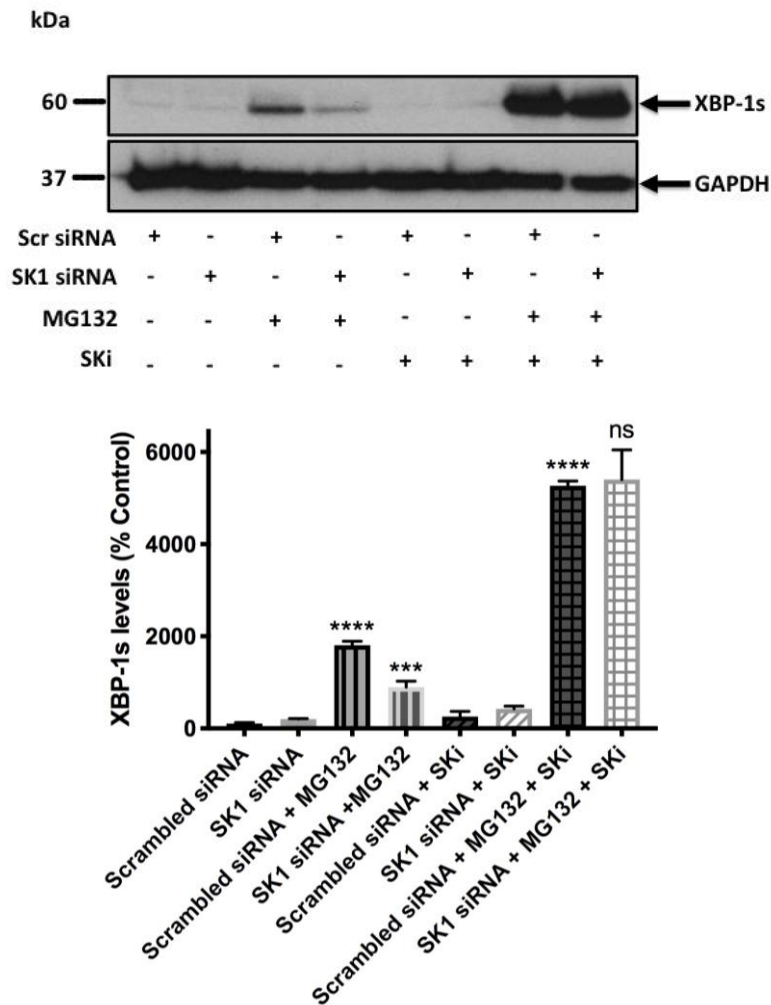


Figure 4.16 *Effect of SK1 siRNA on XBP-1s levels in HEK293T cells.* HEK293T cells were cultured in complete medium containing 10% FCS until ~70% confluent. Cells were transiently transfected with SK1 siRNA or scrambled siRNA at a final concentration of 100 nM in antibiotic free medium for 48 hours. Cells were then pre-treated with MG132 (10 μ M, 30 minutes) before addition of SKi (10 μ M) or with the vehicle alone (DMSO 0.1% v/v) for further 24 hours. XBP-1s levels were detected using SDS PAGE and western blotting with anti-XBP-1s antibody. Blots were stripped and re-probed with anti-GAPDH antibody to ensure comparable protein loading. A representative western blot is shown of an experiment performed at least three independent times. Also shown is the densitometric quantification of XBP-1s/GAPDH ratio immunoreactivity of (Mr 60 kDa), expressed as a percentage of the control (Control=100%). The data was expressed as means \pm SEM for n=3 experiments and analysed by one-way ANOVA multiple comparisons test, *** p <0.001 for SK1 siRNA/MG132 vs Scrambled siRNA/MG132, **** p <0.0001 for Scrambled siRNA/MG132 vs Scrambled siRNA or Scrambled siRNA/MG132/SKi vs Scrambled siRNA/MG132, and ns denotes not statistically significant (p value >0.05) for SK1 siRNA/MG132/SKi vs Scrambled siRNA/MG132/SKi.

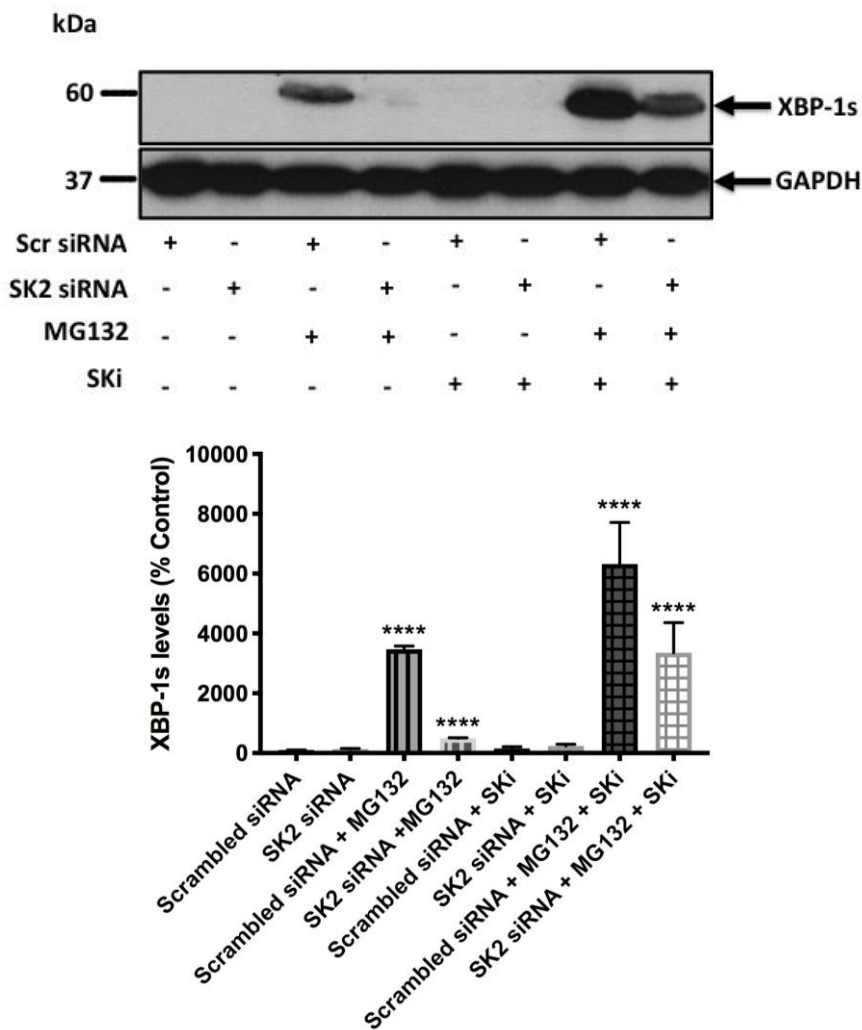


Figure 4.17 Effect of SK2 siRNA on XBP-1s levels in HEK293T cells. HEK293T cells were cultured in complete medium containing 10% FCS until ~70% confluent. Cells were transiently transfected with SK2 siRNA or scrambled siRNA at a final concentration of 100 nM in antibiotic free medium for 48 hours. Cells were then pre-treated with MG132 (10 μ M, 30 minutes) before addition of SKi (10 μ M) or with the vehicle alone (DMSO 0.1% v/v) for further 24 hours. XBP-1s levels were detected using SDS PAGE and western blotting with anti-XBP-1s antibody. Blots were stripped and re-probed with anti-GAPDH antibody to ensure comparable protein loading. A representative western blot is shown of an experiment performed at least three independent times. Also shown is the densitometric quantification of XBP-1s/GAPDH ratio immunoreactivity of (Mr 60 kDa), expressed as a percentage of the control (Control=100%). The data was expressed as means \pm SEM for n=3 experiments and analysed by one-way ANOVA multiple comparisons test, **** p <0.0001 for Scrambled siRNA/MG132 vs Scrambled siRNA or SK2 siRNA/MG132 vs Scrambled siRNA/MG132 or Scrambled siRNA/MG132/SKi vs Scrambled siRNA/MG132 or SK2 siRNA/MG132/SKi vs Scrambled siRNA/MG132/SKi.

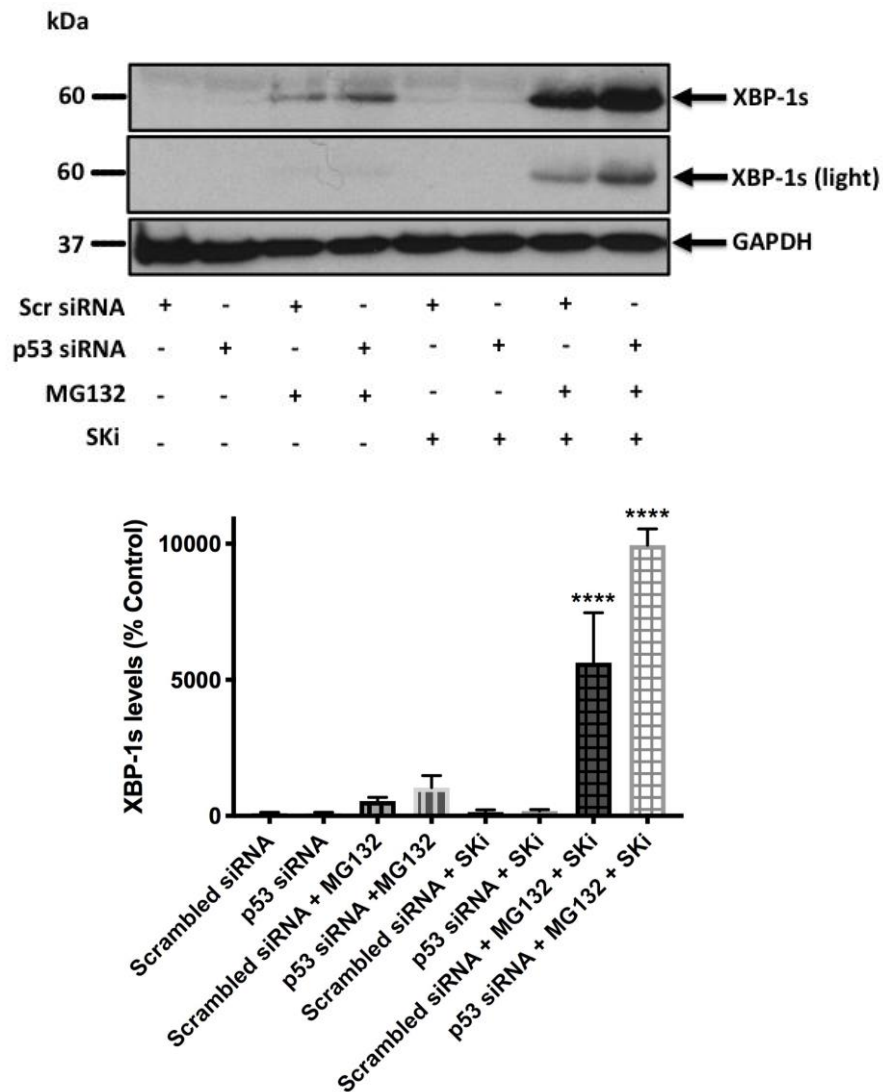


Figure 4.18 Effect of p53 siRNA on XBP-1s levels in HEK293T cells. HEK293T cells were cultured in complete medium containing 10% FCS until ~70% confluent. Cells were transiently transfected with p53 siRNA or scrambled siRNA at a final concentration of 100 nM in antibiotic free medium for 48 hours. Cells were then pre-treated with MG132 (10 μ M, 30 minutes) before addition of SKi (10 μ M) or with the vehicle alone (DMSO 0.1% v/v) for further 24 hours. XBP-1s levels were detected using SDS PAGE and western blotting with anti-XBP-1s antibody. Blots were stripped and re-probed with anti-GAPDH antibody to ensure comparable protein loading. A representative western blot is shown of an experiment performed at least three independent times. A lighter version of XBP-1s levels is also shown. Also shown is the densitometric quantification of XBP-1s/GAPDH ratio immunoreactivity of (Mr 60 kDa), expressed as a percentage of the control (Control=100%). The data was expressed as means \pm SEM for n=3 experiments and analysed by one-way ANOVA multiple comparisons test, ****p<0.0001 for Scrambled siRNA/MG132/SKi vs Scrambled siRNA/MG132 or p53 siRNA/MG132/SKi vs Scrambled siRNA/MG132/SKi.

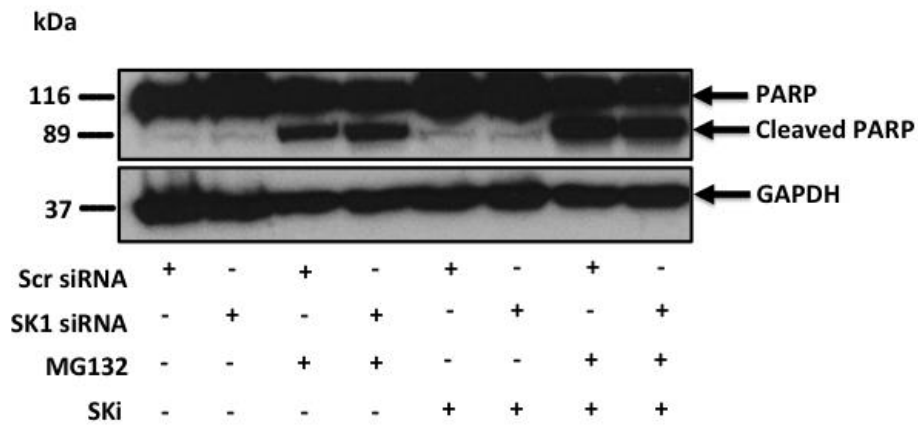


Figure 4.19 *Effect of SK1 siRNA on PARP cleavage in HEK293T cells.* HEK293T cells were cultured in complete medium containing 10% FCS until ~70% confluent. Cells were transiently transfected with SK1 siRNA or scrambled siRNA at a final concentration of 100 nM in antibiotic free medium for 48 hrs. Cells were then pre-treated with MG132 (10 μ M, 30 minutes) before addition of SKi (10 μ M) or with the vehicle alone (DMSO 0.1% v/v) for further 24 hours. PARP cleavage was detected using SDS PAGE and western blotting with anti-PARP antibody. Blots were stripped and re-probed with anti-GAPDH antibody to ensure comparable protein loading. A representative western blot is shown of an experiment performed two independent times.

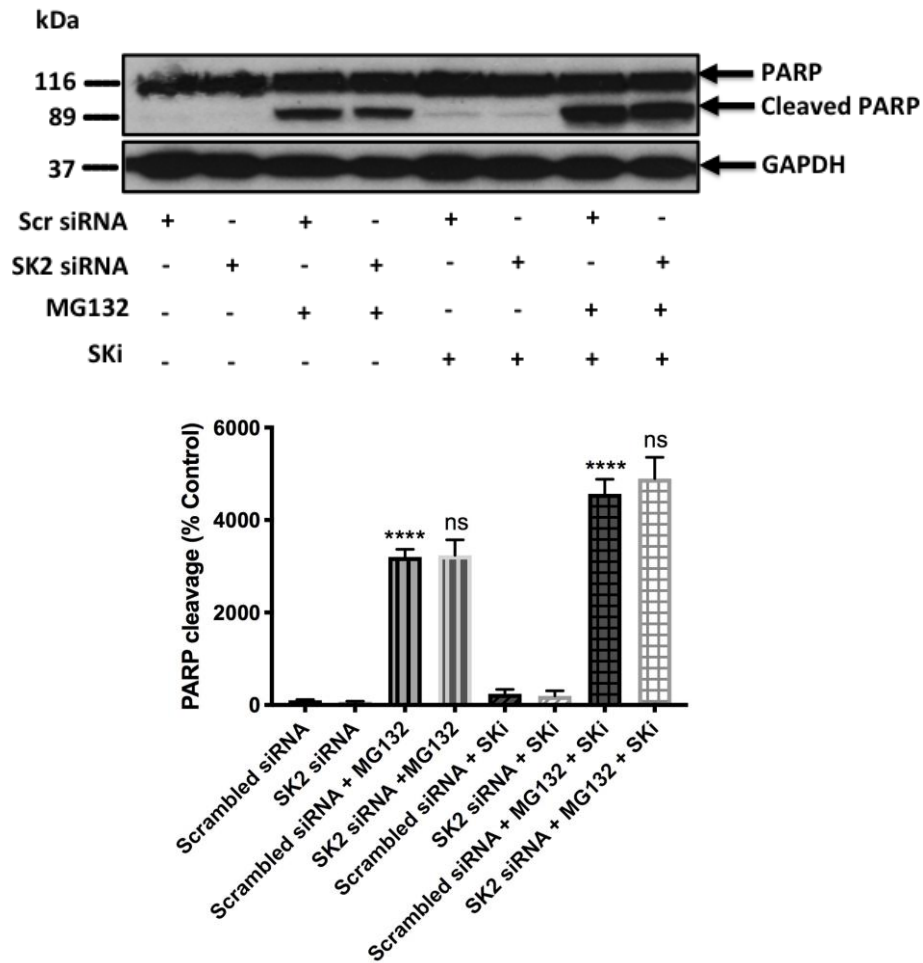


Figure 4.20 Effect of SK2 siRNA on PARP cleavage in HEK293T cells. HEK293T cells were cultured in complete medium containing 10% FCS until ~70% confluent. Cells were transiently transfected with SK2 siRNA or scrambled siRNA at a final concentration of 100 nM in antibiotic free medium for 48 hrs. Cells were then pre-treated with MG132 (10 μ M, 30 minutes) before addition of SKi (10 μ M) or with the vehicle alone (DMSO 0.1% v/v) for further 24 hours. PARP cleavage was detected using SDS PAGE and western blotting with anti-PARP antibody. Blots were stripped and re-probed with anti-GAPDH antibody to ensure comparable protein loading. A representative western blot is shown of an experiment performed at least three independent times. Also shown is the densitometric quantification of cleaved PARP/GAPDH ratio immunoreactivity of (Mr 89 kDa), expressed as a percentage of the control (Control=100%). The data was expressed as means \pm SEM for $n=3$ experiments and analysed by one-way ANOVA multiple comparisons test, **** $p < 0.0001$ for Scrambled siRNA/MG132 vs Scrambled siRNA or Scrambled siRNA/MG132/SKi vs Scrambled siRNA/MG132 and ns denotes not statistically significant (p value > 0.05) for SK2 siRNA/MG132 vs Scrambled siRNA/MG132 or SK2 siRNA/MG132/SKi vs Scrambled siRNA/MG132/SKi.

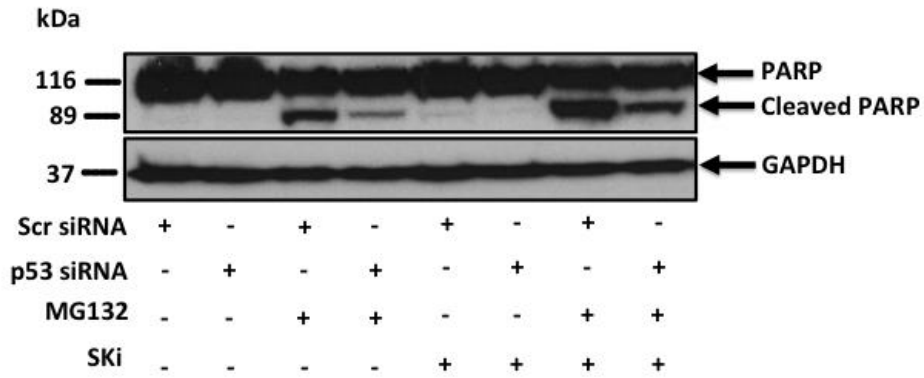


Figure 4.21 *Effect of p53 siRNA on PARP cleavage in HEK293T cells.* HEK293T cells were cultured in complete medium containing 10% FCS until ~70% confluent. Cells were transiently transfected with p53 siRNA or scrambled siRNA at a final concentration of 100 nM in antibiotic free medium for 48 hrs. Cells were then pre-treated with MG132 (10 μ M, 30 minutes) before addition of SKi (10 μ M) or with the vehicle alone (DMSO 0.1% v/v) for further 24 hours. PARP cleavage was detected using SDS PAGE and western blotting with anti-PARP antibody. Blots were stripped and re-probed with anti-GAPDH antibody to ensure comparable protein loading. A representative western blot is shown of an experiment performed two independent times.

4.2.6 Effect of SKi on sphingolipid levels in HEK293T cells

Changes in sphingolipid levels were measured in SKi-treated (10 μ M, 24 hours) HEK293T cells to determine if there is any link with the changes in phosphorylated p38 MAPK, phosphorylated JNK and XBP-1s levels. SK1 or SK2 were knocked down with respective siRNAs in order to confirm which SK is responsible for changes in sphingolipids measurements as well as pro-survival signalling pathways.

There was an increase in levels of dhCers species as well as dhSM in scrambled siRNA/SKi treated HEK293T cells (Appendix, Figures S6A and S7A). Combining SK1 siRNA and SKi did not increase levels of dhCers and dhSM nor did this induce any significant changes in levels of Cers or SM (Appendix, Figure S6A). In contrast, SK1 siRNA/SKi combination treatment significantly increased levels of Sph while decreasing levels of S1P (vs scrambled siRNA/SKi treatment) (Appendix, Figure S6B). These changes suggest involvement of SK1 in the increased p38 MAPK/JNK signalling pathways. However, treatment with either SKi or SK1 siRNA alone had no observable effects on S1P levels (Appendix, Figure S6B), suggesting that SK1, even in low expression levels, can still maintain levels of S1P in HEK293T cells with either of these treatments alone (around 80% SK1 removal in each). HEK293T cells were also treated with SK2 siRNA and this did not affect levels of dhCer species nor increase SKi effects on these sphingolipids (Appendix, Figure S7A). In addition, SK2 siRNA alone increased levels of multiple species of Cers and SM significantly as shown in Appendix, Figure S7A, suggesting a pro-survival function for SK2. Lastly, SK2 siRNA/SKi combination did not affect levels of sphingoid bases (Appendix, Figure S7A).

4.2.7 Effect of SKi, ABC294640, and MG132 on p53 with immunofluorescence microscopy in HEK293T cells

HEK293T cells were treated with SKi (10 μ M, 24 hours) or ABC294640 (25 μ M, 24 hours) or MG132 (10 μ M, 24 hours), then processed for immunofluorescence using the anti-p53 primary antibody and TRITC-tagged secondary antibody (red signal) while cell nuclei were stained with DAPI (blue signal). p53 appears to be located in the nucleus and no discernible effects were observed on the sub-cellular distribution when cells were treated with SKi, ABC294640, or MG132 (Figure 4.22). Treatment of HEK293T cells with SKi or ABC294640 did not affect the nucleus shape. However, treatment with MG132 changed the nucleus to a kidney shape with some fragmentation.

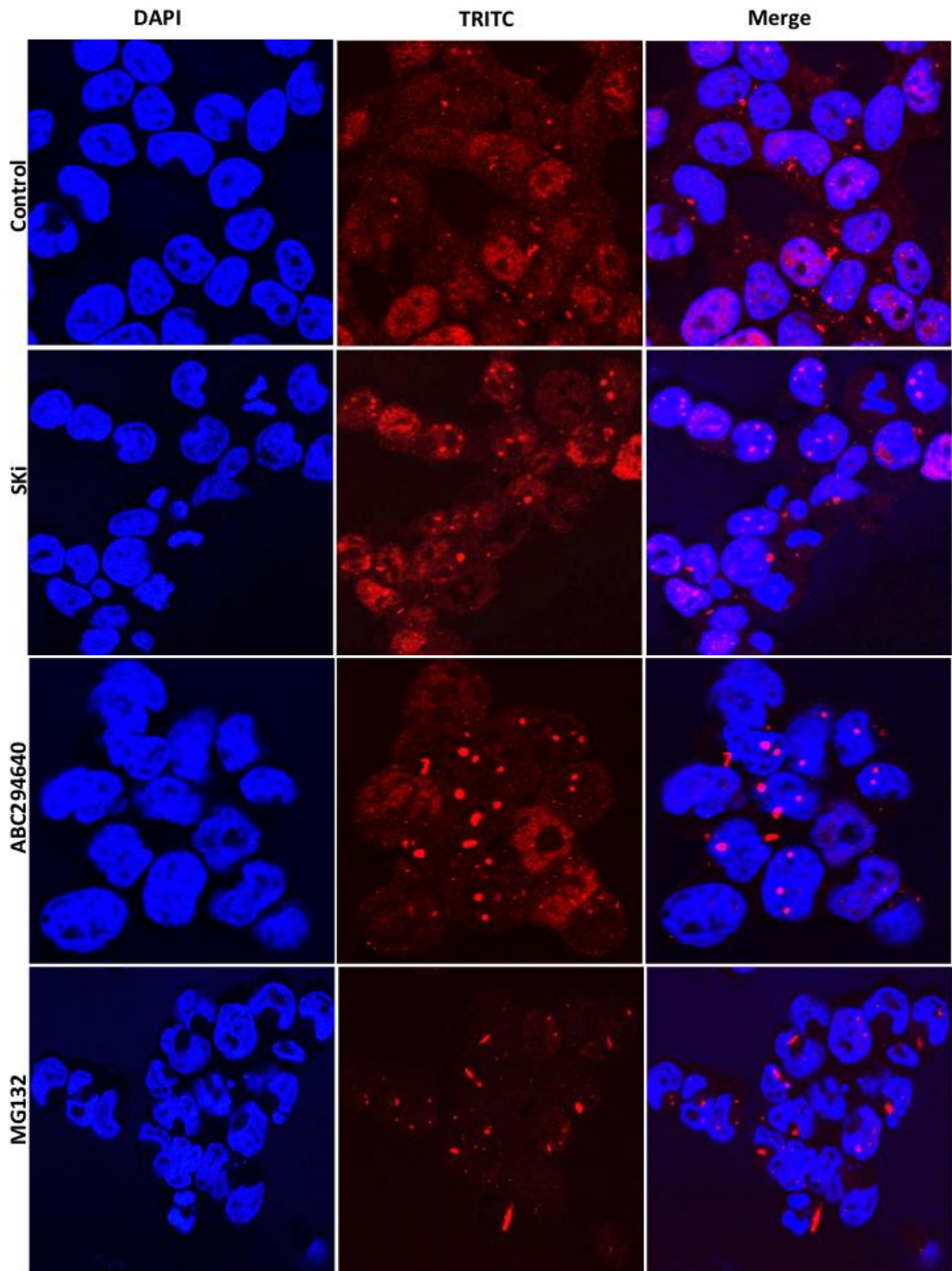


Figure 4.22 *Immunofluorescence microscopy images showing the effect of SKi, ABC294640, and MG132 on p53 in HEK293T cells. HEK293T cells were cultured in complete medium containing 10% FCS until ~70% confluent. Cells were treated with SKi (10 μ M) or ABC294640 (25 μ M) or MG132 (10 μ M) or with the vehicle alone (DMSO 0.1% v/v) for 24 hours. Cells were processed for immunofluorescence (as described under the Methods section) using anti-p53 primary antibody and TRITC-tagged secondary antibody (red signal). Cell nuclei were stained with DAPI (blue signal). Cells were then visualised on Leica SP5 confocal microscope through HC PL APO CS2 20x/0.75 DRY len with 20x magnification. Data are from an individual experiment, typical of 2 others.*

4.3 DISCUSSION

The main finding of this chapter is that the post-translationally modified forms of p53 are induced by SKi in both HEK293T and parental HEK293 cells and that this likely involves ubiquitination. Confirmation of relatedness of p63 and p90 to p53 was based on (i) the reduction in the formation of p63 and p90 in response to SKi by siRNA knockdown of p53 and (ii) immunoprecipitation of p63 and p90 with anti-p53 antibody. The formation of p63 and p90 appears to be due to polyubiquitination as the SKi-induced increase in p63 and p90 levels was enhanced in cells over-expressing HA-tagged ubiquitin, presumably due to the increased availability of ubiquitin as a substrate for the E3 ligase responsible for catalysing the polyubiquitination of p53. Polyubiquitination is catalysed by a family of enzymes called E3 ligases (Zheng and Shabek, 2017), of which Mdm2 is a member. Mdm2 regulates the polyubiquitination of p53 (Moll and Petrenko, 2003) and is a candidate for regulating formation of p63 and p90. This possibility requires further investigation in future work to determine which E3 ligase is involved.

Pre-treatment of HEK293T cells with the proteasome inhibitor MG132 was expected to enhance the formation of p63 and p90. However, the opposite effect was observed, with the complete failure of SKi to induce p63 and p90 formation. Thus, formation of p63 and p90 is likely a consequence of the SKi-induced proteasomal degradation of an unidentified protein that normally functions to suppress the ubiquitination of p53. This protein was proposed to be SK1 because previous results have shown that SKi induces the proteasomal degradation of SK1 and this is reversed with MG132 (Figure 3.11). The ability of SKi, which does not stimulate

apoptosis, to induce formation of p63 and p90 might indicate that this event is associated with inactivation of the death promoting properties of p53. This is supported by the finding that ABC294640 induces apoptosis but importantly, does not promote significant formation of p63 and p90. In addition, a role for SK1 is suggested from evidence showing that knocking down SK1 with gene-specific siRNA enhanced p63 and p90 formation. In this case, if p63 and p90 are inactive forms of p53, then the evidence would suggest that SK1 functions to reduce survival by limiting the conversion of p53 into p63 and p90. In contrast, Lima and colleagues (2018) showed that the SK1 inhibitor SK1-I inhibited cancer cell growth and mediated intrinsic apoptotic cell death in a TP53-dependent manner in WT TP53 cancer cell lines. In this case, p53 plays an essential role in the formation of dilated intracellular vacuoles, which are associated with autophagic-induced apoptosis and which is induced by the inhibition of SK1 in cancer cells (Lima *et al.*, 2018).

Further evidence that SK1 might be pro-apoptotic in HEK293T cells was suggested by the finding that siRNA knockdown of SK1 enhanced the activation of p38 MAPK and JNK, which are pro-survival signalling pathways in these cells. Indeed, combining SK1 siRNA and SKi to completely eliminate the expression of SK1 enhanced the formation of p63 and p90 and pro-survival phosphorylated p38 MAPK and phosphorylated JNK over and above SK1 siRNA or SKi alone (Figures 4.7A and 4.11, respectively). Therefore, it is necessary to completely remove SK1 in order to enhance p38 MAPK and JNK function and the formation of p63 and p90, suggesting that a threshold level of S1P regulates these pathways. A role for SK2 and Degs1 was discounted because knocking down SK2 and Degs1 with respective siRNAs did

not affect the formation of p63 and p90 nor the phosphorylation of JNK and p38 MAPK in response to SKi.

These results are somewhat surprising, as the consensus view is that SK1 functions as a pro-survival protein in numerous mammalian cell types. One explanation might be that SK1 functionally interacts with p53 in a cell context specific manner to affect cell survival or death. In this respect the findings are consistent with Limaye et al. (2009), who reported that the expression levels of SK1 can determine whether the enzyme performs in a pro-survival or apoptotic manner. In this case, modest expression of SK1 was shown to promote survival, whereas high expression of SK1 reduced cell survival, activated caspase-3, inhibited cell cycle, and disrupted cell-cell junctions in endothelial cells (Limaye *et al.*, 2009a). The precise mechanism for this differential action is currently unknown, but it is possible that the expression levels of SK1 are high in HEK293T cells, such that it functions predominantly to promote cell death under conditions of cellular stress. This function might be negated when the enzyme is removed in response to SKi, a consequence of enhanced p63 and p90 formation and protective p38 MAPK and JNK signalling.

S1P produced by SK1 has also been shown to be apoptotic in other cellular settings. For example, Davaille et al. (2002) reported that S1P triggers both apoptotic and survival signals in human hepatic myofibroblasts. The apoptotic effects of S1P were receptor-independent and unrelated to the conversion of S1P into Sph and Cer (Davaille *et al.*, 2002). In contrast, Gennero et al. (2002) showed that S1P-induced apoptosis was linked with increased levels of intracellular Sph and decreased

intracellular S1P levels as a result of enhanced hydrolysis by S1P lyase in mesangial cells cultured at low cellular density (Gennero *et al.*, 2002). Moreover, others have shown that exogenous S1P promotes neuronal apoptosis along with increased expression of IL-17A in microglial cells deprived of oxygen and glucose. In this case, the inhibition of SK1 activity was adequate to reduce neuronal apoptosis and decrease IL-17A production that worsens CNS inflammation (Lv *et al.*, 2016). Finally, the cell functional nature (e.g. whether neuronal, liver, or cancer cell) might also affect how S1P regulates autophagy to determine cell survival or death. Since inhibition of SK1 promotes survival in HEK293T cells, this could also be related to other proliferative signals such as ceramide-1-phosphate (C1P). For example, C1P has been shown to increase cell survival of macrophages when incubated under conditions known to induce apoptosis in these cells. This occurs by inhibition of caspase 9 and 3, to reduce DNA fragmentation (Gómez-Muñoz *et al.*, 2003). C1P has been demonstrated to selectively inhibit the enzyme A-SMase to promote cell survival (Gómez-Muñoz *et al.*, 2004). Whether SKi promotes the formation of C1P in HEK293T cells remains to be determined. In addition, the activation of the PI3-K/PKB pathway has been shown to be required for the anti-apoptotic effect of S1P and C1P in bone marrow-derived macrophages (BMDM) (Gómez-Muñoz *et al.*, 2003; Gómez-Muñoz *et al.*, 2005), although SKi had no effect on this pathway (Figure 3.25) in HEK293T cells.

As previously mentioned in Chapter 3, autophagy is known as a ‘double-edged’ sword that can either promote cell survival (Li *et al.*, 2013) or induce autophagic cell death (Maiuri *et al.*, 2007). Autophagy can be a cytoprotective homeostatic process

that involves digestion of cellular cytoplasmic components or organelles in the lysosomes to redress energy demand. This occurs in response to diverse stress stimuli in order to remove aggregates of misfolded proteins or damaged organelles that might cause disease pathologies (Fulda *et al.*, 2010; Kroemer *et al.*, 2010). Indeed, various links exist between stress and cellular death pathways, such as ER stress and apoptosis that determine cell fate (Karunakaran and van Echten-Deckert, 2017). It is often unclear which signalling interactions might contribute to pro-survival or pro-apoptotic cellular effects due to a complex crosstalk mechanisms that operate between autophagy and apoptosis (Marino *et al.*, 2014). However, Liu *et al.* (2017) identified a core network for regulation of autophagic and apoptotic responses that include cytoplasmic Ca^{2+} , p53, AMPK, calpain, Beclin-1, and Bcl-2. Cell fate ‘decisions’ are tightly controlled through the master regulators, Ca^{2+} and p53 via activation of AMPK and Bax pathways, respectively (Liu *et al.*, 2017). Cytoplasmic p53 inhibits autophagy through deactivation of AMPK (Tasdemir *et al.*, 2008). In contrast, nuclear p53 stimulates autophagy through activation of a lysosomal autophagy-inducing protein termed damage-regulated autophagy modulator (DRAM) (Crichton *et al.*, 2006), and activation of JNK signalling pathways to initiate phosphorylation and inactivation of anti-apoptotic, Bcl-2 (Sui *et al.*, 2011). In contrast, in HEK293T cells, JNK is not promoting apoptosis, but rather enhances cell survival, as discussed in Chapter 3 (Alsanafi *et al.*, 2018). The current results demonstrate that native p53 is involved in ABC294640- and MG132-induced apoptosis. In addition, ABC294640-induced PARP cleavage in HEK293T cells is mediated by the native forms of Degs1 (Chapter 3). Hence both native Degs1 and native p53 appear to function in concert to reduce the survival of HEK293T cells

(Alsanafi *et al.*, 2018). This role of p53 is consistent with its ability to induce the mitochondrial apoptotic pathway stimulated through the ER stress effector Apaf-1, which involves the BH3-only proteins, PUMA and NOXA (Li *et al.*, 2006).

Sphingolipids measurements in HEK293T cells showed that SKi induced an increase in levels of dhCer species as well as levels of dhSM and this is consistent with the SKi-induced ubiquitin-proteasomal degradation of Degr1 (Alsanafi *et al.*, 2018). Treatment of HEK293T cells with combined SK1 siRNA/SKi treatment significantly decreased levels of S1P and increased levels of Sph (vs scrambled siRNA/SKi) suggesting that these changes might underlie enhanced p38 MAPK/JNK and p63/p90 signalling that is achieved by completely removing SK1 from the cells. However, the enhanced p38 MAPK/JNK signalling in response to SK1 siRNA/SKi treatment was not due to changes in levels of dhCer or Cer levels since similar changes were evident in cells treated with SK2 siRNA and which had no effect on p38 MAPK/JNK signalling or p63/p90 formation. It is noteworthy that there is no formal evidence that p53 is linked with p38 MAPK and JNK signalling in HEK293T cells, since p53 siRNA had no effect on p38 MAPK/JNK pathway (Figure 4.13).

The role of p53 in regulating levels of XBP-1s was also tested as sphingosine kinases are known to regulate cell survival and homeostasis through ER stress (Gagliostro *et al.*, 2012; Spassieva *et al.*, 2009; Volmer and Ron, 2015). SK1 siRNA was shown to have no effect on XBP-1s expression induced by combined treatment with SKi and MG132 whereas SK2 siRNA reduced the levels of XBP-1s in response to combined treatment of cells with SKi and MG132. These findings indicate that SK2 is

positively involved in the regulation of XBP-1s expression, which serves as a pro-survival signal in this context. Indeed, previous studies have identified a link between SK2 and XBP-1s. In this case, the SK2 inhibitors ABC294640 and K145 induced ER stress while K145 increased XBP-1s and p-eIF2a expressions (Wallington-Beddoe *et al.*, 2017).

The findings in this Chapter suggest that SK2 functions in a pro-survival context under conditions where the proteasome is inhibited by MG132 (Figure 4.17). However, the enzyme exhibits some versatility, as it functions with p53 in promoting PARP cleavage in response to ABC294640 (Figures 3.24 and 4.14). This differing role of SK2 might be related to the predominance of one of two mechanisms. First, catalytic regulation of S1P might modulate and promote cell survival, while sequestration of Bcl2 by the BH3 domain (Cheng *et al.*, 2001) of SK2 might promote apoptosis. The predominance of these two mechanisms might differ in cells stimulated with ABC294640 or MG132, although this requires further investigation. Nevertheless, there is some support for these possibilities as sphingolipids measurements showed that SK2 siRNA increased Cers levels, which are known to be pro-apoptotic. In this case, it suggests a pro-survival role for the catalytic function of SK2 and which was consistent with SK2 siRNA reducing expression of XBP-1s (Figure 4.17). Moreover, previous findings reported SK2 to function as a pro-survival enzyme as pharmacological inhibition of SK2 induced apoptosis in different cancer cell lines (Lim *et al.*, 2011b). For instance, the SK2-selective inhibitor ABC294640 has been shown to reduce growth, proliferation and cell cycle progression of early stage and advanced prostate cancer cells (Schrecengost *et al.*,

2015). In addition, the selective SK2 inhibitor, (*R*)-FTY720 methyl ether (ROME), promotes autophagic death of T-ALL cell lines as well as patient lymphoblasts (Evangelisti *et al.*, 2014). Moreover, SK2 deficient MCF-7 breast tumor xenografts exhibit retarded tumour growth and tumour associated macrophages display an anti-tumour phenotype (Weigert *et al.*, 2009). Finally, the SK2 inhibitors, K145 and ABC294640, has been reported to stimulate caspase-3-dependent apoptosis of multiple myeloma cells through ER stress/UPR. In addition, K145 and bortezomib synergised in promoting sustained UPR and CHOP-stimulated apoptosis of multiple myeloma cells (Wallington-Beddoe *et al.*, 2017; Pyne and Pyne, 2017).

Treatment of HEK293T cells with p53 siRNA increased MG132- and MG132/SKi-induced XBP-1s expression (Figure 4.18). This is probably mediated by p53 and not the p63 and p90 forms because these forms are not produced in the presence of MG132 (Figure 4.6). Therefore, the native p53 restricts the formation of pro-survival XBP-1s. Apoptosis has been also linked with these findings, and the results showed that p53 siRNA reduced the MG132-induced cleavage of PARP (Figure 4.21) while knocking down SK1 or SK2 expression with gene specific siRNA had no effect on the MG132-induced cleavage of PARP (Figures 4.19 and 4.20). These findings suggest that the maximum p53-induced cell death effects might be produced with MG132 and is therefore not further enhanced by knocking down SK2 expression and is not obviated by knocking down SK1 expression. In this context, the death promoting function of p53 might not be significantly opposed by XBP-1s.

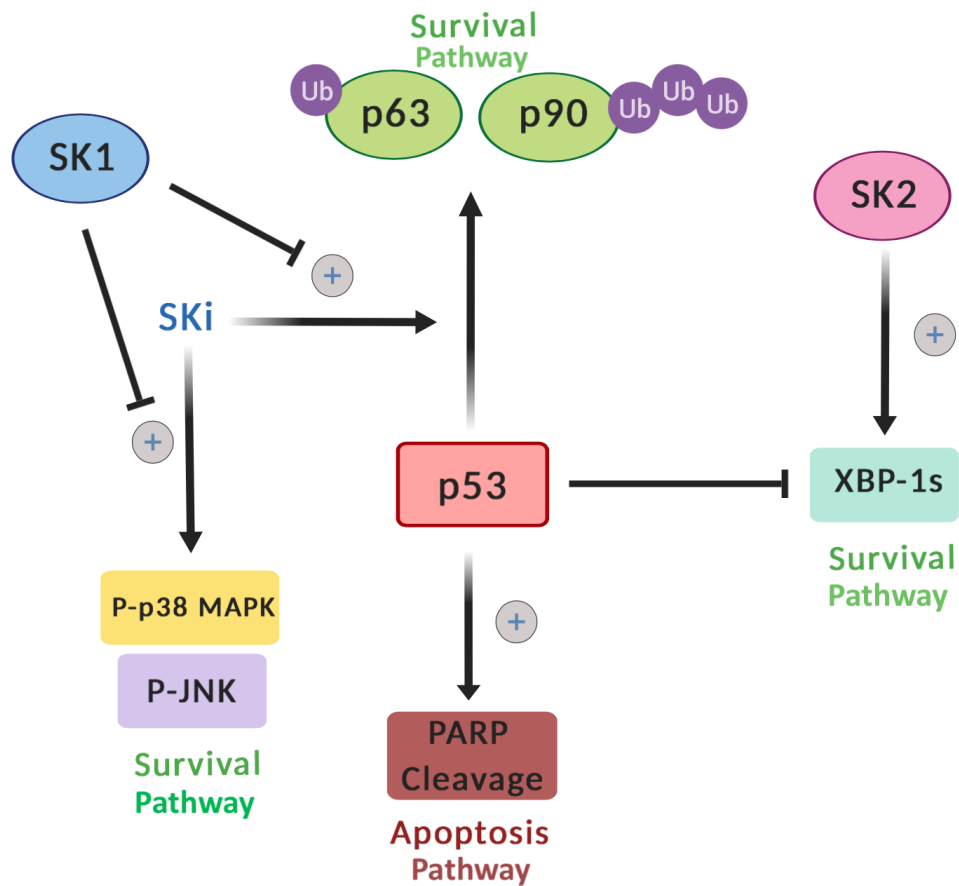


Figure 4.23 Different effects of native p53 and post-translationally modified forms p63/p90 on HEK293T cells fate. Conversion of p53 to ubiquitinated p63/p90 forms with SKi treatment promotes cell survival together with phosphorylated p38 MAPK and phosphorylated JNK. SK1 inhibits these effects while SK2 promotes cells survival through stimulation of XBP-1s expression [Adapted from (Alsanafi et al., 2018)].

One of the control mechanisms of p53 function is the dynamic distribution of p53 between the nucleus and cytoplasm. Although p53 is located in the nucleus, it can also be found in the cytoplasm or the mitochondria. This is significant because the sub-cellular distribution of p53 is crucial in determining its function. Therefore, dysregulation of this process is associated with abnormal and oncogenic cell signalling (Conforti et al., 2015). Under normal conditions, p53 is located in nucleus and functions as a transcription factor to regulate cell cycle arrest and apoptosis and,

in cases of cellular stress, nuclear sequestration of p53 promotes cancer cell death or growth arrest (O’Brate and Giannakakou, 2003). This is reinforced by the concept that tumours in which p53 is ‘trapped’ in the cytoplasm due to a mutation that inhibits its nuclear/cytoplasmic shuttling are more resistant to chemotherapy and patients have poorer clinical prognosis (Ueda *et al.*, 1995; Moll *et al.*, 1995; Sembritzki *et al.*, 2002). In light of these facts, the immunofluorescence microscopy findings of the current study showed no discernible effects on the sub-cellular distribution of p53 when cells were treated with SKi, ABC294640 or MG132 (Figure 4.22). When responding to stress or DNA damage, p53 is subject to several post-translational modifications that lead to its accumulation in the nucleus, stabilisation, and activation as a transcription factor (Inoue *et al.*, 2005). In addition, SKi treatment did not change the nucleus shape, which contrasts with the effect of ABC294640 and MG132. Since DNA damage leads to activation of p53 (O’Brate and Giannakakou, 2003), some compounds could possibly create a DNA damage response that involves generation of ROS and mitochondrial dysfunction which result in activation of native p53 through its nuclear sequestration and inhibition of proteasomal degradation. However, this does not appear to be the case when cells were treated with either ABC294640 or MG132, as there is no major change in the sub-cellular distribution of p53.

In summary, the findings of this study show that SK1 and SK2 are associated with p53 in regulating the survival of HEK293T cells through opposing actions. SK1 restricts the conversion of p53 into p63 and p90 and antagonises pro-survival p38 MAPK/JNK signalling in HEK293T cells. In contrast, SK2 promotes the expression

of pro-survival XBP-1s, which is also inhibited by native p53 in HEK293T cells (Figure 4.23). These novel findings indicate cell type specific function for SK1 and SK2 and suggest complex regulation involving Degr1, p53 and p38 MAPK/JNK/XBP-1s that should be considered when developing therapeutic agents designed to induce apoptosis/senescent death of cancer cells.

CHAPTER 5:

**SPHINGOSINE KINASES LINK WITH
NUCLEAR FACTOR KAPPA B- AND
ACTIVATOR PROTEIN-1-MEDIATED
SIGNALLING IN KERATINOCYTES**

CHAPTER 5: SPHINGOSINE KINASES LINK WITH NUCLEAR FACTOR KAPPA B- AND ACTIVATOR PROTEIN-1-MEDIATED SIGNALLING IN KERATINOCYTES

5.1 INTRODUCTION

Chronic inflammatory diseases, such as chronic obstructive pulmonary disease (COPD), inflammatory bowel disease (IBD), rheumatoid arthritis (RA), psoriatic arthritis, and psoriasis, affect a large proportion of the population. In addition, metabolic diseases, such as atherosclerosis or type 2 diabetes mellitus (T2DM), and even cancer are believed to have an underlying inflammatory mechanistic component (Karin, 2005). In most of these diseases, cytokines and chemotactic/chemoattractant proteins are released that can, in turn, attract innate and adaptive immune cells that if excessive promotes the pathogenesis of disease. The inflammatory process that involves a cascade of events is then activated through the cytokine milieu together with the immune cells (Zhang and Sun, 2015; Lawrence, 2009). The innate immune system involves cellular components such as dendritic cells or macrophages and humoral components of the complement system that react to infectious agents through the activation of Toll-like receptors. Once these receptors are activated, they result in the differentiation of macrophages as well as the production of several cytokines, including TNF α , IL-1, IL-6, or IL-12, which is integrated by adapter molecules such as TRAF6 and MyD88 that eventually stimulate the NF- κ B and AP-1 signalling pathways (Kawai *et al.*, 2004). NF- κ B and AP-1 appear to be central mediators of pro-inflammatory gene induction and functions, and the deregulation of

inflammatory responses can lead to excessive or long-lasting tissue damage, thereby contributing to the development of acute or chronic inflammatory diseases.

AP-1 protein regulates gene transcription of both Jun and Fos and this involves MAPKs pathways and phosphorylation cascades (Palanki, 2002). AP-1 activity is stimulated via growth factors or agents that promote proliferation (Angel and Karin, 1991). AP-1 plays an essential role in initiation and progression of inflammatory disorders and evidence supports its involvement. For instance, Shiozawa *et al.* (1997) showed that when AP-1 decoy oligodeoxynucleotide (ODN) was systematically administered to competitively reduce DNA binding of AP-1, it reduced arthritic joint destruction in mice (Shiozawa *et al.*, 1997). Other studies have also shown that AP-1 is highly expressed in asthmatic patients' airways indicating high activity of this transcription factor in the disease (Demoly *et al.*, 1992; Teo and Kahn, 2004). Moreover, down-regulation of JunB in both human and mice models have been shown to increase cell proliferation and deregulate cytokine expression that lead to initiation of psoriasis lesions (Zenz *et al.*, 2005). Therefore, AP-1 inhibition or inhibition of downstream effectors could act as a promising therapeutic target to treat inflammatory processes and reduce the inflammatory cytokines and chemokines production.

Recent studies have proposed that sphingosine kinases and S1P are essential regulators of inflammatory responses. Some studies have demonstrated the involvement of SK1 in TNF α -dependent signalling through the NF- κ B pathway to form pro-inflammatory mediators. This involves TRAF-2, an essential intermediate

of inflammatory cytokines signalling. In this case, S1P binds to and endows TRAF-2 with E3 ligase activity and this is essential for activation of the NF- κ B pathway. TRAF2 catalyses lysine-63 (K63)-linked polyubiquitination of RIP1 that functions to recruit IKK and promotes the degradation of I κ B and the activation of NF- κ B. These findings suggest that intracellular S1P plays an important role in cytokine-induced inflammatory pathways. In addition, SK1 has been shown to regulate the polyubiquitination of K63 to other proteins involved in novel signalling pathways (Vallabhapurapu *et al.*, 2008; Alvarez *et al.*, 2010). For example, Harikumar and colleagues (2014) reported that interferon-regulatory factor 1 (IRF1) is essential for IL-1-linked K63 polyubiquitination, which involves a complex of apoptosis inhibitor cIAP2, SK1, and IRF1 (Harikumar *et al.*, 2014). However, others have reported contrary data for the involvement of SK1 in TRAF-2 and NF- κ B signalling. For example, Xiong *et al.* (2013) reported neither SK1 nor SK2 are required for the activation of NF- κ B in response to TNF α in macrophages (Xiong *et al.*, 2013). In addition, TRAF-2 has been shown to regulate TNF α and NF- κ B signalling independently of SK1 in keratinocytes, where it suppresses skin inflammation and apoptosis (Etemadi *et al.*, 2015).

In addition, other studies have shown that pharmacological SK1 inhibitors and/or SK1 siRNA decrease the expression of pro-inflammatory cytokines (Nayak *et al.*, 2010; Limaye *et al.*, 2009b). However, this outcome rendered macrophages sensitive to *Mycobacterium smegmatis* infection (Prakash *et al.*, 2010). In addition, SK1 deficiency has been shown to significantly decrease synovial inflammation and joint erosions in TNF α -induced arthritis, which is believed to be mediated through

decreased expression of COX-2, numbers of inflammatory articular Th17 cells, and osteoclastogenesis with increased expression of a member of the suppressor of cytokine signalling (SOCS3) (Baker *et al.*, 2010). SOCS3 works as a negative regulator in the JAK/STAT pathway used by IL-6 receptor signalling that leads to inhibition of prolonged STAT3 phosphorylation and IL-6 downstream inflammatory effects (Crocker *et al.*, 2003). Liang *et al.* also showed that SK1 and the subsequently formed S1P are linked with continuous activation of STAT3, chronic intestinal inflammation, as well as the development of colitis-related cancer (Liang *et al.*, 2013). *Sk1*^{-/-} mice were also shown to be protected from ulcerative colitis (UC), suggesting that SK1 is involved as a pro-inflammatory enzyme in this disease (Snider *et al.*, 2009). Moreover, Jung and colleagues (2007) reported that SK1 overexpression increases the formation of IL-12 from dendritic cells while SK1 RNAi knockdown diminishes the formation of IFN- γ from Th1 cells (Jung *et al.*, 2007). Although SK1 has a pro-inflammatory role in some diseases, others reported that it plays a protective role which suggests disease specificity. For examples, removal of SK1 in mice exacerbated LPS-induced neuroinflammation (Grin'kina *et al.*, 2012) and LPS-induced lung injury compared to WT mice (Wadgaonkar *et al.*, 2009). Furthermore, Adada and colleagues (2013) reported that SK1 regulates the TNF-mediated induction of the chemokine RANTES through p38 MAPK, but it does so independently of NF- κ B activation. In this case, the loss of SK1 reduces TNF α -stimulated phosphorylation of p38 MAPK and induces the RANTES formation and levels of different cytokines and chemokines including IL-8, IL-6, CXCL1, CCL20, and CXCL10 (Adada *et al.*, 2013).

SK2 has also been reported to fulfill a pro-inflammatory and pro-fibrotic role. For example, SK2 deficiency has been shown to attenuate kidney fibrosis in *Sk2*^{-/-} mice compared to the WT mice. This involves regulation of IFN- γ production, and a remarkable reduction in the number of infiltrating CD3⁺ T cells, CD11b⁺ neutrophils, and macrophages. Moreover, an increase in the levels of the pro-inflammatory mediators CXCL1 and CXCL2 was detected in WT and *Sk1*^{-/-} mice, but not *Sk2*^{-/-} mice in response to folic acid (Bajwa *et al.*, 2017). In addition, Yoshimoto *et al.* (2003) proposed that SK2 positively modulates of IL-12 signalling by forming a complex with the IL-12 beta 1 (IL12 β 1) receptor to regulate inflammatory responses in Th1 cells. Indeed, the over-expression of SK2 promotes the formation of IL-12-stimulated IFN- γ in T-cells (Yoshimoto *et al.*, 2003). Furthermore, another study demonstrated that knocking down SK2 exhibited a protective role and reduced the clinical symptoms of experimental autoimmune encephalomyelitis (EAE) in C57BL/6 mice (Imeri *et al.*, 2016). In addition, the SK2-selective inhibitor ROME reduced in the severity of EAE symptoms (Barbour *et al.*, 2017; Lim *et al.*, 2011b) whereas another selective SK2 inhibitor, ABC294640, was shown to have anti-inflammatory effects that attenuated disease progression in rodent models of Crohn's disease (Maines *et al.*, 2010), ulcerative colitis (UC) (Maines *et al.*, 2008), and arthritis (Fitzpatrick *et al.*, 2011). In addition, ABC294640 also decreases inflammation and attenuates graft injury following liver transplantation through the reduction of the expression of TLR4, the activation of NF- κ B, the production of pro-inflammatory cytokines/chemokines, the expression of adhesion molecules, and the infiltration of neutrophils and monocytes/macrophages (Liu *et al.*, 2012).

However, other reports have shown that *Sk1*^{-/-} and *Sk2*^{-/-} mice do not have attenuated inflammatory responses in numerous inflammatory cellular models (Wadgaonkar *et al.*, 2009; Michaud *et al.*, 2006; Zemann *et al.*, 2007). Indeed, in murine macrophages that lack both SK isoenzymes, TNF α or LPS signalling does not involve S1P. Rather, SK2 was proposed to be involved in maintaining sphingolipid homeostasis through the accumulation of sphingolipid metabolites and compensatory autophagy when perturbed (Xiong *et al.*, 2013). Therefore, the role of sphingosine kinases in inflammation is still not well understood in light of the many controversial reports. Thus, in this chapter, the role of SK1 and SK2 was investigated using different SK inhibitors, in order to establish their effect on NF- κ B- and AP-1 signalling and transcriptional regulation in keratinocytes.

5.2 RESULTS

5.2.1 Effect of SK inhibitors on NF- κ B signalling and transcriptional activity in NCTC-NF- κ B reporter keratinocytes

The study initially investigated the effects of different SK1 and SK2 selective inhibitors on the NCTC-NF- κ B reporter cells in which luciferase expression is regulated by an NF- κ B-binding promoter. A previous study by our laboratory showed that SK1 inhibitors induce the proteasomal degradation of SK1 in androgen-independent LNCaP-AI cells (McNaughton *et al.*, 2016). Therefore, the effect of SK inhibitors on SK1 expression levels in NCTC-NF- κ B reporter cells was first investigated by treating these cells with different SK inhibitors for 4 hours. The SK1/SK2 inhibitor, SKi (10 μ M), the SK1 inhibitor/S1P receptor agonist FTY720 (10 μ M), and the nanomolar potent SK1 inhibitor PF-543 (100 nM) reduced the expression of SK1 in NCTC-NF- κ B reporter keratinocytes (Figure 5.1). In contrast, the SK2 selective inhibitors ABC294640 (25 μ M), K145 (10 μ M), and ROME (10 μ M) did not promote the degradation of SK1 (Figure 5.1).

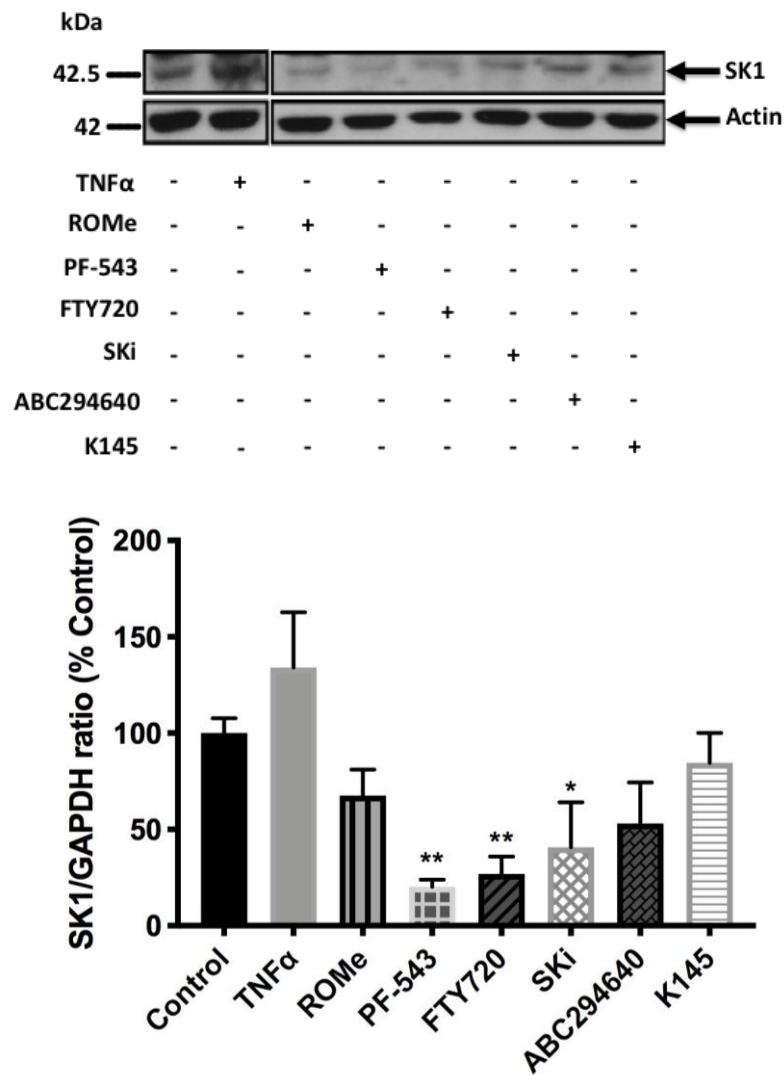


Figure 5.1 *Effect of SK inhibitors on SK1 protein expression in NCTC-NF- κ B reporter keratinocytes.* NCTC-NF- κ B reporter cells were cultured in complete medium containing 10% FCS until ~70% confluent then quiesced with serum-free medium for 24 hours. Cells were treated with SKi (10 μ M) or ABC294640 (25 μ M) or K145 (10 μ M) or ROMe (10 μ M) or PF-543 (100 nM) or FTY720 (10 μ M) or with the vehicle alone (DMSO 0.1% v/v) for 4 hours. SK1 expression was detected using SDS PAGE and western blotting with anti-SK1 antibody. Blots were stripped and re-probed with anti-actin antibody to ensure comparable protein loading. A representative western blot is shown of an experiment performed at least three independent times. Also shown is the densitometric quantification of SK1/actin ratio immunoreactivity of (Mr 42.5 kDa), expressed as a percentage of the control (Control=100%). The data was expressed as means \pm SEM for n=3 experiments and analysed by one-way ANOVA Dunnett's multiple comparisons test, * p <0.05 for SKi vs control, ** p <0.01 for PF-543 or FTY720 vs control.

The next step was to evaluate the effect of SK inhibitors on NF- κ B signalling by testing their effect on I κ B degradation. The pro-inflammatory mediator TNF α was used to promote the degradation of I κ B. Thus, the treatment of cells with TNF α (15 ng/ml) reduced the levels of I κ B in a time-dependent manner, with the maximum reduction being observed at 15 minutes before returning to the baseline by 1 hour (Figure 5.2A). The pre-treatment of cells with the NF- κ B inhibitor BMS345541 (20 μ M) eliminated the effect of TNF α on I κ B degradation (Figure 5.2B).

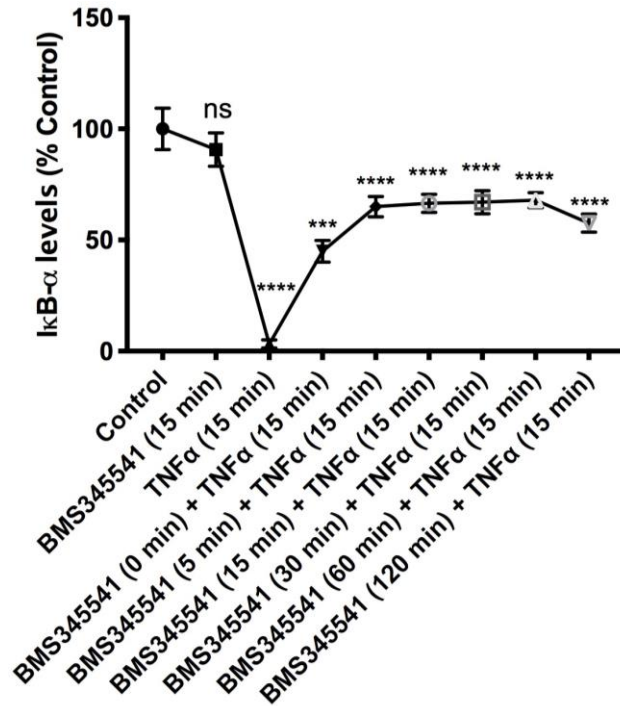
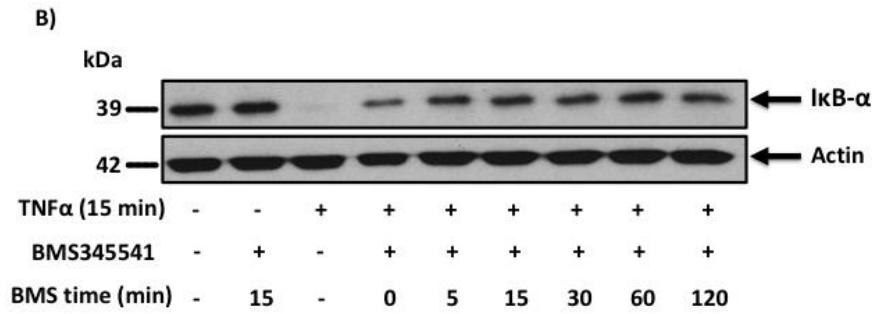
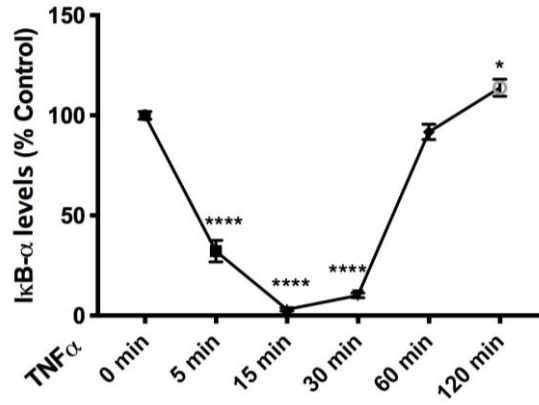
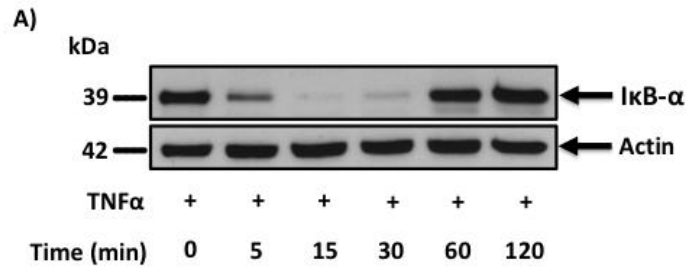
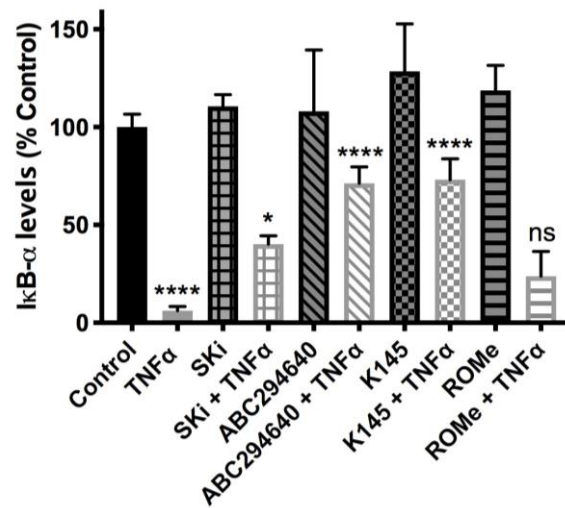
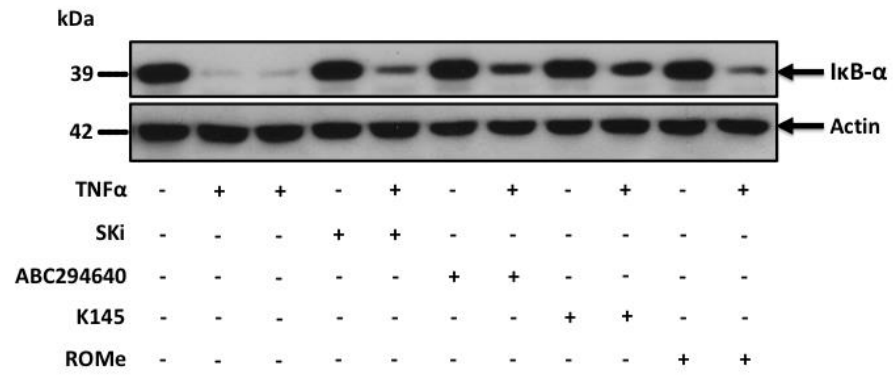


Figure 5.2 *Effect of TNF α on I κ B degradation in NCTC-NF- κ B reporter keratinocytes.* NCTC-NF- κ B reporter cells were cultured in complete medium containing 10% FCS until ~70% confluent then quiesced with serum-free medium for 24 hours. A) Cells were treated with TNF α (15 ng/ml) for a time course (0-120 minutes). B) Cells were pre-treated with BMS345541 (20 μ M) for 30 minutes prior to addition of TNF α (15 ng/ml) or with the vehicle alone (DMSO 0.1% v/v) for the times indicated. I κ B degradation was detected using SDS PAGE and western blotting with anti-I κ B- α antibody. Blots were stripped and re-probed with anti-actin antibody to ensure comparable protein loading. Two representative western blots are shown each of an experiment performed at least three independent times. Also shown is the densitometric quantification of I κ B- α /actin ratio immunoreactivity of (Mr 39 kDa), expressed as a percentage of the control (Control=100%). The data was expressed as means \pm SEM for n=3 experiments and analysed by A) one-way ANOVA Dunnett's multiple comparisons test, * p <0.05 for TNF α (120 min) vs control and **** p <0.0001 for TNF α (5 min) vs control or TNF α (15 min) vs control or TNF α (30 min) vs control. B) one-way ANOVA multiple comparisons test, *** p <0.001 for BMS345541 (0 min)/TNF α vs TNF α and **** p <0.0001 for TNF α vs control or BMS345541 (5 to 120 min)/TNF α vs TNF α and ns denotes not statistically significant (p >0.05) for BMS345541 vs control.

Next, NCTC-NF- κ B reporter cells were pretreated with SK inhibitors prior to the addition of the pro-inflammatory mediator TNF α in order to assess their effect on I κ B degradation. The results showed that the SK2 inhibitors, including SKi, ABC294640, K145, and ROME, reduced TNF α -stimulated I κ B degradation (Figure 5.3A) whereas the potent SK1 selective inhibitor PF-543 and the SK1 inhibitor/S1P receptor agonist FTY720 had no effects on I κ B degradation (Figure 5.3B).

A)



B)

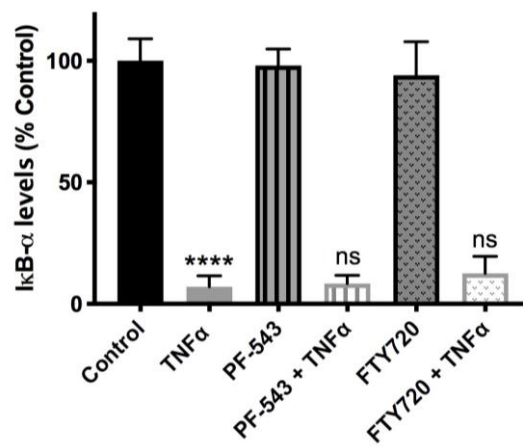
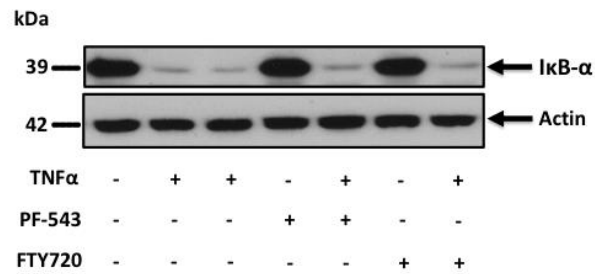
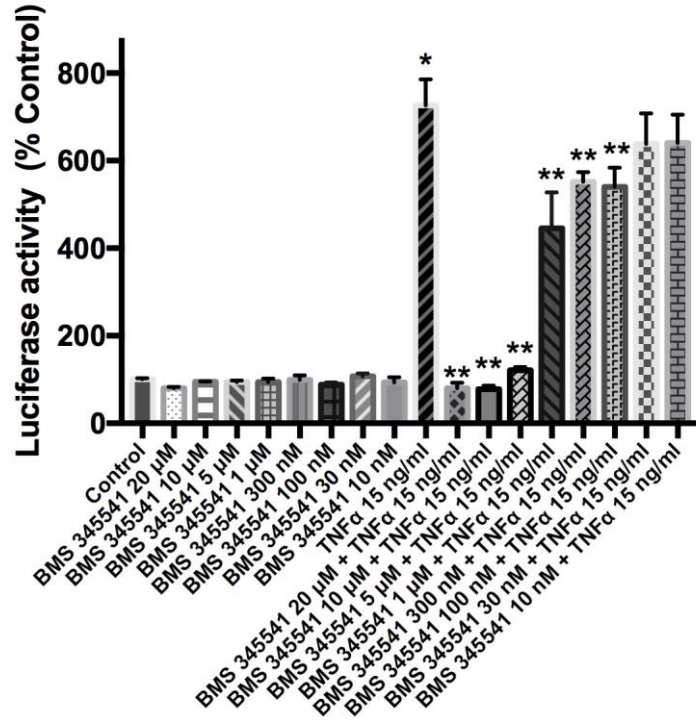


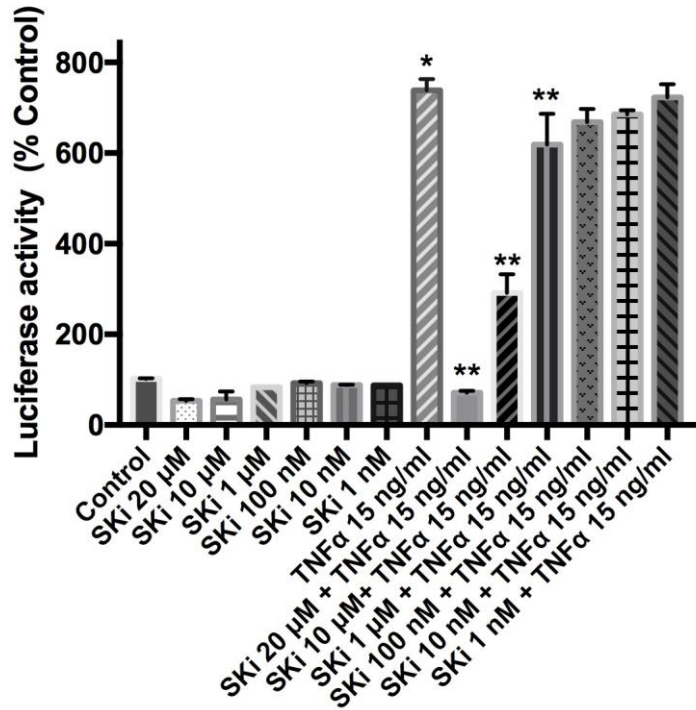
Figure 5.3 *Effect of SK inhibitors on I κ B degradation in NCTC-NF- κ B reporter keratinocytes.* NCTC-NF- κ B reporter cells were cultured in complete medium containing 10% FCS until ~70% confluent then quiesced with serum-free medium for 24 hours. Cells were pre-treated with A) SKi (10 μ M) or ABC294640 (25 μ M) or K145 (10 μ M) or ROME (10 μ M) B) PF-543 (100 nM) or FTY720 (10 μ M) or with the vehicle alone (DMSO 0.1% v/v) for 10 min prior to stimulation with TNF α (15 ng/ml) for 15 min. I κ B degradation was detected using SDS PAGE and western blotting with anti-I κ B- α antibody. Blots were stripped and re-probed with anti-actin antibody to ensure comparable protein loading. Two representative western blots are shown each of an experiment performed at least three independent times. Also shown is the densitometric quantification of I κ B- α /actin ratio immunoreactivity of (Mr 39 kDa), expressed as a percentage of the control (Control=100%). The data was expressed as means \pm SEM for n=3 experiments and analysed by one-way ANOVA multiple comparisons test, A) * p <0.05 for SKi/TNF α vs TNF α , **** p <0.0001 for TNF α vs control or ABC294640/TNF α vs TNF α or K145/ TNF α vs TNF α and ns denotes not statistically significant (p >0.05) for ROME/TNF α vs TNF α . B) **** p <0.0001 for TNF α vs control and ns denotes not statistically significant (p >0.05) for PF-543/TNF α vs TNF α or FTY720/TNF α vs TNF α .

Finally, the effects of NF- κ B and SK inhibitors on NF- κ B-transcriptional activity were measured using the luciferase reporter assay. The NF- κ B inhibitor BMS345541 (100 nM–20 μ M) significantly reduced NF- κ B-mediated transcriptional activity (Figure 5.4A), which validated the responsiveness of the reporter assay for NF- κ B signalling. In addition, all of the tested SK inhibitors significantly reduced NF- κ B-dependent transcriptional activity including SKi (1–20 μ M) (Figure 5.4B), ABC294640 (25–50 μ M) (Figure 5.4C), K145 (10–20 μ M) (Figure 5.4D), ROME (10–30 μ M) (Figure 5.4E), and FTY720 (10–20 μ M) (Figure 5.4G), except PF-543 (Figure 5.4F). The latter reduced NF- κ B-dependent transcriptional activity at 20 μ M but this is much higher than the K_i of PF-543 (4 nM) (Schnute *et al.*, 2012). Although FTY720 (10 μ M) failed to modulate the degradation of I κ B (Figure 5.3B), it induced significant inhibition of NF- κ B transcriptional activity at concentrations (10–20 μ M) (Figure 5.4G) that is known to induce SK1 inhibition (Lim *et al.*, 2011b).

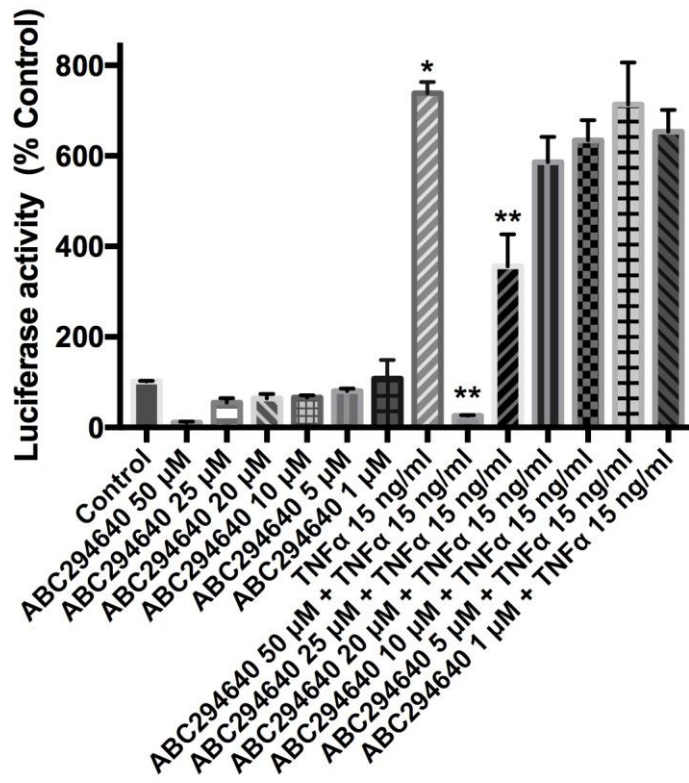
A)



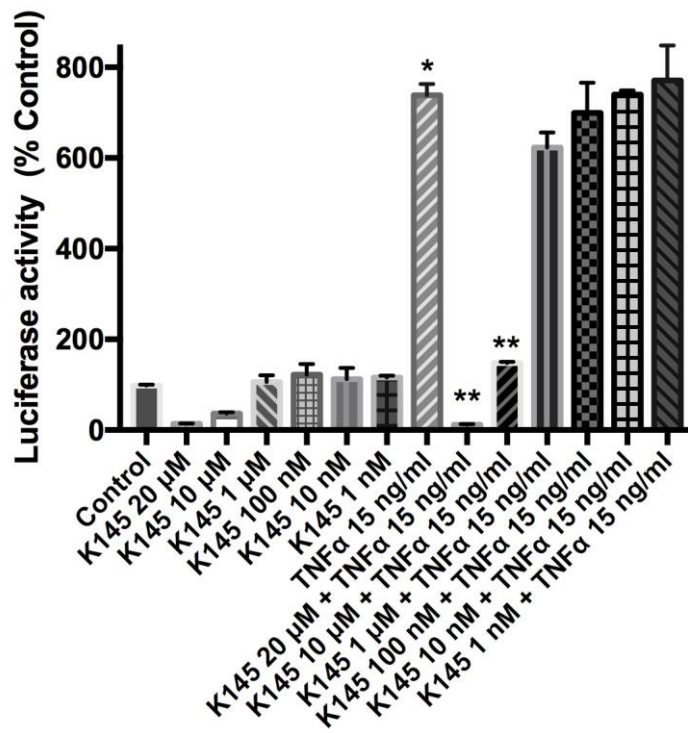
B)



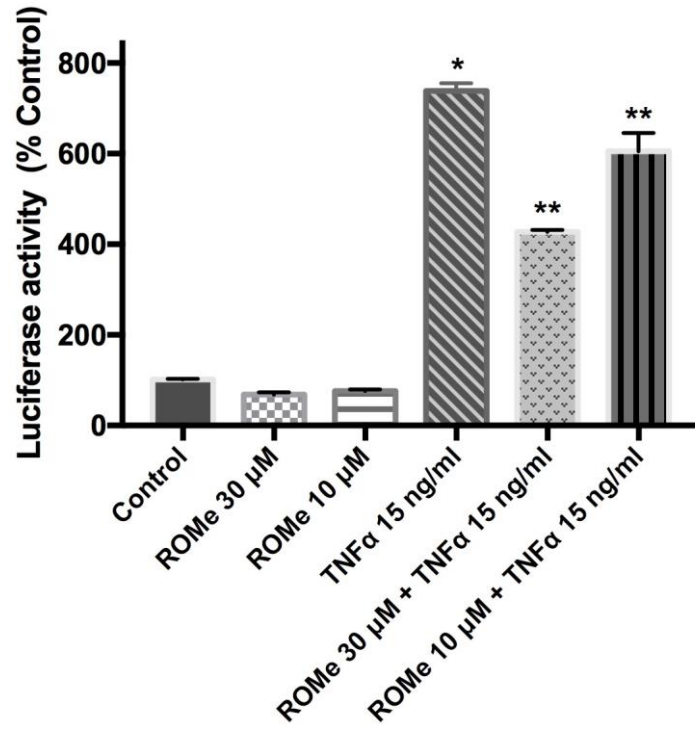
C)



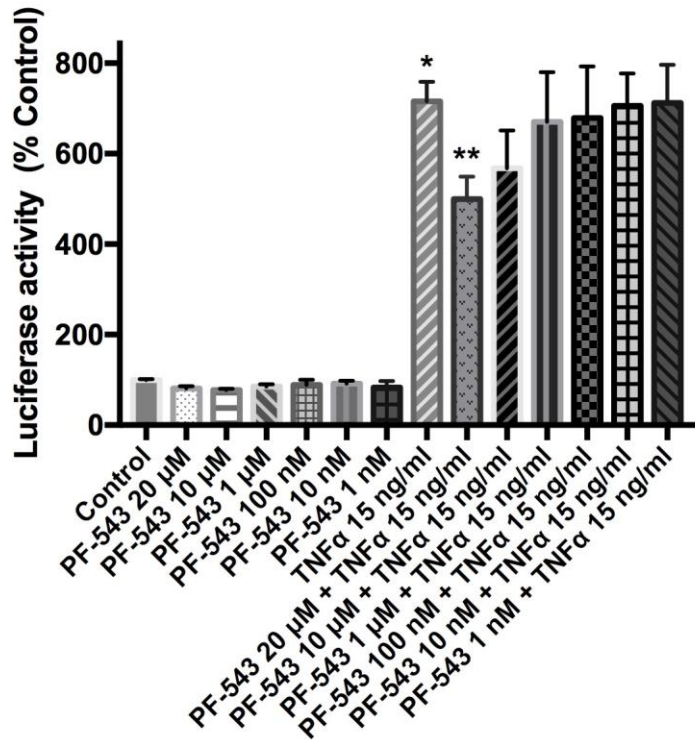
D)



E)



F)



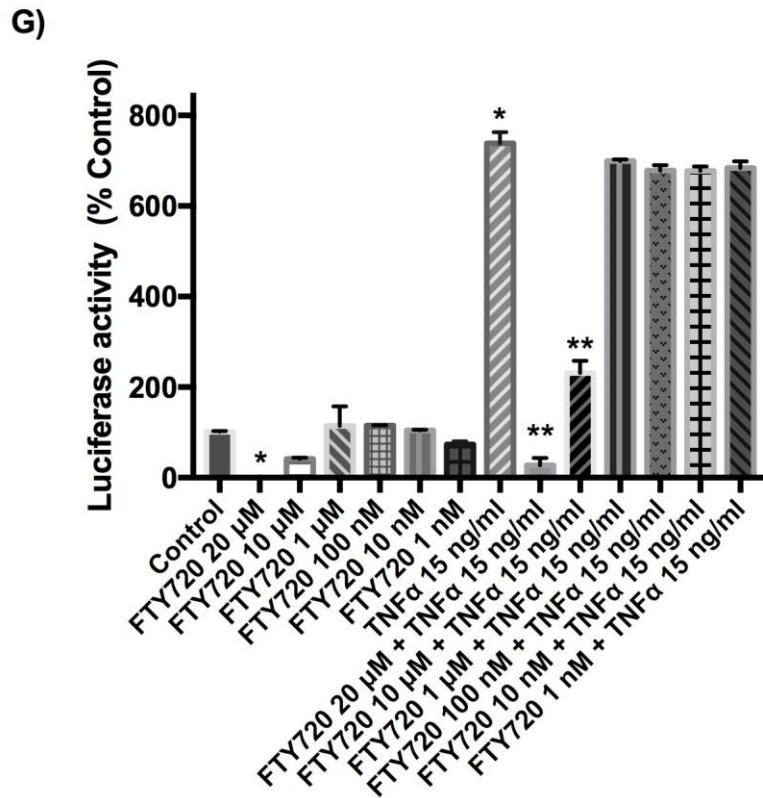


Figure 5.4 *Effect of SK inhibitors on NF-κB-mediated signalling in NCTC-NF-κB reporter keratinocytes.* NCTC-NF-κB reporter cells were cultured in complete medium containing 10% FCS at a density of 10,000 cells/well for 24 hours then quiesced with serum-free medium for another 24 hours. Cells were pre-treated with A) BMS345541 for 30 min or SK inhibitors B) SKi C) ABC294640 D) K145 E) ROME F) PF-543 G) FTY720 for 10 min in concentrations indicated or with the vehicle alone (DMSO 0.1% v/v) prior to stimulation with TNFα (15 ng/ml) for 4 hours before luminescence activity has been measured. Data are expressed as a % of control ± SEM for n=3 experiments. The data was analysed by one-way ANOVA multiple comparisons, * $p < 0.05$ for TNFα vs control and ** $p < 0.05$ for TNFα/SK inhibitor/BMS345541 vs TNFα.

5.2.2 Effect of SK inhibitors on JNK/ERK-1/2 signalling and AP-1 transcriptional activity in NCTC-AP1 reporter keratinocytes

The effect of different SK inhibitors was also investigated against the transcriptional regulation of AP-1 in NCTC-AP1 reporter keratinocytes in which luciferase expression is regulated by an AP-1-binding promoter. The effect of SK inhibitors on SK1 expression levels in NCTC-AP1 reporter cells was assessed by treating these cells with different SK inhibitors for 4 hours. We obtained similar results to those obtained using NCTC-NF- κ B reporter cells—namely, the SK1/SK2 inhibitor SKi (10 μ M), the SK1 inhibitor FTY720 (10 μ M), and the nanomolar-potent SK1 inhibitor PF-543 (100 nM) reduced the expression of SK1 whereas the SK2 selective inhibitors ABC294640 (25 μ M), K145 (10 μ M), and ROME (10 μ M) did not promote the degradation of SK1 (Figure 5.5).

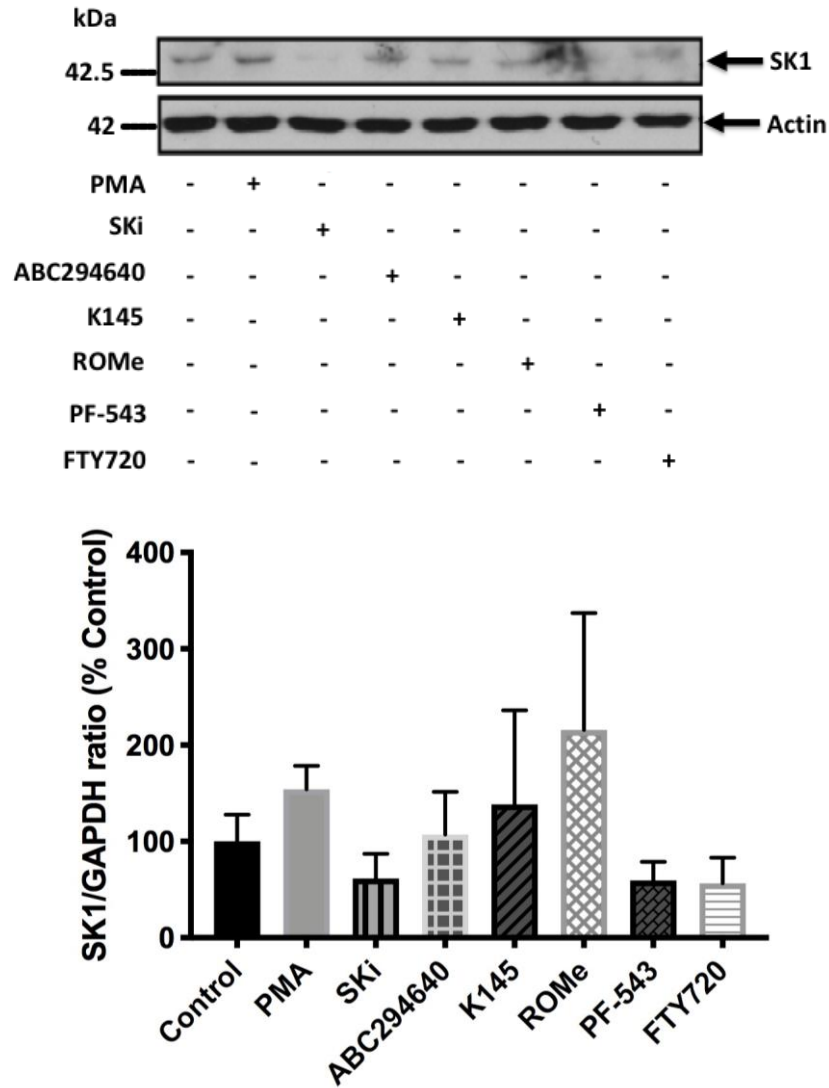


Figure 5.5 *Effect of SK inhibitors on SK1 protein expression in NCTC-API reporter keratinocytes.* NCTC-API reporter cells were cultured in complete medium containing 10% FCS until ~70% confluent then quiesced with serum-free medium for 24 hours. Cells were treated with SKi (10 μ M) or ABC294640 (25 μ M) or K145 (10 μ M) or ROME (10 μ M) or PF-543 (100 nM) or FTY720 (10 μ M) or with the vehicle alone (DMSO 0.1% v/v) for 4 hours. SK1 expression was detected using SDS PAGE and western blotting with anti-SK1 antibody. Blots were stripped and re-probed with anti-actin antibody to ensure comparable protein loading. A representative western blot is shown of an experiment performed at least three independent times. Also shown is the densitometric quantification of SK1/GAPDH ratio immunoreactivity of (Mr 42.5 kDa), expressed as a percentage of the control (Control=100%). The data was expressed as means \pm SEM for n=3 experiments and analysed by one-way ANOVA Dunnett's multiple comparisons test.

AP-1 transcription factor is mainly regulated by JUN and FOS that are regulated by the MAPK pathways, which consist of JNKs, ERK1/2, and p38 pathways. Therefore, phorbol myristate acetate (PMA) was used to promote the activation of the JNK/ERK1/2 pathways. The results showed that PMA (100 nM) stimulates significant activation of P-p46 JNK in a time-dependent manner at 5–60 minutes with maximum effect achieved at 30–60 minutes (Figure 5.6A). In addition, PMA induced activation of P-p54 JNK only at 30-60 minutes (Figure 5.6A). Moreover, PMA (100 nM) promoted the activation of ERK1/2 with maximum activation at 5 minutes, which remained sustained for 2 hours (Figure 5.6B). Next we pre-treated NCTC-AP1 keratinocytes with the JNK inhibitor SP600125 (20 μ M) before the addition of PMA (100 nM) and this abolished the effect of PMA on P-p54 JNK while having no effect on PMA-induced activation of P-p46 JNK or P-ERK1/2 (Figure 5.6B).

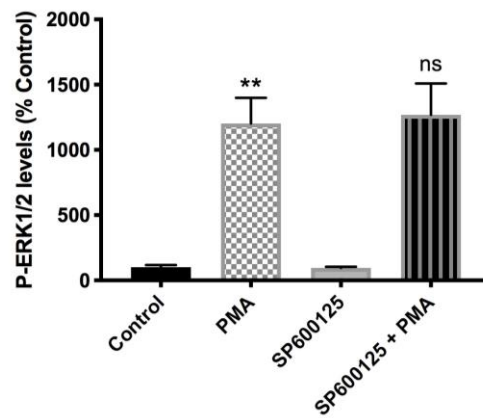
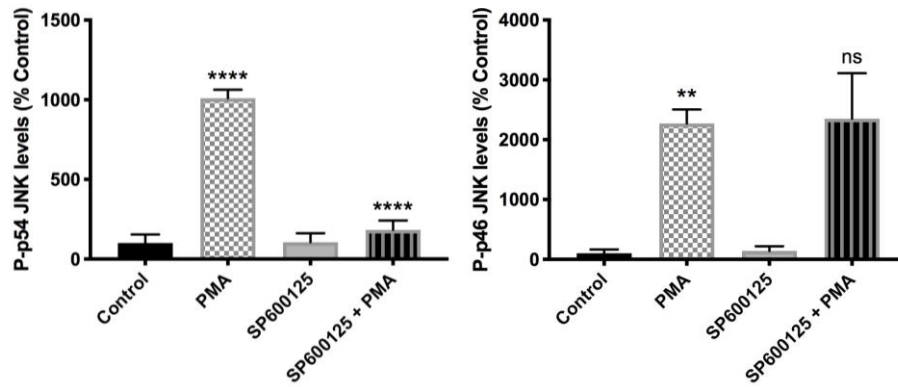
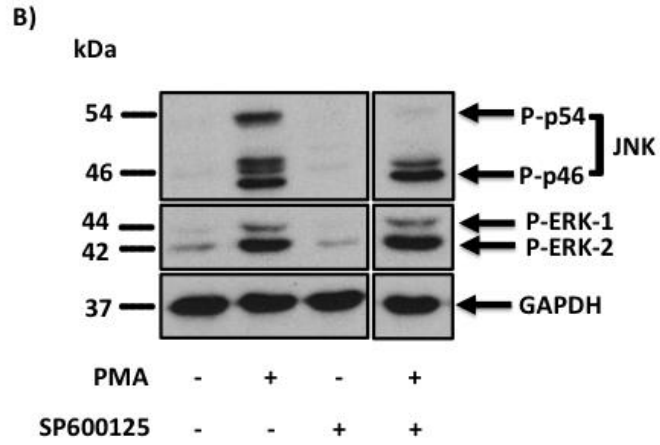
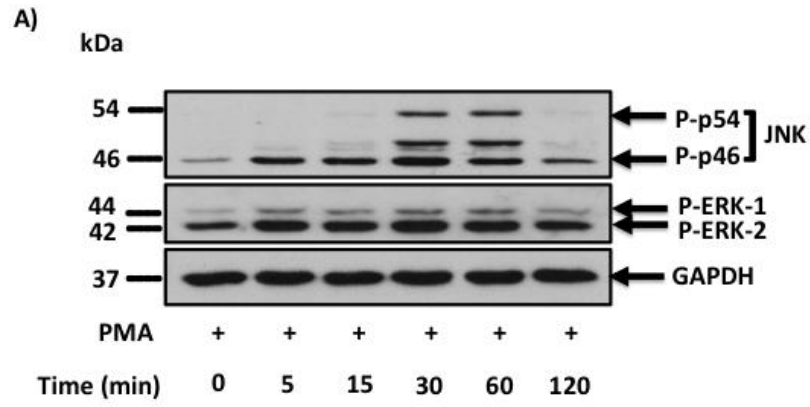


Figure 5.6 *Effect of PMA on JNK phosphorylation and ERK-1/2 activation in NCTC-API reporter keratinocytes.* NCTC-API reporter cells were cultured in complete medium containing 10% FCS until ~70% confluent then quiesced with serum-free medium for 24 hours. A) Cells were treated with PMA (100 nM) for a time course (0-120 minutes). B) Cells were pre-treated with SP600125 (20 μ M) for 30 minutes prior to addition of PMA (100 nM) for another 30 minutes or with the vehicle alone (DMSO 0.1% v/v). P-JNK and P-ERK1/2 levels were detected using SDS PAGE and western blotting with respective antibodies. Blots were stripped and re-probed with anti-GAPDH antibody to ensure comparable protein loading. Two representative western blots are shown of an experiment performed A) two independent times. B) at least three independent times. Also shown is the densitometric quantification of P-p54 JNK/GAPDH, P-p46 JNK/GAPDH, and P-ERK1/2/GAPDH ratios immunoreactivities of (Mr 54, 46, and 42-44 kDa, respectively) of B, expressed as a percentage of the control (Control=100%). The data of B was expressed as means \pm SEM for n=3 experiments and analysed by one-way ANOVA multiple comparisons test; in P-p54 JNK **** p <0.0001 for PMA vs control or SP600125/PMA vs PMA, in P-p46 JNK ** p <0.01 for PMA vs control and ns denotes not statistically significant (p >0.05) for SP600125/PMA vs PMA, in P-ERK1/2 ** p <0.01 for PMA vs control and ns for SP600125/PMA vs PMA.

NCTC-AP1 reporter keratinocytes were pre-treated with SK inhibitors prior to the addition of PMA in order to measure activation on JNK/ERK1/2 pathways. The results showed that the selective SK2 inhibitors ABC294640 (25 μ M) and K145 (10 μ M) as well as the SK1 inhibitor/S1P receptor agonist FTY720 (10 μ M) reduced the PMA-stimulated activation of P-p46-JNK (Figure 5.7). In contrast, ABC294640 (25 μ M) reduced the PMA-stimulated activation of ERK1/2 (Figure 5.7). However the other sphingosine kinase inhibitors used, including the SK1/SK2 inhibitor SKi (10 μ M), the potent SK1 selective inhibitor PF-543 (100 nM), and the SK2 selective inhibitor ROME (10 μ M), had no effect on ERK1/2 phosphorylation (Figure 5.7).

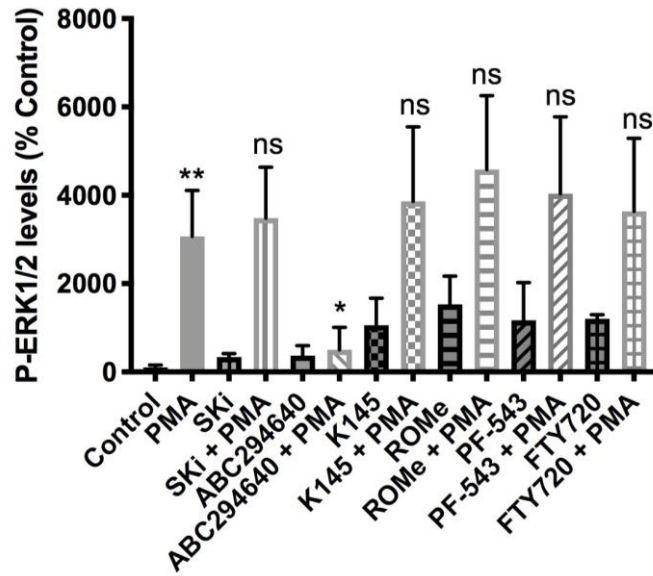
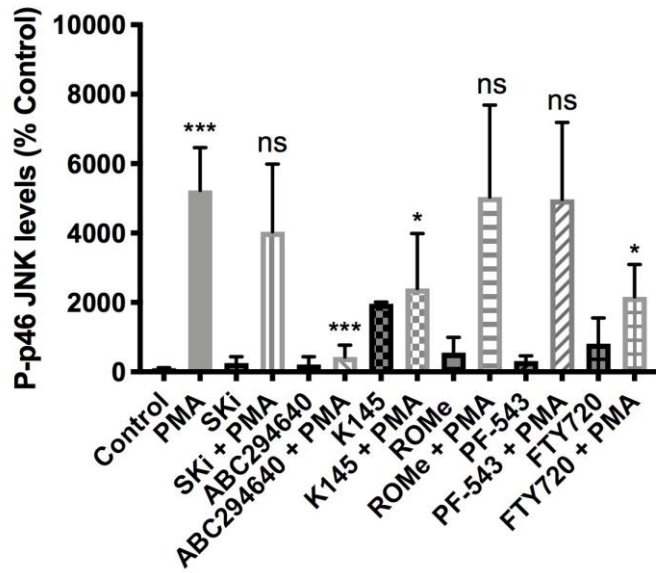
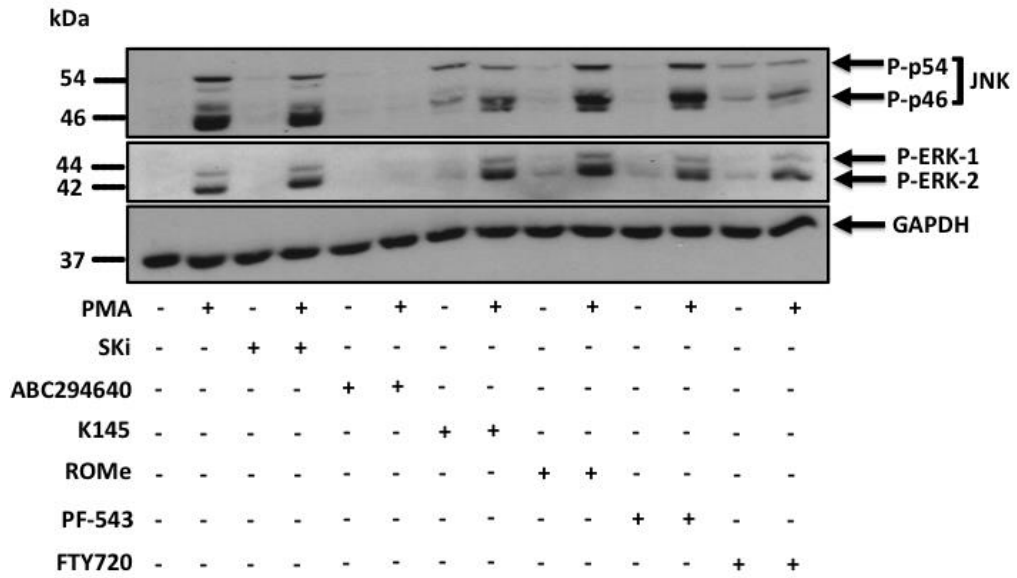
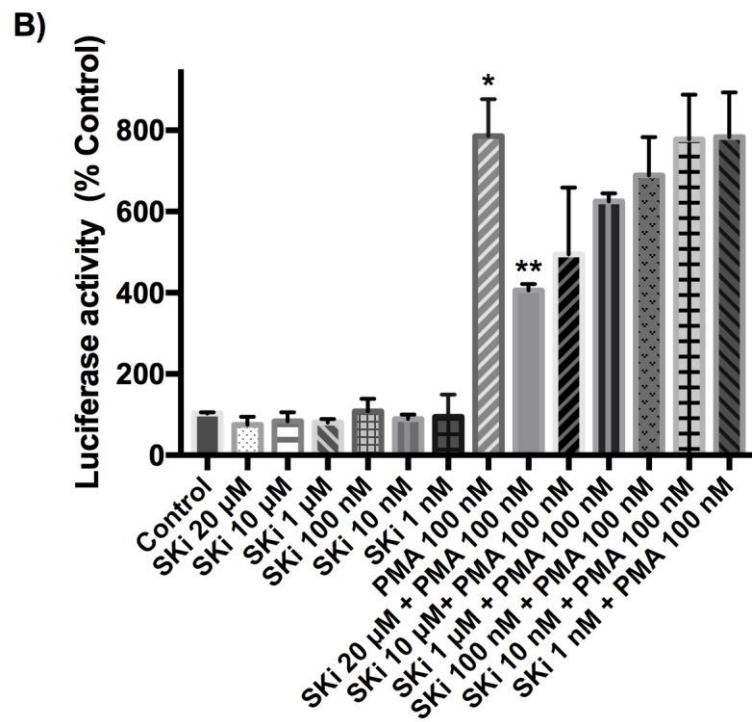
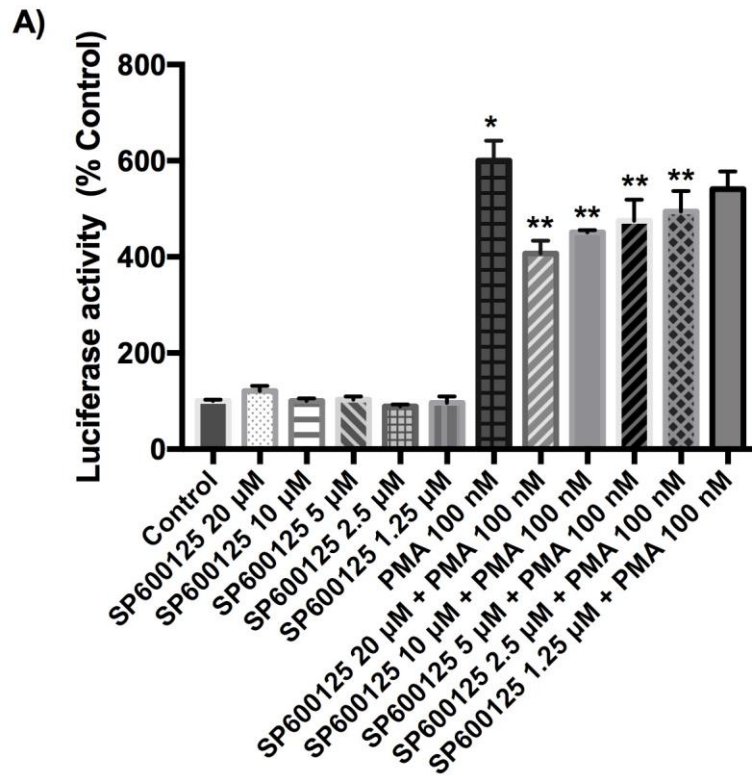
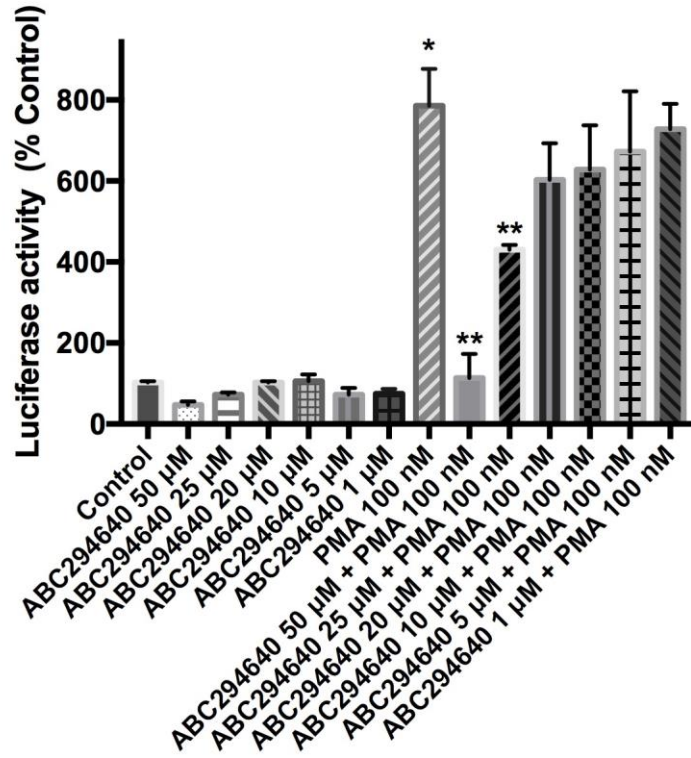


Figure 5.7 Effect of SK inhibitors on PMA-activated JNK and ERK1/2 in NCTC-API reporter keratinocytes. NCTC-API reporter cells were cultured in complete medium containing 10% FCS until ~70% confluent then quiesced with serum-free medium for 24 hours. Cells were pre-treated with SKi (10 μ M) or ABC294640 (25 μ M) or K145 (10 μ M) or ROME (10 μ M) or PF-543 (100 nM) or FTY720 (10 μ M) or with the vehicle alone (DMSO 0.1% v/v) for 10 min prior to stimulation with PMA (100 nM) for 30 min. P-JNK and P-ERK1/2 levels were detected using SDS PAGE and western blotting with respective antibodies. Blots were stripped and re-probed with anti-GAPDH antibody to ensure comparable protein loading. A representative western blot is shown of an experiment performed at least three independent times. Also shown is the densitometric quantification of P46-JNK/GAPDH and P-ERK1/2/GAPDH ratios immunoreactivities of (Mr 46 and 42-44 kDa, respectively), expressed as a percentage of the control (Control=100%). The data was expressed as means \pm SEM for n=3 experiments analysed by one-way ANOVA multiple comparisons test, in P-p46 JNK * p <0.05 for K145/PMA vs PMA or FTY720/PMA vs PMA and *** p <0.001 for PMA vs control or ABC294640/PMA vs PMA and ns denotes not statistically significant (p >0.05) for SKi/PMA vs PMA or ROME/PMA vs PMA or PF-543/PMA; in P-ERK1/2 levels * p <0.05 for ABC294640/PMA vs PMA, ** p <0.01 for PMA vs control, and ns denotes not statistically significant (p >0.05) for SKi/PMA vs PMA or K145/PMA vs PMA or ROME/PMA vs PMA or PF-543/PMA vs PMA or FTY720/PMA vs PMA.

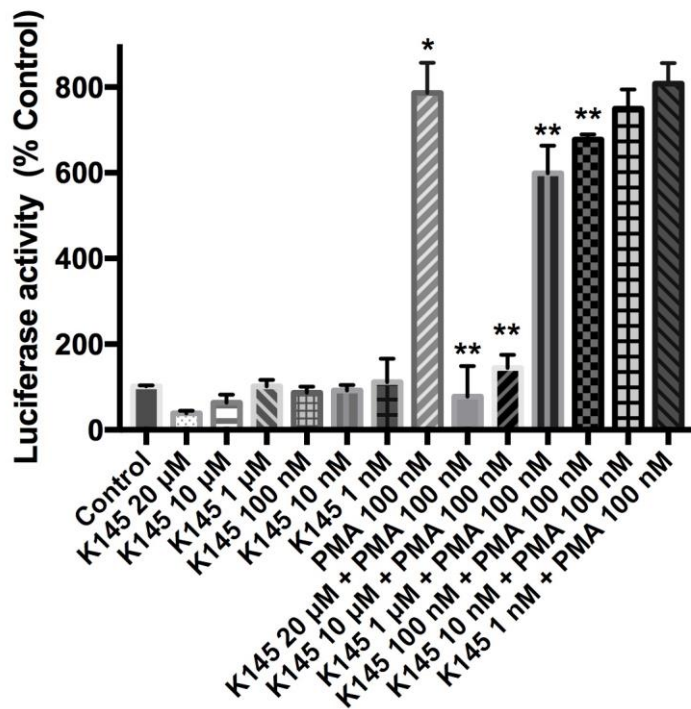
Finally, the effects of JNK and SK inhibitors on AP-1-transcriptional activity was assessed using the luciferase reporter assay. The JNK inhibitor SP600125 (2.5–20 μM) had little effect on the reduction of AP-1-mediated transcriptional activity (Figure 5.8A), which suggests limited requirements for JNK in transcriptional activity of AP-1. The SK2 inhibitors ABC294640 (25–50 μM) (Figure 5.8C) and K145 (1–20 μM) (Figure 5.8D) and the SK1 inhibitor FTY720 (10–20 μM) (Figure 5.8G) significantly reduced the PMA-stimulated transcriptional activity of AP-1. However, the SK1/SK2 inhibitor SKi (20 μM) (Figure 5.8B), the SK1 inhibitor PF-543 (10–20 μM) (Figure 5.8F), and the SK2 inhibitor ROME (30 μM) (Figure 5.8E) induced only a modest reduction in the transcriptional regulation of AP-1 at high concentrations, thereby correlating with limited effect on JNK/ERK1/2.



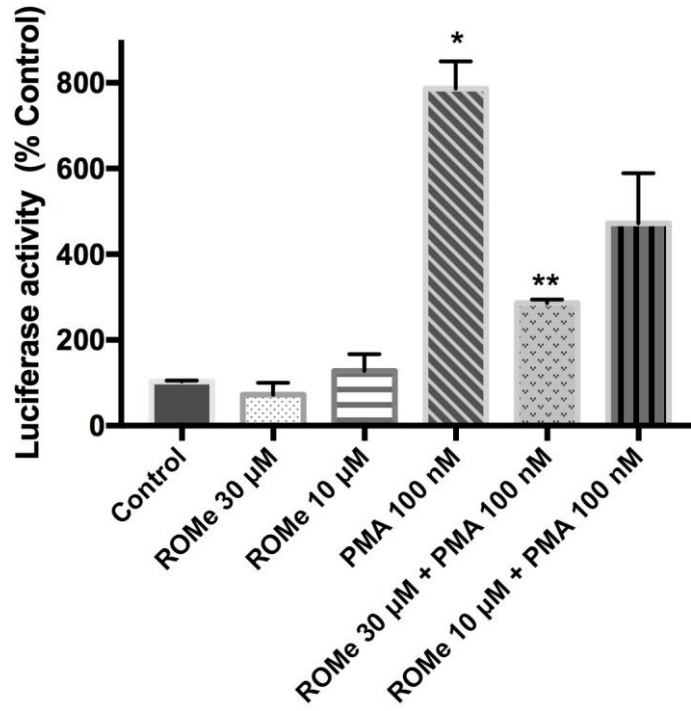
C)



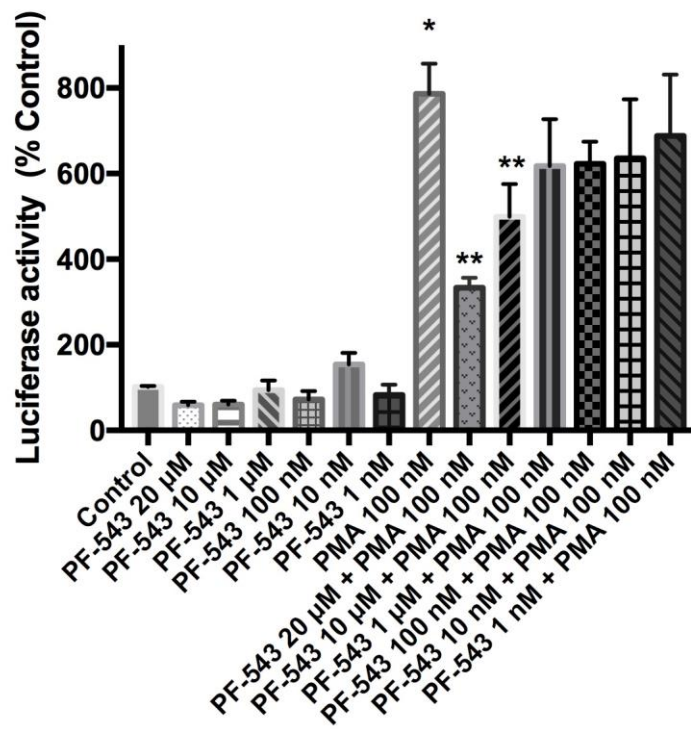
D)



E)



F)



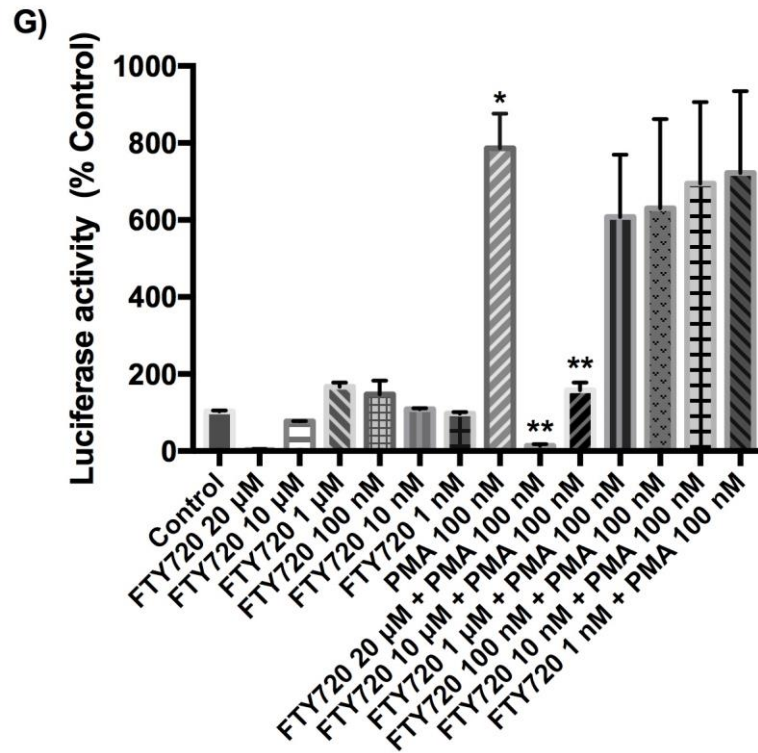


Figure 5.8 *Effect of SK inhibitors on AP1-mediated signalling in NCTC-AP1 reporter keratinocytes.* NCTC-AP1 reporter cells were cultured in complete medium containing 10% FCS at a density of 10,000 cells/well for 24 hours then quiesced with serum-free medium for another 24 hours. Cells were pre-treated with A) SP600125 for 30 min or SK inhibitors B) SKi C) ABC294640 D) K145 E) ROME F) PF-543 G) FTY720 for 10 min in concentrations indicated or with the vehicle alone (DMSO 0.1% v/v) prior to stimulation with PMA (100 nM) for 4 hours before luminescence activity has been measured. Data are expressed as a % of control \pm S.E.M for $n=3$ experiments. The data was analysed by one-way ANOVA multiple comparisons test, $*p<0.05$ for PMA vs control and $**p<0.05$ for PMA/SK inhibitor/SP600125 vs PMA.

5.3 DISCUSSION

The main finding of this study is that SK2, but not SK1, appears to be associated with the NF- κ B-dependent transcriptional regulation in keratinocytes. This is based on the finding that SK2 inhibitors reduced the TNF α -stimulated degradation of I κ B in keratinocytes. The SK1/SK2 inhibitor SKi (1-20 μ M), and the SK2 inhibitors ABC294640 (25-50 μ M), K145 (10-20 μ M), and ROME (10-30 μ M) induced significant reductions in NF- κ B transcriptional activity at concentrations that correlate with their K_i for SK2 inhibition, of ((8 μ M) (Lim *et al.*, 2012; Gao *et al.*, 2012), (10 μ M) (French *et al.*, 2010), (10 μ M) (Liu *et al.*, 2013), and (17 μ M) (Lim *et al.*, 2011a), respectively). A lack of a role for SK1 was supported by the failure of the potent SK1 selective inhibitor PF-543 to reduce TNF α -stimulated I κ B degradation or transcriptional activity of NF- κ B at concentrations known to induce the ubiquitin-proteasomal degradation of SK1 in keratinocytes (100 nM). These findings do not concord with other studies, which showed that S1P formed by SK1 can promote K63 polyubiquitination of RIP1 by binding to TRAF-2 and conferring E3 ligase activity, thereby activating the NF- κ B pathway (Alvarez *et al.*, 2010). The findings also contrast with Jeong *et al.* (2015), who showed that the activation of SK1 using a novel synthetic SK1 activator, (S)-methyl 2-(hexanamide)-3-(4-hydroxyphenyl) propanoate (MHP), improves epidermal innate immunity via the S1P-stimulated production of the antimicrobial peptide cathelicidin (CAMP). In this case, MHP did not reduce activity of S1P lyase that is known to hydrolyse S1P, but instead increased S1P synthesis. Moreover, exogenous MHP has been shown to stimulate production of CAMP mRNA and protein in keratinocytes while SK1 siRNA blocked these responses. Importantly in the context of the current study,

MHP activates the NF- κ B pathway, assessed through nuclear translocation of NF- κ B. Moreover, pre-treatment of cells with a specific SK1 inhibitor (SK1-I) reduced MHP-promoted nuclear translocation of NF- κ B, and considerably decreased the MHP-stimulated production of CAMP (Jeong *et al.*, 2015). In contrast, Etemadi and colleagues (2015) provide support for the current findings by showing that TRAF2 regulates the TNF α signalling and NF- κ B activation independently of SK1 in keratinocytes (Etemadi *et al.*, 2015).

There is substantial evidence that NF- κ B is pro-inflammatory. Libermann and Baltimore (1990) showed that NF- κ B is an essential mediator regulating IL-6 gene expression in response to various stimuli in U-937 and HeLa cells and that alternative inducible enhancer elements regulate the IL-6 gene in a cell-specific manner. Hence mutations in the binding site of NF- κ B eliminated the induction of IL-6 in U-937 cells in response to TNF α , LPS, phytohemagglutinin (PHA), or double-stranded RNA poly (IC) (Libermann and Baltimore, 1990). Similarly, the findings of the current study show that SK2 acts as pro-inflammatory enzyme and SK2 inhibitors are therefore potentially of benefit as anti-inflammatory agents. The findings are consistent with a study by Antoon and colleagues (2011) which reported that selective inhibition of SK2 using the SK2 inhibitor ABC294640 decreased breast cancer chemo-resistance by reducing TNF α -stimulated NF- κ B transcriptional regulation in MCF-7TN-R cells. In this case, S1P stimulates activation of PI3K/Akt pathway and Akt promotes p65 phosphorylation on S536 (Antoon *et al.*, 2011). ABC294640 was shown to inhibit S1P-mediated activation of the Akt pathway and to therefore, reduce levels of phosphorylated p65 to eliminate transcriptional activity.

However, these effects occur independently of I κ B phosphorylation (Antoon *et al.*, 2011). Therefore, this molecular interaction might differ from the current findings showing that ABC294640 inhibited the TNF α -induced degradation of I κ B.

The engagement of SK1 with the different SK inhibitors is evidenced by the proteasomal degradation of SK1 in keratinocytes (Figure 5.1). There is correlation with the K_i for inhibition of SK1 catalytic activity by SK1 inhibitors used in this study, suggesting that they bind directly to SK1 to induce a conformational change that enables ubiquitination and proteasomal degradation of SK1. On the other hand, the SK2 selective inhibitors ABC294640 (25 μ M), K145 (10 μ M), and ROME (10 μ M) did not promote the degradation of SK1 (Figure 5.1), which suggests that the specificity of these compounds for SK2-over-SK1 is maintained in keratinocytes. The S1P produced by SK1 is suggested to be released from cells via an autocrine manner in order to activate S1P receptors. In addition to the intracellular effects of S1P, an autocrine S1P signalling loop is known to enhance the activation of the NF- κ B signalling pathway and survival (Blom *et al.*, 2010). However, this does not appear to be the case in TNF α -stimulated keratinocytes as the nanomolar potent SK1 inhibitor PF-543 failed to affect NF- κ B signalling at concentrations known to inhibit SK1 activity. A reduction in NF- κ B transcriptional activity was observed at higher concentrations of PF-543 (20 μ M), well above the K_i for PF-543 (K_i 4 nM) (Schnute *et al.*, 2012). Additionally, FTY720 which is likely phosphorylated to FTY720-P, was expected to stimulate degradation of I κ B through a receptor-dependent mechanism. However, this was not the case here. Indeed, FTY720 failed to promote or reverse I κ B degradation and which is at odds with its ability of to inhibit NF- κ B

transcriptional activity. It should be noted that FTY720 is also an SK1 inhibitor (Vessey *et al.*, 2007; Tonelli *et al.*, 2010) at μM concentrations, but this is unlikely to be the mechanism of action here due to the inability of low concentrations of PF-543 to modulate I κ B degradation. In this case, Hait and colleagues (2015) have shown that FTY720-P is an inhibitor of HDAC1/2 that regulates transcriptional activity by maintaining histone acetylation, and this might explain the effect of FTY720 on NF- κ B transcriptional activity (Hait *et al.*, 2015).

SK inhibitors have been also shown to reduce transcriptional activity of AP-1. However, the differential effects of these inhibitors in terms of the JNK pathway suggest that their actions on AP-1 transcriptional activity are likely, mediated through SK-independent pathways in keratinocytes. A recent study by Zhou *et al.* (2018) showed that targeting SK2 with ABC294640 reduced the cellular growth of human skin squamous cell carcinoma (SCC) through the activation of JNK, the accumulation of Cer, and the inhibition of S1P and Akt-S6K1 (Zhou *et al.*, 2018). In this case, the inhibition of JNK with SP600125 has been shown to alleviate skin SCC cell apoptosis by ABC294640 (Zhou *et al.*, 2018). In addition, Cer has previously been shown to activate JNK to promote cell apoptosis through thioredoxin-interacting protein-mediated pathway and JNK silencing or mutation significantly reduced Cer-induced cells apoptosis (Chen *et al.*, 2008). Another study showed that a novel SK1 selective inhibitor, SKI-178, promoted the apoptosis of human acute myeloid leukemia (AML) cell lines via a JNK- and CDK1-dependent pathway required to induce apoptosis (Dick *et al.*, 2015). Indeed these studies showed that inhibition of SK1 or SK2 activity stimulates the pro-apoptotic JNK pathway.

However, previous studies showed that JNK has pro- or anti-apoptotic functions, depending on the nature of the death stimulus, duration of JNK activation, cell type and activity of other signalling pathways (Jing and Anning, 2005). Although numerous studies showed that JNK can function as a pro-apoptotic kinase (Bruckner *et al.*, 2001; Lin, 2003; Chen, 2012; Pinal *et al.*, 2019), various others showed that it can function as pro-survival (Gururajan *et al.*, 2005; Ma *et al.*, 2012; Wu *et al.*, 2019) and as evidenced in Chapter 3 by the finding that SKi stimulated pro-survival JNK through the action of polyubiquitinated forms of Degs1 (Alsanafi *et al.*, 2018). However, in the current study, significant inhibition of PMA-stimulated activation of P-p46-JNK signalling was observed when NCTC-AP1 cells treated with FTY720 (10 μ M) or the SK2 inhibitors ABC294640 (25 μ M) and K145 (10 μ M). This was correlated with a reduction in PMA-induced AP1 transcriptional activity, although JNK was shown here to have a very minimal role in regulating AP-1.

ABC294640 (25 μ M) was the only inhibitor to significantly reduce the PMA-stimulated activation of ERK1/2 and, in this case, it is possible that ERK1/2 could be a relevant regulator of AP-1 signalling in these cells. This requires further investigation to identify the main mechanism regulating AP-1 signalling/transcriptional activity in these cells. A previous study conducted by Su and colleagues (1994) proposed that S1P and sphingosine stimulate the DNA binding activity of AP-1 in quiescent Swiss 3T3 fibroblasts and this was inhibited by the SK inhibitor DL-*threo*-dihydrosphingosine (Su *et al.*, 1994). However, the latter compound is also a PKC inhibitor and, therefore we cannot exclude action on this target (Tolan *et al.*, 1996).

In conclusion, the findings of the current study indicate that the differential effects of SK inhibitors on signalling of JNK/ERK-1/2 and the transcriptional activity of AP-1 are likely explained by 'off-target' effects. This is based on the finding that SKi, K145 and ABC294640 have been shown to inhibit SK2 yet exhibit differential effects on JNK signalling. The results also indicate that SK2 might be involved in the signalling and transcriptional regulation of NF- κ B in keratinocytes. These findings suggest that SK2 might be a pharmacological target to treat skin-associated inflammatory disorders.

CHAPTER 6:
GENERAL DISCUSSION AND
FUTURE DIRECTIONS

CHAPTER 6: GENERAL DISCUSSION AND FUTURE DIRECTIONS

6.1 GENERAL DISCUSSION

Sphingolipids are a class of lipids commonly found in cell membranes which have essential roles in signal transduction and cell-cell communication. Sphingolipids are able to trigger functional changes through regulation of their levels or structural membrane changes or protein signalling networks. Sphingolipids are critical and ubiquitous mediators of cellular function and any abnormalities in sphingolipid signalling either due to changes in their quantity, quality or localisation have been implicated in various pathological states (Hannun and Obeid, 2008). Vital enzymes in the sphingolipid signalling pathway including dihydroceramide desaturase (Dggs1) and sphingosine kinases (SK1 and SK2) are responsible for formation of essential bioactive lipids including Cer and S1P. A significant body of evidence has implicated Dggs1 and SKs in autophagic, apoptotic, or proliferative cell responses that are relevant to diseases, including cancer. S1P function is through activation of five G protein-coupled receptors S1P₁₋₅ or intracellularly through binding to proteins, such as HDAC1/2 and TRAF2 to stimulate cell responses (Blaho and Hla, 2014; Hait *et al.*, 2009). Sphingolipid metabolism is a complex process, although major advances have been made in deciphering the different functions of various sphingolipids. However, there is still much to learn (Hannun and Obeid, 2018). In this respect, there is considerable controversy in literature regarding the role of Dggs1 in promoting cell survival/apoptosis, as reviewed in Siddique *et al.* (2015). This provided the impetus to investigate the role and inter-connection of Dggs1 and SKs in regulating cell survival (Chapter 3). Since SKs were known to promote p53-

mediated cell death, the study next (Chapter 4) examined the role of SKs in regulating p53-mediated cell death. Lastly (Chapter 5) the role of SKs in regulating inflammation-based transcriptional factors in keratinocytes was studied due to the controversial reports regarding the role of SK1 in regulating NF- κ B signaling, an important pro-inflammatory pathway in disease.

In Chapter 3, the main finding was that Dags1 undergoes polyubiquitination in response to the SK inhibitor, SKi [2-(*p*-hydroxyanilino)-4-(*p*-chlorophenyl)thiazole] or the Dags1 inhibitor fenretinide. It was also found that the polyubiquitination of Dags1 is linked with the activation of pro-survival pathways, p38 MAPK/c-Jun N-terminal kinase (JNK), and X-box protein 1s (XBP-1s) through a mechanism that involves oxidative stress, and Mdm2 (E3 ligase) in HEK293T cells. In contrast, the SK inhibitor, ABC294640 [3-(4-chlorophenyl)-adamantane-1-carboxylic acid (pyridin-4-ylmethyl)amide] (25 to 50 μ M), did not promote polyubiquitination of Dags1 and appears to use the native form (by substrate induction) to stimulate apoptosis of HEK293T cells possibly through enhanced *de novo* synthesis of Cer. These novel findings are the first to show that the polyubiquitination of Dags1 changes the function of the enzyme from being a pro-apoptotic to pro-survival. These important findings provide clarity to the controversial reports concerning pro-survival *versus* apoptotic functions of the enzyme described within literature and call for a reevaluation of the ubiquitination status of Dags1 in the different cell types studied within the literature. In addition, these novel findings may provide a worthwhile therapeutic approach for various diseases that involve sphingolipids, such as cancers or cardiovascular and metabolic disorders, by use of compounds that

promote the ubiquitin-proteasomal degradation of Dggs1. For example, ceramide has a significant role in cardiovascular diseases and metabolic syndromes (Summers, 2018) and plasma ceramide species have been shown to be elevated in patients with obesity, T2DM, or hepatic stenosis and this was linked to the severity of insulin resistance in these patients (Haus *et al.*, 2009; Chaurasia *et al.*, 2019). Indeed, the depletion of intracellular levels of ceramide has been proposed to represent an effective therapeutic strategy for treatment of obesity and T2DM (Bellini *et al.*, 2015), since there is substantial evidence that ceramide synthesis is upregulated in adipose tissue during inflammation (Glass and Olefsky, 2012; Kang *et al.*, 2013). This was established when the inflammatory mediator TNF α was administered intraperitoneally in C57/BL6 mice to stimulate ceramide synthesis in adipose tissue via a mechanism involving enhanced expression of nSMase, aSMase and SPT (Samad *et al.*, 2006). Additionally, pro-inflammatory lipids, such as lipopolysaccharides (LPS) and palmitate, stimulate TLR4/IKK β signalling and promote the expression of SPT2, CerS1, CerS2 and CerS6 and Dggs1. These changes are associated with ceramide induced insulin resistance in C₂C₁₂ myotubes (Holland *et al.*, 2011). Therefore, inhibition of main enzymes (e.g. Dggs1) that directly catalyse synthesis of ceramides effectively enhances insulin sensitivity (Fang *et al.*, 2019). The deletion of Dggs1 gene has also been shown to induce both anabolic and catabolic signalling pathways (Siddique *et al.*, 2013). These findings can be potentially explained by the existence of two populations of Dggs1 e.g. native and polyubiquitinated forms, with opposing actions (Fang *et al.*, 2019). Thus, the native Dggs1 acts to block Akt/PKB signalling via a ceramide-dependent mechanism. In this case, the deletion of Dggs1 promotes anabolic Akt signalling and

sensitisation of cells to insulin. In contrast, the polyubiquitinated Degr1 are associated with positive regulation of p38 MAPK, which was recently shown to inhibit autophagy (He *et al.*, 2018). These polyubiquitinated forms of Degr1 might be relocalised to specialised lipid micro-domains that could access specific dihydroceramides. Gene deletion of Degr1 will remove both native and polyubiquitinated forms to induce catabolic autophagy as a consequence of the relief of inhibition mediated by p38 MAPK. In addition, the loss of the native form might have a predominant effect in promoting cell survival (Fang *et al.*, 2019). Therefore, targeting a specific population of Degr1 could be a promising pharmacological intervention to treat metabolic and cardiovascular disorders.

The study next investigated p53 regulation in the context of SKs, JNK/p38 MAPK signalling and XBP-1s. SKi promoted ubiquitination of p53 to induce the formation of two higher molecular mass proteins (63 and 90 kDa). SK1 siRNA promoted SKi-induced p63/p90 formation while SK2 or Degr1 siRNAs failed to modulate these responses. These findings suggest that SK1 is a negative regulator of the conversion, which might normally function to inactivate p53 and prevent apoptosis. siRNA mediated elimination of SK1 promoted the activation of p38 MAPK/JNK pathways in response to SKi, suggesting that SK1 also opposes these pro-survival pathways in HEK293T cells. These effects are correlated with a decrease in the intracellular levels of S1P and an increase in Sph suggesting that SK1 might be pro-apoptotic in this context. In cells treated with ABC294640 (which promotes apoptosis), a very weak conversion of p53 to p63 and p90 was found and which might reflect a failure to activate the protective mechanism. Thus SK1 dampens p38

MAPK/JNK activation and p63/p90 formation to restrict pro-survival responses in HEK293T cells. In contrast, ABC294640, which fails to promote the ubiquitination of Degs1 and p63/p90 formation increased ceramide levels and induced PARP cleavage, and decreased DNA synthesis in HEK293T cells. The mechanisms by which ceramide induces cell apoptosis include activation of cathepsin D and protein phosphatase PP2A (Kuzmenko and Klimentyeva, 2016) and the formation of pores in the outer mitochondrial membrane regulated by Bax (Ganesan *et al.*, 2010). In addition, ceramide can promote autophagy/mitophagy linked with cell death (Ganesan *et al.*, 2010). Since ceramide is composed of many chemically distinct species that vary widely, primarily in their N-linked acyl chain length and saturation, their roles in regulating cell biology is complicated and poorly understood (Hannun and Obeid, 2011). Different ceramides have distinct signalling properties. For instance, long chain ceramides (e.g. C₁₆-Cer) are pro-apoptotic, whereas very long chain ceramides (e.g. C₂₄-Cer) can function in a pro-survival context, although this differs according to cell type (Groesch *et al.*, 2012). For instance, resveratrol, a natural phenol, has been shown to induce ER stress, autophagy and apoptotic UPR through a mechanism that involves an increase in C₁₆-ceramide in nasopharyngeal carcinoma (Chow *et al.*, 2014). Indeed, SPT inhibition has been shown to reduce resveratrol-induced apoptosis and ER expansion associated with ER stress (Chow *et al.*, 2014). These findings implicate C₁₆-ceramide as having a pro-apoptotic function.

In this study, the MG132-induced increase in the expression of the pro-survival protein XBP-1s was enhanced by SKi via a mechanism involving polyubiquitinated

Degs1. Knocking down SK2 with gene specific siRNA reduced MG132/SK1-stimulated XBP-1s levels while knocking down p53 promoted this effect. Under these conditions, SK2 is positively involved in the regulation of XBP-1s expression and behaves as a pro-survival signal. In addition, sphingolipids measurements showed that SK2 siRNA increased Cers levels and which is likely to promote apoptosis, thereby reinforcing the idea that SK2 is a pro-survival enzyme in HEK293T cells, consistent with SK2 siRNA reducing expression of XBP-1s. The p53 dependent regulation of XBP-1s is mediated by the native form of p53, i.e. native p53 restricts the formation of pro-survival XBP-1s. Collectively, p53 mediates MG132-induced cell death and this appears to be countered by SK2. These novel findings suggest that the SK1 and SK2 have opposing roles in relation to p53-mediated apoptosis of HEK293T cells.

Research conducted in Chapter 5 explored the role of SKs in regulating inflammation-based nuclear factor kappa B (NF- κ B) or activator protein-1 (AP-1) transcriptional factors in keratinocytes. The main finding suggests that SK2, but not SK1 is associated with the transcriptional regulation of NF- κ B. Inhibition of inhibitor kappa B (κ B) degradation and transcriptional regulation of NF- κ B in TNF α -stimulated NCTC-NF- κ B cells was evident in response to the SK2 inhibitors, ABC294640 or SKi or K145 or ROME. In contrast, the potent SK1 inhibitor, PF-543 did not inhibit TNF α -promoted κ B degradation and very weakly inhibited transcriptional regulation of NF- κ B at a concentration that is 50-fold higher than the K_i of SK1 inhibition. In contrast, the effect of the sphingosine kinases on transcriptional regulation of activator protein-1 (AP-1) showed that inhibitor-induced

effects were due to modulation of SK-independent signalling pathways. This was based on the finding that the effects of the SK2 inhibitors, ABC294640 or K145 on phorbol myristate acetate (PMA)-induction of JNK and ERK-1/2 levels and AP-1 transcriptional activity were not recapitulated by the SK2 inhibitors, SKi and ROME.

6.2 CONCLUSION AND FUTURE DIRECTIONS

The findings of the current study add knowledge to the role of Degr1, SK1 and SK2 in regulating cell survival/apoptosis. Further investigation is required to assess whether the ubiquitin-proteasomal degradation of Degr1 and SK1 can be exploited to develop novel therapeutic agents used to treat cancer, T2D, and metabolic disorders. In addition, knowledge presented herein highlights SK2 as a promising target for inflammatory skin disease.

CHAPTER 7:
REFERENCES

CHAPTER 7: REFERENCES

- ADACHI, K. & CHIBA, K. 2007. FTY720 story. Its discovery and the following accelerated development of sphingosine 1-phosphate receptor agonists as immunomodulators based on reverse pharmacology. *Perspectives in medicinal chemistry*, 1, 1177391X0700100002.
- ADADA, M. M., CANALS, D., JEONG, N., KELKAR, A. D., HERNANDEZ-CORBACHO, M., PULKOSKI-GROSS, M. J., DONALDSON, J. C., HANNUN, Y. A. & OBEID, L. M. 2015. Intracellular sphingosine kinase 2-derived sphingosine-1-phosphate mediates epidermal growth factor-induced ezrin-radixin-moesin phosphorylation and cancer cell invasion. *The FASEB Journal*, 29, 4654-4669.
- ADADA, M. M., ORR-GANDY, K. A., SNIDER, A. J., CANALS, D., HANNUN, Y. A., OBEID, L. M. & CLARKE, C. J. 2013. Sphingosine kinase 1 regulates tumor necrosis factor-mediated RANTES induction through p38 mitogen-activated protein kinase but independently of nuclear factor κ B activation. *Journal of Biological Chemistry*, 288, 27667-27679.
- ADAMS, D. R., PYNE, S. & PYNE, N. J. 2016. Sphingosine kinases: emerging structure-function insights. *Trends in biochemical sciences*, 41, 395-409.
- ALBERTS, B., JOHNSON, A. & LEWIS, J. 2008. *Molecular Biology of the Cell*, New York, NY, USA, Garland Science.
- ALLARD, S. T. & KOPISH, K. 2008. Luciferase reporter assays: powerful, adaptable tools for cell biology research. *Cell Notes*, 21, 23-26.
- ALLENDE, M. L., SASAKI, T., KAWAI, H., OLIVERA, A., MI, Y., VAN ECHTEN-DECKERT, G., HAJDU, R., ROSENBAACH, M., KEOHANE, C. A. & MANDALA, S. 2004. Mice deficient in sphingosine kinase 1 are rendered lymphopenic by FTY720. *Journal of Biological Chemistry*.
- ALSANAFI, M., KELLY, S. L., JUBAIR, K., MCNAUGHTON, M., TATE, R. J., MERRILL, A. H., PYNE, S. & PYNE, N. J. 2018. Native and polyubiquitinated forms of dihydroceramide desaturase are differentially linked to human embryonic kidney cell survival. *Molecular and cellular biology*, 38, e00222-18.
- ALVAREZ, S. E., HARIKUMAR, K. B., HAIT, N. C., ALLEGOOD, J., STRUB, G. M., KIM, E. Y., MACEYKA, M., JIANG, H., LUO, C. & KORDULA, T. 2010. Sphingosine-1-phosphate is a missing cofactor for the E3 ubiquitin ligase TRAF2. *Nature*, 465, 1084.
- AMERIK, A. Y. & HOCHSTRASSER, M. 2004. Mechanism and function of deubiquitinating enzymes. *Biochimica et Biophysica Acta (BBA)-Molecular Cell Research*, 1695, 189-207.
- ANASTASIADOU, S. & KNÖLL, B. 2016. The multiple sclerosis drug fingolimod (FTY720) stimulates neuronal gene expression, axonal growth and regeneration. *Experimental neurology*, 279, 243-260.
- ANDO, K., KERNAN, J. L., LIU, P. H., SANDA, T., LOGETTE, E., TSCHOPP, J., LOOK, A. T., WANG, J., BOUCHIER-HAYES, L. & SIDI, S. 2012. PIDD death-domain phosphorylation by ATM controls prodeath versus prosurvival PIDDosome signaling. *Molecular cell*, 47, 681-693.

- ANGEL, P., IMAGAWA, M., CHIU, R., STEIN, B., IMBRA, R. J., RAHMSDORF, H. J., JONAT, C., HERRLICH, P. & KARIN, M. 1987. Phorbol ester-inducible genes contain a common cis element recognized by a TPA-modulated trans-acting factor. *Cell*, 49, 729-739.
- ANGEL, P. & KARIN, M. 1991. The role of Jun, Fos and the AP-1 complex in cell-proliferation and transformation. *Biochimica et Biophysica Acta (BBA)-Reviews on Cancer*, 1072, 129-157.
- ANTOON, J. W., WHITE, M. D., BUROW, M. E. & BECKMAN, B. S. 2012. Dual inhibition of sphingosine kinase isoforms ablates TNF-induced drug resistance. *Oncology reports*, 27, 1779-1786.
- ANTOON, J. W., WHITE, M. D., MEACHAM, W. D., SLAUGHTER, E. M., MUIR, S. E., ELLIOTT, S., RHODES, L. V., ASHE, H. B., WIESE, T. E. & SMITH, C. D. 2010. Antiestrogenic effects of the novel sphingosine kinase-2 inhibitor ABC294640. *Endocrinology*, 151, 5124-5135.
- ANTOON, J. W., WHITE, M. D., SLAUGHTER, E. M., DRIVER, J. L., KHALILI, H. S., ELLIOTT, S., SMITH, C. D., BUROW, M. E. & BECKMAN, B. S. 2011. Targeting NFκB mediated breast cancer chemoresistance through selective inhibition of sphingosine kinase-2. *Cancer biology & therapy*, 11, 678-689.
- APRAIZ, A., IDKOWIAK-BALDYS, J. K., BOYANO, M. D., PÉREZ-YARZA, G., HANNUN, Y. A. & ASUMENDI, A. 2011. Evaluation of bioactive sphingolipids in 4-HPR-resistant leukemia cells. *BMC cancer*, 11, 477.
- ASHER, G., LOTEM, J., KAMA, R., SACHS, L. & SHAUL, Y. 2002. NQO1 stabilizes p53 through a distinct pathway. *Proceedings of the National Academy of Sciences*, 99, 3099-3104.
- ASLE-ROUSTA, M., KOLAHDOOZ, Z., ORYAN, S., AHMADIANI, A. & DARGAHI, L. 2013. FTY720 (Fingolimod) Attenuates Beta-amyloid Peptide (Aβ 42)-Induced Impairment of Spatial Learning and Memory in Rats. *Journal of molecular neuroscience*, 50, 524-532.
- AUGUSTIN, M., BAMBERGER, C., PAUL, D. & SCHMALE, H. 1998. Cloning and chromosomal mapping of the human p53-related KET gene to chromosome 3q27 and its murine homolog Ket to mouse chromosome 16. *Mammalian genome*, 9, 899-902.
- AURELIO, L., SCULLINO, C. V., PITMAN, M. R., SEXTON, A., OLIVER, V., DAVIES, L., REBELLO, R. J., FURIC, L., CREEK, D. J. & PITSON, S. M. 2016. From sphingosine kinase to dihydroceramide desaturase: A structure-activity relationship (SAR) study of the enzyme inhibitory and anticancer activity of 4-((4-(4-chlorophenyl) thiazol-2-yl) amino) phenol (SKI-II). *Journal of medicinal chemistry*, 59, 965-984.
- AZZAM, R., HARIRI, F., EL-HACHEM, N., KAMAR, A., DBAIBO, G., NEMER, G. & BITAR, F. 2013. Regulation of de novo ceramide synthesis: the role of dihydroceramide desaturase and transcriptional factors NFATC and Hand2 in the hypoxic mouse heart. *DNA and cell biology*, 32, 310-319.
- BAJWA, A., HUANG, L., KURMAEVA, E., YE, H., DONDETI, K. R., CHROSCICKI, P., FOLEY, L. S., BALOGUN, Z. A., ALEXANDER, K. J. & PARK, H. 2017. Sphingosine kinase 2 deficiency attenuates kidney fibrosis via IFN-γ. *Journal of the American Society of Nephrology*, 28, 1145-1161.

- BAKER, D. A., BARTH, J., CHANG, R., OBEID, L. M. & GILKESON, G. S. 2010. Genetic sphingosine kinase 1 deficiency significantly decreases synovial inflammation and joint erosions in murine TNF- α -induced arthritis. *The Journal of Immunology*, 185, 2570-2579.
- BAKER, S. J., FEARON, E. R., NIGRO, J. M., PREISINGER, A., JESSUP, J., LEDBETTER, D., BARKER, D., NAKAMURA, Y., WHITE, R. & VOGELSTEIN, B. 1989. Chromosome 17 deletions and p53 gene mutations in colorectal carcinomas. *Science*, 244, 217-221.
- BANERJEE, A., LANG, J. Y., HUNG, M.-C., SENGUPTA, K., BANERJEE, S. K., BAKSI, K. & BANERJEE, D. K. 2011. Unfolded protein response is required in nu/nu mice microvasculature for treating breast tumor with tunicamycin. *Journal of Biological Chemistry*, jbc. M110. 169771.
- BARBOUR, M., MCNAUGHTON, M., BOOMKAMP, S. D., MACRITCHIE, N., JIANG, H. R., PYNE, N. J. & PYNE, S. 2017. Effect of sphingosine kinase modulators on interleukin-1 β release, sphingosine 1-phosphate receptor 1 expression and experimental autoimmune encephalomyelitis. *British journal of pharmacology*, 174, 210-222.
- BARNES, P. J. 2015. Mechanisms of development of multimorbidity in the elderly. *European Respiratory Journal*, ERJ-02297-2014.
- BARR, R. K., LYNN, H. E., MORETTI, P. A., KHEW-GOODALL, Y. & PITSON, S. M. 2008. Deactivation of sphingosine kinase 1 by protein phosphatase 2A. *Journal of Biological Chemistry*, 283, 34994-35002.
- BASU, J. & LI, Z. 1998. The Des-1 protein, required for central spindle assembly and cytokinesis, is associated with mitochondria along the meiotic spindle apparatus and with the contractile ring during male meiosis in *Drosophila melanogaster*. *Molecular and General Genetics MGG*, 259, 664-673.
- BAYRAKTAR, O., OZKIRIMLI, E. & ULGEN, K. 2017. Sphingosine kinase 1 (SK1) allosteric inhibitors that target the dimerization site. *Computational biology and chemistry*, 69, 64-76.
- BEG, A., RUBEN, S., SCHEINMAN, R., HASKILL, S., ROSEN, C. & BALDWIN, A. S. 1992. I kappa B interacts with the nuclear localization sequences of the subunits of NF-kappa B: a mechanism for cytoplasmic retention. *Genes & development*, 6, 1899-1913.
- BEHRANGI, N., FISCHBACH, F. & KIPP, M. 2019. Mechanism of Siponimod: Anti-Inflammatory and Neuroprotective Mode of Action. *Cells*, 8, 24.
- BELJANSKI, V., KNAAK, C. & SMITH, C. D. 2010. A novel sphingosine kinase inhibitor induces autophagy in tumor cells. *Journal of Pharmacology and Experimental Therapeutics*, 333, 454-464.
- BELJANSKI, V., LEWIS, C. S. & SMITH, C. D. 2011. Antitumor activity of sphingosine kinase 2 inhibitor ABC294640 and sorafenib in hepatocellular carcinoma xenografts. *Cancer biology & therapy*, 11, 524-534.
- BELLINI, L., CAMPANA, M., MAHFOUZ, R., CARLIER, A., VÉRET, J., MAGNAN, C., HAJDUCH, E. & LE STUNFF, H. 2015. Targeting sphingolipid metabolism in the treatment of obesity/type 2 diabetes. *Expert opinion on therapeutic targets*, 19, 1037-1050.

- BENETTI, R., DEL SAL, G., MONTE, M., PARONI, G., BRANCOLINI, C. & SCHNEIDER, C. 2001. The death substrate Gas2 binds m-calpain and increases susceptibility to p53-dependent apoptosis. *The EMBO Journal*, 20, 2702-2714.
- BENNETT, M. K., WALLINGTON-BEDDOE, C. T. & PITSON, S. M. 2019. Sphingolipids and the unfolded protein response. *Biochimica et Biophysica Acta (BBA)-Molecular and Cell Biology of Lipids*.
- BERDYSHEV, E. V., GORSHKOVA, I., SKOBELEVA, A., BITTMAN, R., LU, X., DUDEK, S. M., MIRZAPOIAZOVA, T., GARCIA, J. G. & NATARAJAN, V. 2009. FTY720 inhibits ceramide synthases and upregulates dihydrosphingosine-1-phosphate formation in human lung endothelial cells. *Journal of Biological Chemistry*.
- BIDÈRE, N., LORENZO, H. K., CARMONA, S., LAFORGE, M., HARPER, F., DUMONT, C. & SENIK, A. 2003. Cathepsin D triggers Bax activation, resulting in selective apoptosis-inducing factor (AIF) relocation in T lymphocytes entering the early commitment phase to apoptosis. *Journal of Biological Chemistry*, 278, 31401-31411.
- BIELAWSKA, A., CRANE, H. M., LIOTTA, D., OBEID, L. M. & HANNUN, Y. A. 1993. Selectivity of ceramide-mediated biology. Lack of activity of erythro-dihydroceramide. *Journal of Biological Chemistry*, 268, 26226-26232.
- BIKMAN, B. T., GUAN, Y., SHUI, G., SIDDIQUE, M. M., HOLLAND, W. L., KIM, J. Y., FABRIAS, G., WENK, M. R. & SUMMERS, S. A. 2012. Fenretinide prevents lipid-induced insulin resistance by blocking ceramide biosynthesis. *Journal of Biological Chemistry*, jbc.M112.359950.
- BILLICH, A., BORNANCIN, F., DÉVAY, P., MECHTCHERIAKOVA, D., URTZ, N. & BAUMRUKER, T. 2003. Phosphorylation of the immunomodulatory drug FTY720 by sphingosine kinases. *Journal of Biological Chemistry*, 278, 47408-47415.
- BLAHO, V. A. & HLA, T. 2014. An update on the biology of sphingosine 1-phosphate receptors. *Journal of lipid research*, 55, 1596-1608.
- BLOM, T., BERGELIN, N., MEINANDER, A., LÖF, C., SLOTTE, J. P., ERIKSSON, J. E. & TÖRNQUIST, K. 2010. An autocrine sphingosine-1-phosphate signaling loop enhances NF- κ B-activation and survival. *BMC cell biology*, 11, 45.
- BOKOCH, G. M., REILLY, A. M., DANIELS, R. H., KING, C. C., OLIVERA, A., SPIEGEL, S. & KNAUS, U. G. 1998. A GTPase-independent Mechanism of p21-activated Kinase Activation REGULATION BY SPHINGOSINE AND OTHER BIOLOGICALLY ACTIVE LIPIDS. *Journal of Biological Chemistry*, 273, 8137-8144.
- BONIZZI, G., BEBIEN, M., OTERO, D. C., JOHNSON- VROOM, K. E., CAO, Y., VU, D., JEGGA, A. G., ARONOW, B. J., GHOSH, G. & RICKERT, R. C. 2004. Activation of IKK α target genes depends on recognition of specific κ B binding sites by RelB: p52 dimers. *The EMBO Journal*, 23, 4202-4210.
- BONIZZI, G. & KARIN, M. 2004. The two NF- κ B activation pathways and their role in innate and adaptive immunity. *Trends in immunology*, 25, 280-288.
- BOSSIS, G., FERRARA, P., ACQUAVIVA, C., JARIEL-ENCONTRE, I. & PIECHACZYK, M. 2003. c-Fos proto-oncoprotein is degraded by the proteasome

- independently of its own ubiquitylation in vivo. *Molecular and cellular biology*, 23, 7425-7436.
- BOSSIS, G., MALNOU, C. E., FARRAS, R., ANDERMARCHER, E., HIPSKIND, R., RODRIGUEZ, M., SCHMIDT, D., MULLER, S., JARIEL-ENCONTRE, I. & PIECHACZYK, M. 2005. Down-regulation of c-Fos/c-Jun AP-1 dimer activity by sumoylation. *Molecular and cellular biology*, 25, 6964-6979.
- BOURBON, N. A., SANDIRASEGARANE, L. & KESTER, M. 2002. Ceramide-induced Inhibition of Akt Is Mediated through Protein Kinase C ζ IMPLICATIONS FOR GROWTH ARREST. *Journal of Biological Chemistry*, 277, 3286-3292.
- BOURDON, J.-C., RENZING, J., ROBERTSON, P., FERNANDES, K. & LANE, D. 2002. Scotin, a novel p53-inducible proapoptotic protein located in the ER and the nuclear membrane. *J Cell Biol*, 158, 235-246.
- BOURS, V., BONIZZI, G., BENTIRES-ALJ, M., BUREAU, F., PIETTE, J., LEKEUX, P. & MERVILLE, M.-P. 2000. NF- κ B activation in response to toxic and therapeutical agents: role in inflammation and cancer treatment. *Toxicology*, 153, 27-38.
- BREEN, P., JOSEPH, N., THOMPSON, K., KRAVEKA, J. M., GUDZ, T. I., LI, L., RAHMANIYAN, M., BIELAWSKI, J., PIERCE, J. S. & VAN BUREN, E. 2013. Dihydroceramide desaturase knockdown impacts sphingolipids and apoptosis after photodamage in human head and neck squamous carcinoma cells. *Anticancer research*, 33, 77-84.
- BRESLOW, D. K., COLLINS, S. R., BODENMILLER, B., AEBERSOLD, R., SIMONS, K., SHEVCHENKO, A., EJSING, C. S. & WEISSMAN, J. S. 2010. Orm family proteins mediate sphingolipid homeostasis. *Nature*, 463, 1048.
- BRIDGES, D. & MOORHEAD, G. B. 2005. 14-3-3 proteins: a number of functions for a numbered protein. *Sci. STKE*, 2005, re10-re10.
- BRINKMANN, V. 2007. Sphingosine 1-phosphate receptors in health and disease: mechanistic insights from gene deletion studies and reverse pharmacology. *Pharmacology & therapeutics*, 115, 84-105.
- BRITTEN, C. D., GARRETT-MAYER, E., CHIN, S. H., SHIRAI, K., OGRETMEN, B., BENTZ, T. A., BRISENDINE, A., ANDERTON, K., CUSACK, S. L. & MAINES, L. W. 2017. A phase I study of ABC294640, a first-in-class sphingosine kinase-2 inhibitor, in patients with advanced solid tumors. *Clinical Cancer Research*.
- BRODIE, C. & BLUMBERG, P. 2003. Regulation of cell apoptosis by protein kinase c δ . *Apoptosis*, 8, 19-27.
- BRUCKNER, S. R., TAMMARIELLO, S. P., KUAN, C. Y., FLAVELL, R. A., RAKIC, P. & ESTUS, S. 2001. JNK3 contributes to c- Jun activation and apoptosis but not oxidative stress in nerve growth factor- deprived sympathetic neurons. *Journal of neurochemistry*, 78, 298-303.
- BURKHARD, P., STETEFELD, J. & STRELKOV, S. V. 2001. Coiled coils: a highly versatile protein folding motif. *Trends in cell biology*, 11, 82-88.
- BYRDWELL, C. & BORCHMAN, D. 1997. Liquid chromatography/mass-spectrometric characterization of sphingomyelin and dihydrosphingomyelin of human lens membranes. *Ophthalmic research*, 29, 191-206.

- BYUN, H.-S., PYNE, S., MACRITCHIE, N., PYNE, N. J. & BITTMAN, R. 2013. Novel sphingosine-containing analogues selectively inhibit sphingosine kinase (SK) isozymes, induce SK1 proteasomal degradation and reduce DNA synthesis in human pulmonary arterial smooth muscle cells. *Medchemcomm*, 4, 1394-1399.
- CAMP, S. M., CHIANG, E. T., SUN, C., USATYUK, P. V., BITTMAN, R., NATARAJAN, V., GARCIA, J. G. & DUDEK, S. M. 2016. Pulmonary endothelial cell barrier enhancement by novel FTY720 analogs: methoxy-FTY720, fluoro-FTY720, and β -glucuronide-FTY720. *Chemistry and physics of lipids*, 194, 85-93.
- CARROLL, B. L., BONICA, J., SHAMSEDDINE, A. A., HANNUN, Y. A. & OBEID, L. M. 2018. A role for caspase- 2 in sphingosine kinase 1 proteolysis in response to doxorubicin in breast cancer cells—implications for the CHK1- suppressed pathway. *FEBS open bio*, 8, 27-40.
- CASASAMPERE, M., ORDÓÑEZ, Y. F., CASAS, J. & FABRIAS, G. 2017. Dihydroceramide desaturase inhibitors induce autophagy via dihydroceramide-dependent and independent mechanisms. *Biochimica et Biophysica Acta (BBA)-General Subjects*, 1861, 264-275.
- CAUSERET, C., GEERAERT, L., VAN DER HOEVEN, G., MANNAERTS, G. P. & VAN VELDHOVEN, P. P. 2000. Further characterization of rat dihydroceramide desaturase: tissue distribution, subcellular localization, and substrate specificity. *Lipids*, 35, 1117-1125.
- CHALFANT, C. E. & SPIEGEL, S. 2005. Sphingosine 1-phosphate and ceramide 1-phosphate: expanding roles in cell signaling. *J Cell Sci*, 118, 4605-12.
- CHAN, H. & PITSON, S. M. 2013. Post-translational regulation of sphingosine kinases. *Biochimica et Biophysica Acta (BBA)-Molecular and Cell Biology of Lipids*, 1831, 147-156.
- CHAN, S.-W. & EGAN, P. A. 2005. Hepatitis C virus envelope proteins regulate CHOP via induction of the unfolded protein response. *The FASEB journal*, 19, 1510-1512.
- CHAURASIA, B., TIPPETTS, T. S., MONIBAS, R. M., LIU, J., LI, Y., WANG, L., WILKERSON, J. L., SWEENEY, C. R., PEREIRA, R. F. & SUMIDA, D. H. 2019. Targeting a ceramide double bond improves insulin resistance and hepatic steatosis. *Science*, 365, 386-392.
- CHEN, C.-L., LIN, C.-F., CHANG, W.-T., HUANG, W.-C., TENG, C.-F. & LIN, Y.-S. 2008. Ceramide induces p38 MAPK and JNK activation through a mechanism involving a thioredoxin-interacting protein-mediated pathway. *Blood*, 111, 4365-4374.
- CHEN, F. 2012. JNK-induced apoptosis, compensatory growth, and cancer stem cells. *Cancer research*, 72, 379-386.
- CHEN, Q., KANG, J. & FU, C. 2018. The independence of and associations among apoptosis, autophagy, and necrosis. *Signal transduction and targeted therapy*, 3, 18.
- CHEN, Z. J. & SUN, L. J. 2009. Nonproteolytic functions of ubiquitin in cell signaling. *Molecular cell*, 33, 275-286.
- CHENG, E., WEI, M., WEILER, S., FLAVELL, R., MAK, T., LINDSTEN, T. & KORSMEYER, S. 2001. BCL-2, BCL-X (L) sequester BH3 domain-only

- molecules preventing BAX-and BAK-mediated mitochondrial apoptosis. *Molecular cell*, 8, 705.
- CHENG, X., FENG, H., WU, H., JIN, Z., SHEN, X., KUANG, J., HUO, Z., CHEN, X., GAO, H. & YE, F. 2018. Targeting autophagy enhances apatinib-induced apoptosis via endoplasmic reticulum stress for human colorectal cancer. *Cancer letters*, 431, 105-114.
- CHIPUK, J. E., MCSTAY, G. P., BHARTI, A., KUWANA, T., CLARKE, C. J., SISKIND, L. J., OBEID, L. M. & GREEN, D. R. 2012. Sphingolipid metabolism cooperates with BAK and BAX to promote the mitochondrial pathway of apoptosis. *Cell*, 148, 988-1000.
- CHOI, J. W., LEE, C.-W. & CHUN, J. 2008. Biological roles of lysophospholipid receptors revealed by genetic null mice: an update. *Biochimica et Biophysica Acta (BBA)-Molecular and Cell Biology of Lipids*, 1781, 531-539.
- CHOW, S.-E., KAO, C.-H., LIU, Y.-T. A., CHENG, M.-L., YANG, Y.-W., HUANG, Y.-K., HSU, C.-C. & WANG, J.-S. 2014. Resveratrol induced ER expansion and ER caspase-mediated apoptosis in human nasopharyngeal carcinoma cells. *Apoptosis*, 19, 527-541.
- CHRISTOFFERSEN, C., OBINATA, H., KUMARASWAMY, S. B., GALVANI, S., AHNSTRÖM, J., SEVVANA, M., EGERER-SIEBER, C., MULLER, Y. A., HLA, T. & NIELSEN, L. B. 2011. Endothelium-protective sphingosine-1-phosphate provided by HDL-associated apolipoprotein M. *Proceedings of the National Academy of Sciences*, 108, 9613-9618.
- CHUN, J., GOETZL, E. J., HLA, T., IGARASHI, Y., LYNCH, K. R., MOOLENAAR, W., PYNE, S. & TIGYI, G. 2002. International union of pharmacology. XXXIV. Lysophospholipid receptor nomenclature. *Pharmacological reviews*, 54, 265-269.
- CHUN, J. & HARTUNG, H.-P. 2010. Mechanism of action of oral fingolimod (FTY720) in multiple sclerosis. *Clinical neuropharmacology*, 33, 91.
- CHUN, J., HLA, T., LYNCH, K. R., SPIEGEL, S. & MOOLENAAR, W. H. 2010. International union of basic and clinical pharmacology. LXXVIII. Lysophospholipid receptor nomenclature. *Pharmacological reviews*, 62, 579-587.
- CINGOLANI, F., CASASAMPERE, M., SANLLEHÍ, P., CASAS, J., BUJONS, J. & FABRIAS, G. 2014. Inhibition of dihydroceramide desaturase activity by the sphingosine kinase inhibitor SKI II. *Journal of lipid research*, 55, 1711-1720.
- CLARKE, R., COOK, K. L., HU, R., FACEY, C. O., TAVASSOLY, I., SCHWARTZ, J. L., BAUMANN, W. T., TYSON, J. J., XUAN, J. & WANG, Y. 2012. Endoplasmic reticulum stress, the unfolded protein response, autophagy, and the integrated regulation of breast cancer cell fate. *Cancer research*, 72, 1321-1331.
- COLOMBINI, M. 2010. Ceramide channels and their role in mitochondria-mediated apoptosis. *Biochimica et Biophysica Acta (BBA)-Bioenergetics*, 1797, 1239-1244.
- COLOMBINI, M. 2013. Membrane channels formed by ceramide. *Sphingolipids: Basic Science and Drug Development*. Springer.

- CONFORTI, F., WANG, Y., RODRIGUEZ, J. A., ALBEROBELLO, A. T., ZHANG, Y.-W. & GIACCONE, G. 2015. Molecular pathways: anticancer activity by inhibition of nucleocytoplasmic shuttling. *Clinical Cancer Research*, 21, 4508-4513.
- COURTOIS, G. & GILMORE, T. D. 2006. Mutations in the NF-kappaB signaling pathway: implications for human disease. *Oncogene*, 25, 6831-43.
- CREASY, D. M. & COTTRELL, J. S. 2004. Unimod: Protein modifications for mass spectrometry. *Proteomics*, 4, 1534-1536.
- CRIGHTON, D., WILKINSON, S., O'PREY, J., SYED, N., SMITH, P., HARRISON, P. R., GASCO, M., GARRONE, O., CROOK, T. & RYAN, K. M. 2006. DRAM, a p53-induced modulator of autophagy, is critical for apoptosis. *Cell*, 126, 121-134.
- CROKER, B. A., KREBS, D. L., ZHANG, J.-G., WORMALD, S., WILLSON, T. A., STANLEY, E. G., ROBB, L., GREENHALGH, C. J., FÖRSTER, I. & CLAUSEN, B. E. 2003. SOCS3 negatively regulates IL-6 signaling in vivo. *Nature immunology*, 4, 540.
- CUVILLIER, O. 2002. Sphingosine in apoptosis signaling. *Biochimica Et Biophysica Acta (BBA)-Molecular and Cell Biology of Lipids*, 1585, 153-162.
- CUVILLIER, O., NAVA, V., MURTHY, S., EDSALL, L., LEVADE, T., MILSTIEN, S. & SPIEGEL, S. 2001. Sphingosine generation, cytochrome c release, and activation of caspase-7 in doxorubicin-induced apoptosis of MCF7 breast adenocarcinoma cells. *Cell death and differentiation*, 8, 162.
- CUVILLIER, O., PIRIANOV, G., KLEUSER, B., VANEK, P. G., COSO, O. A., GUTKIND, S. & SPIEGEL, S. 1996. Suppression of ceramide-mediated programmed cell death by sphingosine-1-phosphate. *Nature*, 381, 800-803.
- DAI, C. 2014. *p90 and UHRF1, Two Novel Regulators of the p53 Signaling Pathway*. Columbia University.
- DAI, C., TANG, Y., JUNG, S. Y., QIN, J., AARONSON, S. A. & GU, W. 2011. Differential effects on p53-mediated cell cycle arrest vs. apoptosis by p90. *Proceedings of the National Academy of Sciences*, 108, 18937-18942.
- DAUJAT, S., NEEL, H. & PIETTE, J. 2001. MDM2: life without p53. *TRENDS in Genetics*, 17, 459-464.
- DAVAILLE, J., LI, L., MALLAT, A. & LOTERSZTAJN, S. 2002. Sphingosine 1-phosphate triggers both apoptotic and survival signals for human hepatic myofibroblasts. *Journal of Biological Chemistry*, 277, 37323-37330.
- DAVIS, R. J., GIRONES, N. & FAUCHER, M. 1988. Two alternative mechanisms control the interconversion of functional states of the epidermal growth factor receptor. *Journal of Biological Chemistry*, 263, 5373-5379.
- DBAIBO, G. S., PUSHKAREVA, M. Y., RACHID, R. A., ALTER, N., SMYTH, M. J., OBEID, L. M. & HANNUN, Y. A. 1998. p53-dependent ceramide response to genotoxic stress. *The Journal of clinical investigation*, 102, 329-339.
- DE- FREITAS- JUNIOR, J. C. M., BASTOS, L. G., FREIRE- NETO, C. A., ROCHER, B. D., ABDELHAY, E. S. F. W. & MORGADO- DÍAZ, J. A. 2012. N- glycan biosynthesis inhibitors induce in vitro anticancer activity in colorectal cancer cells. *Journal of cellular biochemistry*, 113, 2957-2966.

- DEB, S. P. 2002. Function and dysfunction of the human oncoprotein MDM2. *Front Biosci*, 7, d235-d243.
- DELEO, A. B., JAY, G., APPELLA, E., DUBOIS, G. C., LAW, L. W. & OLD, L. J. 1979. Detection of a transformation-related antigen in chemically induced sarcomas and other transformed cells of the mouse. *Proceedings of the National Academy of Sciences*, 76, 2420-2424.
- DELMAS, D., SOLARY, E. & LATRUFFE, N. 2011. Resveratrol, a phytochemical inducer of multiple cell death pathways: apoptosis, autophagy and mitotic catastrophe. *Current medicinal chemistry*, 18, 1100-1121.
- DEMOLY, P., BASSET-SEGUIN, N., CHANEZ, P., CAMPBELL, A. M., GAUTHIER-ROUVIERE, C., GODARD, P., MICHEL, F. B. & BOUSQUET, J. 1992. C-fos proto-oncogene expression in bronchial biopsies of asthmatics. *American journal of respiratory cell and molecular biology*, 7, 128-128.
- DENG, X., GAO, F. & MAY, W. S. 2009. Protein phosphatase 2A inactivates Bcl2's antiapoptotic function by dephosphorylation and up-regulation of Bcl2-p53 binding. *Blood*, 113, 422-428.
- DENG, X., XIAO, L., LANG, W., GAO, F., RUVOLO, P. & MAY, W. S. 2001. Novel role for JNK as a stress-activated Bcl2 kinase. *Journal of Biological Chemistry*, 276, 23681-23688.
- DEVLIN, C. M., LAHM, T., HUBBARD, W. C., VAN DEMARK, M., WANG, K. C., WU, X., BIELAWSKA, A., OBEID, L. M., IVAN, M. & PETRACHE, I. 2011. Dihydroceramide-based response to hypoxia. *Journal of Biological Chemistry*, 286, 38069-38078.
- DI MENNA, L., MOLINARO, G., DI NUZZO, L., RIOZZI, B., ZAPPULLA, C., POZZILLI, C., TURRINI, R., CARACI, F., COPANI, A. & BATTAGLIA, G. 2013. Fingolimod protects cultured cortical neurons against excitotoxic death. *Pharmacological research*, 67, 1-9.
- DICK, T. E., HENGST, J. A., FOX, T. E., COLLEDGE, A. L., KALE, V. P., SUNG, S.-S., SHARMA, A., AMIN, S., LOUGHRAN, T. P. & KESTER, M. 2015. The apoptotic mechanism of action of the sphingosine kinase 1 selective inhibitor SKI-178 in human acute myeloid leukemia cell lines. *Journal of Pharmacology and Experimental Therapeutics*, 352, 494-508.
- DING, G., SONODA, H., YU, H., KAJIMOTO, T., GOPARAJU, S. K., JAHANGEER, S., OKADA, T. & NAKAMURA, S.-I. 2007. Protein kinase D-mediated phosphorylation and nuclear export of sphingosine kinase 2. *Journal of Biological Chemistry*, 282, 27493-27502.
- DING, W. X. & YIN, X. M. 2004. Dissection of the multiple mechanisms of TNF- α - induced apoptosis in liver injury. *Journal of cellular and molecular medicine*, 8, 445-454.
- DING, X., CHAITEERAKIJ, R., MOSER, C. D., SHALEH, H., BOAKYE, J., CHEN, G., NDZENGUE, A., LI, Y., ZHOU, Y. & HUANG, S. 2016. Antitumor effect of the novel sphingosine kinase 2 inhibitor ABC294640 is enhanced by inhibition of autophagy and by sorafenib in human cholangiocarcinoma cells. *Oncotarget*, 7, 20080.
- DING, X., ZHANG, Y., HUANG, T., XU, G., PENG, C., CHEN, G., KONG, B., FRIESS, H., SHEN, S. & LV, Y. 2019. Targeting sphingosine kinase 2 suppresses cell growth and synergizes with BCL2/BCL-XL inhibitors through NOXA-

- mediated MCL1 degradation in cholangiocarcinoma. *American Journal of Cancer Research*, 9, 546.
- DONEHOWER, L. A., HARVEY, M., SLAGLE, B. L., MCARTHUR, M. J., MONTGOMERY JR, C. A., BUTEL, J. S. & BRADLEY, A. 1992. Mice deficient for p53 are developmentally normal but susceptible to spontaneous tumours. *Nature*, 356, 215.
- DÖTSCH, V., BERNASSOLA, F., COUTANDIN, D., CANDI, E. & MELINO, G. 2010. p63 and p73, the ancestors of p53. *Cold Spring Harbor perspectives in biology*, a004887.
- DUKSIN, D. & MAHONEY, W. 1982. Relationship of the structure and biological activity of the natural homologues of tunicamycin. *Journal of Biological Chemistry*, 257, 3105-3109.
- EFERL, R. & WAGNER, E. F. 2003. AP-1: a double-edged sword in tumorigenesis. *Nature Reviews Cancer*, 3, 859.
- EL-ASSAAD, W., KOZHAYA, L., ARAYSI, S., PANJARIAN, S., BITAR, F. F., BAZ, E., EL-SABBAN, M. E. & DBAIBO, G. S. 2003. Ceramide and glutathione define two independently regulated pathways of cell death initiated by p53 in Molt-4 leukaemia cells. *Biochem. J*, 376, 725-732.
- EL-DEIRY, W. S., KERN, S. E., PIETENPOL, J. A., KINZLER, K. W. & VOGELSTEIN, B. 1992. Definition of a consensus binding site for p53. *Nature genetics*, 1, 45.
- EL-DEIRY, W. S., TOKINO, T., VELCULESCU, V. E., LEVY, D. B., PARSONS, R., TRENT, J. M., LIN, D., MERCER, W. E., KINZLER, K. W. & VOGELSTEIN, B. 1993. WAF1, a potential mediator of p53 tumor suppression. *Cell*, 75, 817-825.
- ELBEIN, A. D. 1981. The tunicamycins—useful tools for studies on glycoproteins. *Trends in Biochemical Sciences*, 6, 219-221.
- ENDO, K., AKIYAMA, T., KOBAYASHI, S. & OKADA, M. 1996. Degenerative spermatocyte, a novel gene encoding a transmembrane protein required for the initiation of meiosis in *Drosophila* spermatogenesis. *Molecular and General Genetics MGG*, 253, 157-165.
- ERDREICH-EPSTEIN, A., TRAN, L. B., BOWMAN, N. N., WANG, H., CABOT, M. C., DURDEN, D. L., VLCKOVA, J., REYNOLDS, C. P., STINS, M. F. & GROSHEN, S. 2002. Ceramide signaling in fenretinide-induced endothelial cell apoptosis. *Journal of Biological Chemistry*, 277, 49531-49537.
- ETEMADI, N., CHOPIN, M., ANDERTON, H., TANZER, M. C., RICKARD, J. A., ABEYSEKERA, W., HALL, C., SPALL, S. K., WANG, B. & XIONG, Y. 2015. TRAF2 regulates TNF and NF- κ B signalling to suppress apoptosis and skin inflammation independently of Sphingosine kinase 1. *Elife*, 4, e10592.
- EVANGELISTI, C., EVANGELISTI, C., TETI, G., CHIARINI, F., FALCONI, M., MELCHIONDA, F., PESSION, A., BERTAINA, A., LOCATELLI, F. & MCCUBREY, J. A. 2014. Assessment of the effect of sphingosine kinase inhibitors on apoptosis, unfolded protein response and autophagy of T-cell acute lymphoblastic leukemia cells; indications for novel therapeutics. *Oncotarget*, 5, 7886.

- FABRIAS, G., MUÑOZ-OLAYA, J., CINGOLANI, F., SIGNORELLI, P., CASAS, J., GAGLIOSTRO, V. & GHIDONI, R. 2012. Dihydroceramide desaturase and dihydrosphingolipids: debutant players in the sphingolipid arena. *Progress in lipid research*, 51, 82-94.
- FANG, S. & WEISSMAN, A. 2004. A field guide to ubiquitylation. *Cellular and molecular life sciences: CMLS*, 61, 1546-1561.
- FANG, Z., PYNE, S. & PYNE, N. J. 2019. Ceramide and sphingosine 1-phosphate in adipose dysfunction. *Progress in lipid research*, 100991.
- FANGER, G. R., GERWINS, P., WIDMANN, C., JARPE, M. B. & JOHNSON, G. L. 1997. MEKKs, GCKs, MLKs, PAKs, TAKs, and tpls: upstream regulators of the c-Jun amino-terminal kinases? *Current opinion in genetics & development*, 7, 67-74.
- FARLEY, A. R. & LINK, A. J. 2009. Identification and quantification of protein posttranslational modifications. *Methods in enzymology*. Elsevier.
- FITZPATRICK, L. R., GREEN, C., FRAUENHOFFER, E. E., FRENCH, K. J., ZHUANG, Y., MAINES, L. W., UPSON, J. J., PAUL, E., DONAHUE, H. & MOSHER, T. J. 2011. Attenuation of arthritis in rodents by a novel orally-available inhibitor of sphingosine kinase. *Inflammopharmacology*, 19, 75-87.
- FRENCH, K. J., SCHRECENGOST, R. S., LEE, B. D., ZHUANG, Y., SMITH, S. N., EBERLY, J. L., YUN, J. K. & SMITH, C. D. 2003. Discovery and evaluation of inhibitors of human sphingosine kinase. *Cancer research*, 63, 5962-5969.
- FRENCH, K. J., ZHUANG, Y., MAINES, L. W., GAO, P., WANG, W., BELJANSKI, V., UPSON, J. J., GREEN, C. L., KELLER, S. N. & SMITH, C. D. 2010. Pharmacology and antitumor activity of ABC294640, a selective inhibitor of sphingosine kinase-2. *Journal of Pharmacology and Experimental Therapeutics*, 333, 129-139.
- FRISZ, J. F., LOU, K., KLITZING, H. A., HANAFIN, W. P., LIZUNOV, V., WILSON, R. L., CARPENTER, K. J., KIM, R., HUTCHEON, I. D. & ZIMMERBERG, J. 2013. Direct chemical evidence for sphingolipid domains in the plasma membranes of fibroblasts. *Proceedings of the National Academy of Sciences*, 110, E613-E622.
- FUCHS, S. Y., ADLER, V., BUSCHMANN, T., YIN, Z., WU, X., JONES, S. N. & RONAI, Z. E. 1998. JNK targets p53 ubiquitination and degradation in nonstressed cells. *Genes & development*, 12, 2658-2663.
- FULDA, S., GORMAN, A. M., HORI, O. & SAMALI, A. 2010. Cellular stress responses: cell survival and cell death. *International journal of cell biology*, 2010.
- FYRST, H. & SABA, J. D. 2010. An update on sphingosine-1-phosphate and other sphingolipid mediators. *Nat Chem Biol*, 6, 489-97.
- GAGLIOSTRO, V., CASAS, J., CARETTI, A., ABAD, J. L., TAGLIAVACCA, L., GHIDONI, R., FABRIAS, G. & SIGNORELLI, P. 2012. Dihydroceramide delays cell cycle G1/S transition via activation of ER stress and induction of autophagy. *The international journal of biochemistry & cell biology*, 44, 2135-2143.
- GALVANI, S., SANSON, M., BLAHO, V. A., SWENDEMAN, S. L., OBINATA, H., CONGER, H., DAHLBÄCK, B., KONO, M., PROIA, R. L. & SMITH, J. D. 2015. HDL-bound sphingosine 1-phosphate acts as a biased agonist for the

- endothelial cell receptor S1P1 to limit vascular inflammation. *Sci. Signal*, 8, ra79-ra79.
- GANDY, K. A. O. & OBEID, L. M. 2013. Targeting the sphingosine kinase/sphingosine 1-phosphate pathway in disease: review of sphingosine kinase inhibitors. *Biochimica et Biophysica Acta (BBA)-Molecular and Cell Biology of Lipids*, 1831, 157-166.
- GANESAN, V., PERERA, M. N., COLOMBINI, D., DATSKOVSKIY, D., CHADHA, K. & COLOMBINI, M. 2010. Ceramide and activated Bax act synergistically to permeabilize the mitochondrial outer membrane. *Apoptosis*, 15, 553-562.
- GAO, P., PETERSON, Y. K., SMITH, R. A. & SMITH, C. D. 2012. Characterization of isoenzyme-selective inhibitors of human sphingosine kinases. *PloS one*, 7, e44543.
- GAO, P. & SMITH, C. D. 2011. Ablation of sphingosine kinase-2 inhibits tumor cell proliferation and migration. *Molecular Cancer Research*, molcanres.0336.2011.
- GAULT, C. R. & OBEID, L. M. 2011. Still benched on its way to the bedside: sphingosine kinase 1 as an emerging target in cancer chemotherapy. *Critical reviews in biochemistry and molecular biology*, 46, 342-351.
- GAULT, C. R., OBEID, L. M. & HANNUN, Y. A. 2010. An overview of sphingolipid metabolism: from synthesis to breakdown. *Sphingolipids as Signaling and Regulatory Molecules*. Springer.
- GEFFIN, R., MARTINEZ, R., DE LAS POZAS, A., ISSAC, B. & MCCARTHY, M. 2017. Fingolimod induces neuronal-specific gene expression with potential neuroprotective outcomes in maturing neuronal progenitor cells exposed to HIV. *Journal of neurovirology*, 23, 808-824.
- GENNERO, I., FAUVEL, J., NIÉTO, M., CARIVEN, C., GAITS, F., BRIAND-MÉSANGE, F., CHAP, H. & SALLES, J. P. 2002. Apoptotic effect of sphingosine 1-phosphate and increased sphingosine 1-phosphate hydrolysis on mesangial cells cultured at low cell density. *Journal of Biological Chemistry*, 277, 12724-12734.
- GERONDAKIS, S., FULFORD, T. S., MESSINA, N. L. & GRUMONT, R. J. 2014. NF- κ B control of T cell development. *Nature immunology*, 15, 15.
- GHOSH, S. & HAYDEN, M. S. 2008. New regulators of NF- κ B in inflammation. *Nature Reviews Immunology*, 8, 837.
- GHOSH, S., MAY, M. J. & KOPP, E. B. 1998. NF- κ B and Rel proteins: evolutionarily conserved mediators of immune responses. *Annual review of immunology*, 16, 225-260.
- GLASS, C. K. & OLEFSKY, J. M. 2012. Inflammation and lipid signaling in the etiology of insulin resistance. *Cell metabolism*, 15, 635-645.
- GLOVER, J. M. & HARRISON, S. C. 1995. Crystal structure of the heterodimeric bZIP transcription factor c-Fos-c-Jun bound to DNA. *Nature*, 373, 257.
- GOETZL, E. J., KONG, Y. & MEI, B. 1999. Lysophosphatidic acid and sphingosine 1-phosphate protection of T cells from apoptosis in association with suppression of Bax. *The Journal of Immunology*, 162, 2049-2056.
- GOMEZ, L., PAILLARD, M., PRICE, M., CHEN, Q., TEIXEIRA, G., SPIEGEL, S. & LESNEFSKY, E. J. 2011. A novel role for mitochondrial sphingosine-1-phosphate produced by sphingosine kinase-2 in PTP-mediated cell

- survival during cardioprotection. *Basic research in cardiology*, 106, 1341-1353.
- GÓMEZ-MUÑOZ, A., KONG, J., SALH, B. & STEINBRECHER, U. P. 2003. Sphingosine- 1- phosphate inhibits acid sphingomyelinase and blocks apoptosis in macrophages. *FEBS letters*, 539, 56-60.
- GÓMEZ-MUÑOZ, A., KONG, J. Y., PARHAR, K., WANG, S. W., GANGOITI, P., GONZÁLEZ, M., EIVEMARK, S., SALH, B., DURONIO, V. & STEINBRECHER, U. P. 2005. Ceramide- 1- phosphate promotes cell survival through activation of the phosphatidylinositol 3- kinase/protein kinase B pathway. *FEBS letters*, 579, 3744-3750.
- GÓMEZ-MUÑOZ, A., KONG, J. Y., SALH, B. & STEINBRECHER, U. P. 2004. Ceramide-1-phosphate blocks apoptosis through inhibition of acid sphingomyelinase in macrophages. *Journal of lipid research*, 45, 99-105.
- GOPARAJU, S. K., JOLLY, P. S., WATTERSON, K. R., BEKTAS, M., ALVAREZ, S., SARKAR, S., MEL, L., ISHII, I., CHUN, J. & MILSTIEN, S. 2005. The S1P2 receptor negatively regulates platelet-derived growth factor-induced motility and proliferation. *Molecular and cellular biology*, 25, 4237-4249.
- GRASSMÉ, H., JENDROSSEK, V., BOCK, J., RIEHLE, A. & GULBINS, E. 2002. Ceramide-rich membrane rafts mediate CD40 clustering. *The Journal of Immunology*, 168, 298-307.
- GRASSMÉ, H., SCHWARZ, H. & GULBINS, E. 2001. Molecular mechanisms of ceramide-mediated CD95 clustering. *Biochemical and biophysical research communications*, 284, 1016-1030.
- GREEN, D. R. & KROEMER, G. 2009. Cytoplasmic functions of the tumour suppressor p53. *Nature*, 458, 1127.
- GRIN'KINA, N. M., KARNABI, E. E., DAMANIA, D., WADGAONKAR, S., MUSLIMOV, I. A. & WADGAONKAR, R. 2012. Sphingosine kinase 1 deficiency exacerbates LPS-induced neuroinflammation. *PLoS One*, 7, e36475.
- GROESCH, S., SCHIFFMANN, S. & GEISSLINGER, G. 2012. Chain length-specific properties of ceramides. *Progress in lipid research*, 51, 50-62.
- GRÖSCH, S., SCHIFFMANN, S. & GEISSLINGER, G. 2012. Chain length-specific properties of ceramides. *Progress in lipid research*, 51, 50-62.
- GROVES, A., KIHARA, Y. & CHUN, J. 2013. Fingolimod: direct CNS effects of sphingosine 1-phosphate (S1P) receptor modulation and implications in multiple sclerosis therapy. *Journal of the neurological sciences*, 328, 9-18.
- GUENTHER, G. G., PERALTA, E. R., ROSALES, K. R., WONG, S. Y., SISKIND, L. J. & EDINGER, A. L. 2008. Ceramide starves cells to death by downregulating nutrient transporter proteins. *Proceedings of the National Academy of Sciences*, 105, 17402-17407.
- GUPTA, S., BARRETT, T., WHITMARSH, A. J., CAVANAGH, J., SLUSS, H. K., DERIJARD, B. & DAVIS, R. J. 1996. Selective interaction of JNK protein kinase isoforms with transcription factors. *The EMBO journal*, 15, 2760-2770.
- GURURAJAN, M., CHUI, R., KARUPPANNAN, A. K., KE, J., JENNINGS, C. D. & BONDADA, S. 2005. c-Jun N-terminal kinase (JNK) is required for survival and proliferation of B-lymphoma cells. *Blood*, 106, 1382-1391.

- HABRUKOWICH, C., HAN, D. K., LE, A., REZAUL, K., PAN, W., GHOSH, M., LI, Z., DODGE-KAFKA, K., JIANG, X. & BITTMAN, R. 2010. Sphingosine interaction with acidic leucine-rich nuclear phosphoprotein-32A (ANP32A) regulates PP2A activity and cyclooxygenase (COX)-2 expression in human endothelial cells. *Journal of Biological Chemistry*, 285, 26825-26831.
- HÄCKER, H. & KARIN, M. 2006. Regulation and function of IKK and IKK-related kinases. *Sci. Stke*, 2006, re13-re13.
- HAGLUND, K., SIGISMUND, S., POLO, S., SZYMKIEWICZ, I., DI FIORE, P. P. & DIKIC, I. 2003. Multiple monoubiquitination of RTKs is sufficient for their endocytosis and degradation. *Nature cell biology*, 5, 461.
- HAIL, N., KIM, H. A. & LOTAN, R. 2006. Mechanisms of fenretinide-induced apoptosis. *Apoptosis*, 11, 1677-1694.
- HAIT, N. C., ALLEGOOD, J., MACEYKA, M., STRUB, G. M., HARIKUMAR, K. B., SINGH, S. K., LUO, C., MARMORSTEIN, R., KORDULA, T. & MILSTIEN, S. 2009. Regulation of histone acetylation in the nucleus by sphingosine-1-phosphate. *Science*, 325, 1254-1257.
- HAIT, N. C., AVNI, D., YAMADA, A., NAGAHASHI, M., AOYAGI, T., AOKI, H., DUMUR, C. I., ZELENKO, Z., GALLAGHER, E. & LEROITH, D. 2015. The phosphorylated prodrug FTY720 is a histone deacetylase inhibitor that reactivates ER α expression and enhances hormonal therapy for breast cancer. *Oncogenesis*, 4, e156.
- HAIT, N. C., BELLAMY, A., MILSTIEN, S., KORDULA, T. & SPIEGEL, S. 2007. Sphingosine kinase type 2 activation by ERK-mediated phosphorylation. *Journal of Biological Chemistry*, 282, 12058-12065.
- HAIT, N. C., OSKERITZIAN, C. A., PAUGH, S. W., MILSTIEN, S. & SPIEGEL, S. 2006. Sphingosine kinases, sphingosine 1-phosphate, apoptosis and diseases. *Biochim Biophys Acta*, 1758, 2016-26.
- HAIT, N. C., SARKAR, S., LE STUNFF, H., MIKAMI, A., MACEYKA, M., MILSTIEN, S. & SPIEGEL, S. 2005. Role of sphingosine kinase 2 in cell migration towards epidermal growth factor. *Journal of Biological Chemistry*.
- HAMAGUCHI, A., SUZUKI, E., MURAYAMA, K., FUJIMURA, T., HIKITA, T., IWABUCHI, K., HANDA, K., WITHERS, D. A., MASTERS, S. C. & FU, H. 2003. Sphingosine-dependent protein kinase-1, directed to 14-3-3, is identified as the kinase domain of protein kinase C δ . *Journal of Biological Chemistry*, 278, 41557-41565.
- HAN, G., GUPTA, S. D., GABLE, K., NIRANJANAKUMARI, S., MOITRA, P., EICHLER, F., BROWN, R. H., HARMON, J. M. & DUNN, T. M. 2009. Identification of small subunits of mammalian serine palmitoyltransferase that confer distinct acyl-CoA substrate specificities. *Proceedings of the National Academy of Sciences*, 106, 8186-8191.
- HANADA, K., KUMAGAI, K., YASUDA, S., MIURA, Y., KAWANO, M., FUKASAWA, M. & NISHIJIMA, M. 2003. Molecular machinery for non-vesicular trafficking of ceramide. *Nature*, 426, 803.
- HANNUN, Y. A. & LUBERTO, C. 2000. Ceramide in the eukaryotic stress response. *Trends in cell biology*, 10, 73-80.

- HANNUN, Y. A., LUBERTO, C. & ARGRAVES, K. M. 2001. Enzymes of sphingolipid metabolism: from modular to integrative signaling. *Biochemistry*, 40, 4893-4903.
- HANNUN, Y. A. & OBEID, L. M. 2008. Principles of bioactive lipid signalling: lessons from sphingolipids. *Nature reviews Molecular cell biology*, 9, 139.
- HANNUN, Y. A. & OBEID, L. M. 2011. Many ceramides. *Journal of Biological Chemistry*, 286, 27855-27862.
- HANNUN, Y. A. & OBEID, L. M. 2018. Sphingolipids and their metabolism in physiology and disease. *Nature reviews Molecular cell biology*, 19, 175.
- HANSON, D., MURRAY, P., COULSON, T., SUD, A., OMOKANYE, A., STRATTA, E., SAKHINIA, F., BONSHK, C., WILSON, L. & WAKELING, E. 2012a. Mutations in CUL7, OBSL1 and CCDC8 in 3-M syndrome lead to disordered growth factor signalling. *Journal of molecular endocrinology*, 49, 267.
- HANSON, D., MURRAY, P. G., O'SULLIVAN, J., URQUHART, J., DALY, S., BHASKAR, S. S., BIESECKER, L. G., SKAE, M., SMITH, C. & COLE, T. 2011. Exome sequencing identifies CCDC8 mutations in 3-M syndrome, suggesting that CCDC8 contributes in a pathway with CUL7 and OBSL1 to control human growth. *The American Journal of Human Genetics*, 89, 148-153.
- HANSON, M. A., ROTH, C. B., JO, E., GRIFFITH, M. T., SCOTT, F. L., REINHART, G., DESALE, H., CLEMONS, B., CAHALAN, S. M. & SCHUERER, S. C. 2012b. Crystal structure of a lipid G protein-coupled receptor. *Science*, 335, 851-855.
- HARDING, H. P., CALFON, M., URANO, F., NOVOA, I. & RON, D. 2002. Transcriptional and translational control in the mammalian unfolded protein response. *Annual review of cell and developmental biology*, 18.
- HARDING, H. P., NOVOA, I., ZHANG, Y., ZENG, H., WEK, R., SCHAPIRA, M. & RON, D. 2000a. Regulated translation initiation controls stress-induced gene expression in mammalian cells. *Molecular cell*, 6, 1099-1108.
- HARDING, H. P., ZHANG, Y., BERTOLOTTI, A., ZENG, H. & RON, D. 2000b. Perk is essential for translational regulation and cell survival during the unfolded protein response. *Molecular cell*, 5, 897-904.
- HARDING, H. P., ZHANG, Y. & RON, D. 1999. Protein translation and folding are coupled by an endoplasmic-reticulum-resident kinase. *Nature*, 397, 271.
- HARIKUMAR, K. B., YESTER, J. W., SURACE, M. J., OYENIRAN, C., PRICE, M. M., HUANG, W.-C., HAIT, N. C., ALLEGOOD, J. C., YAMADA, A. & KONG, X. 2014. K63-linked polyubiquitination of transcription factor IRF1 is essential for IL-1-induced production of chemokines CXCL10 and CCL5. *Nature immunology*, 15, 231.
- HAUGLAND, R. P. 2005. *The handbook: a guide to fluorescent probes and labeling technologies*. Univerza v Ljubljani, Fakulteta za farmacijo.
- HAUPT, Y., ROWAN, S., SHAULIAN, E., VOUSDEN, K. & OREN, M. 1995. Induction of apoptosis in HeLa cells by trans-activation-deficient p53. *Genes & development*, 9, 2170-2183.
- HAUS, J. M., KASHYAP, S. R., KASUMOV, T., ZHANG, R., KELLY, K. R., DEFRONZO, R. A. & KIRWAN, J. P. 2009. Plasma ceramides are elevated in obese

- subjects with type 2 diabetes and correlate with the severity of insulin resistance. *Diabetes*, 58, 337-343.
- HAYASHI, Y., NEMOTO-SASAKI, Y., TANIKAWA, T., OKA, S., TSUCHIYA, K., ZAMA, K., MITSUTAKE, S., SUGIURA, T. & YAMASHITA, A. 2014. Sphingomyelin synthase 2, but not sphingomyelin synthase 1, is involved in HIV-1 envelope-mediated membrane fusion. *Journal of Biological Chemistry*, 289, 30842-30856.
- HAYDEN, M. & GHOSH, S. 2004. Signaling to NF- κ B. *Genes & development*.
- HAYDEN, M. S. & GHOSH, S. 2008. Shared principles in NF- κ B signaling. *Cell*, 132, 344-362.
- HE, Y., SHE, H., ZHANG, T., XU, H., CHENG, L., YEPES, M., ZHAO, Y. & MAO, Z. 2018. p38 MAPK inhibits autophagy and promotes microglial inflammatory responses by phosphorylating ULK1. *J Cell Biol*, 217, 315-328.
- HECKELMAN, P. E., KINNEARY, J. F., O'NEIL, M. J. & SMITH, A. 1996. *The Merck index: an encyclopedia of chemicals, drugs, and biologicals*.
- HEINRICH, M., NEUMEYER, J., JAKOB, M., HALLAS, C., TCHIKOV, V., WINOTOMORBACH, S., WICKEL, M., SCHNEIDER-BRACHER, W., TRAUZOLD, A. & HETHKE, A. 2004. Cathepsin D links TNF-induced acid sphingomyelinase to Bid-mediated caspase-9 and -3 activation. *Cell death and differentiation*, 11, 550.
- HEMMATI, F., DARGAHI, L., NASOOHI, S., OMIDBAKHSR, R., MOHAMED, Z., CHIK, Z., NAIDU, M. & AHMADIANI, A. 2013. Neurorestorative effect of FTY720 in a rat model of Alzheimer's disease: comparison with memantine. *Behavioural brain research*, 252, 415-421.
- HERNÁNDEZ-CORBACHO, M. J., SALAMA, M. F., CANALS, D., SENKAL, C. E. & OBEID, L. M. 2017. Sphingolipids in mitochondria. *Biochimica et Biophysica Acta (BBA)-Molecular and Cell Biology of Lipids*, 1862, 56-68.
- HERNÁNDEZ-TIEDRA, S., FABRIAS, G., DÁVILA, D., SALANUEVA, I. J., CASAS, J., MONTES, L. R., ANTÓN, Z., GARCÍA-TABOADA, E., SALAZAR-ROA, M. & LORENTE, M. 2016. Dihydroceramide accumulation mediates cytotoxic autophagy of cancer cells via autolysosome destabilization. *Autophagy*, 12, 2213-2229.
- HÉRON-MILHAVET, L. & LE ROITH, D. 2002. IGF-I induces MDM2-dependent degradation of p53 via the p38 MAP kinase pathway in response to DNA damage. *Journal of Biological Chemistry*.
- HERSHKO, A. & CIECHANOVER, A. 1998. The ubiquitin system. Annual Reviews 4139 El Camino Way, PO Box 10139, Palo Alto, CA 94303-0139, USA.
- HERSHKO, A., HELLER, H., ELIAS, S. & CIECHANOVER, A. 1983. Components of ubiquitin-protein ligase system. Resolution, affinity purification, and role in protein breakdown. *Journal of Biological Chemistry*, 258, 8206-8214.
- HESS, J., ANGEL, P. & SCHORPP-KISTNER, M. 2004. AP-1 subunits: quarrel and harmony among siblings. *Journal of cell science*, 117, 5965-5973.
- HLA, T., VENKATARAMAN, K. & MICHAUD, J. 2008. The vascular S1P gradient—cellular sources and biological significance. *Biochimica et Biophysica Acta (BBA)-Molecular and Cell Biology of Lipids*, 1781, 477-482.

- HOBSON, J. P., ROSENFELDT, H. M., BARAK, L. S., OLIVERA, A., POULTON, S., CARON, M. G., MILSTIEN, S. & SPIEGEL, S. 2001. Role of the sphingosine-1-phosphate receptor EDG-1 in PDGF-induced cell motility. *Science*, 291, 1800-1803.
- HOCHSTRASSER, M. 2006. Lingering mysteries of ubiquitin-chain assembly. *Cell*, 124, 27-34.
- HOCHSTRASSER, M., PAPA, F., CHEN, P., SWAMINATHAN, S., JOHNSON, P., STILLMAN, L., AMERIK, A. & LI, S.-J. The DOA pathway: studies on the functions and mechanisms of ubiquitin-dependent protein degradation in the yeast *Saccharomyces cerevisiae*. Cold Spring Harbor symposia on quantitative biology, 1995. Cold Spring Harbor Laboratory Press, 503-513.
- HOLLAND, W. L., BIKMAN, B. T., WANG, L.-P., YUGUANG, G., SARGENT, K. M., BULCHAND, S., KNOTTS, T. A., SHUI, G., CLEGG, D. J. & WENK, M. R. 2011. Lipid-induced insulin resistance mediated by the proinflammatory receptor TLR4 requires saturated fatty acid-induced ceramide biosynthesis in mice. *The Journal of clinical investigation*, 121, 1858-1870.
- HOLLIDAY JR, M. W., COX, S. B., KANG, M. H. & MAURER, B. J. 2013. C22: 0-and C24: 0-dihydroceramides confer mixed cytotoxicity in T-cell acute lymphoblastic leukemia cell lines. *PLoS One*, 8, e74768.
- HONDA, R., TANAKA, H. & YASUDA, H. 1997. Oncoprotein MDM2 is a ubiquitin ligase E3 for tumor suppressor p53. *FEBS letters*, 420, 25-27.
- HUITEMA, K., VAN DEN DIKKENBERG, J., BROUWERS, J. F. & HOLTHUIS, J. C. 2004. Identification of a family of animal sphingomyelin synthases. *The EMBO journal*, 23, 33-44.
- HUWILER, A., DÖLL, F., REN, S., KLAWITTER, S., GREENING, A., RÖMER, I., BUBNOVA, S., REINSBERG, L. & PFEILSCHIFTER, J. 2006. Histamine increases sphingosine kinase-1 expression and activity in the human arterial endothelial cell line EA.hy 926 by a PKC- α -dependent mechanism. *Biochimica et Biophysica Acta (BBA)-Molecular and Cell Biology of Lipids*, 1761, 367-376.
- HUWILER, A., KOLTER, T., PFEILSCHIFTER, J. & SANDHOFF, K. 2000. Physiology and pathophysiology of sphingolipid metabolism and signaling. *Biochimica et Biophysica Acta (BBA)-Molecular and Cell Biology of Lipids*, 1485, 63-99.
- HYDE, R., HAJDUCH, E., POWELL, D. J., TAYLOR, P. M. & HUNDAL, H. S. 2005. Ceramide down-regulates System A amino acid transport and protein synthesis in rat skeletal muscle cells. *The FASEB journal*, 19, 461-463.
- ICHIMURA, Y., KIRISAKO, T., TAKAO, T., SATOMI, Y., SHIMONISHI, Y., ISHIHARA, N., MIZUSHIMA, N., TANIDA, I., KOMINAMI, E. & OHSUMI, M. 2000. A ubiquitin-like system mediates protein lipidation. *Nature*, 408, 488.
- IDKOWIAK-BALDYS, J., APRAIZ, A., LI, L., RAHMANIYAN, M., CLARKE, C. J., KRAVEKA, J. M., ASUMENDI, A. & HANNUN, Y. A. 2010. Dihydroceramide desaturase activity is modulated by oxidative stress. *Biochemical Journal*, 427, 265-274.

- IKEDA, F. & DIKIC, I. 2008. Atypical ubiquitin chains: new molecular signals. *EMBO reports*, 9, 536-542.
- ILLUZZI, G., BERNACCHIONI, C., AURELI, M., PRIONI, S., FRERA, G., DONATI, C., VALSECCHI, M., CHIGORNO, V., BRUNI, P. & SONNINO, S. 2010. Sphingosine kinase mediates resistance to the synthetic retinoid N-(4-hydroxyphenyl) retinamide in human ovarian cancer cells. *Journal of Biological Chemistry*, 285, 18594-18602.
- IMERI, F., SCHWALM, S., LYCK, R., ZIVKOVIC, A., STARK, H., ENGELHARDT, B., PFEILSCHIFTER, J. & HUWILER, A. 2016. Sphingosine kinase 2 deficient mice exhibit reduced experimental autoimmune encephalomyelitis: Resistance to FTY720 but not ST-968 treatments. *Neuropharmacology*, 105, 341-350.
- INOUE, T., WU, L., STUART, J. & MAKI, C. G. 2005. Control of p53 nuclear accumulation in stressed cells. *FEBS letters*, 579, 4978-4984.
- ISHIKAWA, Y., MUKAIDA, N., KUNO, K., RICE, N., OKAMOTO, S.-I. & MATSUSHIMA, K. 1995. Establishment of lipopolysaccharide-dependent nuclear factor κ B activation in a cell-free system. *Journal of Biological Chemistry*, 270, 4158-4164.
- JACKS, T., REMINGTON, L., WILLIAMS, B. O., SCHMITT, E. M., HALACHMI, S., BRONSON, R. T. & WEINBERG, R. A. 1994. Tumor spectrum analysis in p53-mutant mice. *Current biology*, 4, 1-7.
- JARMAN, K. E., MORETTI, P. A., ZEBOL, J. R. & PITSON, S. M. 2010. Translocation of sphingosine kinase 1 to the plasma membrane is mediated by calcium- and integrin-binding protein 1. *Journal of Biological Chemistry*, 285, 483-492.
- JEONG, S. K., KIM, Y. I., SHIN, K.-O., KIM, B.-W., LEE, S. H., JEON, J. E., KIM, H. J., LEE, Y.-M., MAURO, T. M. & ELIAS, P. M. 2015. Sphingosine kinase 1 activation enhances epidermal innate immunity through sphingosine-1-phosphate stimulation of cathelicidin production. *Journal of dermatological science*, 79, 229-234.
- JIANG, W. & OGRETMEN, B. 2013. Ceramide stress in survival versus lethal autophagy paradox: ceramide targets autophagosomes to mitochondria and induces lethal mitophagy. *Autophagy*, 9, 258-259.
- JIN, R., CHEN, Z., XUE, H. & CHEN, M. 2018. Blockage of bone marrow kinase in chromosome X enhances ABC294640-induced growth inhibition and apoptosis of colorectal cancer cells. *Tropical Journal of Pharmaceutical Research*, 17, 761-766.
- JIN, S. V. & WHITE, E. 2008. Tumor suppression by autophagy through the management of metabolic stress. *Autophagy*, 4, 563-566.
- JING, L. & ANNING, L. 2005. Role of JNK activation in apoptosis: a double-edged sword. *Cell research*, 15, 36.
- JUNG, I. D., LEE, J. S., KIM, Y. J., JEONG, Y.-I., LEE, C.-M., BAUMRUKER, T., BILLLICH, A., BANNO, Y., LEE, M. G. & AHN, S.-C. 2007. Sphingosine kinase inhibitor suppresses a Th1 polarization via the inhibition of immunostimulatory activity in murine bone marrow-derived dendritic cells. *International immunology*, 19, 411-426.

- JUNG, Y.-H., LIM, E. J., HEO, J., KWON, T. K. & KIM, Y.-H. 2012. Tunicamycin sensitizes human prostate cells to TRAIL-induced apoptosis by upregulation of TRAIL receptors and downregulation of cIAP2. *International journal of oncology*, 40, 1941-1948.
- KAGHAD, M., BONNET, H., YANG, A., CREANCIER, L., BISCAN, J.-C., VALENT, A., MINTY, A., CHALON, P., LELIAS, J.-M. & DUMONT, X. 1997. Monoallelically expressed gene related to p53 at 1p36, a region frequently deleted in neuroblastoma and other human cancers. *cell*, 90, 809-819.
- KAKUDO, Y., SHIBATA, H., OTSUKA, K., KATO, S. & ISHIOKA, C. 2005. Lack of correlation between p53-dependent transcriptional activity and the ability to induce apoptosis among 179 mutant p53s. *Cancer research*, 65, 2108-2114.
- KANG, S.-C., KIM, B.-R., LEE, S.-Y. & PARK, T.-S. 2013. Sphingolipid metabolism and obesity-induced inflammation. *Frontiers in endocrinology*, 4, 67.
- KARIN, M. 2005. Inflammation-activated protein kinases as targets for drug development. *Proceedings of the American Thoracic Society*, 2, 386-390.
- KARIN, M. & BEN-NERIAH, Y. 2000. Phosphorylation meets ubiquitination: the control of NF- κ B activity. *Annual review of immunology*, 18, 621-663.
- KARIN, M., CAO, Y., GRETEN, F. R. & LI, Z.-W. 2002. NF- κ B in cancer: from innocent bystander to major culprit. *Nature reviews cancer*, 2, 301.
- KARSAI, G., KRAFT, F., HAAG, N., KORENKE, G. C., HÄNISCH, B., OTHMAN, A., SURIYANARAYANAN, S., STEINER, R., KNOPP, C. & MULL, M. 2019. DEGS1-associated aberrant sphingolipid metabolism impairs nervous system function in humans. *The Journal of clinical investigation*, 129, 1229-1239.
- KARUNAKARAN, I. & VAN ECHTEN-DECKERT, G. 2017. Sphingosine 1-phosphate—A double edged sword in the brain. Elsevier.
- KATO JR, T., DELHASE, M., HOFFMANN, A. & KARIN, M. 2003. CK2 is a C-terminal I κ B kinase responsible for NF- κ B activation during the UV response. *Molecular cell*, 12, 829-839.
- KAUFMAN, R. J., SCHEUNER, D., SCHRÖDER, M., SHEN, X., LEE, K., LIU, C. Y. & ARNOLD, S. M. 2002. The unfolded protein response in nutrient sensing and differentiation. *Nature Reviews Molecular Cell Biology*, 3, 411.
- KAWAHARA, A., NISHI, T., HISANO, Y., FUKUI, H., YAMAGUCHI, A. & MOCHIZUKI, N. 2009. The sphingolipid transporter spns2 functions in migration of zebrafish myocardial precursors. *Science*, 323, 524-527.
- KAWAI, T., SATO, S., ISHII, K. J., COBAN, C., HEMMI, H., YAMAMOTO, M., TERAJ, K., MATSUDA, M., INOUE, J.-I. & UEMATSU, S. 2004. Interferon- α induction through Toll-like receptors involves a direct interaction of IRF7 with MyD88 and TRAF6. *Nature immunology*, 5, 1061.
- KEYES, W. M., WU, Y., VOGEL, H., GUO, X., LOWE, S. W. & MILLS, A. A. 2005. p63 deficiency activates a program of cellular senescence and leads to accelerated aging. *Genes & development*, 19, 1986-1999.
- KIM, I., XU, W. & REED, J. C. 2008. Cell death and endoplasmic reticulum stress: disease relevance and therapeutic opportunities. *Nature reviews Drug discovery*, 7, 1013.

- KIM, S. S., CHAE, H.-S., BACH, J.-H., LEE, M. W., KIM, K. Y., LEE, W. B., JUNG, Y.-M., BONVENTRE, J. V. & SUH, Y.-H. 2002. p53 mediates ceramide-induced apoptosis in SKN-SH cells. *Oncogene*, 21, 2020.
- KING, C. C., ZENKE, F. T., DAWSON, P. E., DUTIL, E. M., NEWTON, A. C., HEMMING, B. A. & BOKOCH, G. M. 2000. Sphingosine is a novel activator of 3-phosphoinositide-dependent kinase 1. *Journal of Biological Chemistry*, 275, 18108-18113.
- KIRKIN, V., MCEWAN, D. G., NOVAK, I. & DIKIC, I. 2009. A role for ubiquitin in selective autophagy. *Molecular cell*, 34, 259-269.
- KISHIMOTO, T., ISHITSUKA, R. & KOBAYASHI, T. 2016. Detectors for evaluating the cellular landscape of sphingomyelin- and cholesterol-rich membrane domains. *Biochimica et Biophysica Acta (BBA)-Molecular and Cell Biology of Lipids*, 1861, 812-829.
- KOHAMA, T., OLIVERA, A., EDSALL, L., NAGIEC, M. M., DICKSON, R. & SPIEGEL, S. 1998. Molecular cloning and functional characterization of murine sphingosine kinase. *Journal of Biological Chemistry*, 273, 23722-23728.
- KOLESNICK, R. & HEMER, M. 1990. Characterization of a ceramide kinase activity from human leukemia (HL-60) cells. Separation from diacylglycerol kinase activity. *Journal of Biological Chemistry*, 265, 18803-18808.
- KOUMENIS, C., NACZKI, C., KORITZINSKY, M., RASTANI, S., DIEHL, A., SONENBERG, N., KOROMILAS, A. & WOUTERS, B. G. 2002. Regulation of protein synthesis by hypoxia via activation of the endoplasmic reticulum kinase PERK and phosphorylation of the translation initiation factor eIF2 α . *Molecular and cellular biology*, 22, 7405-7416.
- KOVAL, M. & PAGANO, R. E. 1991. Intracellular transport and metabolism of sphingomyelin. *Biochimica et Biophysica Acta (BBA)-Lipids and Lipid Metabolism*, 1082, 113-125.
- KRESS, M., MAY, E., CASSINGENA, R. & MAY, P. 1979. Simian virus 40-transformed cells express new species of proteins precipitable by anti-simian virus 40 tumor serum. *Journal of virology*, 31, 472-483.
- KROEMER, G., MARIÑO, G. & LEVINE, B. 2010. Autophagy and the integrated stress response. *Molecular cell*, 40, 280-293.
- KUBBUTAT, M. & VOUSDEN, K. H. 1997. Proteolytic cleavage of human p53 by calpain: a potential regulator of protein stability. *Molecular and Cellular Biology*, 17, 460-468.
- KULKARNI, Y. M., KAUSHIK, V., AZAD, N., WRIGHT, C., ROJANASAKUL, Y., O'DOHERTY, G. & IYER, A. K. V. 2016. Autophagy- Induced Apoptosis in Lung Cancer Cells by a Novel Digitoxin Analog. *Journal of cellular physiology*, 231, 817-828.
- KUNKEL, G. T., MACEYKA, M., MILSTIEN, S. & SPIEGEL, S. 2013. Targeting the sphingosine-1-phosphate axis in cancer, inflammation and beyond. *Nature reviews Drug discovery*, 12, 688.
- KUO, Y.-C., HUANG, K.-Y., YANG, C.-H., YANG, Y.-S., LEE, W.-Y. & CHIANG, C.-W. 2008. Regulation of phosphorylation of Thr-308 of Akt, cell proliferation, and survival by the B55 α regulatory subunit targeting of the protein

- phosphatase 2A holoenzyme to Akt. *Journal of Biological Chemistry*, 283, 1882-1892.
- KUZMENKO, D. & KLIMENTYEVA, T. 2016. Role of ceramide in apoptosis and development of insulin resistance. *Biochemistry (Moscow)*, 81, 913-927.
- LANE, D. P. 1992. Cancer. p53, guardian of the genome. *Nature*, 358, 15-16.
- LANE, D. P. & CRAWFORD, L. V. 1979. T antigen is bound to a host protein in SY40-transformed cells. *Nature*, 278, 261-263.
- LAW, J. H., LI, Y., TO, K., WANG, M., ASTANEHE, A., LAMBIE, K., DHILLON, J., JONES, S. J., GLEAVE, M. E. & EAVES, C. J. 2010. Molecular decoy to the Y-box binding protein-1 suppresses the growth of breast and prostate cancer cells whilst sparing normal cell viability. *PloS one*, 5.
- LAWRENCE, T. 2009. The nuclear factor NF- κ B pathway in inflammation. *Cold Spring Harbor perspectives in biology*, 1, a001651.
- LEBMAN, D. A. & SPIEGEL, S. 2008. Thematic review series: sphingolipids. Cross-talk at the crossroads of sphingosine-1-phosphate, growth factors, and cytokine signaling. *Journal of lipid research*, 49, 1388-1394.
- LEE, H., ROTOLO, J. A., MESICEK, J., PENATE-MEDINA, T., RIMNER, A., LIAO, W.-C., YIN, X., RAGUPATHI, G., EHLEITER, D. & GULBINS, E. 2011. Mitochondrial ceramide-rich macrodomains functionalize Bax upon irradiation. *PloS one*, 6, e19783.
- LEE, K., TIRASOPHON, W., SHEN, X., MICHALAK, M., PRYWES, R., OKADA, T., YOSHIDA, H., MORI, K. & KAUFMAN, R. J. 2002. IRE1-mediated unconventional mRNA splicing and S2P-mediated ATF6 cleavage merge to regulate XBP1 in signaling the unfolded protein response. *Genes & development*, 16, 452-466.
- LEILI, H., NASSER, S., NADEREH, R., SIAVOUSH, D. & POURAN, K. 2018. Sphingosine kinase-2 inhibitor ABC294640 enhances doxorubicin-induced apoptosis of NSCLC cells via altering survivin expression. *Drug research*, 68, 45-53.
- LENGAUER, C., KINZLER, K. W. & VOGELSTEIN, B. 1998. Genetic instabilities in human cancers. *Nature*, 396, 643.
- LEVINE, B. & YUAN, J. 2005. Autophagy in cell death: an innocent convict? *The Journal of clinical investigation*, 115, 2679-2688.
- LEWIS, A. C., WALLINGTON-BEDDOE, C. T., POWELL, J. A. & PITSON, S. M. 2018. Targeting sphingolipid metabolism as an approach for combination therapies in haematological malignancies. *Cell Death Discovery*, 4, 72.
- LI, J., LEE, B. & LEE, A. S. 2006. Endoplasmic reticulum stress-induced apoptosis multiple pathways and activation of p53-up-regulated modulator of apoptosis (puma) and noxa by p53. *Journal of Biological Chemistry*, 281, 7260-7270.
- LI, Y., XU, K.-P., JIANG, D., ZHAO, J., GE, J.-F. & ZHENG, S.-Y. 2015. Relationship of Fas, FasL, p53 and bcl-2 expression in human non-small cell lung carcinomas. *International journal of clinical and experimental pathology*, 8, 13978.
- LI, Y., ZHU, H., ZENG, X., FAN, J., QIAN, X., WANG, S., WANG, Z., SUN, Y., WANG, X. & WANG, W. 2013. Suppression of autophagy enhanced growth

- inhibition and apoptosis of interferon- β in human glioma cells. *Molecular neurobiology*, 47, 1000-1010.
- LI, Y.-P., CHEN, Y., JOHN, J., MOYLAN, J., JIN, B., MANN, D. L. & REID, M. B. 2005. TNF- α acts via p38 MAPK to stimulate expression of the ubiquitin ligase atrogin1/MAFbx in skeletal muscle. *The FASEB Journal*, 19, 362-370.
- LIANG, J., NAGAHASHI, M., KIM, E. Y., HARIKUMAR, K. B., YAMADA, A., HUANG, W.-C., HAIT, N. C., ALLEGOOD, J. C., PRICE, M. M. & AVNI, D. 2013. Sphingosine-1-phosphate links persistent STAT3 activation, chronic intestinal inflammation, and development of colitis-associated cancer. *Cancer cell*, 23, 107-120.
- LIBERMANN, T. A. & BALTIMORE, D. 1990. Activation of interleukin-6 gene expression through the NF-kappa B transcription factor. *Molecular and cellular biology*, 10, 2327-2334.
- LIM, K. G., SUN, C., BITTMAN, R., PYNE, N. J. & PYNE, S. 2011a. (R)-FTY720 methyl ether is a specific sphingosine kinase 2 inhibitor: effect on sphingosine kinase 2 expression in HEK 293 cells and actin rearrangement and survival of MCF-7 breast cancer cells. *Cellular signalling*, 23, 1590-1595.
- LIM, K. G., TONELLI, F., BERDYSHEV, E., GORSHKOVA, I., LECLERCQ, T., PITSON, S. M., BITTMAN, R., PYNE, S. & PYNE, N. J. 2012. Inhibition kinetics and regulation of sphingosine kinase 1 expression in prostate cancer cells: functional differences between sphingosine kinase 1a and 1b. *The international journal of biochemistry & cell biology*, 44, 1457-1464.
- LIM, K. G., TONELLI, F., LI, Z., LU, X., BITTMAN, R., PYNE, S. & PYNE, N. J. 2011b. FTY720 analogues as sphingosine kinase 1 inhibitors: enzyme inhibition kinetics, allostereism, proteasomal degradation and actin rearrangement in MCF-7 breast cancer cells. *Journal of Biological Chemistry*, jbc. M111. 220756.
- LIMA, S., TAKABE, K., NEWTON, J., SAURABH, K., YOUNG, M. M., LEOPOLDINO, A. M., HAIT, N. C., ROBERTS, J. L., WANG, H.-G. & DENT, P. 2018. TP53 is required for BECN1-and ATG5-dependent cell death induced by sphingosine kinase 1 inhibition. *Autophagy*, 1-16.
- LIMAYE, V., VADAS, M. A., PITSON, S. M. & GAMBLE, J. R. 2009a. The effects of markedly raised intracellular sphingosine kinase-1 activity in endothelial cells. *Cellular & molecular biology letters*, 14, 411.
- LIMAYE, V., XIA, P., HAHN, C., SMITH, M., VADAS, M. A., PITSON, S. M. & GAMBLE, J. R. 2009b. Chronic increases in sphingosine kinase-1 activity induce a pro-inflammatory, pro-angiogenic phenotype in endothelial cells. *Cellular & molecular biology letters*, 14, 424.
- LIN, A. 2003. Activation of the JNK signaling pathway: breaking the brake on apoptosis. *Bioessays*, 25, 17-24.
- LIN, Q. & LONDON, E. 2015. Ordered raft domains induced by outer leaflet sphingomyelin in cholesterol-rich asymmetric vesicles. *Biophysical journal*, 108, 2212-2222.
- LINGWOOD, D. & SIMONS, K. 2010. Lipid rafts as a membrane-organizing principle. *science*, 327, 46-50.

- LINZER, D. I. & LEVINE, A. J. 1979. Characterization of a 54K dalton cellular SV40 tumor antigen present in SV40-transformed cells and uninfected embryonal carcinoma cells. *Cell*, 17, 43-52.
- LIU, B., OLTVAI, Z. N., BAYIR, H., SILVERMAN, G. A., PAK, S. C., PERLMUTTER, D. H. & BAHAR, I. 2017. Quantitative assessment of cell fate decision between autophagy and apoptosis. *Scientific reports*, 7, 17605.
- LIU, H., SUGIURA, M., NAVA, V. E., EDSALL, L. C., KONO, K., POULTON, S., MILSTIEN, S., KOHAMA, T. & SPIEGEL, S. 2000. Molecular cloning and functional characterization of a novel mammalian sphingosine kinase type 2 isoform. *Journal of Biological Chemistry*.
- LIU, H., TOMAN, R. E., GOPARAJU, S. K., MACEYKA, M., NAVA, V. E., SANKALA, H., PAYNE, S. G., BEKTAS, M., ISHII, I. & CHUN, J. 2003. Sphingosine kinase type 2 is a putative BH3-only protein that induces apoptosis. *Journal of Biological Chemistry*, 278, 40330-40336.
- LIU, K., GUO, T. L., HAIT, N. C., ALLEGOOD, J., PARIKH, H. I., XU, W., KELLOGG, G. E., GRANT, S., SPIEGEL, S. & ZHANG, S. 2013. Biological characterization of 3-(2-amino-ethyl)-5-[3-(4-butoxyl-phenyl)-propylidene]-thiazolidine-2, 4-dione (K145) as a selective sphingosine kinase-2 inhibitor and anticancer agent. *PloS one*, 8, e56471.
- LIU, Q., REHMAN, H., SHI, Y., KRISHNASAMY, Y., LEMASTERS, J. J., SMITH, C. D. & ZHONG, Z. 2012. Inhibition of sphingosine kinase-2 suppresses inflammation and attenuates graft injury after liver transplantation in rats. *Plos one*, 7, e41834.
- LIU, Y.-C., PENNINGER, J. & KARIN, M. 2005. Immunity by ubiquitylation: a reversible process of modification. *Nature Reviews Immunology*, 5, 941.
- LONG, J. S., NATARAJAN, V., TIGYI, G., PYNE, S. & PYNE, N. J. 2006. The functional PDGF β receptor-S1P1 receptor signaling complex is involved in regulating migration of mouse embryonic fibroblasts in response to platelet derived growth factor. *Prostaglandins & other lipid mediators*, 80, 74-80.
- LOVERIDGE, C., TONELLI, F., LECLERCQ, T., LIM, K. G., LONG, J. S., BERDYSHEV, E., TATE, R. J., NATARAJAN, V., PITSON, S. M. & PYNE, N. J. 2010. The sphingosine kinase 1 inhibitor 2-(p-hydroxyanilino)-4-(p-chlorophenyl) thiazole induces proteasomal degradation of sphingosine kinase 1 in mammalian cells. *Journal of Biological Chemistry*, 285, 38841-38852.
- LUOMA, P. V. 2013. Elimination of endoplasmic reticulum stress and cardiovascular, type 2 diabetic, and other metabolic diseases. *Annals of medicine*, 45, 194-202.
- LV, M., ZHANG, D., DAI, D., ZHANG, W. & ZHANG, L. 2016. Sphingosine kinase 1/sphingosine-1-phosphate regulates the expression of interleukin-17A in activated microglia in cerebral ischemia/reperfusion. *Inflammation Research*, 65, 551-562.
- MA, J., ZHANG, L., HAN, W., SHEN, T., MA, C., LIU, Y., NIE, X., LIU, M., RAN, Y. & ZHU, D. 2012. Activation of JNK/c-Jun is required for the proliferation, survival, and angiogenesis induced by EET in pulmonary artery endothelial cells. *Journal of lipid research*, 53, 1093-1105.

- MA, Y., BREWER, J. W., DIEHL, J. A. & HENDERSHOT, L. M. 2002. Two distinct stress signaling pathways converge upon the CHOP promoter during the mammalian unfolded protein response. *Journal of molecular biology*, 318, 1351-1365.
- MA, Y. & HENDERSHOT, L. M. 2001. The unfolding tale of the unfolded protein response. *Cell*, 107, 827-830.
- MA, Y., PITSON, S., HERCUS, T., MURPHY, J., LOPEZ, A. & WOODCOCK, J. 2005. Sphingosine activates protein kinase A type II by a novel cAMP-independent mechanism. *Journal of Biological Chemistry*, 280, 26011-26017.
- MACEYKA, M., HARIKUMAR, K. B., MILSTIEN, S. & SPIEGEL, S. 2012. Sphingosine-1-phosphate signaling and its role in disease. *Trends in cell biology*, 22, 50-60.
- MACEYKA, M., SANKALA, H., HAIT, N. C., LE STUNFF, H., LIU, H., TOMAN, R., COLLIER, C., ZHANG, M., SATIN, L. & MERRILL, A. H. 2005. Sphk1 and Sphk2: Sphingosine kinase isoenzymes with opposing functions in sphingolipid metabolism. *Journal of Biological Chemistry*.
- MACEYKA, M. & SPIEGEL, S. 2014. Sphingolipid metabolites in inflammatory disease. *Nature*, 510, 58.
- MACLACHLAN, T. K. & EL-DEIRY, W. S. 2002. Apoptotic threshold is lowered by p53 transactivation of caspase-6. *Proceedings of the National Academy of Sciences*, 99, 9492-9497.
- MACRITCHIE, N., VOLPERT, G., AL WASHIH, M., WATSON, D. G., FUTERMAN, A. H., KENNEDY, S., PYNE, S. & PYNE, N. J. 2016. Effect of the sphingosine kinase 1 selective inhibitor, PF-543 on arterial and cardiac remodelling in a hypoxic model of pulmonary arterial hypertension. *Cellular signalling*, 28, 946-955.
- MAHIPAL, A., KOMMALAPATI, A., TELLA, S. H., LIM, A. & KIM, R. 2018. Novel targeted treatment options for advanced cholangiocarcinoma. *Expert opinion on investigational drugs*, 27, 709-720.
- MAINES, L. W., FITZPATRICK, L. R., FRENCH, K. J., ZHUANG, Y., XIA, Z., KELLER, S. N., UPSON, J. J. & SMITH, C. D. 2008. Suppression of ulcerative colitis in mice by orally available inhibitors of sphingosine kinase. *Digestive diseases and sciences*, 53, 997-1012.
- MAINES, L. W., FITZPATRICK, L. R., GREEN, C. L., ZHUANG, Y. & SMITH, C. D. 2010. Efficacy of a novel sphingosine kinase inhibitor in experimental Crohn's disease. *Inflammopharmacology*, 18, 73-85.
- MAIURI, M. C., ZALCKVAR, E., KIMCHI, A. & KROEMER, G. 2007. Self-eating and self-killing: crosstalk between autophagy and apoptosis. *Nature reviews Molecular cell biology*, 8, 741.
- MALKIN, D., LI, F. P., STRONG, L. C., FRAUMENI, J. F., NELSON, C. E., KIM, D. H., KASSEL, J., GRYKA, M. A., BISCHOFF, F. Z. & TAINSKY, M. A. 1990. Germ line p53 mutations in a familial syndrome of breast cancer, sarcomas, and other neoplasms. *Science*, 250, 1233-1238.
- MANNI, S., MAUBAN, J. H., WARD, C. W. & BOND, M. 2008. Phosphorylation of the cAMP-dependent protein kinase (PKA) regulatory subunit modulates

- PKA-AKAP interaction, substrate phosphorylation, and calcium signaling in cardiac cells. *Journal of Biological Chemistry*, 283, 24145-24154.
- MAO, C. & OBEID, L. M. 2008. Ceramidases: regulators of cellular responses mediated by ceramide, sphingosine, and sphingosine-1-phosphate. *Biochimica et Biophysica Acta (BBA)-Molecular and Cell Biology of Lipids*, 1781, 424-434.
- MARINO, G., NISO-SANTANO, M., BAEHRECKE, E. H. & KROEMER, G. 2014. Self-consumption: the interplay of autophagy and apoptosis. *Nature reviews Molecular cell biology*, 15, 81.
- MARTIN, J. L., DE SILVA, H. C., LIN, M. Z., SCOTT, C. D. & BAXTER, R. C. 2014. Inhibition of Insulin-like Growth Factor-Binding Protein-3 Signaling through Sphingosine Kinase-1 Sensitizes Triple-Negative Breast Cancer Cells to EGF Receptor Blockade. *Molecular cancer therapeutics*, 13, 316-328.
- MASTRANDREA, L. D., SESSANNA, S. M. & LAYCHOCK, S. G. 2005. Sphingosine kinase activity and sphingosine-1 phosphate production in rat pancreatic islets and INS-1 cells: response to cytokines. *Diabetes*, 54, 1429-1436.
- MAY, M. J., MARIENFELD, R. B. & GHOSH, S. 2002. Characterization of the I κ B-kinase NEMO binding domain. *Journal of Biological Chemistry*, 277, 45992-46000.
- MCDONALD, O., HANNUN, Y., REYNOLDS, C. & SAHYOUN, N. 1991. Activation of casein kinase II by sphingosine. *Journal of Biological Chemistry*, 266, 21773-21776.
- MCNAUGHTON, M., PITMAN, M., PITSON, S. M., PYNE, N. J. & PYNE, S. 2016. Proteasomal degradation of sphingosine kinase 1 and inhibition of dihydroceramide desaturase by the sphingosine kinase inhibitors, SKi or ABC294640, induces growth arrest in androgen-independent LNCaP-AI prostate cancer cells. *Oncotarget*, 7, 16663.
- MEACCI, E., CENCETTI, F., DONATI, C., NUTI, F., FARNARARO, M., KOHNO, T., IGARASHI, Y. & BRUNI, P. 2003. Down-regulation of EDG5/S1P2 during myogenic differentiation results in the specific uncoupling of sphingosine 1-phosphate signalling to phospholipase D. *Biochimica et Biophysica Acta (BBA)-Molecular and Cell Biology of Lipids*, 1633, 133-142.
- MEGIDISH, T., COOPER, J., ZHANG, L., FU, H. & HAKOMORI, S.-I. 1998. A novel sphingosine-dependent protein kinase (SDK1) specifically phosphorylates certain isoforms of 14-3-3 protein. *Journal of Biological Chemistry*, 273, 21834-21845.
- MEI, Y., HAHN, A. A., HU, S. & YANG, X. 2011. The USP19 deubiquitinase regulates the stability of c-IAP1 and c-IAP2. *Journal of Biological Chemistry*, jbc. M111. 282020.
- MELERO, J., STITT, D. T., MANGEL, W. F. & CARROLL, R. B. 1979. Identification of new polypeptide species (48-55K) immunoprecipitable by antiserum to purified large T antigen and present in SV40-infected and-transformed cells. *Virology*, 93, 466-480.
- MELINO, G., LU, X., GASCO, M., CROOK, T. & KNIGHT, R. A. 2003. Functional regulation of p73 and p63: development and cancer. *Trends in biochemical sciences*, 28, 663-670.

- MENENDEZ, D., INGA, A. & RESNICK, M. A. 2009. The expanding universe of p53 targets. *Nature reviews Cancer*, 9, 724.
- MERCADO, N., KIZAWA, Y., UEDA, K., XIONG, Y., KIMURA, G., MOSES, A., CURTIS, J. M., ITO, K. & BARNES, P. J. 2014. Activation of transcription factor Nrf2 signalling by the sphingosine kinase inhibitor SKI-II is mediated by the formation of Keap1 dimers. *PLoS One*, 9, e88168.
- MERCURIO, F. & MANNING, A. M. 1999. Multiple signals converging on NF- κ B. *Current opinion in cell biology*, 11, 226-232.
- MERCURIO, F., ZHU, H., MURRAY, B. W., SHEVCHENKO, A., BENNETT, B. L., WU LI, J., YOUNG, D. B., BARBOSA, M., MANN, M. & MANNING, A. 1997. IKK-1 and IKK-2: cytokine-activated I κ B kinases essential for NF- κ B activation. *Science*, 278, 860-866.
- MERRILL, A. H. 2002. De novo sphingolipid biosynthesis: a necessary, but dangerous, pathway. *Journal of Biological Chemistry*, 277, 25843-25846.
- MERRILL, A. H. 2008. Sphingolipids. *Biochemistry of Lipids, Lipoproteins and Membranes (Fifth Edition)*. Elsevier.
- MICHAEL, D. & OREN, M. 2002. The p53 and Mdm2 families in cancer. *Current opinion in genetics & development*, 12, 53-59.
- MICHAUD, J., KOHNO, M., PROIA, R. L. & HLA, T. 2006. Normal acute and chronic inflammatory responses in sphingosine kinase 1 knockout mice. *FEBS letters*, 580, 4607-4612.
- MICHEL, C. & VAN ECHTEN-DECKERT, G. 1997. Conversion of dihydroceramide to ceramide occurs at the cytosolic face of the endoplasmic reticulum. *FEBS letters*, 416, 153-155.
- MICHEL, C., VAN ECHTEN-DECKERT, G., ROTHER, J., SANDHOFF, K., WANG, E. & MERRILL, A. H. 1997. Characterization of ceramide synthesis a dihydroceramide desaturase introduces the 4, 5-trans-double bond of sphingosine at the level of dihydroceramide. *Journal of Biological Chemistry*, 272, 22432-22437.
- MILLER, D. M. & SHAKES, D. C. 1995. Immunofluorescence microscopy. *Methods in cell biology*. Elsevier.
- MILLS, A. A., ZHENG, B., WANG, X.-J., VOGEL, H., ROOP, D. R. & BRADLEY, A. 1999. p63 is a p53 homologue required for limb and epidermal morphogenesis. *Nature*, 398, 708.
- MIN, J., MESIKA, A., SIVAGURU, M., VAN VELDHoven, P. P., ALEXANDER, H., FUTERMAN, A. H. & ALEXANDER, S. 2007. (Dihydro) ceramide synthase 1-regulated sensitivity to cisplatin is associated with the activation of p38 mitogen-activated protein kinase and is abrogated by sphingosine kinase 1. *Molecular Cancer Research*, 5, 801-812.
- MIRON, V. E., LUDWIN, S. K., DARLINGTON, P. J., JARJOUR, A. A., SOLIVEN, B., KENNEDY, T. E. & ANTEL, J. P. 2010. Fingolimod (FTY720) enhances remyelination following demyelination of organotypic cerebellar slices. *The American journal of pathology*, 176, 2682-2694.
- MIYAJI, M., JIN, Z.-X., YAMAOKA, S., AMAKAWA, R., FUKUHARA, S., SATO, S. B., KOBAYASHI, T., DOMAE, N., MIMORI, T. & BLOOM, E. T. 2005. Role of membrane sphingomyelin and ceramide in platform formation for Fas-mediated apoptosis. *Journal of Experimental Medicine*, 202, 249-259.

- MIZUGISHI, K., YAMASHITA, T., OLIVERA, A., MILLER, G. F., SPIEGEL, S. & PROIA, R. L. 2005. Essential role for sphingosine kinases in neural and vascular development. *Molecular and cellular biology*, 25, 11113-11121.
- MIZUTANI, Y., KIHARA, A. & IGARASHI, Y. 2004. Identification of the human sphingolipid C4- hydroxylase, hDES2, and its up- regulation during keratinocyte differentiation. *FEBS letters*, 563, 93-97.
- MOLL, U. M., LAQUAGLIA, M., BÉNARD, J. & RIOU, G. 1995. Wild-type p53 protein undergoes cytoplasmic sequestration in undifferentiated neuroblastomas but not in differentiated tumors. *Proceedings of the National Academy of Sciences*, 92, 4407-4411.
- MOLL, U. M. & PETRENKO, O. 2003. The MDM2-p53 interaction. *Molecular cancer research*, 1, 1001-1008.
- MOMAND, J., WU, H.-H. & DASGUPTA, G. 2000. MDM2—master regulator of the p53 tumor suppressor protein. *Gene*, 242, 15-29.
- MORAD, S. A. & CABOT, M. C. 2013. Ceramide-orchestrated signalling in cancer cells. *Nature Reviews Cancer*, 13, 51.
- MORRIS, M. R., RICKETTS, C., GENTLE, D., MCRONALD, F., CARLI, N., KHALILI, H., BROWN, M., KISHIDA, T., YAO, M. & BANKS, R. E. 2011. Genome-wide methylation analysis identifies epigenetically inactivated candidate tumour suppressor genes in renal cell carcinoma. *Oncogene*, 30, 1390-1401.
- MUKHOPADHYAY, D. & RIEZMAN, H. 2007. Proteasome-independent functions of ubiquitin in endocytosis and signaling. *Science*, 315, 201-205.
- MÜLLER, M., WILDER, S., BANNASCH, D., ISRAELI, D., LEHLBACH, K., LI-WEBER, M., FRIEDMAN, S. L., GALLE, P. R., STREMMEL, W. & OREN, M. 1998. p53 activates the CD95 (APO-1/Fas) gene in response to DNA damage by anticancer drugs. *Journal of Experimental Medicine*, 188, 2033-2045.
- MURRAY-ZMIJEWSKI, F., LANE, D. & BOURDON, J. 2006. p53/p63/p73 isoforms: an orchestra of isoforms to harmonise cell differentiation and response to stress. *Cell death and differentiation*, 13, 962.
- MYU, P., KHAN, W., ALESSENKO, A., SAHYOUN, N. & HANNUN, Y. 1992. Sphingosine activation of protein kinases in Jurkat T cells. In vitro phosphorylation of endogenous protein substrates and specificity of action. *Journal of Biological Chemistry*, 267, 15246-15251.
- NAKANO, K. & VOUSDEN, K. H. 2001. PUMA, a novel proapoptotic gene, is induced by p53. *Molecular cell*, 7, 683-694.
- NAKATSUKASA, K. & BRODSKY, J. L. 2008. The recognition and retrotranslocation of misfolded proteins from the endoplasmic reticulum. *Traffic*, 9, 861-870.
- NASR, R., EL-SABBAN, M. E., KARAM, J.-A., DBAIBO, G., KFOURY, Y., ARNULF, B., LEPELLETIER, Y., BEX, F., DE THÉ, H. & HERMINE, O. 2005. Efficacy and mechanism of action of the proteasome inhibitor PS-341 in T-cell lymphomas and HTLV-I associated adult T-cell leukemia/lymphoma. *Oncogene*, 24, 419.
- NAVA, V. E., HOBSON, J. P., MURTHY, S., MILSTIEN, S. & SPIEGEL, S. 2002. Sphingosine kinase type 1 promotes estrogen-dependent tumorigenesis of breast cancer MCF-7 cells. *Experimental cell research*, 281, 115-127.

- NAYAK, D., HUO, Y., KWANG, W., PUSHPARAJ, P., KUMAR, S., LING, E.-A. & DHEEN, S. 2010. Sphingosine kinase 1 regulates the expression of proinflammatory cytokines and nitric oxide in activated microglia. *Neuroscience*, 166, 132-144.
- NEUBAUER, H. A. & PITSON, S. M. 2013. Roles, regulation and inhibitors of sphingosine kinase 2. *The FEBS journal*, 280, 5317-5336.
- NEWTON, J., LIMA, S., MACEYKA, M. & SPIEGEL, S. 2015. Revisiting the sphingolipid rheostat: Evolving concepts in cancer therapy. *Exp Cell Res*, 333, 195-200.
- NISHI, T., KOBAYASHI, N., HISANO, Y., KAWAHARA, A. & YAMAGUCHI, A. 2014. Molecular and physiological functions of sphingosine 1-phosphate transporters. *Biochimica et Biophysica Acta (BBA)-Molecular and Cell Biology of Lipids*, 1841, 759-765.
- NOACK, J., CHOI, J., RICHTER, K., KOPP-SCHNEIDER, A. & REGNIER-VIGOUROUX, A. 2014. A sphingosine kinase inhibitor combined with temozolomide induces glioblastoma cell death through accumulation of dihydrosphingosine and dihydroceramide, endoplasmic reticulum stress and autophagy. *Cell death & disease*, 5, e1425.
- O'SHEA, J. M. & PERKINS, N. D. 2008. Regulation of the RelA (p65) transactivation domain. Portland Press Limited.
- O'BRATE, A. & GIANNAKAKOU, P. 2003. The importance of p53 location: nuclear or cytoplasmic zip code? *Drug resistance updates*, 6, 313-322.
- OBEID, L. M., LINARDIC, C. M., KAROLAK, L. A. & HANNUN, Y. A. 1993. Programmed cell death induced by ceramide. *Science*, 259, 1769-1771.
- ODA, E., OHKI, R., MURASAWA, H., NEMOTO, J., SHIBUE, T., YAMASHITA, T., TOKINO, T., TANIGUCHI, T. & TANAKA, N. 2000. Noxa, a BH3-only member of the Bcl-2 family and candidate mediator of p53-induced apoptosis. *Science*, 288, 1053-1058.
- ODA, Y., HOSOKAWA, N., WADA, I. & NAGATA, K. 2003. EDEM as an acceptor of terminally misfolded glycoproteins released from calnexin. *Science*, 299, 1394-1397.
- OHOTSKI, J., ROSEN, H., BITTMAN, R., PYNE, S. & PYNE, N. J. 2014. Sphingosine kinase 2 prevents the nuclear translocation of sphingosine 1-phosphate receptor-2 and tyrosine 416 phosphorylated c-Src and increases estrogen receptor negative MDA-MB-231 breast cancer cell growth: The role of sphingosine 1-phosphate receptor-4. *Cellular signalling*, 26, 1040-1047.
- OLIVERA, A., EISNER, C., KITAMURA, Y., DILLAHUNT, S., ALLENDE, L., TUYMETOVA, G., WATFORD, W., MEYLAN, F., DIESNER, S. C. & LI, L. 2010. Sphingosine kinase 1 and sphingosine-1-phosphate receptor 2 are vital to recovery from anaphylactic shock in mice. *The Journal of clinical investigation*, 120, 1429-1440.
- OLIVERA, A., KOHAMA, T., EDSALL, L., NAVA, V., CUVILLIER, O., POULTON, S. & SPIEGEL, S. 1999. Sphingosine kinase expression increases intracellular sphingosine-1-phosphate and promotes cell growth and survival. *The Journal of cell biology*, 147, 545-558.

- OLIVERA, A., KOHAMA, T., TU, Z., MILSTIEN, S. & SPIEGEL, S. 1998. Purification and characterization of rat kidney sphingosine kinase. *Journal of Biological Chemistry*, 273, 12576-12583.
- OLIVERA, A., ROSENTHAL, J. & SPIEGEL, S. 1996. Effect of acidic phospholipids on sphingosine kinase. *Journal of cellular biochemistry*, 60, 529-537.
- OLIVERA, A. & SPIEGEL, S. 1993. Sphingosine-1-phosphate as second messenger in cell proliferation induced by PDGF and FCS mitogens. *Nature*, 365, 557.
- OMAE, F., MIYAZAKI, M., ENOMOTO, A. & SUZUKI, A. 2004a. Identification of an essential sequence for dihydroceramide C-4 hydroxylase activity of mouse DES2. *FEBS letters*, 576, 63-67.
- OMAE, F., MIYAZAKI, M., ENOMOTO, A., SUZUKI, M., SUZUKI, Y. & SUZUKI, A. 2004b. DES2 protein is responsible for phytoceramide biosynthesis in the mouse small intestine. *Biochemical Journal*, 379, 687.
- OREN, M. 2003. Decision making by p53: life, death and cancer. *Cell death and differentiation*, 10, 431.
- OSAKI, M., OSHIMURA, M. A. & ITO, H. 2004. PI3K-Akt pathway: its functions and alterations in human cancer. *Apoptosis*, 9, 667-676.
- OSKOUIAN, B. & SABA, J. D. 2010. Cancer treatment strategies targeting sphingolipid metabolism. *Sphingolipids as Signaling and Regulatory Molecules*. Springer.
- OSLOWSKI, C. M. & URANO, F. 2010. The binary switch between life and death of ER stressed beta cells. *Current opinion in endocrinology, diabetes, and obesity*, 17, 107.
- PALANKI, M. 2002. Inhibitors of AP-1 and NF- κ B mediated transcriptional activation: therapeutic potential in autoimmune diseases and structural diversity. *Current medicinal chemistry*, 9, 219-227.
- PANGENI, R. P., CHANNATHODIYIL, P., HUEN, D. S., EAGLES, L. W., JOHAL, B. K., PASHA, D., HADJISTEPHANOU, N., NEVELL, O., DAVIES, C. L. & ADEWUMI, A. I. 2015. The GALNT9, BNC1 and CCDC8 genes are frequently epigenetically dysregulated in breast tumours that metastasise to the brain. *Clinical epigenetics*, 7, 57.
- PARK, E.-S., CHOI, S., SHIN, B., YU, J., YU, J., HWANG, J.-M., YUN, H., CHUNG, Y.-H., CHOI, J.-S. & CHOI, Y. 2015. Tumor necrosis factor (TNF) receptor-associated factor (TRAF)-interacting protein (TRIP) negatively regulates the TRAF2 ubiquitin-dependent pathway by suppressing the TRAF2-sphingosine 1-phosphate (S1P) interaction. *Journal of Biological Chemistry*, 290, 9660-9673.
- PARK, J.-B., LEE, J.-K., PARK, E.-Y. & RIEW, K. D. 2008. Fas/FasL interaction of nucleus pulposus and cancer cells with the activation of caspases. *International orthopaedics*, 32, 835-840.
- PASCHALL, A. V., YANG, D., LU, C., CHOI, J.-H., LI, X., LIU, F., FIGUEROA, M., OBERLIES, N. H., PEARCE, C. & BOLLAG, W. B. 2015. H3K9 trimethylation silences Fas expression to confer colon carcinoma immune escape and 5-fluorouracil chemoresistance. *The Journal of Immunology*, 1402243.

- PATTINGRE, S., BAUVY, C., LEVADE, T., LEVINE, B. & CODOGNO, P. 2009. Ceramide-induced autophagy: to junk or to protect cells? *Autophagy*, 5, 558-560.
- PATWARDHAN, G. A., BEVERLY, L. J. & SISKIND, L. J. 2016. Sphingolipids and mitochondrial apoptosis. *Journal of bioenergetics and biomembranes*, 48, 153-168.
- PAUGH, S. W., PAYNE, S. G., BARBOUR, S. E., MILSTIEN, S. & SPIEGEL, S. 2003. The immunosuppressant FTY720 is phosphorylated by sphingosine kinase type 2. *FEBS letters*, 554, 189-193.
- PÉBAY, A., WONG, R. C., PITSON, S. M., WOLVETANG, E. J., PEH, G. S. L., FILIPCZYK, A., KOH, K. L., TELLIS, I., NGUYEN, L. T. & PERA, M. F. 2005. Essential Roles of Sphingosine-1-Phosphate and Platelet-Derived Growth Factor in the Maintenance of Human Embryonic Stem Cells. *Stem Cells*, 23, 1541-1548.
- PENG, J., SCHWARTZ, D., ELIAS, J. E., THOREEN, C. C., CHENG, D., MARSISCHKY, G., ROELOFS, J., FINLEY, D. & GYGI, S. P. 2003. A proteomics approach to understanding protein ubiquitination. *Nature biotechnology*, 21, 921.
- PERKINS, N. & GILMORE, T. 2006. Good cop, bad cop: the different faces of NF- κ B. *Cell death and differentiation*, 13, 759.
- PICK, L. & BIELSCHOWSKY, M. 1927. Über lipoidzellige Splenomegalie (Typus Niemann-Pick) und amaurotische Idiotie. *Klin Wschr*, 6, 1631-1632.
- PICKART, C. M. 2001. Ubiquitin enters the new millennium. *Molecular cell*, 8, 499-504.
- PICKART, C. M. & FUSHMAN, D. 2004. Polyubiquitin chains: polymeric protein signals. *Current opinion in chemical biology*, 8, 610-616.
- PINAL, N., CALLEJA, M. & MORATA, G. 2019. Pro-apoptotic and pro-proliferation functions of the JNK pathway of Drosophila: roles in cell competition, tumorigenesis and regeneration. *Open biology*, 9, 180256.
- PITMAN, M. R., COSTABILE, M. & PITSON, S. M. 2016. Recent advances in the development of sphingosine kinase inhibitors. *Cellular signalling*, 28, 1349-1363.
- PITMAN, M. R., WOODCOCK, J. M., LOPEZ, A. F. & PITSON, S. M. 2012. Molecular targets of FTY720 (fingolimod). *Current molecular medicine*, 12, 1207-1219.
- PITSON, S. M. 2011a. Regulation of sphingosine kinase and sphingolipid signaling. *Trends in biochemical sciences*, 36, 97-107.
- PITSON, S. M. 2011b. Regulation of sphingosine kinase and sphingolipid signaling. *Trends Biochem Sci*, 36, 97-107.
- PITSON, S. M., MORETTI, P. A., ZEBOL, J. R., LYNN, H. E., XIA, P., VADAS, M. A. & WATTENBERG, B. W. 2003. Activation of sphingosine kinase 1 by ERK1/2-mediated phosphorylation. *The EMBO journal*, 22, 5491-5500.
- PITSON, S. M., MORETTI, P. A., ZEBOL, J. R., ZAREIE, R., DERIAN, C. K., DARROW, A. L., QI, J., D'ANDREA, R. J., BAGLEY, C. J. & VADAS, M. A. 2002. The nucleotide-binding site of human sphingosine kinase 1. *Journal of Biological Chemistry*, 277, 49545-49553.
- PITSON, S. M., XIA, P., LECLERCQ, T. M., MORETTI, P. A., ZEBOL, J. R., LYNN, H. E., WATTENBERG, B. W. & VADAS, M. A. 2005. Phosphorylation-dependent

- translocation of sphingosine kinase to the plasma membrane drives its oncogenic signalling. *Journal of Experimental Medicine*, 201, 49-54.
- PLOTNIKOV, A., ZEHORAI, E., PROCACCIA, S. & SEGER, R. 2011. The MAPK cascades: signaling components, nuclear roles and mechanisms of nuclear translocation. *Biochimica et Biophysica Acta (BBA)-Molecular Cell Research*, 1813, 1619-1633.
- POZNIAK, C. D., RADINOVIC, S., YANG, A., MCKEON, F., KAPLAN, D. R. & MILLER, F. D. 2000. An anti-apoptotic role for the p53 family member, p73, during developmental neuron death. *Science*, 289, 304-306.
- PRAKASH, H., LÜTH, A., GRINKINA, N., HOLZER, D., WADGAONKAR, R., GONZALEZ, A. P., ANES, E. & KLEUSER, B. 2010. Sphingosine kinase-1 (SphK-1) regulates Mycobacterium smegmatis infection in macrophages. *PLoS One*, 5, e10657.
- PULKOSKI-GROSS, M. J., JENKINS, M. L., TRUMAN, J.-P., SALAMA, M. F., CLARKE, C. J., BURKE, J. E., HANNUN, Y. A. & OBEID, L. M. 2018. An intrinsic lipid-binding interface controls sphingosine kinase 1 function. *Journal of lipid research*, 59, 462-474.
- PYNE, N. J., MCNAUGHTON, M., BOOMKAMP, S., MACRITCHIE, N., EVANGELISTI, C., MARTELLI, A. M., JIANG, H.-R., UBHI, S. & PYNE, S. 2016a. Role of sphingosine 1-phosphate receptors, sphingosine kinases and sphingosine in cancer and inflammation. *Advances in biological regulation*, 60, 151-159.
- PYNE, N. J. & PYNE, S. 2010. Sphingosine 1-phosphate and cancer. *Nature Reviews Cancer*, 10, 489.
- PYNE, N. J. & PYNE, S. 2017. Sphingosine kinase 2 and multiple myeloma. *Oncotarget*, 8, 43596.
- PYNE, S., ADAMS, D. R. & PYNE, N. J. 2016b. Sphingosine 1-phosphate and sphingosine kinases in health and disease: recent advances. *Progress in lipid research*, 62, 93-106.
- PYNE, S., ADAMS, D. R. & PYNE, N. J. 2018. Sphingosine kinases as druggable targets.
- PYNE, S., CHAPMAN, J., STEELE, L. & PYNE, N. J. 1996. Sphingomyelin- derived lipids differentially regulate the extracellular signal- regulated kinase 2 (ERK- 2) and c- Jun N- terminal kinase (JNK) signal cascades in airway smooth muscle. *European journal of biochemistry*, 237, 819-826.
- PYNE, S., LEE, S. C., LONG, J. & PYNE, N. J. 2009. Role of sphingosine kinases and lipid phosphate phosphatases in regulating spatial sphingosine 1-phosphate signalling in health and disease. *Cellular signalling*, 21, 14-21.
- PYNE, S. & PYNE, N. J. 2000. Sphingosine 1-phosphate signalling in mammalian cells. *Biochem J*, 349, 385-402.
- PYNE, S. & PYNE, N. J. 2011. Translational aspects of sphingosine 1-phosphate biology. *Trends Mol Med*, 17, 463-72.
- RAHMANIYAN, M., CURLEY, R. W., OBEID, L. M., HANNUN, Y. A. & KRAVEKA, J. M. 2011. Identification of dihydroceramide desaturase as a direct in vitro target for fenretinide. *Journal of Biological Chemistry*, jbc. M111. 250779.

- RAMAKRISHNA, S., KIM, K.-S. & BAEK, K.-H. 2014. Posttranslational modifications of defined embryonic reprogramming transcription factors. *Cellular reprogramming*, 16, 108-120.
- RAMAKRISHNA, S., SURESH, B. & BAEK, K.-H. 2011. The role of deubiquitinating enzymes in apoptosis. *Cellular and Molecular Life Sciences*, 68, 15-26.
- RAMAKRISHNA, S., SURESH, B. & BAEK, K.-H. 2015. Biological functions of hyaluronan and cytokine-inducible deubiquitinating enzymes. *Biochimica et Biophysica Acta (BBA)-Reviews on Cancer*, 1855, 83-91.
- REGGIORI, F. & KLIONSKY, D. J. 2002. Autophagy in the eukaryotic cell. *Eukaryotic cell*, 1, 11-21.
- REN, S., XIN, C., PFEILSCHIFTER, J. & HUWILER, A. 2010. A novel mode of action of the putative sphingosine kinase inhibitor 2-(p-hydroxyanilino)-4-(p-chlorophenyl) thiazole (SKI II): induction of lysosomal sphingosine kinase 1 degradation. *Cellular physiology and biochemistry*, 26, 97-104.
- REYES-TURCU, F. E., VENTII, K. H. & WILKINSON, K. D. 2009. Regulation and cellular roles of ubiquitin-specific deubiquitinating enzymes. *Annual review of biochemistry*, 78, 363-397.
- RICH, T., ALLEN, R. L. & WYLLIE, A. H. 2000. Defying death after DNA damage. *Nature*, 407, 777.
- RIENTO, K., ZHANG, Q., CLARK, J., BEGUM, F., STEPHENS, E., WAKELAM, M. J. & NICHOLS, B. J. 2018. Flotillin proteins recruit sphingosine to membranes and maintain cellular sphingosine-1-phosphate levels. *PLoS one*, 13, e0197401.
- RODRIGUEZ-CUENCA, S., BARBARROJA, N. & VIDAL-PUIG, A. 2015. Dihydroceramide desaturase 1, the gatekeeper of ceramide induced lipotoxicity. *Biochimica et Biophysica Acta (BBA)-Molecular and Cell Biology of Lipids*, 1851, 40-50.
- ROMIEU-MOUREZ, R., LANDESMAN-BOLLAG, E., SELDIN, D. C. & SONENSHEIN, G. E. 2002. Protein kinase CK2 promotes aberrant activation of nuclear factor- κ B, transformed phenotype, and survival of breast cancer cells. *Cancer research*, 62, 6770-6778.
- RON, D. & WALTER, P. 2007. Signal integration in the endoplasmic reticulum unfolded protein response. *Nature reviews Molecular cell biology*, 8, 519.
- ROTHWARF, D. M., ZANDI, E., NATOLI, G. & KARIN, M. 1998. IKK- γ is an essential regulatory subunit of the I κ B kinase complex. *Nature*, 395, 297.
- RUVOLO, P. P. 2003. Intracellular signal transduction pathways activated by ceramide and its metabolites. *Pharmacological research*, 47, 383-392.
- RUVOLO, P. P., DENG, X., ITO, T., CARR, B. K. & MAY, W. S. 1999. Ceramide induces Bcl2 dephosphorylation via a mechanism involving mitochondrial PP2A. *Journal of Biological Chemistry*, 274, 20296-20300.
- SADAHIRA, Y., RUAN, F., HAKOMORI, S.-I. & IGARASHI, Y. 1992. Sphingosine 1-phosphate, a specific endogenous signaling molecule controlling cell motility and tumor cell invasiveness. *Proceedings of the National Academy of Sciences*, 89, 9686-9690.
- SADOWSKI, M., SURYADINATA, R., TAN, A. R., ROESLEY, S. N. A. & SARCEVIC, B. 2012. Protein monoubiquitination and polyubiquitination generate

- structural diversity to control distinct biological processes. *IUBMB life*, 64, 136-142.
- SAKAKURA, C., SWEENEY, E., SHIRAHAMA, T., RUAN, F., SOLCA, F., KOHNO, M., HAKOMORI, S., FISCHER, E. & IGARASHI, Y. 1997. Inhibition of MAP kinase by sphingosine and its methylated derivative, N, N-dimethylsphingosine. *International journal of oncology*, 11, 31-39.
- SALVAT, C., JARIEL-ENCONTRE, I., ACQUAVIVA, C., OMURA, S. & PIECHACZYK, M. 1998. Differential directing of c-Fos and c-Jun proteins to the proteasome in serum-stimulated mouse embryo fibroblasts. *Oncogene*, 17, 327.
- SAMAD, F., HESTER, K. D., YANG, G., HANNUN, Y. A. & BIELAWSKI, J. 2006. Altered adipose and plasma sphingolipid metabolism in obesity: a potential mechanism for cardiovascular and metabolic risk. *Diabetes*, 55, 2579-2587.
- SANCHEZ, T., ESTRADA-HERNANDEZ, T., PAIK, J.-H., WU, M.-T., VENKATARAMAN, K., BRINKMANN, V., CLAFFEY, K. & HLA, T. 2003. Phosphorylation and action of the immunomodulator FTY720 inhibits VEGF-induced vascular permeability. *Journal of Biological Chemistry*.
- SANKALA, H. M., HAIT, N. C., PAUGH, S. W., SHIDA, D., LÉPINE, S., ELMORE, L. W., DENT, P., MILSTIEN, S. & SPIEGEL, S. 2007. Involvement of sphingosine kinase 2 in p53-independent induction of p21 by the chemotherapeutic drug doxorubicin. *Cancer research*, 67, 10466-10474.
- SCARLATTI, F., BAUVY, C., VENTRUTI, A., SALA, G., CLUZEAUD, F., VANDEWALLE, A., GHIDONI, R. & CODOGNO, P. 2004. Ceramide-mediated macroautophagy involves inhibition of protein kinase B and up-regulation of beclin 1. *Journal of Biological Chemistry*, 279, 18384-18391.
- SCHEIDEREIT, C. 2006. I κ B kinase complexes: gateways to NF- κ B activation and transcription. *Oncogene*, 25, 6685.
- SCHIEFLER, C., PIONTEK, G., DOESCHER, J., SCHUETTLER, D., MISSLBEC, M., RUDELIUS, M., HAUG, A., REITER, R., BROCKHOFF, G. & PICKHARD, A. 2014. Inhibition of SphK1 reduces radiation-induced migration and enhances sensitivity to cetuximab treatment by affecting the EGFR/SphK1 crosstalk. *Oncotarget*, 5, 9877.
- SCHMITZ, M. L. & BAEUERLE, P. A. 1991. The p65 subunit is responsible for the strong transcription activating potential of NF- κ B. *The EMBO journal*, 10, 3805-3817.
- SCHNUTE, M. E., MCREYNOLDS, M. D., KASTEN, T., YATES, M., JEROME, G., RAINS, J. W., HALL, T., CHRENCIK, J., KRAUS, M. & CRONIN, C. N. 2012. Modulation of cellular S1P levels with a novel, potent and specific inhibitor of sphingosine kinase-1. *Biochemical Journal*, 444, 79-88.
- SCHÖNTHAL, A. H. 2012. Endoplasmic reticulum stress: its role in disease and novel prospects for therapy. *Scientifica*, 2012.
- SCHRADER, E. K., HARSTAD, K. G. & MATOUSCHEK, A. 2009. Targeting proteins for degradation. *Nature chemical biology*, 5, 815.
- SCHRECENGOST, R. S., KELLER, S. N., SCHIEWER, M. J., KNUDSEN, K. E. & SMITH, C. D. 2015. Downregulation of critical oncogenes by the selective SK2

- inhibitor ABC294640 hinders prostate cancer progression. *Molecular cancer research*, molcanres. 0626.2014.
- SCHUBERT, K. M., SCHEID, M. P. & DURONIO, V. 2000. Ceramide inhibits protein kinase B/Akt by promoting dephosphorylation of serine 473. *Journal of Biological Chemistry*, 275, 13330-13335.
- SEMBRITZKI, O., HAGEL, C., LAMSZUS, K., DEPPERT, W. & BOHN, W. 2002. Cytoplasmic localization of wild-type p53 in glioblastomas correlates with expression of vimentin and glial fibrillary acidic protein. *Neuro-oncology*, 4, 171-178.
- SEN, R. & BALTIMORE, D. 1986. Multiple nuclear factors interact with the immunoglobulin enhancer sequences. *cell*, 46, 705-716.
- SENTELLE, R. D., SENKAL, C. E., JIANG, W., PONNUSAMY, S., GENCER, S., SELVAM, S. P., RAMSHESH, V. K., PETERSON, Y. K., LEMASTERS, J. J. & SZULC, Z. M. 2012. Ceramide targets autophagosomes to mitochondria and induces lethal mitophagy. *Nature chemical biology*, 8, 831.
- SETHI, G., AHN, K., CHATURVEDI, M. & AGGARWAL, B. 2007. Epidermal growth factor (EGF) activates nuclear factor- κ B through I κ B α kinase-independent but EGF receptor-kinase dependent tyrosine 42 phosphorylation of I κ B α . *Oncogene*, 26, 7324.
- SEZGIN, E., LEVENTAL, I., GRZYBEK, M., SCHWARZMANN, G., MUELLER, V., HONIGMANN, A., BELOV, V. N., EGGELING, C., COSKUN, Ü. & SIMONS, K. 2012. Partitioning, diffusion, and ligand binding of raft lipid analogs in model and cellular plasma membranes. *Biochimica et Biophysica Acta (BBA)-Biomembranes*, 1818, 1777-1784.
- SHANER, R. L., ALLEGOOD, J. C., PARK, H., WANG, E., KELLY, S., HAYNES, C. A., SULLARDS, M. C. & MERRILL, A. H. 2009. Quantitative analysis of sphingolipids for lipidomics using triple quadrupole and quadrupole linear ion trap mass spectrometers. *Journal of lipid research*, 50, 1692-1707.
- SHARPLESS, N. E. & DEPINHO, R. A. 2002. p53: good cop/bad cop. *Cell*, 110, 9-12.
- SHAULIAN, E. & KARIN, M. 2002. AP-1 as a regulator of cell life and death. *Nature cell biology*, 4, E131.
- SHAW, P., BOVEY, R., TARDY, S., SAHLI, R., SORDAT, B. & COSTA, J. 1992. Induction of apoptosis by wild-type p53 in a human colon tumor-derived cell line. *Proceedings of the National Academy of Sciences*, 89, 4495-4499.
- SHEN, H., GIORDANO, F., WU, Y., CHAN, J., ZHU, C., MILOSEVIC, I., WU, X., YAO, K., CHEN, B. & BAUMGART, T. 2014. Coupling between endocytosis and sphingosine kinase 1 recruitment. *Nature cell biology*, 16, 652.
- SHIOZAWA, S., SHIMIZU, K., TANAKA, K. & HINO, K. 1997. Studies on the contribution of c-fos/AP-1 to arthritic joint destruction. *The Journal of clinical investigation*, 99, 1210-1216.
- SIDDIQUE, M. M., BIKMAN, B. T., WANG, L., YING, L., REINHARDT, E., SHUI, G., WENK, M. R. & SUMMERS, S. A. 2012. Ablation of dihydroceramide desaturase confers resistance to etoposide-induced apoptosis in vitro. *PLoS One*, 7, e44042.

- SIDDIQUE, M. M., LI, Y., CHAURASIA, B., KADDAI, V. A. & SUMMERS, S. A. 2015. Dihydroceramides: from bit players to lead actors. *Journal of Biological Chemistry*, 290, 15371-15379.
- SIDDIQUE, M. M., LI, Y., WANG, L., CHING, J., MAL, M., ILKAYEVA, O., WU, Y. J., BAY, B. H. & SUMMERS, S. A. 2013. Ablation of dihydroceramide desaturase 1, a therapeutic target for the treatment of metabolic diseases, simultaneously stimulates anabolic and catabolic signaling. *Molecular and cellular biology*, 33, 2353-2369.
- SIDI, S., SANDA, T., KENNEDY, R. D., HAGEN, A. T., JETTE, C. A., HOFFMANS, R., PASCUAL, J., IMAMURA, S., KISHI, S. & AMATRUDA, J. F. 2008. Chk1 suppresses a caspase-2 apoptotic response to DNA damage that bypasses p53, Bcl-2, and caspase-3. *Cell*, 133, 864-877.
- SIGNORELLI, P., MUNOZ-OLAYA, J. M., GAGLIOSTRO, V., CASAS, J., GHIDONI, R. & FABRIÀS, G. 2009. Dihydroceramide intracellular increase in response to resveratrol treatment mediates autophagy in gastric cancer cells. *Cancer letters*, 282, 238-243.
- SIMONS, K. & IKONEN, E. 1997. Functional rafts in cell membranes. *Nature*, 387, 569.
- SISKIND, L. J. 2005. Mitochondrial ceramide and the induction of apoptosis. *Journal of bioenergetics and biomembranes*, 37, 143-153.
- SISKIND, L. J. & COLOMBINI, M. 2000. The lipids C2-and C16-ceramide form large stable channels Implications for apoptosis. *Journal of Biological Chemistry*, 275, 38640-38644.
- SKOURA, A. & HLA, T. 2009a. Lysophospholipid receptors in vertebrate development, physiology, and pathology. *Journal of lipid research*, 50, S293-S298.
- SKOURA, A. & HLA, T. 2009b. Regulation of vascular physiology and pathology by the S1P2 receptor subtype. *Cardiovascular research*, 82, 221-228.
- SMITH, A. E., SMITH, R. & PAUCHA, E. 1979. Characterization of different tumor antigens present in cells transformed by simian virus 40. *Cell*, 18, 335-346.
- SMITH, E., MERRILL, A., OBEID, L. M. & HANNUN, Y. A. 2000. Effects of sphingosine and other sphingolipids on protein kinase C. *Methods in enzymology*, 312, 361-373.
- SNIDER, A. J., KAWAMORI, T., BRADSHAW, S. G., ORR, K. A., GILKESON, G. S., HANNUN, Y. A. & OBEID, L. M. 2009. A role for sphingosine kinase 1 in dextran sulfate sodium-induced colitis. *The FASEB Journal*, 23, 143-152.
- SOLOFF, M. S., IZBAN, M. G., COOK JR, D. L., JENG, Y.-J. & MIFFLIN, R. C. 2006. Interleukin-1-induced NF- κ B recruitment to the oxytocin receptor gene inhibits RNA polymerase II-promoter interactions in cultured human myometrial cells. *Molecular human reproduction*, 12, 619-624.
- SONG, K., DAI, L., LONG, X., CUI, X., LIU, Y. & DI, W. 2019. Sphingosine kinase 2 inhibitor ABC294640 displays anti-epithelial ovarian cancer activities in vitro and in vivo. *OncoTargets and Therapy*, 12, 4437-4449.
- SPASSIEVA, S. D., MULLEN, T. D., TOWNSEND, D. M. & OBEID, L. M. 2009. Disruption of ceramide synthesis by CerS2 down-regulation leads to

- autophagy and the unfolded protein response. *Biochemical Journal*, 424, 273-283.
- SPIEGEL, S. & MILSTIEN, S. 2003. Sphingosine-1-phosphate: an enigmatic signalling lipid. *Nature reviews Molecular cell biology*, 4, 397.
- SRIDEVI, P., ALEXANDER, H., LAVIAD, E. L., MIN, J., MESIKA, A., HANNINK, M., FUTERMAN, A. H. & ALEXANDER, S. 2010. Stress-induced ER to Golgi translocation of ceramide synthase 1 is dependent on proteasomal processing. *Experimental cell research*, 316, 78-91.
- SRIVASTAVA, S., ZOU, Z., PIROLLO, K., BLATTNER, W. & CHANG, E. H. 1990. Germ-line transmission of a mutated p53 gene in a cancer-prone family with Li-Fraumeni syndrome. *Nature*, 348, 747.
- STAHELIN, R. V., HWANG, J. H., KIM, J.-H., PARK, Z.-Y., JOHNSON, K. R., OBEID, L. M. & CHO, W. 2005. The mechanism of membrane targeting of human sphingosine kinase 1. *Journal of Biological Chemistry*, 280, 43030-43038.
- STIBAN, J., FISTERE, D. & COLOMBINI, M. 2006. Dihydroceramide hinders ceramide channel formation: implications on apoptosis. *Apoptosis*, 11, 773-780.
- STROCHLIC, L., DWIVEDY, A., VAN HORCK, F. P., FALK, J. & HOLT, C. E. 2008. A role for S1P signalling in axon guidance in the *Xenopus* visual system. *Development*, 135, 333-342.
- STRUB, G. M., MACEYKA, M., HAIT, N. C., MILSTIEN, S. & SPIEGEL, S. 2010. Extracellular and intracellular actions of sphingosine-1-phosphate. *Sphingolipids as Signaling and Regulatory Molecules*. Springer.
- STRUB, G. M., PAILLARD, M., LIANG, J., GOMEZ, L., ALLEGOOD, J. C., HAIT, N. C., MACEYKA, M., PRICE, M. M., CHEN, Q. & SIMPSON, D. C. 2011. Sphingosine-1-phosphate produced by sphingosine kinase 2 in mitochondria interacts with prohibitin 2 to regulate complex IV assembly and respiration. *The FASEB Journal*, 25, 600-612.
- SU, Y., ROSENTHAL, D., SMULSON, M. & SPIEGEL, S. 1994. Sphingosine 1-phosphate, a novel signaling molecule, stimulates DNA binding activity of AP-1 in quiescent Swiss 3T3 fibroblasts. *Journal of Biological Chemistry*, 269, 16512-16517.
- SUGIKI, H., HOZUMI, Y., MAESHIMA, H., KATAGATA, Y., MITSUHASHI, Y. & KONDO, S. 2000. C2- ceramide induces apoptosis in a human squamous cell carcinoma cell line. *British Journal of Dermatology*, 143, 1154-1163.
- SUI, X., JIN, L., HUANG, X., GENG, S., HE, C. & HU, X. 2011. p53 signaling and autophagy in cancer: a revolutionary strategy could be developed for cancer treatment. *Autophagy*, 7, 565-571.
- SULLARDS, M. C., LIU, Y., CHEN, Y. & MERRILL JR, A. H. 2011. Analysis of mammalian sphingolipids by liquid chromatography tandem mass spectrometry (LC-MS/MS) and tissue imaging mass spectrometry (TIMS). *Biochimica et Biophysica Acta (BBA)-Molecular and Cell Biology of Lipids*, 1811, 838-853.
- SUMMERS, S. A. 2018. Could ceramides become the new cholesterol? *Cell metabolism*, 27, 276-280.
- SUNDARAMOORTHY, P., GASPARETTO, C. & KANG, Y. 2018. The combination of a sphingosine kinase 2 inhibitor (ABC294640) and a Bcl- 2 inhibitor

- (ABT- 199) displays synergistic anti- myeloma effects in myeloma cells without at (11; 14) translocation. *Cancer medicine*, 7, 3257-3268.
- SURESH, B., LEE, J., KIM, K.-S. & RAMAKRISHNA, S. 2016. The importance of ubiquitination and deubiquitination in cellular reprogramming. *Stem cells international*, 2016.
- SUTO, M. J. & RANSONE, L. J. 1997. Novel Approaches for the Treatment of Inflammatory Diseases: Inhibitors of NF- κ B and AP-1. *Current pharmaceutical design*, 3, 515.
- SVENSSON, C., PART, K., KÜNNIS-BERES, K., KALDMÄE, M., FERNAEUS, S. Z. & LAND, T. 2011. Pro-survival effects of JNK and p38 MAPK pathways in LPS-induced activation of BV-2 cells. *Biochemical and biophysical research communications*, 406, 488-492.
- SWEENEY, E. A., INOKUCHI, J.-I. & IGARASHI, Y. 1998. Inhibition of sphingolipid induced apoptosis by caspase inhibitors indicates that sphingosine acts in an earlier part of the apoptotic pathway than ceramide. *FEBS letters*, 425, 61-65.
- TAHA, T. A., HANNUN, Y. A. & OBEID, L. M. 2006a. Sphingosine kinase: biochemical and cellular regulation and role in disease. *BMB Reports*, 39, 113-131.
- TAHA, T. A., KITATANI, K., EL-ALWANI, M., BIELAWSKI, J., HANNUN, Y. A. & OBEID, L. M. 2006b. Loss of sphingosine kinase-1 activates the intrinsic pathway of programmed cell death: modulation of sphingolipid levels and the induction of apoptosis. *The FASEB journal*, 20, 482-484.
- TAKABE, K., PAUGH, S. W., MILSTIEN, S. & SPIEGEL, S. 2008. "Inside-out" signaling of sphingosine-1-phosphate: therapeutic targets. *Pharmacological reviews*, 60, 181-195.
- TALBOTT, C. M., VOROBYOV, I., BORCHMAN, D., TAYLOR, K. G., DUPRÉ, D. B. & YAPPERT, M. C. 2000. Conformational studies of sphingolipids by NMR spectroscopy. II. Sphingomyelin. *Biochimica et Biophysica Acta (BBA)-Biomembranes*, 1467, 326-337.
- TANI, M., ITO, M. & IGARASHI, Y. 2007. Ceramide/sphingosine/sphingosine 1-phosphate metabolism on the cell surface and in the extracellular space. *Cellular signalling*, 19, 229-237.
- TANIDA, I., UENO, T. & KOMINAMI, E. 2004. Human light chain 3/MAP1LC3B is cleaved at its carboxyl-terminal Met121 to expose Gly120 for lipidation and targeting to autophagosomal membranes. *Journal of Biological Chemistry*, 279, 47704-47710.
- TASDEMIR, E., MAIURI, M. C., GALLUZZI, L., VITALE, I., DJAVAHERI-MERGNY, M., D'AMELIO, M., CRIOLLO, A., MORSELLI, E., ZHU, C. & HARPER, F. 2008. Regulation of autophagy by cytoplasmic p53. *Nature cell biology*, 10, 676.
- TEO, J.-L. & KAHN, M. 2004. AP-1 as a potential therapeutic target in allergic airways inflammation. *Drugs Future*, 29, 693-703.
- TERNES, P., FRANKE, S., ZÄHRINGER, U., SPERLING, P. & HEINZ, E. 2002. Identification and characterization of a sphingolipid Δ 4-desaturase family. *Journal of Biological Chemistry*, 277, 25512-25518.

- THOMPSON, R., SHAH, R. B., LIU, P. H., GUPTA, Y. K., ANDO, K., AGGARWAL, A. K. & SIDI, S. 2015. An inhibitor of PIDDosome formation. *Molecular cell*, 58, 767-779.
- THUDICUM, J. 1884. A treatise on the chemical composition of the brain. *Bailliere, Tindall and Cox, London*.
- TOLAN, D., CONWAY, A. M., STEELE, L., PYNE, S. & PYNE, N. J. 1996. The identification of DL- threo dihydrosphingosine and sphingosine as novel inhibitors of extracellular signal- regulated kinase signalling in airway smooth muscle. *British journal of pharmacology*, 119, 185-186.
- TONELLI, F., ALOSSAIMI, M., NATARAJAN, V., GORSHKOVA, I., BERDYSHEV, E., BITTMAN, R., WATSON, D. G., PYNE, S. & PYNE, N. J. 2013. The roles of sphingosine kinase 1 and 2 in regulating the metabolome and survival of prostate cancer cells. *Biomolecules*, 3, 316-333.
- TONELLI, F., LIM, K. G., LOVERIDGE, C., LONG, J., PITSON, S. M., TIGYI, G., BITTMAN, R., PYNE, S. & PYNE, N. J. 2010. FTY720 and (S)-FTY720 vinylphosphonate inhibit sphingosine kinase 1 and promote its proteasomal degradation in human pulmonary artery smooth muscle, breast cancer and androgen-independent prostate cancer cells. *Cellular signalling*, 22, 1536-1542.
- TRAVERS, K. J., PATIL, C. K., WODICKA, L., LOCKHART, D. J., WEISSMAN, J. S. & WALTER, P. 2000. Functional and genomic analyses reveal an essential coordination between the unfolded protein response and ER-associated degradation. *Cell*, 101, 249-258.
- TREIER, M., STASZEWSKI, L. M. & BOHMANN, D. 1994. Ubiquitin-dependent c-Jun degradation in vivo is mediated by the δ domain. *Cell*, 78, 787-798.
- UEDA, H., ULLRICH, S. J., GANGEMI, J. D., KAPPEL, C. A., NGO, L., FEITELSON, M. A. & JAY, G. 1995. Functional inactivation but not structural mutation of p53 causes liver cancer. *Nature genetics*, 9, 41.
- UYAMA, R., HONG, S., NAKAGAWA, T., YAZAWA, M., KADOSAWA, T., MOCHIZUKI, M., TSUJIMOTO, H., NISHIMURA, R. & SASAKI, N. 2005. Establishment and characterization of eight feline mammary adenocarcinoma cell lines. *The Journal of veterinary medical science*, 67, 1273-1276.
- VACARU, A. M., TAFESSE, F. G., TERNES, P., KONDYLLIS, V., HERMANSSON, M., BROUWERS, J. F., SOMERHARJU, P., RABOUILLE, C. & HOLTHUIS, J. C. 2009. Sphingomyelin synthase-related protein SMSr controls ceramide homeostasis in the ER. *The Journal of cell biology*, 185, 1013-1027.
- VALLABHAPURAPU, S., MATSUZAWA, A., ZHANG, W., TSENG, P.-H., KEATS, J. J., WANG, H., VIGNALI, D. A., BERGSAGEL, P. L. & KARIN, M. 2008. Nonredundant and complementary functions of TRAF2 and TRAF3 in a ubiquitination cascade that activates NIK-dependent alternative NF- κ B signaling. *Nature immunology*, 9, 1364.
- VAN MEER, G. & HOLTHUIS, J. C. 2000. Sphingolipid transport in eukaryotic cells. *Biochimica et Biophysica Acta (BBA)-Molecular and Cell Biology of Lipids*, 1486, 145-170.
- VENABLE, M. E., LEE, J. Y., SMYTH, M. J., BIELAWSKA, A. & OBEID, L. M. 1995. Role of ceramide in cellular senescence. *Journal of Biological Chemistry*, 270, 30701-30708.

- VENABLE, M. E. & YIN, X. 2009. Ceramide induces endothelial cell senescence. *Cell Biochemistry and Function: Cellular biochemistry and its modulation by active agents or disease*, 27, 547-551.
- VENANT, H., RAHMANYAN, M., JONES, E. E., LU, P., LILLY, M. B., GARRETT-MAYER, E., DRAKE, R. R., KRAVEKA, J. M., SMITH, C. D. & VOELKEL-JOHNSON, C. 2015. The sphingosine kinase 2 inhibitor ABC294640 reduces the growth of prostate cancer cells and results in accumulation of dihydroceramides in vitro and in vivo. *Molecular cancer therapeutics*, 14, 2744-2752.
- VENKATA, J. K., AN, N., STUART, R., COSTA, L. J., CAI, H., COKER, W., SONG, J. H., GIBBS, K., MATSON, T. & GARRETT-MAYER, E. 2014. Inhibition of sphingosine kinase 2 down-regulates the expression of c-Myc and Mcl-1 and induces apoptosis in multiple myeloma. *Blood*, blood-2014-03-559385.
- VESSEY, D. A., KELLEY, M., ZHANG, J., LI, L., TAO, R. & KARLINER, J. S. 2007. Dimethylsphingosine and FTY720 inhibit the SK1 form but activate the SK2 form of sphingosine kinase from rat heart. *Journal of biochemical and molecular toxicology*, 21, 273-279.
- VIATOUR, P., MERVILLE, M.-P., BOURS, V. & CHARIOT, A. 2005. Phosphorylation of NF- κ B and I κ B proteins: implications in cancer and inflammation. *Trends in biochemical sciences*, 30, 43-52.
- VIGNERON, A. & VOUSDEN, K. H. 2010. p53, ROS and senescence in the control of aging. *Aging (Albany NY)*, 2, 471.
- VILLANI, M. G., APPIERTO, V., CAVADINI, E., BETTIGA, A., PRINETTI, A., CLAGETT-DAME, M., CURLEY, R. W. & FORMELLI, F. 2006. 4-oxo-fenretinide, a recently identified fenretinide metabolite, induces marked G2-M cell cycle arrest and apoptosis in fenretinide-sensitive and fenretinide-resistant cell lines. *Cancer research*, 66, 3238-3247.
- VOGELSTEIN, B., LANE, D. & LEVINE, A. J. 2000. Surfing the p53 network. *Nature*, 408, 307.
- VOLMER, R. & RON, D. 2015. Lipid-dependent regulation of the unfolded protein response. *Current opinion in cell biology*, 33, 67-73.
- VOLMER, R., VAN DER PLOEG, K. & RON, D. 2013. Membrane lipid saturation activates endoplasmic reticulum unfolded protein response transducers through their transmembrane domains. *Proceedings of the National Academy of Sciences*, 110, 4628-4633.
- VON HAEFEN, C., WIEDER, T., GILLISSEN, B., STAÈRCK, L., GRAUPNER, V., DOÈRKEN, B. & DANIEL, P. T. 2002. Ceramide induces mitochondrial activation and apoptosis via a Bax-dependent pathway in human carcinoma cells. *Oncogene*, 21, 4009.
- VOUSDEN, K. H. & LU, X. 2002. Live or let die: the cell's response to p53. *Nature Reviews Cancer*, 2, 594.
- VU, T. M., ISHIZU, A.-N., FOO, J. C., TOH, X. R., ZHANG, F., WHEE, D. M., TORTA, F., CAZENAVE-GASSIOT, A., MATSUMURA, T. & KIM, S. 2017. Mfsd2b is essential for the sphingosine-1-phosphate export in erythrocytes and platelets. *Nature*, 550, 524.

- WADGAONKAR, R., PATEL, V., GRINKINA, N., ROMANO, C., LIU, J., ZHAO, Y., SAMMANI, S., PROIA, R., GARCIA, J. G. & NATARAJAN, V. 2009. Differential regulation of sphingosine kinases 1 and 2 in lung injury. *American Journal of Physiology-Lung Cellular and Molecular Physiology*.
- WAHL, G. M. & CARR, A. M. 2001. The evolution of diverse biological responses to DNA damage: insights from yeast and p53. *Nature cell biology*, 3, E277.
- WALLINGTON-BEDDOE, C. T., BENNETT, M. K., VANDYKE, K., DAVIES, L., ZEBOL, J. R., MORETTI, P. A., PITMAN, M. R., HEWETT, D. R., ZANNETTINO, A. C. & PITSON, S. M. 2017. Sphingosine kinase 2 inhibition synergises with bortezomib to target myeloma by enhancing endoplasmic reticulum stress. *Oncotarget*, 8, 43602.
- WALLINGTON-BEDDOE, C. T., POWELL, J. A., TONG, D., PITSON, S. M., BRADSTOCK, K. F. & BENDALL, L. J. 2014. Sphingosine kinase 2 promotes acute lymphoblastic leukemia by enhancing MYC expression. *Cancer research*, canres. 2732.2013.
- WANG, A., AL-KUHLANI, M., JOHNSTON, S. C., OJCIUS, D. M., CHOU, J. & DEAN, D. 2013a. Transcription factor complex AP-1 mediates inflammation initiated by *Chlamydia pneumoniae* infection. *Cellular microbiology*, 15, 779-794.
- WANG, H., MAURER, B. J., LIU, Y.-Y., WANG, E., ALLEGOOD, J. C., KELLY, S., SYMOLON, H., LIU, Y., MERRILL, A. H. & GOUAZÉ-ANDERSSON, V. 2008. N-(4-Hydroxyphenyl) retinamide increases dihydroceramide and synergizes with dimethylsphingosine to enhance cancer cell killing. *Molecular cancer therapeutics*, 7, 2967-2976.
- WANG, J., CUI, D., GU, S., CHEN, X., BI, Y., XIONG, X. & ZHAO, Y. 2018. Autophagy regulates apoptosis by targeting NOXA for degradation. *Biochimica et Biophysica Acta (BBA)-Molecular Cell Research*, 1865, 1105-1113.
- WANG, J., KNAPP, S., PYNE, N. J., PYNE, S. & ELKINS, J. M. 2014. Crystal structure of sphingosine kinase 1 with PF-543. *ACS medicinal chemistry letters*, 5, 1329-1333.
- WANG, X. & RON, D. 1996. Stress-induced phosphorylation and activation of the transcription factor CHOP (GADD153) by p38 MAP kinase. *Science*, 272, 1347-1349.
- WANG, Z., MIN, X., XIAO, S.-H., JOHNSTONE, S., ROMANOW, W., MEININGER, D., XU, H., LIU, J., DAI, J. & AN, S. 2013b. Molecular basis of sphingosine kinase 1 substrate recognition and catalysis. *Structure*, 21, 798-809.
- WATSON, D. G., TONELLI, F., ALOSSAIMI, M., WILLIAMSON, L., CHAN, E., GORSHKOVA, I., BERDYSHEV, E., BITTMAN, R., PYNE, N. J. & PYNE, S. 2013. ti. *Cellular signalling*, 25, 1011-1017.
- WATTENBERG, B. W. 2010. Role of sphingosine kinase localization in sphingolipid signaling. *World journal of biological chemistry*, 1, 362.
- WEI, M. C., ZONG, W.-X., CHENG, E. H.-Y., LINDSTEN, T., PANOUTSAKOPOULOU, V., ROSS, A. J., ROTH, K. A., MACGREGOR, G. R., THOMPSON, C. B. & KORSMEYER, S. J. 2001. Proapoptotic BAX and BAK: a requisite gateway to mitochondrial dysfunction and death. *Science*, 292, 727-730.

- WEI, Y., PATTINGRE, S., SINHA, S., BASSIK, M. & LEVINE, B. 2008. JNK1-mediated phosphorylation of Bcl-2 regulates starvation-induced autophagy. *Molecular cell*, 30, 678-688.
- WEIGERT, A., SCHIFFMANN, S., SEKAR, D., LEY, S., MENRAD, H., WERNO, C., GROSCH, S., GEISSLINGER, G. & BRÜNE, B. 2009. Sphingosine kinase 2 deficient tumor xenografts show impaired growth and fail to polarize macrophages towards an anti-inflammatory phenotype. *International journal of cancer*, 125, 2114-2121.
- WEISSMAN, A. M. 2001. Ubiquitin and proteasomes: themes and variations on ubiquitylation. *Nature reviews Molecular cell biology*, 2, 169.
- WENK, M. R. 2005. The emerging field of lipidomics. *Nature reviews Drug discovery*, 4, 594.
- WHITE-GILBERTSON, S., HUA, Y. & LIU, B. 2013. The role of endoplasmic reticulum stress in maintaining and targeting multiple myeloma: a double-edged sword of adaptation and apoptosis. *Frontiers in genetics*, 4, 109.
- WOODCOCK, J. M., COOLEN, C., GOODWIN, K. L., BAEK, D. J., BITTMAN, R., SAMUEL, M. S., PITSON, S. M. & LOPEZ, A. F. 2015. Destabilisation of dimeric 14-3-3 proteins as a novel approach to anti-cancer therapeutics. *Oncotarget*, 6, 14522.
- WOODCOCK, J. M., MURPHY, J., STOMSKI, F. C., BERNDT, M. C. & LOPEZ, A. F. 2003. The dimeric versus monomeric status of 14-3-3 ζ is controlled by phosphorylation of Ser58 at the dimer interface. *Journal of Biological Chemistry*, 278, 36323-36327.
- WOOLFSON, D. N. 2005. The design of coiled-coil structures and assemblies. *Advances in protein chemistry*. Elsevier.
- WU, G. S., BURNS, T. F., MCDONALD, E. R., JIANG, W., MENG, R., KRANTZ, I. D., KAO, G., GAN, D.-D., ZHOU, J.-Y. & MUSCHEL, R. 1997. KILLER/DR5 is a DNA damage-inducible p53-regulated death receptor gene. *Nature genetics*, 17, 141-143.
- WU, J., DIPIETRANTONIO, A. & HSIEH, T.-C. 2001. Mechanism of fenretinide (4-HPR)-induced cell death. *Apoptosis*, 6, 377-388.
- WU, Q., WU, W., FU, B., SHI, L., WANG, X. & KUCA, K. 2019. JNK signaling in cancer cell survival. *Medicinal research reviews*.
- XIA, P., WANG, L., GAMBLE, J. R. & VADAS, M. A. 1999. Activation of sphingosine kinase by tumor necrosis factor- α inhibits apoptosis in human endothelial cells. *Journal of Biological Chemistry*, 274, 34499-34505.
- XIA, P., WANG, L., MORETTI, P. A., ALBANESE, N., CHAI, F., PITSON, S. M., D'ANDREA, R. J., GAMBLE, J. R. & VADAS, M. A. 2002. Sphingosine kinase interacts with TRAF2 and dissects tumor necrosis factor- α signaling. *Journal of Biological Chemistry*, 277, 7996-8003.
- XIA, Y., WANG, J., LIU, T.-J., YUNG, W. A., HUNTER, T. & LU, Z. 2007. c-Jun downregulation by HDAC3-dependent transcriptional repression promotes osmotic stress-induced cell apoptosis. *Molecular cell*, 25, 219-232.

- XIA, Z., DICKENS, M., RAINGEAUD, J., DAVIS, R. J. & GREENBERG, M. E. 1995. Opposing effects of ERK and JNK-p38 MAP kinases on apoptosis. *Science*, 270, 1326-1331.
- XIN, M. & DENG, X. 2006. Protein phosphatase 2A enhances the proapoptotic function of Bax through dephosphorylation. *Journal of Biological Chemistry*, 281, 18859-18867.
- XING, H., ZHANG, S., WEINHEIMER, C., KOVACS, A. & MUSLIN, A. J. 2000. 14- 3- 3 proteins block apoptosis and differentially regulate MAPK cascades. *The EMBO journal*, 19, 349-358.
- XIONG, Y., LEE, H. J., MARIKO, B., LU, Y.-C., DANNENBERG, A. J., HAKA, A. S., MAXFIELD, F. R., CAMERER, E., PROIA, R. L. & HLA, T. 2013. Sphingosine kinases are not required for inflammatory responses in macrophages. *Journal of Biological Chemistry*, 288, 32563-32573.
- XU, L., JIN, L., YANG, B., WANG, L., XIA, Z., ZHANG, Q. & XU, J. 2018. The sphingosine kinase 2 inhibitor ABC294640 inhibits cervical carcinoma cell growth. *Oncotarget*, 9, 2384.
- XU, T., LI, L., HUANG, C., PENG, Y. & LI, J. 2014. Sphingosine kinase 2: a controversial role in arthritis. *Rheumatology international*, 34, 1015-1016.
- YAMAGUCHI, K., LANTOWSKI, A., DANNENBERG, A. J. & SUBBARAMAIAH, K. 2005. Histone deacetylase inhibitors suppress the induction of c-Jun and its target genes including COX-2. *Journal of Biological Chemistry*, 280, 32569-32577.
- YAMAJI, T. & HANADA, K. 2015. Sphingolipid metabolism and interorganellar transport: localization of sphingolipid enzymes and lipid transfer proteins. *Traffic*, 16, 101-122.
- YANG, A., KAGHAD, M., WANG, Y., GILLETT, E., FLEMING, M. D., DÖTSCH, V., ANDREWS, N. C., CAPUT, D. & MCKEON, F. 1998. p63, a p53 homolog at 3q27-29, encodes multiple products with transactivating, death-inducing, and dominant-negative activities. *Molecular cell*, 2, 305-316.
- YANG, A. & MCKEON, F. 2000. P63 and P73: P53 mimics, menaces and more. *Nature reviews Molecular cell biology*, 1, 199.
- YANG, A., SCHWEITZER, R., SUN, D., KAGHAD, M., WALKER, N., BRONSON, R. T., TABIN, C., SHARPE, A., CAPUT, D. & CRUM, C. 1999. p63 is essential for regenerative proliferation in limb, craniofacial and epithelial development. *Nature*, 398, 714.
- YANG, A., WALKER, N., BRONSON, R., KAGHAD, M., OOSTERWEGEL, M., BONNIN, J., VAGNER, C., BONNET, H., DIKES, P. & SHARPE, A. 2000. p73-deficient mice have neurological, pheromonal and inflammatory defects but lack spontaneous tumours. *Nature*, 404, 99.
- YASUO, M., MIZUNO, S., ALLEGOOD, J., KRASKAUSKAS, D., BOGAARD, H. J., SPIEGEL, S. & VOELKEL, N. F. 2013. Fenretinide causes emphysema, which is prevented by sphingosine 1-phosphate. *PloS one*, 8, e53927.
- YATOMI, Y., IGARASHI, Y., YANG, L., HISANO, N., QI, R., ASAZUMA, N., SATOH, K., OZAKI, Y. & KUME, S. 1997. Sphingosine 1-phosphate, a bioactive sphingolipid abundantly stored in platelets, is a normal constituent of human plasma and serum. *The Journal of Biochemistry*, 121, 969-973.

- YE, J., RAWSON, R. B., KOMURO, R., CHEN, X., DAVÉ, U. P., PRYWES, R., BROWN, M. S. & GOLDSTEIN, J. L. 2000. ER stress induces cleavage of membrane-bound ATF6 by the same proteases that process SREBPs. *Molecular cell*, 6, 1355-1364.
- YE, Y. & RAPE, M. 2009. Building ubiquitin chains: E2 enzymes at work. *Nature reviews Molecular cell biology*, 10, 755.
- YONISH-ROUACH, E., RESNFTZKY, D., LOTEM, J., SACHS, L., KIMCHI, A. & OREN, M. 1991. Wild-type p53 induces apoptosis of myeloid leukaemic cells that is inhibited by interleukin-6. *Nature*, 352, 345.
- YOSHIDA, H., MATSUI, T., HOSOKAWA, N., KAUFMAN, R. J., NAGATA, K. & MORI, K. 2003. A time-dependent phase shift in the mammalian unfolded protein response. *Developmental cell*, 4, 265-271.
- YOSHIMOTO, T., FURUHATA, M., KAMIYA, S., HISADA, M., MIYAJI, H., MAGAMI, Y., YAMAMOTO, K., FUJIWARA, H. & MIZUGUCHI, J. 2003. Positive modulation of IL-12 signaling by sphingosine kinase 2 associating with the IL-12 receptor β 1 cytoplasmic region. *The Journal of Immunology*, 171, 1352-1359.
- YUNG, L. M., WEI, Y., QIN, T., WANG, Y., SMITH, C. D. & WAEBER, C. 2012. Sphingosine kinase 2 mediates cerebral preconditioning and protects the mouse brain against ischemic injury. *Stroke*, 43, 199-204.
- ZEMANN, B., URTZ, N., REUSCHEL, R., MECHTCHERIAKOVA, D., BORNANCIN, F., BADEGRUBER, R., BAUMRUKER, T. & BILLICH, A. 2007. Normal neutrophil functions in sphingosine kinase type 1 and 2 knockout mice. *Immunology letters*, 109, 56-63.
- ZENZ, R., EFERL, R., KENNER, L., FLORIN, L., HUMMERICH, L., MEHIC, D., SCHEUCH, H., ANGEL, P., TSCHACHLER, E. & WAGNER, E. F. 2005. Psoriasis-like skin disease and arthritis caused by inducible epidermal deletion of Jun proteins. *Nature*, 437, 369.
- ZHAN, F., BARLOGIE, B., ARZOUMANIAN, V., HUANG, Y., WILLIAMS, D. R., HOLLMIG, K., PINEDA-ROMAN, M., TRICOT, G., VAN RHEE, F. & ZANGARI, M. 2007. Gene-expression signature of benign monoclonal gammopathy evident in multiple myeloma is linked to good prognosis. *Blood*, 109, 1692-1700.
- ZHANG, C., YONG, C., ADACHI, M. T., OSHIRO, S., ASO, T., KAUFMAN, R. J. & KITAJIMA, S. 2001. ci. *Journal of Biological Chemistry*.
- ZHANG, F., XIA, Y., YAN, W., ZHANG, H., ZHOU, F., ZHAO, S., WANG, W., ZHU, D., XIN, C. & LEE, Y. 2016. Sphingosine 1-phosphate signaling contributes to cardiac inflammation, dysfunction, and remodeling following myocardial infarction. *American journal of physiology. Heart and circulatory physiology*, 310, H250-61.
- ZHANG, H., DESAI, N. N., OLIVERA, A., SEKI, T., BROOKER, G. & SPIEGEL, S. 1991. Sphingosine-1-phosphate, a novel lipid, involved in cellular proliferation. *The Journal of cell biology*, 114, 155-167.
- ZHANG, H. & SUN, S.-C. 2015. NF- κ B in inflammation and renal diseases. *Cell & bioscience*, 5, 63.
- ZHANG, H.-G., WANG, J., YANG, X., HSU, H.-C. & MOUNTZ, J. D. 2004. Regulation of apoptosis proteins in cancer cells by ubiquitin. *Oncogene*, 23, 2009.

- ZHANG, K. & KAUFMAN, R. J. 2004. Signaling the unfolded protein response from the endoplasmic reticulum. *Journal of Biological Chemistry*, 279, 25935-25938.
- ZHANG, Y., BERKA, V., SONG, A., SUN, K., WANG, W., ZHANG, W., NING, C., LI, C., ZHANG, Q. & BOGDANOV, M. 2014. Elevated sphingosine-1-phosphate promotes sickling and sickle cell disease progression. *The Journal of clinical investigation*, 124, 2750-2761.
- ZHANG, Y. & XIONG, Y. 2001. A p53 amino-terminal nuclear export signal inhibited by DNA damage-induced phosphorylation. *Science*, 292, 1910-1915.
- ZHAO, P., YANG, X., YANG, L., LI, M., WOOD, K., LIU, Q. & ZHU, X. 2016. Neuroprotective effects of fingolimod in mouse models of Parkinson's disease. *The FASEB Journal*, 31, 172-179.
- ZHENG, N. & SHABEK, N. 2017. Ubiquitin ligases: structure, function, and regulation. *Annual review of biochemistry*, 86, 129-157.
- ZHENG, W., KOLLMEYER, J., SYMOLON, H., MOMIN, A., MUNTER, E., WANG, E., KELLY, S., ALLEGOOD, J. C., LIU, Y. & PENG, Q. 2006. Ceramides and other bioactive sphingolipid backbones in health and disease: lipidomic analysis, metabolism and roles in membrane structure, dynamics, signaling and autophagy. *Biochimica et Biophysica Acta (BBA)-Biomembranes*, 1758, 1864-1884.
- ZHOU, B.-B. S. & ELLEDGE, S. J. 2000. The DNA damage response: putting checkpoints in perspective. *Nature*, 408, 433.
- ZHOU, H., SUMMERS, S. A., BIRNBAUM, M. J. & PITTMAN, R. N. 1998. Inhibition of Akt kinase by cell-permeable ceramide and its implications for ceramide-induced apoptosis. *Journal of Biological Chemistry*, 273, 16568-16575.
- ZHOU, J., CHEN, J. & YU, H. 2018. Targeting sphingosine kinase 2 by ABC294640 inhibits human skin squamous cell carcinoma cell growth. *Biochemical and biophysical research communications*, 497, 535-542.
- ZHU, W., GLIDDON, B. L., JARMAN, K. E., MORETTI, P. A., TIN, T., PARISE, L. V., WOODCOCK, J. M., POWELL, J. A., RUSZKIEWICZ, A. & PITTMAN, M. R. 2017a. CIB1 contributes to oncogenic signalling by Ras via modulating the subcellular localisation of sphingosine kinase 1. *Oncogene*, 36, 2619.
- ZHU, W., JARMAN, K. E., LOKMAN, N. A., NEUBAUER, H. A., DAVIES, L. T., GLIDDON, B. L., TAING, H., MORETTI, P. A., OEHLER, M. K. & PITTMAN, M. R. 2017b. CIB2 negatively regulates oncogenic signaling in ovarian cancer via sphingosine kinase 1. *Cancer research*, 77, 4823-4834.
- ZHU, Y., MAO, X. O., SUN, Y., XIA, Z. & GREENBERG, D. A. 2002. p38 Mitogen-activated protein kinase mediates hypoxic regulation of Mdm2 and p53 in neurons. *Journal of Biological Chemistry*, 277, 22909-22914.

APPENDIX:
SUPPLEMENTARY DATA

APPENDIX: SUPPLEMENTARY DATA

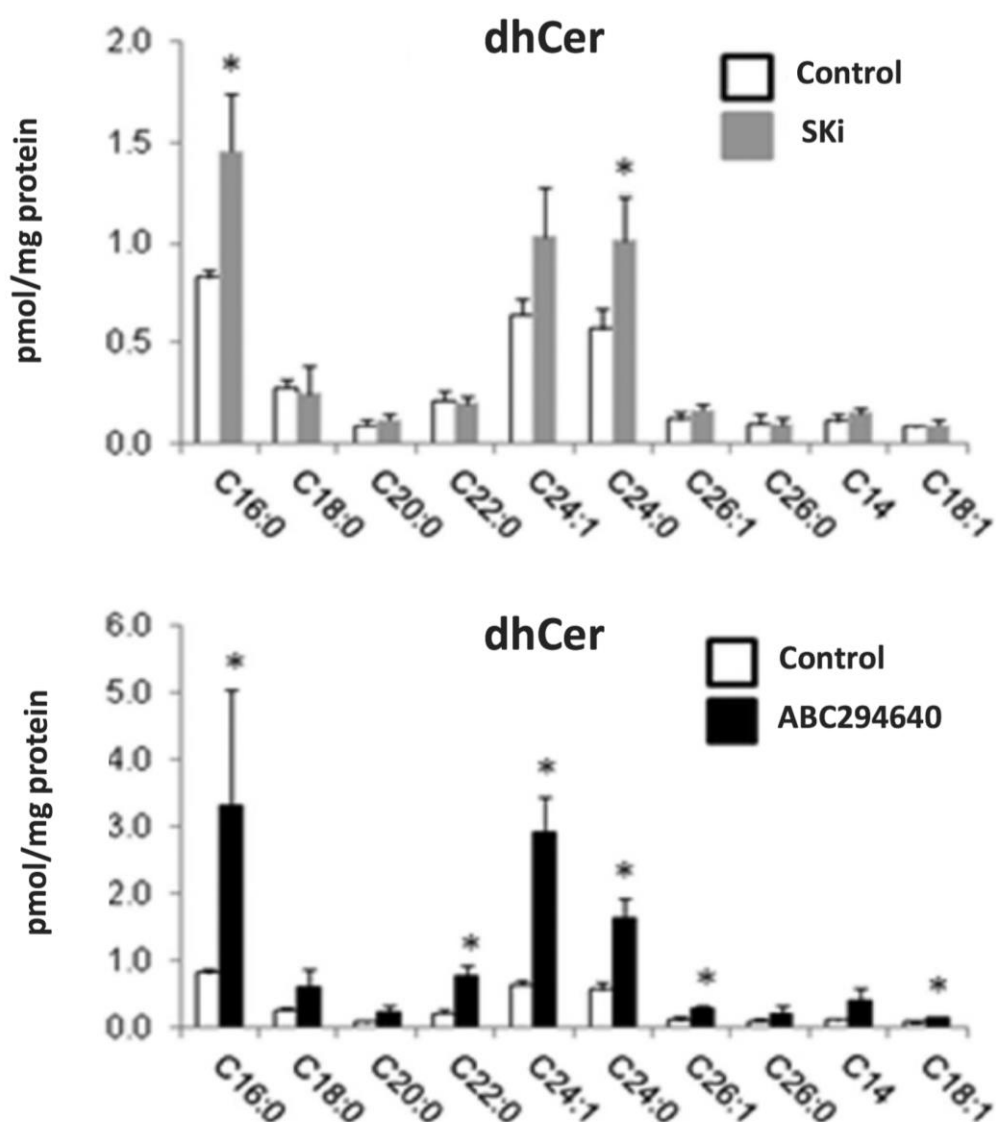


Figure S1 MS analysis of dihydroceramide levels in HEK293T cells treated with SKi or ABC294640. HEK293T cells were cultured in complete medium containing 10% FCS until ~70% confluent. Cells were treated with SKi (10 μ M) or ABC294640 (25 μ M) or with the vehicle alone (DMSO 0.1% v/v) for 24 hours before snap-freezing. Lipid extracts were analyzed by LC-MS for dihydroceramide (dhCer). The data was expressed as means \pm SEM for $n=3$ experiments and analysed by Unpaired t -test multiple comparisons, $*p<0.05$ for SKi or ABC294640 versus control. The x axis annotates different N-acyl chain lengths and double-bond molecular species.

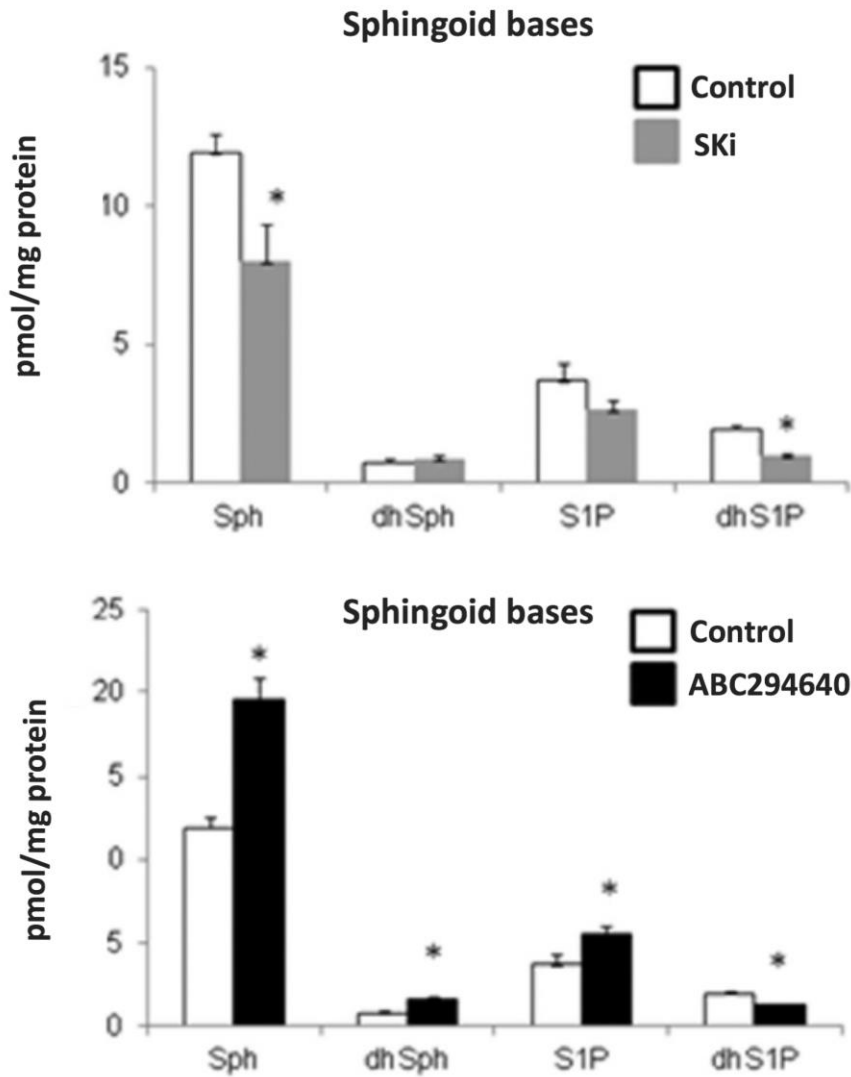


Figure S2 MS analysis of sphingoid bases levels in HEK293T cells treated with SKi or ABC294640. HEK293T cells were cultured in complete medium containing 10% FCS until ~70% confluent. Cells were treated with SKi (10 μ M) or ABC294640 (25 μ M) or with the vehicle alone (DMSO 0.1% v/v) for 24 hours before snap-freezing. Lipid extracts were analyzed by LC-MS for sphingoid bases (Sphinganine/dihydrosphingosine, dhSph; sphinganine 1-phosphate, dhS1P). The data was expressed as means \pm SEM for $n=3$ experiments and analysed by Unpaired t -test multiple comparisons, $*p<0.05$ for SKi or ABC294640 versus control.

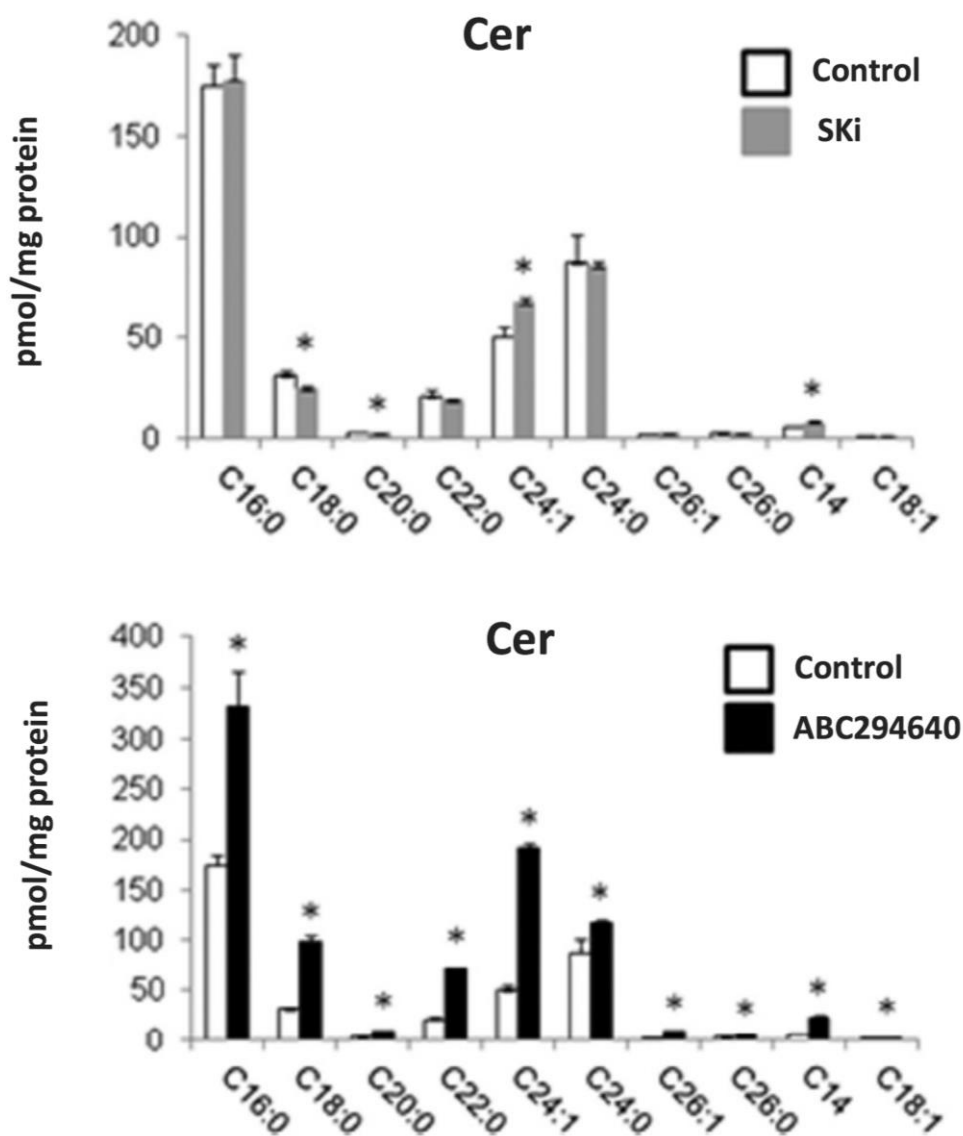


Figure S3 MS analysis of ceramide levels in HEK293T cells treated with SKi or ABC294640. HEK293T cells were cultured in complete medium containing 10% FCS until ~70% confluent. Cells were treated with SKi (10 μ M) or ABC294640 (25 μ M) or with the vehicle alone (DMSO 0.1% v/v) for 24 hours before snap-freezing. Lipid extracts were analyzed by LC-MS for ceramide (Cer). The data was expressed as means \pm SEM for $n=3$ experiments and analysed by Unpaired t -test multiple comparisons, $*p<0.05$ for SKi or ABC294640 versus control. The x axis annotates different N-acyl chain lengths and double-bond molecular species.

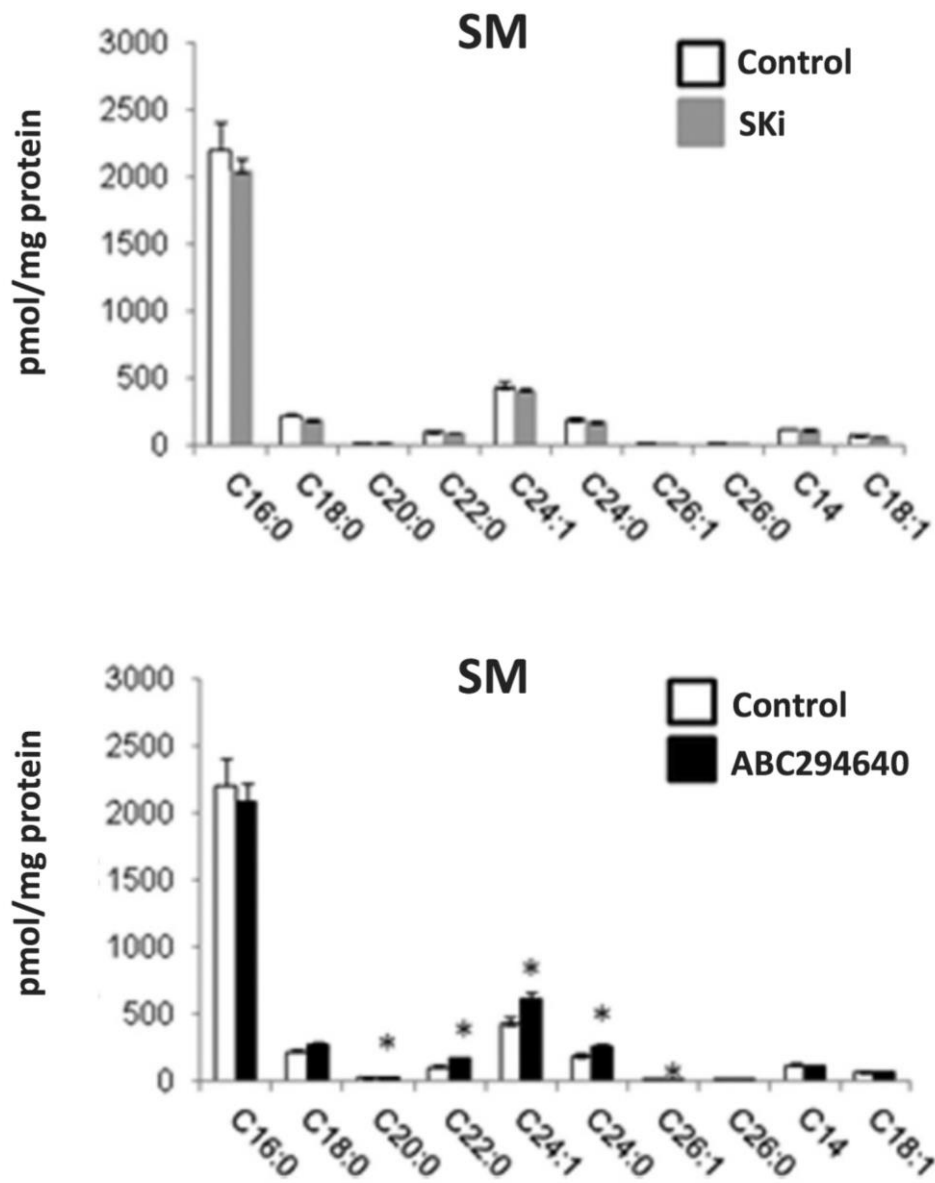


Figure S4 MS analysis of sphingomyelin levels in HEK293T cells treated with SKi or ABC294640. HEK293T cells were cultured in complete medium containing 10% FCS until ~70% confluent. Cells were treated with SKi (10 μ M) or ABC294640 (25 μ M) or with the vehicle alone (DMSO 0.1% v/v) for 24 hours before snap-freezing. Lipid extracts were analyzed by LC-MS for sphingomyelin (SM). The data was expressed as means \pm SEM for $n=3$ experiments and analysed by Unpaired t-test multiple comparisons, * $p < 0.05$ for SKi or ABC294640 versus control. The x axis annotates different N-acyl chain lengths and double-bond molecular species.

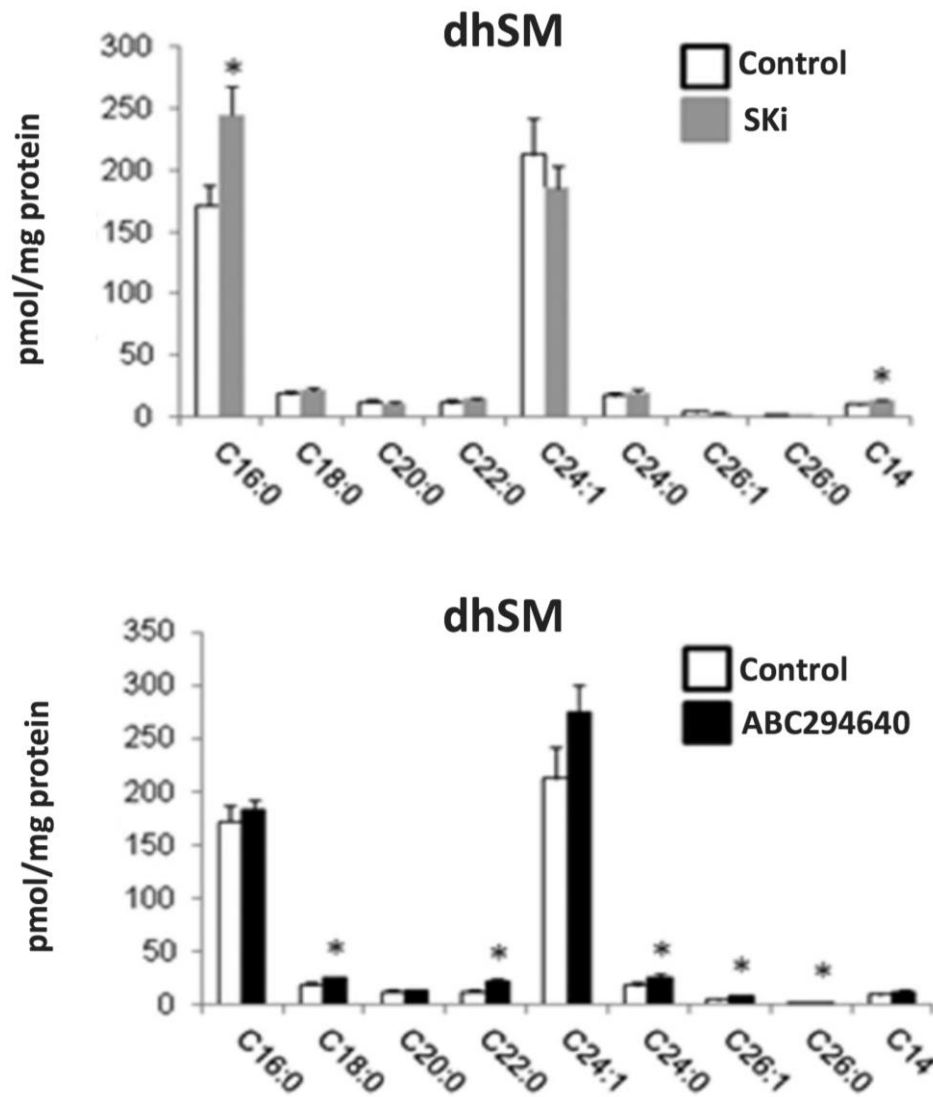


Figure S5 MS analysis of dihydrosphingomyelin levels in HEK293T cells treated with SKi or ABC294640. HEK293T cells were cultured in complete medium containing 10% FCS until ~70% confluent. Cells were treated with SKi (10 μ M) or ABC294640 (25 μ M) or with the vehicle alone (DMSO 0.1% v/v) for 24 hours before snap-freezing. Lipid extracts were analyzed by LC-MS for dihydrosphingomyelin (dhSM). The data was expressed as means \pm SEM for $n=3$ experiments and analysed by Unpaired t -test multiple comparisons, $*p<0.05$ for SKi or ABC294640 versus control. The x axis annotates different N-acyl chain lengths and double-bond molecular species.

